

**THE EVOLUTION OF ANTIBACTERIAL CHEMOTHERAPY:  
TARGETING RECA TO SABOTAGE  
ANTIBIOTIC TOLERANCE AND RESISTANCE MECHANISMS**

by

**TIM J. WIGLE**

A dissertation submitted to the faculty of the University of North Carolina at Chapel Hill  
in partial fulfillment of the requirements for the degree of  
Doctor of Philosophy in the School of Pharmacy

CHAPEL HILL  
2007

APPROVED BY:

Scott Singleton, Ph.D.

Harold Kohn, Ph.D.

Kenneth Bastow, Ph.D.

Michael Jartsfer, Ph.D.

Rob Nicholas, Ph.D.

## ABSTRACT

### **The Evolution of Antibacterial Chemotherapy: Targeting RecA to Sabotage Antibiotic Tolerance and Resistance Mechanisms**

by

**Tim J. Wagle**

Antibiotic resistant bacteria are rendering the current supply of available antibacterial drugs ineffective at an alarming rate and there is a dearth of novel drug targets for the treatment of bacterial infectious diseases. New strategies are required to combat pathogenic bacteria and in this context RecA has emerged as an intriguing candidate for inhibition studies. In the bacterial kingdom, the RecA protein is a highly conserved recombinase enzyme that mediates DNA repair and horizontal gene transfer and across all species it almost uniformly regulates the SOS response to DNA damage. Recent evidence suggests that these RecA-controlled processes are responsible for an increased tolerance to antibiotic chemotherapy and they up-regulate pathways which ultimately lead to full-fledged antibiotic resistance. We propose targeting RecA with small molecules to sabotage the molecular mechanisms which are believed to cause antibiotic chemotherapy to fail. Towards the goal of validating RecA as an important and novel target for the chemotherapeutic treatment of bacterial infectious diseases we have studied the interaction of metal–dithiols, nucleotide analogs and drug-like small molecules with the RecA protein. Upon activation RecA binds ssDNA and performs ATP hydrolysis, therefore we observed either a reduction of RecA-ssDNA binding or ATP hydrolysis in the presence of potential inhibitors using fast and

efficient screening assays. As the size and complexity of the compound libraries increased in our studies, the methods we employed to identify inhibitors evolved to meet the demand they imposed. In all, more than 64,000 compounds were assayed against RecA and we identified several lead structures which were active against RecA in *Escherichia coli* cell cultures. We demonstrate that cell-permeable inhibitors of RecA are capable of abrogating the SOS response and potentiate the toxicity of bactericidal antibiotics, e.g. ciprofloxacin. The results of this study suggests that RecA may serve as a novel antibacterial drug target not belonging to any class of currently prescribed antibiotics, and which has not previously been examined in this regard.

To my beautiful wife Lawna, whose love and support has made this work possible, and to my parents James and Jeannine who have provided with me with an excellent foundation for learning and who have bailed me out of trouble more times than I can count. I made it guys!

## ACKNOWLEDGMENTS

I am grateful for the opportunity I have had to pursue my doctorate degree at the University of North Carolina and want to thank all those who been instrumental in my success. I have had quite an enjoyable and satisfying four and a half years and I feel I have experienced tremendous growth as a person. I have particularly enjoyed my time on this beautiful campus and the infectious Tarheel spirit that has turned me into a die-hard UNC basketball fan.

I thank Dr. Scott Singleton for giving me an opportunity to flourish under his supervision. I was his first graduate student at the University of North Carolina and I have been fortunate to take on the lead role in his most exciting and rewarding projects and I particularly enjoyed having the opportunity to help spend large sums of his R01 grant! Dr. Singleton has been a tremendous advisor and has polished my rough edges, teaching me how to think about science and how to effectively present my findings. I appreciate his willingness to allow me to speak with blunt honesty and operate in a way which suits my personality and skills. I also feel fortunate to have had an advisor that sent me to three excellent conferences which have broadened my scientific perspective.

I extend thanks to my dissertation committee, Dr. Kohn, Dr. Bastow, Dr. Jarstfer and Dr. Nicholas for their constructive criticism and helpful advice. More thanks go out to my collaborators at North Carolina Central University, particularly Dr. Sexton for allowing me to get a taste of high-throughput screening and for introducing me to high-content microscopy.

I have enjoyed the company and camaraderie of Singleton research group members past and present: Dr. Andrew Lee, Dr. Bu-Bing Zeng, Chris Ross, Dr. Daniel Cline, Dr. Mallinath Hadimani, Dr. Anna Gromova, Will Horton, Keri Flanagan and Demet Guntas. They are a brave and tolerant lot for putting up with some of my antics. I have also enjoyed hanging out with other students from the Division of Medicinal Chemistry and wish them success in their future endeavours.

Thanks to all my friends outside of school, the Canadian Gang, the Woody's Crew and my teammates from the Shockers hockey team who provide ample distraction from a busy week on Sunday nights. Thanks to all my childhood friends and those friends from along the way who don't let me forget where I come from.

Last but not least I am in debt to my family for allowing me to succeed in all aspects of life. My parents have helped me out in more ways than they can imagine and there is no possible way to repay them for everything they have done for me. The bond between my brother and I has become stronger with distance and I always look forward to spending time with him. My wife Lawna has been a tremendous source of support and love and she does a great job of keeping me in line. I only met her because I decided to take a leap of faith and attend UNC and for that I am eternally grateful.

## TABLE OF CONTENTS

	<b>PAGE</b>
LIST OF TABLES.....	xi
LIST OF FIGURES.....	xii
ABBREVIATIONS.....	xvi
CHAPTER I INTRODUCTION.....	1
The Significance of Bacterial Drug Resistance.....	1
The Molecular Origins of Antibiotic Resistance.....	4
The Physiology of the RecA Protein.....	5
RecA and the SOS Response to DNA Damage.....	7
RecA and Recombination.....	10
Other Roles of RecA in Pathogenicity.....	14
RecA and Tolerance to Antibiotic Chemotherapy.....	14
RecA and Resistance to Antibiotic Chemotherapy.....	19
RecA and the Overall Antibiotic Response.....	21
The Necessity of RecA.....	22
RecA as a Novel Target for the Chemotherapy of Bacterial Infectious Diseases.....	22
Our Efforts to Develop RecA Inhibitors.....	27
CHAPTER II BISMUTH-DITHIOL AND METAL-CATION MEDIATED INHIBITION OF RECA.....	31

Screening Metal Cations for Irreversible Inactivation of RecA.....	34
Investigating the Dependence of ATPase Cofactors for RecA Aggregation.....	35
Effect of Thiol Ligands on RecA Inhibition by the Bismuth Cation.....	36
Mechanism of RecA Inhibition by Bi <sub>3</sub> BAL.....	38
Conformationally Selective Inhibition of RecA by Bi <sub>3</sub> BAL.....	40
In Vivo Studies of Bi <sub>3</sub> BAL vs. RecA: Using a Reporter Gene to Follow SOS Induction.....	42
In Vivo Studies of Bi <sub>3</sub> BAL: Antibacterial Synergism with Mitomycin C.....	44
Conclusions.....	45
Materials and Methods.....	46
 CHAPTER III THE NUCLEOTIDE BINDING SPECIFICITY OF RECA: A LIGAND-BASED ANALYSIS OF THE ATP-BINDING SITE AND THE DESIGN OF ATP-COMPETITIVE INHIBITORS.....	 53
Criteria for ATP-Competitive Inhibitor Design.....	56
Structural Analysis of the RecA ATP-Binding Site.....	57
Comparative Analysis of the ATP-Binding Site.....	59
ADP is Bound in an Unusual Orientation .....	61
Internal Cavity Adjacent to ADP .....	61
Merging Structural Knowledge of the RecA ATP-Binding Site with Nucleotide Analog Binding Data.....	62
Probing the Substrate Specificity of RecA.....	64
Probing the Ability of Non-Substrate Nucleotide Analogs to Bind and Inhibit RecA.....	70
Application of Selectivity Filters to ADP and ATP Analogs.....	71



	Prospective Inhibitors in Other Structural Classes.....	74
	Molecular Screening Assays for RecA Activities.....	75
	Inhibition of RecA-DNA Filament ATPase Activity.....	77
	Inhibition of RecA-DNA Filament Assembly.....	80
	Inhibition of RecA-Mediated DNA Three-Strand Exchange Reaction.....	83
	Functionally Selective Inhibition of RecA.....	85
	Structural Basis For Inhibition by ADP and ATP Analogs.....	89
	Implications for Future Rational Design Modification Procedures.....	92
	Conclusions.....	95
	Materials and Methods.....	96
CHAPTER IV	DIRECTED MOLECULAR SCREENING FOR RECA ATPASE INHIBITORS.....	111
	Selection of a Focused Mini-Library of Potential Inhibitors.....	111
	Development of Novel HTS-Compatible Fluorescent ATPase Assays.....	113
	Screening the Focused Library.....	117
	Insights Into the Mechanism of Inhibition by Poly-Sulfated Naphthyl Compounds.....	119
	Conclusions.....	121
	Materials and Methods.....	121
CHAPTER V	HIGH-THROUGHPUT SCREENING FOR INHIBITORS OF RECA.....	126
	Assay Optimization and Validation.....	128
	PMB ATPase Assay Trial Run on the National Cancer Insititute Libraries.....	131

Screening a 33,600 Compound Library Against RecA.....	132
Investigating the Mechanism of Action of Group A Compounds....	136
Group A Compounds Effect a Reduction in RecA-Dependent SOS Expression.....	138
Group A Compounds Display Antibacterial Synergism With Ciprofloxacin.....	141
Conclusions.....	143
Materials and Methods.....	145
CHAPTER VI CONCLUSIONS.....	150
REFEREED PUBLICATIONS.....	155
CONFERENCE PRESENTATIONS.....	156
REFERENCES.....	157

## LIST OF TABLES

Table 3.1.	Kinetics of NTP hydrolysis by the RecA protein.....	65
Table 3.2.	Commercial sources of nucleotides used.....	97
Table 4.2.	Commercial sources of the focused library.....	122

## LIST OF FIGURES

Figure 1.1.	The timeline of antibiotic deployment vs. the observation of resistant strains.....	3
Figure 1.2.	Dangerous antibiotic-related trends.....	4
Figure 1.3.	Molecular bases for antibiotic resistance.....	5
Figure 1.4.	The dynamic balance mediated by RecA.....	6
Figure 1.5.	The SOS response to DNA damage.....	8
Figure 1.6.	RecA-mediated recombinational DNA repair pathways.....	12
Figure 1.7.	Targets of currently prescribed antibiotics.....	16
Figure 1.8.	The hydroxyl radical pathway stimulated by DNA-damaging antibiotics.....	17
Figure 1.9.	The importance of the SOS response and RecA for mitigating the effects of bactericidal antibiotics.....	18
Figure 1.10.	Antibiotic treatment induces RecA-mediated competence and recombination.....	20
Figure 1.11.	RecA and the antibiotic response.....	21
Figure 1.12.	Three possible therapeutic outcomes of RecA inhibitor treatment.....	25
Figure 2.1.	Metal-cation induced RecA aggregation under conditions of active ATP hydrolysis measured by light-scattering.....	34
Figure 2.2.	Enhancement of bismuth-mediated inhibition by thiol ligands.....	37
Figure 2.3.	Determining if Bi <sub>3</sub> BAL is competitive with ATP or ssDNA.....	39
Figure 2.4.	Mechanistic exploration of inactivation of RecA by bismuth using a light-scattering assay to measure protein aggregation.....	41

Figure 2.5.	Cartoon depicting the conformational states of RecA which are targeted by bismuth.....	42
Figure 2.6.	In vivo experiments studying the effect of Bi <sub>3</sub> BAL on SOS induction and the antibacterial synergism of Bi <sub>3</sub> BAL.....	44
Figure 3.1.	Nucleotides can be classified based on their mode of inhibition of RecA.....	55
Figure 3.2.	Targeting the inactive vs. active conformations of NTP-binding proteins.....	57
Figure 3.4.	Structural models of the RecA ATP-binding site.....	58
Figure 3.3.	Comparative analysis of the RecA ATP-binding site.....	60
Figure 3.5.	Flowchart for analyzing the binding of nucleotide analogs to RecA.....	63
Figure 3.6.	Non-natural nucleotide triphosphate analogs examined as substrates for hydrolysis by RecA.....	65
Figure 3.7.	Analysis of structure-activity relationships for RecA-catalyzed NTP hydrolysis of ATP analogs.....	67
Figure 3.8.	<i>N</i> <sup>6</sup> -modified purine analogs examined as inhibitors of RecA.....	72
Figure 3.9.	Ribose-modified purine analogs examined as inhibitors of RecA.....	72
Figure 3.10.	TTP analogs screened as potential inhibitors of RecA.....	74
Figure 3.11.	Nucleotide analogs with di- and triphosphate replacements screened as potential inhibitors of RecA.....	75
Figure 3.12.	Activities of nucleotide analogs screened against RecA in the ATPase and filament assembly assays.....	76
Figure 3.13.	MESG-coupled ATPase assay used to screen for nucleotide analog inhibitors of ATP hydrolysis by RecA.....	78
Figure 3.14.	Biotin-dT <sub>36</sub> magnetic pull-down assay used to screen for inhibitors of RecA-DNA filament assembly.....	81
Figure 3.15.	Inhibition of RecA-mediated three-strand exchange assay by TNP-ADP.....	84
Figure 3.16.	Functionally selective inhibition of RecA.....	85

Figure 3.17.	Adenosine scaffold substitutions create conformationally selective inhibitors of RecA.....	93
Figure 4.1.	Five classes of compounds screened for RecA inhibition.....	112
Figure 4.2.	Two fluorescent ATPase assays developed to monitor ATP hydrolysis by RecA in the presence of small molecules which may be UV-active.....	114
Figure 4.3.	The resorufin ADP/P <sub>i</sub> reporter molecule provides a convenient colorimetric indicator that the reaction is complete.....	115
Figure 4.4.	Interday and intercolumn precision for the ADP-linked fluorescent ATPase assay.....	117
Figure 4.5.	Results of the directed screen of 18 selected compounds against RecA ATP hydrolysis activity.....	118
Figure 4.6.	Suramin inhibits the RecA-mediated DNA three-strand exchange reaction.....	120
Figure 5.1.	PMB ATPase assay used to identify inhibitors of RecA.....	128
Figure 5.2.	Optimization of the phosphomolybdate blue ATPase adapted for use with RecA.....	129
Figure 5.3.	Z' factor determination for the phosphomolybdate blue ATPase assay adapted for use with RecA.....	130
Figure 5.4.	Scatter plot of the ATPase inhibition effected by the NCI Compounds.....	131
Figure 5.5.	Statistical analyses of each 384-well plate to determine the quality of the HTS assay performed on the donated Biogen Idec compounds.....	132
Figure 5.6.	A total of 33,600 were screened using the phosphomolybdate blue ATPase assay.....	133
Figure 5.7.	Four classes of hits mined in the Biogen library.....	133
Figure 5.8.	IC <sub>50</sub> study for selected scaffold class A compounds.....	134
Figure 5.9.	IC <sub>50</sub> study for selected scaffold class B compounds.....	135
Figure 5.10.	IC <sub>50</sub> study for selected scaffold class C compounds.....	135
Figure 5.11.	Determining if A1 is competitive with ATP or ssDNA.....	136

Figure 5.12.	RecA mediated three-strand exchange is inhibited by A1.....	137
Figure 5.13.	The ciprofloxacin-induced SOS response measured by a GFP reporter gene expression assay.....	139
Figure 5.14.	Inhibition of SOS induction by A1.....	140
Figure 5.15.	Compound A1 synergistically enhances the toxicity of ciprofloxacin in <i>E. coli</i> .....	142

## LIST OF ABBREVIATIONS

Amp	Ampicillin
ANS	8-Anilino-1-naphthalenesulfonic acid
ATP $\gamma$ S	Adenosine 5'-[ $\gamma$ -thio]triphosphate
BAL	British anti-Lewisite; 3,4-dimercapto-butan-1-ol
BME	$\beta$ -mercaptoethanol
CFU	Colony-forming units
Cipro	Ciprofloxacin
cssDNA	circular single-stranded DNA
<i>cycloSal</i>	<i>cycloSaligenyl</i>
DHF	dihydrofolate
DOS	Diversity-oriented synthesis
DSB	Double-strand break
dsDNA	double-stranded DNA
DTT	Dithiothreitol
Em	Emission
Ex	Excitation
FQRP	Fluoroquinolone-resistant <i>Pseudomonas aeruginosa</i>
GHL	Gyrase-Hsp90-like



HGT	Horizontal Gene Transfer
HTS	High-throughput screening
IRA	Inhibitor of RecA
Kan	Kanamycin
LB	Luria Bertani
LPA	Reduced lipoic acid
MESG	2-amino-6-mercapto-7-methylpurine riboside
MMC	Mitomycin C
MRSA	Methicillin-resistant <i>Staphylococcus aureus</i>
NAD <sup>+</sup>	$\beta$ -Nicotinamide adenine dinucleotide, oxidized
NADH	$\beta$ -Nicotinamide adenine dinucleotide, reduced
NCI	National Cancer Insitute
NER	Nucleotide excision repair
NMP	Nucleotide monophosphate
NDP	Nucleotide diphosphate
NTP	Nucleotide triphosphate
NXP	Nucleotide mono-, di- or triphosphate
Nor	Norfloxacin
NPF	Nucleoprotein filament
nts	nucleotides (in reference to DNA oligomer concentration)
O <sub>2</sub> <sup>-</sup>	Superoxide
OD	Optical density
OH <sup>•</sup>	Hydroxyl radical

ONPG	2-Nitrophenyl- $\beta$ -D-galactopyranoside
PABA	para-amino benzoic acid
P <sub>i</sub>	Inorganic phosphate
P-loop	Phosphate binding loop
PMB	Phosphomolybdate blue
PNP	Purine nucleoside phosphorylase
PolIV	DNA polymerase IV
PolV	DNA polymerase V
RDR	Recombinational DNA repair
SA-PMP	Streptavidin paramagnetic particle
ssDNA	Single-stranded DNA
SSB	Single-stranded DNA binding protein
TCA cycle	Tricarboxylic acid cycle
THF	Tetrahydrofolate
tsDNA	Triple-stranded DNA
UV	Ultraviolet
VRE	Vancomycin-resistant <i>enterococci</i>
wt	wild-type

## CHAPTER I

### INTRODUCTION

#### **The significance of bacterial drug resistance**

Bacteria are ubiquitous unicellular organisms that have evolved to inhabit every imaginable environment, including extremely harsh ones such as thermal vents in the Earth's crust with temperatures of up to 85 °C, deep ocean trenches with pressures 1000 times that of the atmosphere, and sites of radioactive contamination with 1500 times the dose of radiation considered lethal to humans. Although bacteria cover almost every square inch of the planet's surface, many species have evolved to preferentially invade and multiply within animals, making them a potential threat to the host if they cause a persistent infection that leads to debilitating illness or death. In and on the human body alone, commensal bacteria outnumber host cells 10:1, but these bacteria prevent colonization and infection by pathogenic bacteria and even facilitate digestion and the uptake of essential nutrients.<sup>[7]</sup> Unfortunately, even commensal bacteria, which are normally kept in check by the host's immune system, can become pathogenic under opportunistic conditions.

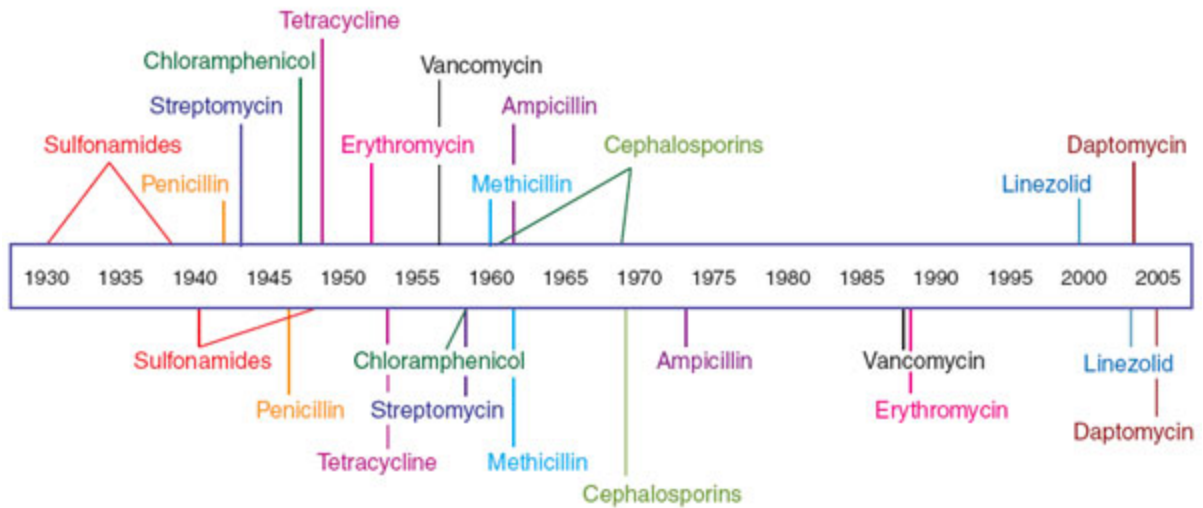
Humans have been at odds with bacteria throughout history. The discovery of Penicillin,<sup>[8]</sup> a natural product secreted by *Penicillium* mold, by Fleming, Florey and Chain in the 1930's was a landmark in the war on bacteria. Prior to this period, humans relied on personal hygiene, public sanitation, a few crude chemotherapeutics and their immune systems to combat microorganisms, but Penicillin offered a revolutionary way to approach

the treatment of infectious bacteria. The acid test for Penicillins came in World War II when an estimated 15% of wounded soldiers were saved and an untold number of amputations of gangrenous limbs were prevented by the heavy use of these newly mass-produced wonder compounds. For their pioneering work in the field of antibiotics, Fleming, Florey and Chain were awarded a Nobel Prize in 1945. In his Nobel Laureate speech, Fleming made an ominous prediction: he guaranteed that bacteria would develop resistance to Penicillins and the next-generation antibiotics under development at the time, and he stated that the misuse of antibiotics would exacerbate this problem,

“...I would like to sound one note of warning. Penicillin is to all intents and purposes non-poisonous so there is no need to worry about giving an overdose and poisoning the patient. There may be a danger however, though, in underdosage. It is not difficult to make microbes resistant to penicillin in the laboratory by exposing them to concentrations not sufficient to kill them, and the same thing has occasionally happened in the body. The time may come when penicillin can be bought by anyone in the shops. Then the danger is the ignorant man may easily underdose himself and by exposing his microbes to non-lethal quantities of the drug make them resistant. Here is a hypothetical illustration. Mr. X has a sore throat. He buys some penicillin and gives himself, not enough to kill the streptococci but enough to educate them to resist penicillin. He then infects his wife. Mrs. X gets pneumonia and is treated with penicillin. As the streptococci are now resistant to penicillin the treatment fails. Mrs. X dies. Who is responsible for Mrs. X's death? Why Mr. X, whose negligent use of Penicillin changed the nature of the microbe. *Moral:* If you use penicillin, use enough.” – excerpt from Alexander Fleming's Nobel Laureate speech, December 11<sup>th</sup>, 1945.

Fleming's prophecy was stunningly accurate, such that today, at the beginning of the 21<sup>st</sup> century, a myriad bacterial strains display resistance to at least one antibiotic, and some strains exist which display resistance to nearly all of the almost 100 available antibiotics. Novel antibiotics rapidly become obsolete as bacteria quickly develop resistance,

## Antibiotic deployment



## Antibiotic resistance observed

**Figure 1.1. The timeline of antibiotic deployment vs. the observation of resistant strains.** This figure was reproduced from Clatworthy et al, (2007).<sup>[1]</sup>

leaving medical professionals with limited treatment options in some cases. Figure 1.1<sup>[1]</sup> summarizes the relationship between the introduction of new antibiotics and the timeframe in which resistance was first observed.

The rate at which bacteria are developing resistance to current therapeutics is increasing uncontrollably, while the economic challenges of antibacterial research and development over the past 25 years has resulted in the downsizing, and in some cases complete elimination of Big Pharma's antibiotic pipeline.<sup>[9]</sup> Coupled together, the alarming rise in antibiotic resistant bacterial strains and a diminishing supply of new antibiotics are disturbing trends that are intersecting with dangerous consequences (Figure 1.2). Several factors such as international travel, bioterrorism, and antibiotic misuse are destined to exacerbate this dilemma. The Infectious Diseases Society of America states that bacterial infections claimed approximately 600% more lives in the year 2006 than they did in 1992, and the treatment of bacterial infections costs the U.S. health care system in the vicinity

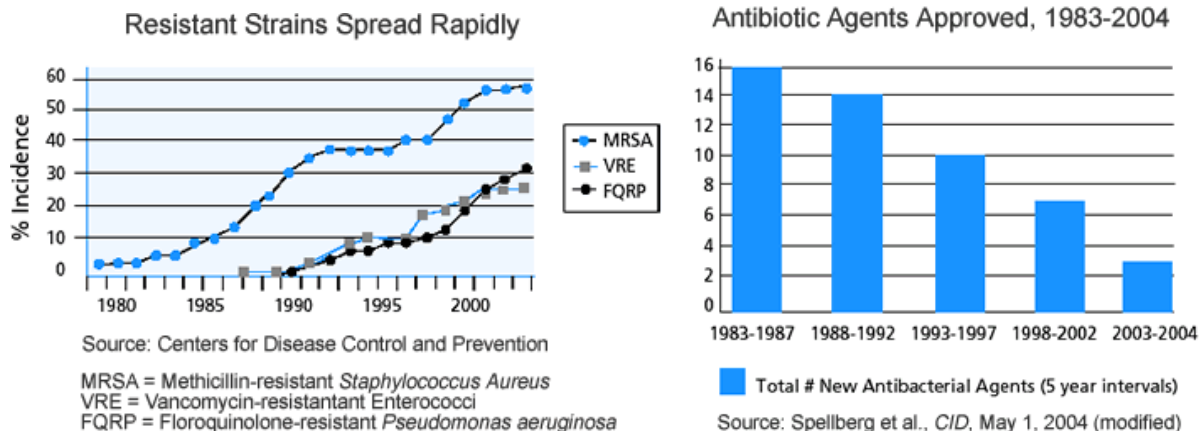


**Figure 1.2. Dangerous antibiotic-related trends.** *Left Panel:* The % incidence increase in nosocomial infections involving Methicillin-Resistant *Staphylococcus aureus* (MRSA), Vancomycin-Resistant *Enterococci* (VRE) and Fluoroquinolone-Resistant *Pseudomonas aeruginosa* (FQRP) in the past 25 years. *Right Panel:* The decreasing number of approved antibiotics in the past 20 years. This figure was obtained from the Infectious Diseases Society of America website, <http://www.idsociety.org/>.

of \$30 billion a year. Indeed, in the United States, MRSA alone results in over 18,000 deaths each year, outpacing AIDS as the most lethal infectious disease in this country.<sup>[10]</sup>

The goal behind the work undertaken in this dissertation aimed to increase our knowledge of the role of RecA in bacterial infectious diseases and potentially present RecA as a novel therapeutic target in the treatment of these diseases.

### The molecular origins of antibiotic resistance

Antibiotic resistance may either be intrinsic to the organism or acquired via adaptive mutations and the transfer of DNA encoding drug-resistant proteins.<sup>[11]</sup> While intrinsic resistance is naturally present in a bacterial species without any further genetic modifications, acquired resistance occurs through the natural selection of individual mutants that arise during exposure to one or more particular antibiotics. Acquired resistance employs one of these common molecular strategies<sup>[12]</sup> (Figure 1.3): (1) drug inactivation, (2) modification of

the drug target, (3) decreasing the amount of drug reaching the target (usually by modifying influx/efflux pump expression), and (4) altering a metabolic pathway.

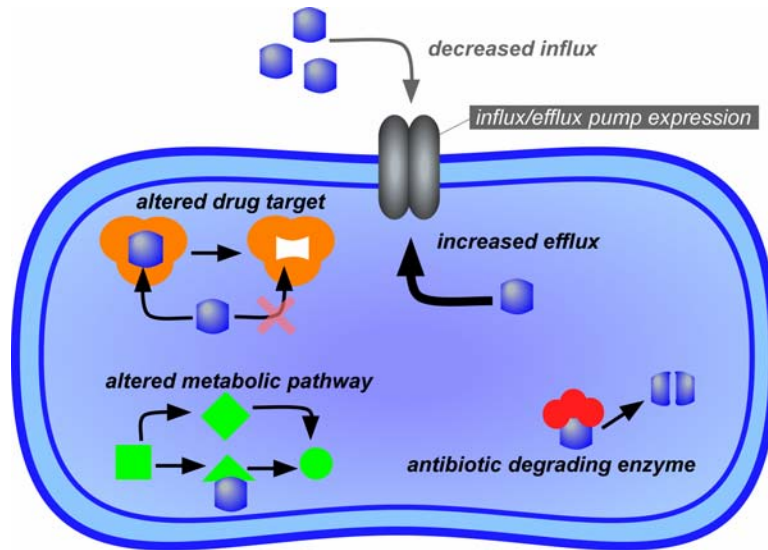


**Figure 1.3. Molecular bases for antibiotic resistance.** A heritable change in a bacterium's DNA causes a bacteria to become antibiotic resistant by altering the target of the drug, altering a metabolic pathway, creating an antibiotic inactivating enzyme or modifying drug permeability. RecA has been implicated in the mutation and horizontal gene transfer pathways which lead to the expression of these modified proteins and/or protein expression profiles.

In each of these cases, a heritable change in a cell's DNA must be made, either through mutation or the acquisition of foreign DNA elements. Antibiotic-induced metabolic stress has been shown to increase the frequency and efficacy of these evolutionary activities<sup>[3, 13, 14]</sup> and RecA has emerged as a key player in both pathways.<sup>[15-21]</sup>

### The physiology of the RecA protein

Living organisms must achieve a dynamic balance between the need to preserve genetic information to maintain a functional genome and the need to vary that same genetic information for adaptive purposes. Among bacteria, RecA is a highly conserved protein that mediates important processes on both sides of this equilibrium and is elemental to the

survival and viability of the organism.<sup>[5, 22]</sup> RecA, discovered over 40 years ago by Clark and Margulies,<sup>[23]</sup> is classically known to be activated by DNA damaging elements, but its activation is not limited to UV- and chemical-induced damage. Many factors such as antibiotic treatment, starvation, oxidative stress, heat shock and pressure cause metabolic and physiologic stress which indirectly lead to DNA damage, exposing persistent stretches of ssDNA, the rare substrate which activates RecA.<sup>[24-28]</sup>

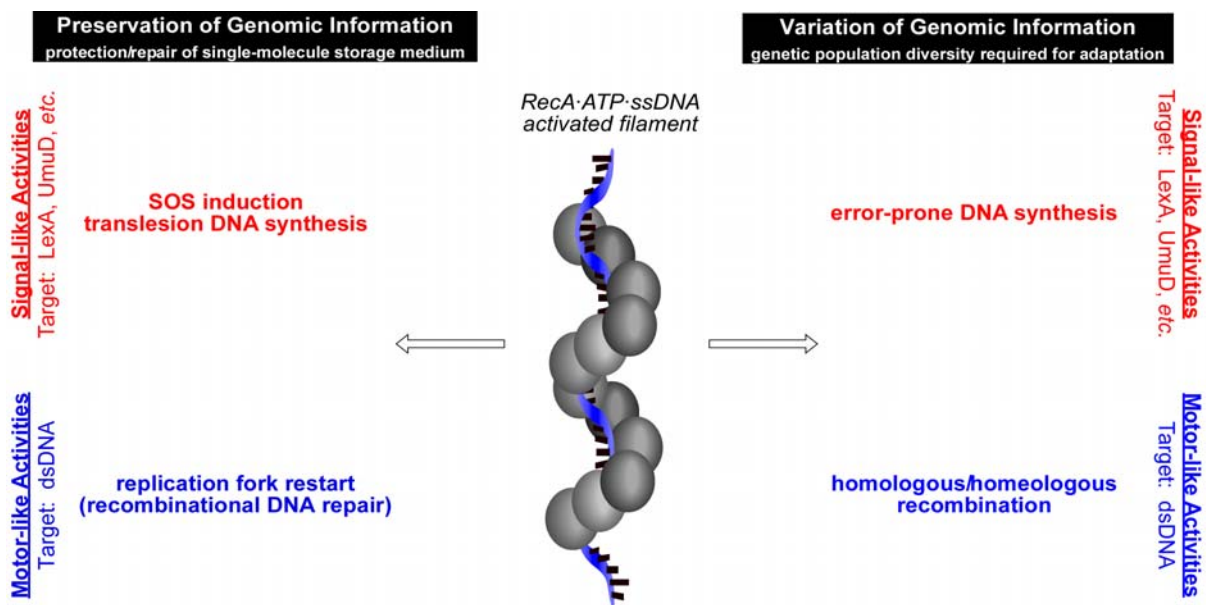


**Figure 1.4. The dynamic balance mediated by RecA.** The activated RecA-ssDNA filament initiates signaling of the SOS response and mediates several motor-like recombination activities, eloquently balancing the tendencies of bacteria towards preserving or varying genomic information.

RecA is an unusual protein in that a monomer of RecA has no relevant biological activity, but hundreds to thousands of monomers homopolymerize in the presence of ssDNA, a hallmark of DNA damage, and ATP to form an activated nucleoprotein filament (NPF) that possesses inherent signaling and ATP-hydrolysis dependent activities.<sup>[5]</sup> The activated RecA NPF initiates the SOS response to DNA damage by stimulating LexA repressor autoproteolysis<sup>[29-31]</sup> and also carries out ATP-hydrolysis driven recombinational motor



activities<sup>[32, 33]</sup> necessary for horizontal gene transfer and recombinational DNA repair, including the re-start of stalled replication forks.<sup>[34]</sup> The outcomes of RecA-mediated SOS signaling and recombination activities can both act to maintain a high fidelity genome, or serve to create advantageous mutations which enable species survival and proliferation under adverse conditions (see Figure 1.4).

### **RecA and the SOS response to DNA damage**

The bacterial SOS response is a graded response to DNA damage that initially up-regulates DNA-excision repair and recombination repair processes, then eventually promotes cell-cycle arrest and global mutagenesis if the DNA damage persists (see Figure 1.5). The LexA repressor is a dimeric protein that binds to a specific set of related sequences – the SOS box – in the promoter region of SOS genes and prevents access of RNA polymerase to their promoter.<sup>[35]</sup> Upon activation, the RecA nucleoprotein filament causes LexA to undergo autoproteolytic cleavage, a signaling-like function of RecA which is dependent on the formation of an ATP·RecA·ssDNA nucleoprotein filament but which does *not* require ATP hydrolysis.<sup>[36-38]</sup> The RecA filament can be considered a sentinel of the SOS response, as its activation and ability to interact with LexA require recognition and binding to ssDNA, a rather rare substrate occurring only when DNA damage has occurred or when DNA synthesis is interrupted and stalled replication forks are observed.<sup>[39]</sup> The cleavage of LexA sequentially de-represses up to 40 genes involved in DNA repair and mutagenic translesion DNA synthesis.<sup>[25, 31, 40-43]</sup> The order in which they are de-repressed depends upon the

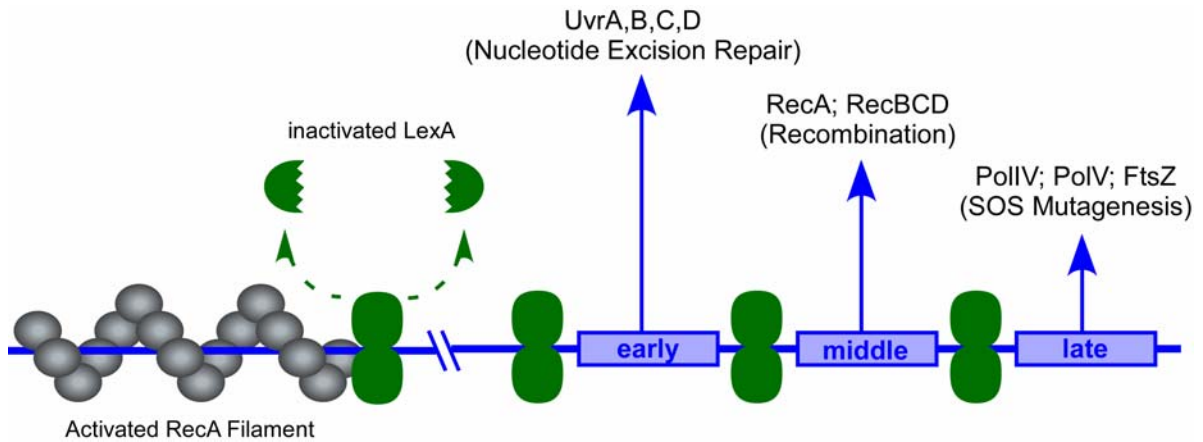


**Figure 1.5. The SOS response to DNA damage.** In the SOS response in *Escherichia coli* up to 40 early, middle and late genes are temporally expressed upon RecA-stimulated autoproteolysis of the LexA repressor. The genes expressed in the early and middle stages are instrumental to the repair of DNA damage, while the genes expressed in the late stages facilitate global mutagenesis of the bacterial genome.

sequence of their SOS box and the position and strength of their promoter, but they can generally be classified as early, middle and late SOS genes<sup>[40, 42-44]</sup> (see figure 1.5).

Initially, the products of the early SOS genes *uvrA*, *uvrB*, *uvrD* and the exonuclease *uvrC* catalyze nucleotide excision repair (NER) to fix small amounts of DNA damage without fully committing the organism to a full-fledged SOS response.<sup>[35]</sup> If the DNA damage persists after roughly 20 min, pools of LexA are further diminished and the middle phase SOS genes are heavily transcribed.<sup>[45]</sup> Notable genes involved in the middle phase of the SOS response encode the double-stranded break repair proteins RecBCD and RecA itself.<sup>[35]</sup> The proteins expressed in the middle phase are able to repair large amounts of DNA damage by exchanging strands containing thousands of bases worth of homologous DNA. The damaged DNA strand can either be paired with a sister chromatid or can be paired with homologous DNA acquired from another organism. The middle phase of the SOS response leads to a spike in the level of RecA in an organism from 8000-10,000 molecules

per cell to 70,000 per cell,<sup>[5]</sup> which translates to 1-2% of the total protein.<sup>[45]</sup> The end result is the perpetuation the SOS response at an accelerated rate.

Finally, about 40 min into the SOS response, if the aggravating DNA damage has not been tempered by nucleotide excision or recombinational DNA repair, the late genes encoding the mutagenic Y-family polymerases are expressed.<sup>[35]</sup> This includes the expression of DNA Polymerase IV (PolIV) and UmuC & UmuD which form the DNA polymerase V holoenzyme (PolV). Akin to its interaction with LexA, RecA directly controls the activity of PolV by stimulating UmuD to undergo autoproteolytic cleavage,<sup>[39]</sup> and the by-product binds UmuC in a 2:1 ratio to form DNA Polymerase V. Both PolIV and PolV lack a proof-reading function but they are useful to the bacteria for two different reasons.<sup>[16]</sup> PolV is essential in lesion bypass DNA synthesis, allowing for a gap across from the site of a lesion to be filled by any nucleotide.<sup>[46]</sup> In contrast, PolIV has poor lesion bypass activity and rather its major function likely is the production of mutations during times of metabolic stress which severely hinder growth.<sup>[47-49]</sup> Furthermore, in the late stages of the SOS response, Sula is expressed and arrests cell division by binding to FtsZ,<sup>[50]</sup> a key cytoskeletal element responsible for abutting the membrane during cell division to form two new daughter bacteria.<sup>[51]</sup> Arresting cell division is crucial to divert the bacterium's resources towards stress bypass and to allow the mutagenic Y-family polymerases supplemental time to introduce stationary phase mutations which provide bacteria with an evolutionary "escape pod" in the face of metabolic and genomic stress.

The SOS response appears to be almost universally conserved in the bacterial kingdom and is essential for the repair of spontaneous and environmentally-induced DNA damage.<sup>[19, 20, 35, 52-54]</sup> While most bacteria demonstrate a DNA damage inducible SOS

response, a small number of bacteria are known to lack this feature. Bacteria in this class seem to have evolved to colonize animals, and it is advantageous to forgo the SOS response for reasons such as their localization to internal anaerobic environments such as the intestinal tract and reproductive system which are essentially free of DNA-damaging elements such as UV light and oxygen radicals.<sup>[52]</sup> Members of this class include *Neisseriaceae*,<sup>[52, 55]</sup> *Acinetobacter calcoaceticus*,<sup>[56]</sup> *Thiobacillus ferrooxidans*,<sup>[57]</sup> and *Bacteroides fragilis*.<sup>[58]</sup> Even though these bacterial species lack a defined SOS response, RecA remains highly conserved and its recombinational activity is nonetheless still crucial to the repair of DNA damage and remains an integral component in aspects of pathogenicity and virulence. Some of these unique organisms will be more closely examined in the following section on the recombinational activity of RecA.

### **RecA and recombination**

Recombinase proteins are ubiquitous in all living organisms,<sup>[59, 60]</sup> and RecA is the archetypal member of this superfamily of enzymes. While much is now known of RecA and its contributions to the SOS response, RecA was first identified as “Recombinase A”, the most widely studied and biologically important recombinase enzyme in bacteria.<sup>[23]</sup> In general, all recombinases share a universal structural organization when activated, forming a spiraling homopolymer that coats the substrate DNA, and this entire complex is referred to as the nucleoprotein filament or presynaptic complex.<sup>[61]</sup> What makes RecA unique is that unlike its homologs, there is a requirement for a motor function powered by ATP hydrolysis for the strand exchange reaction to proceed *in vitro*. The initial pairing of homologous DNAs only requires ATP-binding, and the subsequent cooperative hydrolysis of this bound ATP by

individual RecA monomers in the filament makes the strand exchange reaction unidirectional, permits the reaction to proceed past substantial structural barriers present in the target DNAs and can involve up to four strands of DNA.<sup>[62]</sup>

RecA-mediated recombinational DNA repair (RDR) is essential for the survival of bacteria in the face of stalled or collapsed replication forks, double-stranded DNA breaks and cross-linked DNA strands.<sup>[5]</sup> It has been observed that even in conditions of ideal aerobic growth in rich media, between 10% and 50% of replication forks encounter a DNA lesion or double-stranded break.<sup>[63]</sup> Each type of aforementioned DNA damage exposes ssDNA or is processed to ssDNA by other accessory proteins. Stalled or collapsed replication forks naturally expose ssDNA<sup>[64]</sup> (see Figure 1.6A). Upon DNA cross-link damage, the UvrABC exonuclease system nicks and removes small stretches of DNA from one strand of the damaged duplex before and after the site of cross-linking, leaving a short ssDNA gap<sup>[65]</sup> (see Figure 1.6B). The RecBCD protein is activated in the presence of double-stranded breaks, and uses a combination of helicase and exo- and endonuclease activities to unwind and degrade one of the strands to expose ssDNA.<sup>[66]</sup> RecBCD utilizes “recombination hotspots” consisting of a short conserved 8-base sequence known as a *chi* site as a reference point when creating these large ssDNA gaps<sup>[67]</sup> (see Figure 1.6C). In each of these 3 cases, RecA recognizes this ssDNA as its cue to activate and hundreds to thousands of RecA monomers coat the ssDNA, forming a nucleoprotein filament. The activated RecA NPF searches out homologous DNA (usually from a sister chromatid present during replication) and facilitates a local strand invasion of the ssDNA substrate into the homologous duplex DNA, forming a Holliday-type structure<sup>[68]</sup> (Figure 1.6). Branch migration is perpetuated by the RuvA, B and C proteins and this processive activity rapidly exchanges the strands.<sup>[69]</sup> It is interesting to

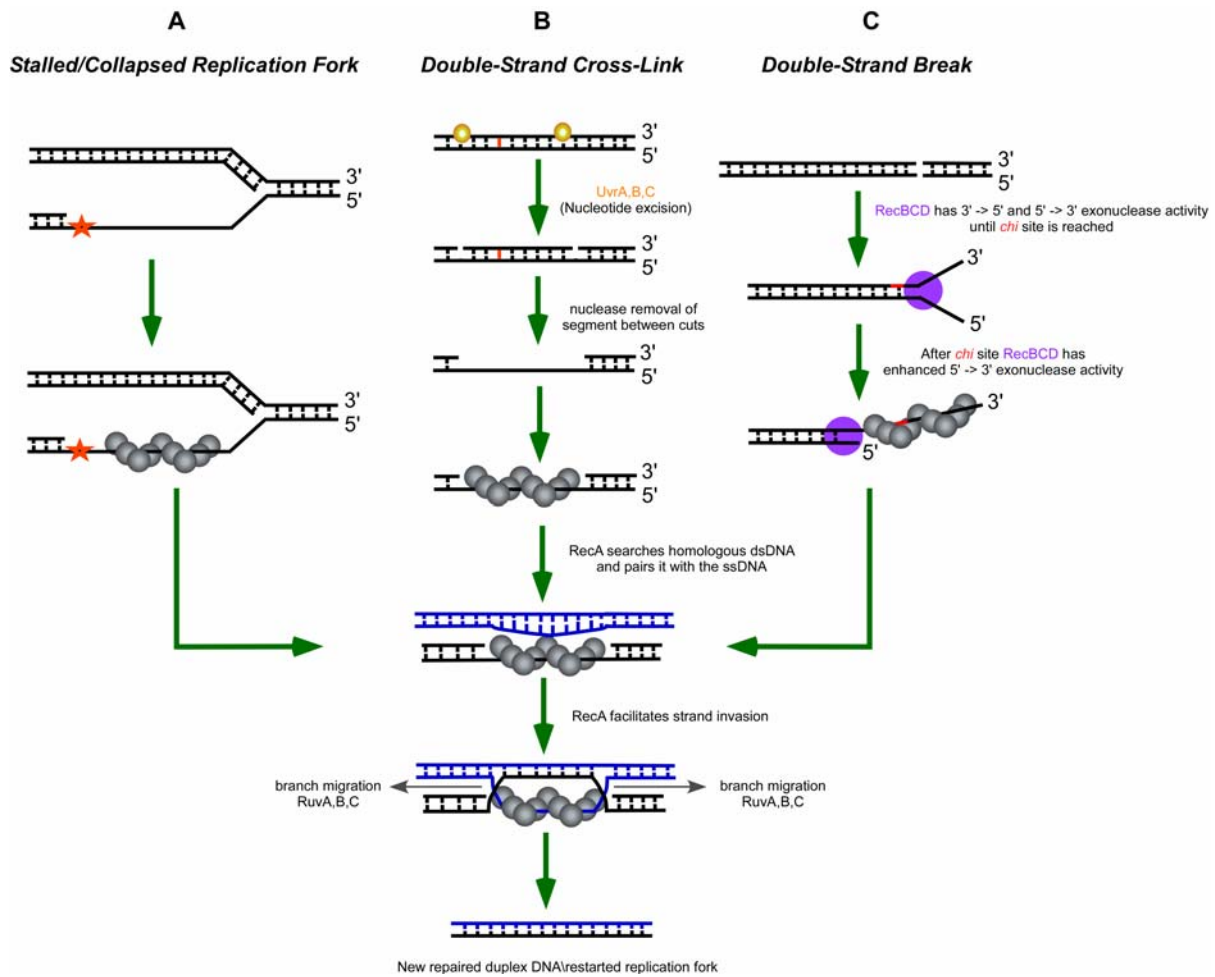


**Figure 1.6. RecA-mediated recombinational DNA repair pathways.** **A)** Once a DNA polymerase (usually PolIII) becomes stalled, RecA quickly forms a nucleoprotein filament on the exposed ssDNA. In this pathway, the newly synthesized DNA on the opposite side of the replication fork becomes the dsDNA substrate used in the recombination reaction. **B)** In double-stranded cross-link repair, the UvrABCD system nicks one strand several bases up and down of the damaged site. Nucleases remove the segment of strands between the nicks, exposing a short gap of ssDNA on which RecA forms a nucleoprotein filament. **C)** In double-stranded break repair, RecBCD finds the site of the break, and travels across the duplex with  $3' \rightarrow 5'$  and  $5' \rightarrow 3'$  exonuclease activity. Once the *chi* site is reached (shown in red), the RecBCD enzyme has enhanced  $5' \rightarrow 3'$  exonuclease activity and  $3' \rightarrow 5'$  activity is inhibited, producing a free ssDNA 3'-OH end to which RecA binds. In all cases, the activated RecA nucleoprotein filament will search out homologous duplex DNA and form a Holliday-type structure which quickly undergoes branch migration perpetuated by the RuvABC proteins. (This figure was adapted from Roca & Cox, 1997<sup>[5]</sup>).

note that RecA is capable of resolving the new DNA products in vitro in the absence of the RuvA, B and C proteins but in the presence of single-stranded DNA binding protein (SSB).<sup>[70]</sup>

While recombinational DNA repair by RecA is formally a non-mutagenic process by which bacteria resolve problems arising from DNA damage, RecA-mediated recombination can also serve to incorporate foreign or “mutant” genes originating from exogenous homologous DNA into the host genome in a process known as horizontal gene transfer.<sup>[16, 49, 71]</sup> Bacteria are capable of taking up duplex DNA from bacteria of the same or different species by the processes of conjugation, transduction and transformation and when searching out homologous dsDNA for recombination, RecA may pair ssDNA from the host bacteria with this dsDNA. The impact that horizontal gene transfer has on bacterial evolution is embodied by the fact that foreign DNA may represent up to one-fifth of a given bacterial genome.<sup>[72]</sup>

In the rare bacterial species which lack a defined SOS response, the expression of RecA is generally still DNA damage-inducible,<sup>[73]</sup> with only those few exceptions noted above.<sup>[56-58]</sup> In SOS-deficient *Neisseria gonorrhoeae* and *Neisseria meningitidis*, RecA plays an immense role in the repair of DNA damage and is essential for several processes relating to pathogenicity. Both species of *Neisseria* have been shown to be extremely transformation competent, with normal transformation frequencies of  $10^{-3}$ - $10^{-2}$ , but which can reach as high as 50% when large amounts of cloned gonococcal DNA are available.<sup>[74]</sup> Unlike other bacterial species, *Neisseriaceae* are extremely transformation competent for their entire life cycle,<sup>[75]</sup> and use the recombinational activities of RecA to incorporate this transformed DNA into their genome to enhance their ability to survive in the human body. Moreover, in their co-evolution with humans, *Neisseriaceae* have come to rely heavily on RecA-mediated recombination for surface antigen variation to enhance their ability to evade the human immune system.<sup>[55]</sup>

### **Other roles of RecA in pathogenicity**

Additionally, RecA-mediated recombination has also been shown to play a role in the colonization of host environments,<sup>[76]</sup> induction of toxin biosynthesis,<sup>[77, 78]</sup> competence,<sup>[13, 79]</sup> virulence factor production<sup>[80]</sup> and the genetic diversification of biofilms.<sup>[81]</sup> Therefore, in many diverse bacterial species, and even in those lacking a defined SOS-like system, RecA and its associated recombinase activity play an important role in survival and pathogenicity.

### **RecA and tolerance to antibiotic chemotherapy**

The ability to respond to and repair DNA damage is an essential process required by all forms of cellular life. Bacteria often colonize harsh environments and are continually subjected to DNA-damaging phenomena such as UV light, oxygen radicals and chemical agents. The SOS response is a programmed response that allows bacteria to cope with the effects of this DNA damage. RecA is the mastermind of the SOS response, using the exposed ssDNA as a template to form active RecA filaments that control the state of the LexA repressor to orchestrate a timed series of events which escalate the actions taken towards any DNA damage that threatens the organism. In the early and middle stages of the SOS response the bacterium overexpresses proteins, including RecA, involved in the repair of DNA damage. If this attempt at DNA repair is not successful, the late stage of the SOS response is initiated and the production of the mutagenic Y-family polymerases, PolIV and PolV, allows the organism to introduce mutations until it has adapted to the stressful environment, providing bacteria with a last-ditch attempt at proliferating in less than ideal conditions which promote DNA damage.



The ability of the SOS response to enhance bacterial survival in the face of environmental assaults on DNA fidelity has enormous pharmacotherapeutic implications. While many naturally occurring phenomena are capable of stimulating RecA to initiate the SOS response, it has been shown that antibiotic treatment also serves as a powerful instigator of the SOS response.<sup>[3, 11, 14-16, 19, 20, 49, 82-100]</sup> For example, ciprofloxacin is a fluoroquinolone-based inhibitor of bacterial type II DNA topoisomerases, including gyrase and topoisomerase IV, which targets a protein-DNA intermediate leading to double-stranded DNA breaks and stalled replication forks. As outlined earlier (see Figure 1.6), double-stranded breaks are processed by RecBCD to ssDNA and stalled replication forks inherently expose ssDNA. This ssDNA substrate resulting from exposure to ciprofloxacin activates RecA which in turn jump-starts the SOS response.<sup>[19, 20, 84]</sup>

While the ability of ciprofloxacin to stimulate the SOS response is obvious given its DNA-specific mechanism of action, the power of antibiotic chemotherapy to stimulate SOS activation extends to other classes of antibiotics. Currently prescribed antibiotics can be divided into at least 6 traditional classes distinguished by their cellular target (see Figure 1.7). Among these antibiotics,  $\beta$ -lactams have been shown to activate SOS expression through a two-component signaling pathway,<sup>[86]</sup> and trimethoprim starves bacteria of dTTP, creating SOS-activating disruptions of DNA synthesis.<sup>[82]</sup> Antibiotics can further be categorized into two general categories based on their mode of action<sup>[101]</sup>: (1) bactericidal antibiotics, which kill bacteria with an efficiency of >99.9%, and (2) bacteriostatic antibiotics, which inhibit growth and allow the immune system to clear the infection. Recently, the Collins group at Boston University has successfully demonstrated that all bactericidal antibiotics induce a

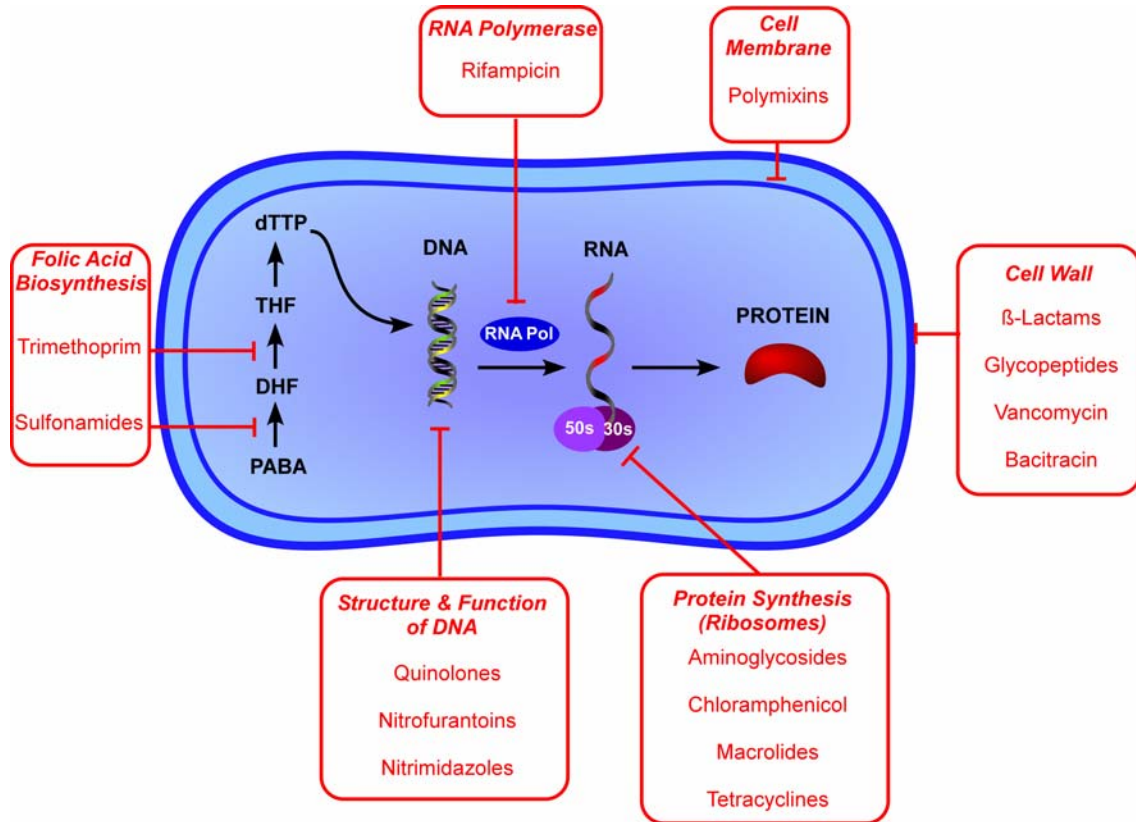


**Figure 1.7. Targets of currently prescribed antibiotics.** Antibiotics are traditionally classified into 6 groups depending on their mode of action. An inhibitor of RecA would not fit the profile of one of these current therapeutic classes, but may increase their potency and delay the onset of resistance to them.

common mechanism of cellular death whereby they stimulate the formation of lethal amounts of hydroxyl radicals via the Fenton reaction.<sup>[3]</sup> In their insightful study, Collins and coworkers found that quinolones,  $\beta$ -lactams and aminoglycosides, all bactericidal antibiotics with different cellular targets, converge downstream upon the tricarboxylic acid (TCA) cycle and induce a rapid accumulation of NADH. This overproduction of NADH hyperactivates the electron transport chain, producing superoxide as it is rapidly depleted. Superoxide then de-stabilizes iron-sulfur clusters, leeching away ferrous iron that becomes available for oxidation by the Fenton reaction, ultimately resulting in the formation of hydroxyl radicals that destroy protein, lipids and importantly, DNA (see Figure 1.8 for an overview of this pathway).

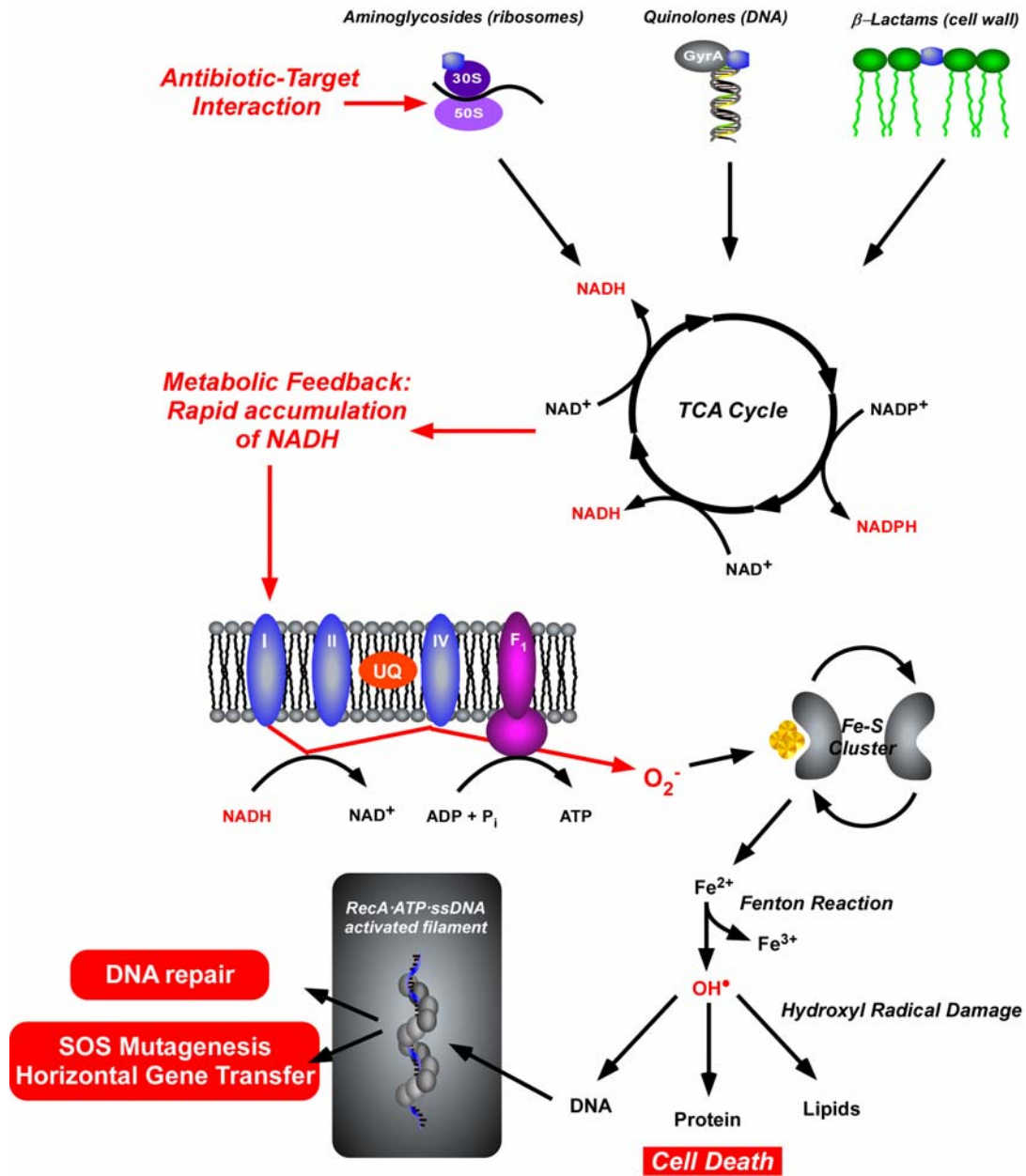


**Figure 1.8. The hydroxyl radical pathway stimulated by bactericidal antibiotics.** The primary drug-target interactions (aminoglycoside with the ribosome, quinolone with DNA gyrase, and  $\beta$ -lactam with cell wall proteins) stimulate overproduction of NADH, hyperactivating the electron transport chain and ultimately resulting in superoxide formation. Superoxide damages iron-sulfur clusters, making ferrous iron available for oxidation by the Fenton reaction. The Fenton reaction leads to hydroxyl radical formation, and these radicals damage DNA, proteins, and lipids, which results in cell death. The oxidative DNA damage activates RecA, allowing bacteria to tolerate higher doses of the antibiotic and stimulates the pathways leading to drug resistance. This figure was adapted from Kohanski et al, (2007).<sup>[3]</sup>

Additional experiments performed by the Collins group demonstrate the link between bactericidal antibiotics, oxidative radicals, the SOS response and RecA. SOS induction was

measured using a GFP reporter and found to substantially increase in the presence of quinolones and  $\beta$ -lactams, but the experiment was inconclusive for the aminoglycosides as the assay relies on expression of the reporter protein GFP, yet aminoglycosides inhibit protein expression (Figure 1.9, left). An additional experiment demonstrating the potentiation of these three classes of bactericidal antibiotics in  $\Delta recA$  *E. coli* further clarified this issue. In each case, the  $\Delta recA$  *E. coli* were 100- to 1000-fold more sensitive to bactericidal antibiotics, highlighting the importance of RecA and a DNA-damage inducible repair system for mitigating the effects of bactericidal antibiotics (Figure 1.9, right). Irregardless of the mechanism of action by which antibiotics induce the SOS response, the end result is the same: an increased tolerance to antibiotic treatment by enhancing the repair of DNA damage that ultimately accumulates from metabolic and oxidative stress.

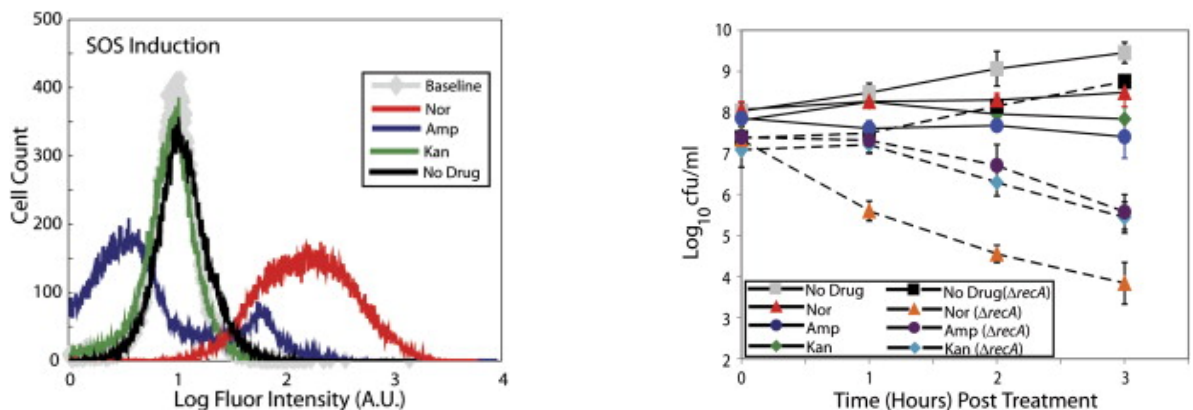


**Figure 1.9. The importance of the SOS response and RecA for mitigating the effects of bactericidal antibiotics.** *Left panel:* Activation of the SOS response was measured by RecA/LexA-controlled GFP expression in the presence of norfloxacin (Nor), ampicillin (Amp) and kanamycin (Kan). The quinolone norfloxacin and the  $\beta$ -lactam ampicillin activated SOS, but this was not detected for the aminoglycoside kanamycin due to its effect on protein expression. *Right panel:*  $\Delta recA$  *E. coli* are 100- to 1000-fold more sensitive to the same three bactericidal antibiotics examined for SOS activation in the left panel. This figure is reproduced from Kohanski et al, (2007).<sup>[3]</sup>

## **RecA and resistance to antibiotic chemotherapy**

Stress-induced mutation, encompassing both error-prone DNA synthesis and recombination, is much more efficient at producing antibiotic resistance genes than if the organism were to rely on spontaneous mutation.<sup>[102]</sup> While RecA-mediated processes initially serve to repair DNA damage arising in the course of antibiotic chemotherapy, these same processes eventually promote a hypermutable phenotype that facilitates the de novo development and transmission of antibiotic resistance genes.

In the late stages of the DNA-damage inducible SOS response, the low-fidelity Y-family DNA polymerases are expressed and create resistance-conferring mutations. The mutagenic action of these polymerases may only create mutations sufficient to bestow resistance in a small fraction of the bacterial population, but this small subset of the population proliferates exponentially until the entire bacterial population is composed of resistant bacteria.

Bacteria may also follow a different route towards becoming drug-resistant, acquiring resistance genes from exogenous DNA taken up through one of the extensively characterized processes of conjugation, transformation and transduction in a phenomenon known as horizontal gene transfer. The first evidence of horizontal gene transfer facilitating the dissemination of antibiotic resistance came from an experiment by Hotchkiss,<sup>[103]</sup> in which he demonstrated that DNA from heat-killed penicillin-resistant *Streptococcus pneumoniae* cultures was capable of conferring a penicillin-resistant phenotype on cultures of *Streptococcus pneumoniae* which previously displayed no resistance to the antibiotic. Resistance genes may either be expressed from conjugative plasmids<sup>[104]</sup> or may be integrated into the host genome by the recombinational activity of RecA.<sup>[15, 105]</sup> Additionally,

in *Streptococcus pneumoniae*, RecA has been shown to be instrumental in stimulating the production of competence factors when the bacteria are under antibiotic-induced stress.<sup>[13]</sup> These competence factors greatly enhance the up-take of exogenous DNA, which is eventually integrated into the chromosome by RecA-mediated recombination.<sup>[13]</sup> Recent findings have also provided concrete evidence that in *Bacillus subtilis*, RecA is part of a complex of 6 proteins which enhance transformation competence.<sup>[106]</sup> This group of soluble and membrane-bound proteins co-localize into large complexes at the cell poles<sup>[106]</sup> and mediate the binding and uptake of foreign DNA, protecting it from cellular nucleases and stimulating its recombinational integration into the recipient chromosome.<sup>[79, 106]</sup> See Figure 1.10 for an overview of this process.

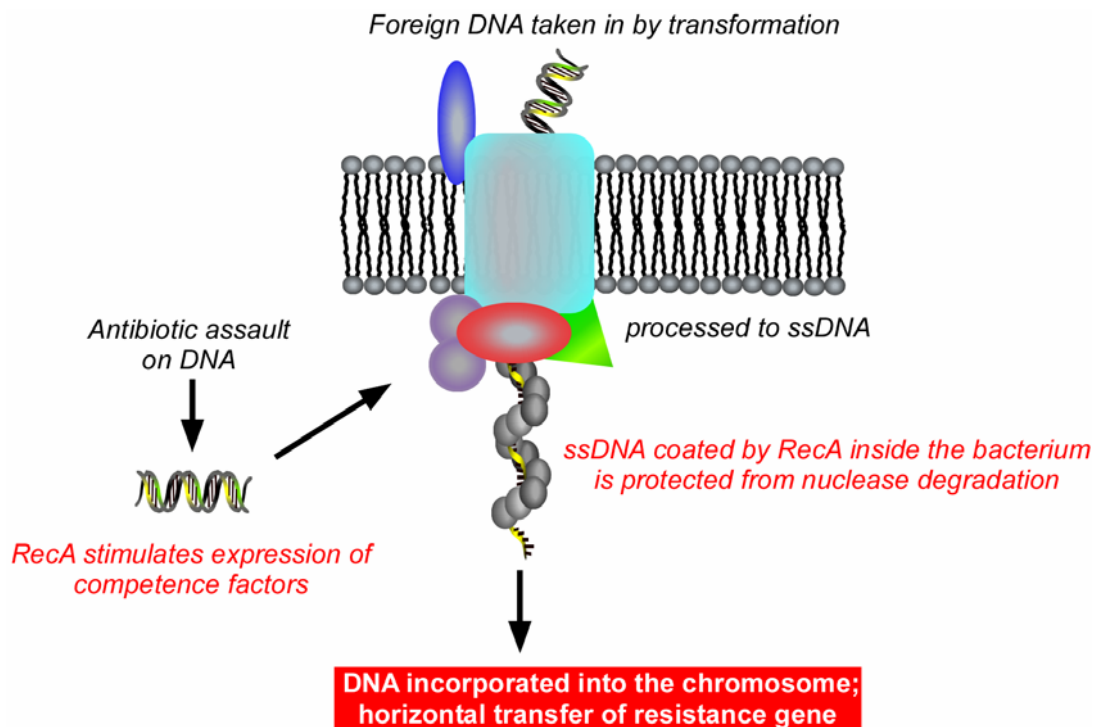


**Figure 1.10. Antibiotic treatment induces RecA-mediated competence and recombination.** Antibiotic-induced stress activates RecA, and as a result competence genes are expressed. This gives rise to the enhanced transformability of the bacteria, culminating in the uptake of exogenous DNA which is processed to ssDNA. RecA meets the ssDNA inside the cell, coating it and integrating it into the genome via recombination. The consequences of these processes are ultimately genetic diversification; thus, antibiotics have the potential to drive the acquisition resistance to themselves by stimulating natural transformation and recombination through the activation of RecA.

## RecA and the overall antibiotic response

In summary, antibiotics are capable of activating RecA by directly causing DNA damage or by virtue of their downstream metabolic effects, including the induction of a common pathway which leads to the production of DNA-damaging hydroxyl radicals. Once activated, RecA controls the balance of ostensibly antagonistic pathways which attempt to restore normal function by repairing DNA damage or which are programmed to hypermutate genomic DNA and accelerate adaptive evolution in response to stress. This suggests that RecA, whose expression ultimately leads to antibiotic tolerance and resistance (see overview

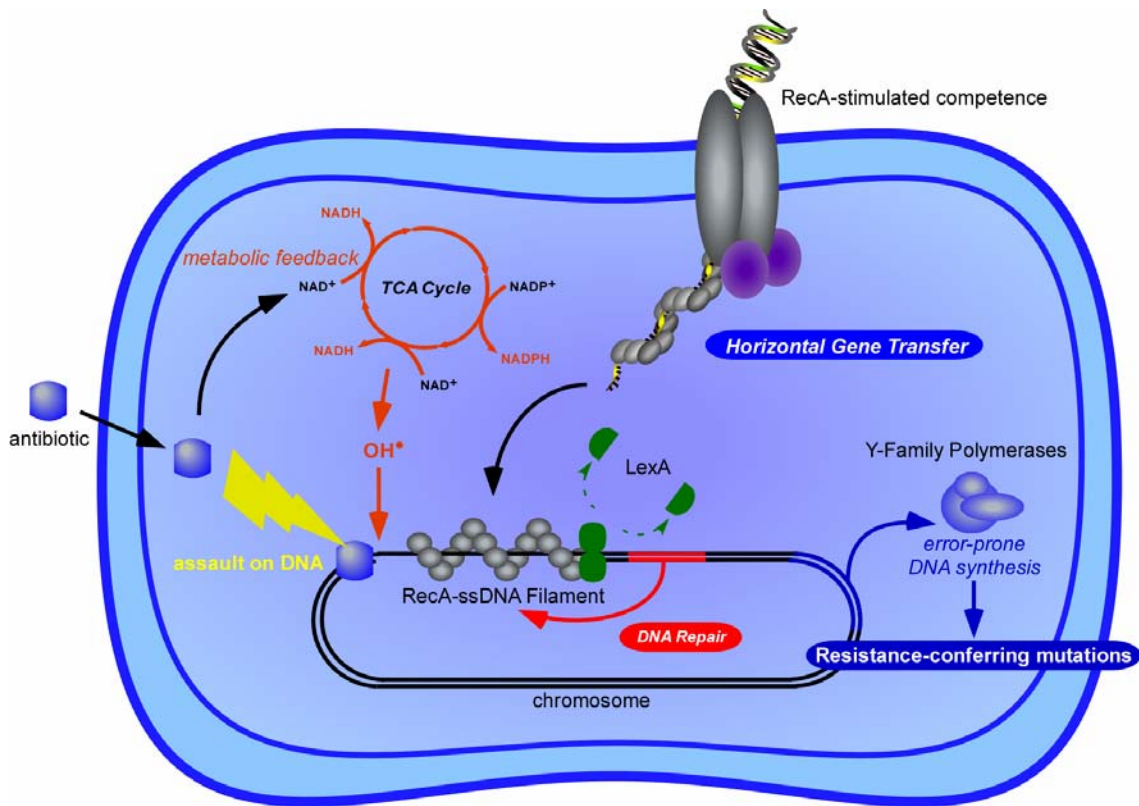


**Figure 1.11. RecA and the antibiotic response.** Antibiotic treatment can activate RecA by directly assaulting DNA or activates metabolic feedback pathways whose downstream effects lead to DNA damage. RecA is activated to repair DNA and protect the genome, or to promote diversification of the genome to escape antibiotic-induced stress. The repair pathways enhance tolerance to bactericidal antibiotics, while the mutational pathways may lead to a drug-resistant phenotype. Inhibiting RecA could potentiate the effectiveness of known antibiotics and prevent the evolution and transmission of resistance genes.

in Figure 1.11), and which has also been shown to enhance aspects of pathogenicity, may be a novel druggable target in the war on infectious bacteria. An inhibitor of RecA would not fall into any of the established classes of antibiotics and may have several outcomes as described in the next sections.

### **The necessity of RecA**

RecA has been shown to be required for the steady proliferation of bacterial populations, especially for its role in replication fork re-start and DNA repair.<sup>[63]</sup> RecA<sup>-</sup> bacteria can be grown *ex vivo* in a laboratory setting using rich media, but the absence of the *recA* gene significantly impacts the rate of DNA replication and cell division leading to an overall reduction in bacterial viability.<sup>[107-110]</sup> More relevant to the purpose of our research is the fact that to this day no RecA<sup>-</sup> bacteria have been successfully isolated from naturally occurring sources, and *recA* has been identified as belonging to a minimal set of genes required for cellular life.<sup>[111, 112]</sup> Taken together, this indicates that in the wild RecA<sup>-</sup> bacteria are not competitive with their counterparts having a functional *recA* gene.

### **RecA as a novel target for the chemotherapy of bacterial infectious diseases**

Antibiotic resistance is a “catch-22” problem in the chemotherapy of bacterial infectious diseases<sup>[113-115]</sup> and creates a health-care dilemma: from an industry perspective the profitability of developing new antibacterial chemotherapeutics is undermined by the short time frame in which drug resistant bacterial populations arise.<sup>[116]</sup> Genes endowing drug resistance are either created by the increased rates of genetic mutation during the late stages of stress induced DNA repair,<sup>[14, 117-119]</sup> effectively accelerating the rate at which evolution



occurs, or they are acquired via the uptake and incorporation of resistance genes into the genome.<sup>[15, 120]</sup> Novel strategies are required to counter these phenomena and in this context the bacterial RecA protein has emerged as an intriguing target for the small molecule suppression of antibiotic tolerance and resistance.

The ability to selectively control the activities of RecA would permit the dissection of bacterial DNA repair pathways and would expose their contributions to stress-induced mutagenesis and adaptive mutation. A small molecule inhibitor of RecA would therefore enable a greater understanding of the role of RecA in the bacterial stress response. While it may be possible to target other components of these pathways, such as LexA or the Y-family polymerases, small molecule control of RecA may prove to be even more effective as RecA controls LexA and PolV in a switch-like manner and RecA actively participates in DNA repair and horizontal gene transfer by virtue of its recombinational activities. We have hypothesized that targeting RecA for antibiotic chemotherapy will ultimately prevent the induction of the SOS response, impacting both DNA repair and stress-induced mutagenesis pathways which are activated as a result of exposure a wide array of antibiotics. In a pharmacotherapeutic context, we propose that RecA may be a novel druggable target in the war on bacterial infectious diseases and we expect that an inhibitor of RecA activities may lead to one or more of the following outcomes (see Figure 1.12):

**(1)** *An inhibitor of RecA may serve as an adjuvant to bactericidal antibiotic chemotherapy by potentiating the toxicity of the primary antibiotic.* The RecA-controlled SOS response is stimulated by bactericidal antibiotic exposure and up-regulates DNA repair processes, including RecA-mediated recombinational DNA repair, to overcome substantial barriers to

growth and enhance drug tolerance. It has been shown that RecA<sup>-</sup> bacteria are susceptible to much lower doses of a wide variety of antibiotics than are their wild-type counterparts.<sup>[3]</sup> A small molecule inhibitor would synergistically enhance the killing effect of currently therapeutically useful antibiotics, (e.g. creating “Super-Cipro”) and the use of lower effective doses of antibacterials may allow the re-examination of the potential applications of antibiotics deemed too cytotoxic for use in humans.

**(2)** *An inhibitor of RecA serve as an adjuvant to traditional antibiotic chemotherapy by reducing the rate at which resistance genes emerge or are transferred.* RecA<sup>-</sup> bacteria have been shown to have a reduced or non-existent capacity for developing drug resistance (Singleton, unpublished results). RecA stimulates the induction of the SOS response, promoting global mutagenesis of a bacterial genome to create resistant proteins and RecA also participates in horizontal gene transfer, a process by which resistant genes are shared among bacteria of the same and different species. Inhibition of one or both of these activities will delay or completely prevent the onset of antibiotic resistance evolution and transmission.

**(3)** *An inhibitor of RecA could be a standalone antibiotic.* The inability of RecA<sup>-</sup> bacteria to compete with their wild-type counterparts<sup>[111, 112]</sup> in a natural setting suggests that environmental stress in a bacteria having a chemical knockout of RecA would lead to persistent stalled replication forks and oxidative DNA damage would naturally accumulate to debilitating levels, arresting proliferation. The bacteria would be in a weakened state and would be more easily cleared by the host’s immune system.

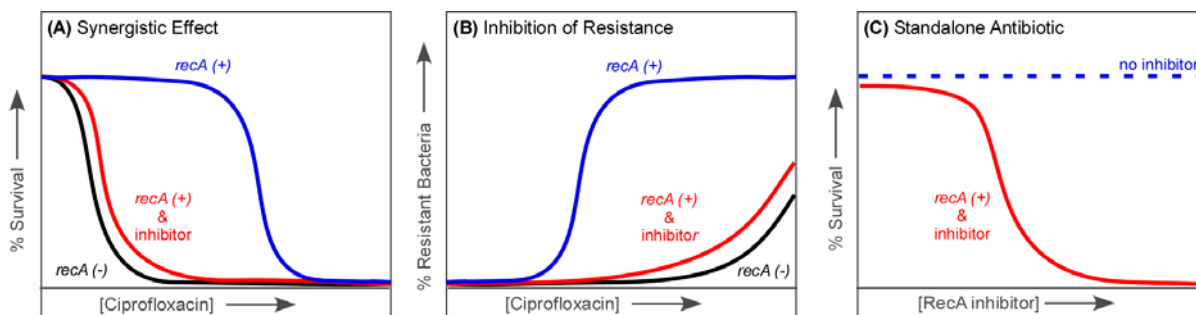


**Figure 1.12: Three possible therapeutic outcomes of RecA inhibitor treatment.** (A) An inhibitor of RecA could act synergistically with a frontline antibiotic such as Ciprofloxacin to increase its potency. (B) An inhibitor of RecA could delay the occurrence of antibiotic resistance to a frontline antibiotic such as ciprofloxacin. (C) An inhibitor of RecA could act as a standalone antibiotic by leaving the bacteria vulnerable to naturally occurring DNA damage.

When developing an inhibitor of any protein, especially in the context of pharmaceutical research, the obvious desire is to create a chemotherapeutic agent that is selective for one target only. Off-target effects greatly increase the potential toxicity of a particular chemical agent and convolute the interpretation of the phenotype resulting from exposure to the agent. An inhibitor of RecA with potential therapeutic applications must not interfere with homologous eukaryotic DNA repair machinery. All eukaryotic cells do possess RecA orthologs, chiefly Rad51 and its paralogs. The nature of the relationship between RecA and Rad51 is mostly functional, as evolution has rendered these proteins structurally and biochemically distinct.<sup>[121, 122]</sup> They share only one domain in common, the core ATP-binding domain, and even these domains are only modestly similar. Additionally, Rad51 does not rely on ATP hydrolysis for its main recombinational duties.<sup>[33]</sup> Across bacterial species, RecA is a very highly conserved protein, both structurally and functionally and the likelihood that an inhibitor of RecA from one bacterial species will cross-inhibit the RecA from another bacterial species is very high.

As RecA is an ATPase whose functions rely upon active nucleoprotein filament formation stimulated by the simultaneous binding of ATP and ssDNA, we envisaged two

major approaches towards targeting RecA for inhibition: (1) inhibitors that interact with the inactive conformation of RecA and prevent active nucleoprotein filament assembly, and (2) inhibitors that interact with structural features of the DNA-bound active nucleoprotein filament. Inhibitors of the former class would negate both the SOS-signaling and processive recombinational activities of RecA by preventing the assembly of the active filament altogether. Inhibitors of the latter class would potentially permit the SOS-signaling function of RecA but would prevent the ATP hydrolysis dependent motor activities that result in recombination. Such functionally selective inhibitors of the RecA-mediated stress response would permit a greater understanding of the antibiotic-induced bacterial stress response.

We have hypothesized that the activities of RecA are required to mitigate the effects of bactericidal antibiotics and enhance the development and transmission of antibiotic resistance. Furthering this hypothesis, we predict that an inhibitor of RecA would allow us to demonstrate that RecA is indeed a novel candidate for the development of a new class of pharmacotherapeutics that would synergistically enhance the lethality of antibiotic-induced DNA damage. However, to date, no natural product inhibitors of RecA have been successfully identified and with this dearth of known molecular modulators of RecA, our laboratory's research efforts are driven to meet this demand imposed by our hypothesis. Towards this end, our research group has screened and rationally developed select metal cations,<sup>[123]</sup> nucleotide analogs,<sup>[17, 124]</sup> polysulfated naphthyl compounds<sup>[21]</sup> and alpha helical peptides<sup>[125]</sup> as inhibitors of RecA. Recent findings in our laboratory also suggest that RecA is inhibited by a few scaffolds from combinatorial synthetic libraries. This dissertation will examine all of these inhibitor classes with the exception of alpha-helical peptides.

## **Our efforts to develop inhibitors of RecA**

Inspired by recent reports from Harold Kohn's laboratory on the inhibition of the rho transcription terminator by zinc and bismuth metal cations,<sup>[126-128]</sup> we explored the effects of several different metal cations free in solution and in organometallic complexes against the activity of RecA. The rationale for this investigation is rooted in the fact that rho is structurally homologous to RecA.<sup>[61]</sup> Both enzymes are nucleic acid binding molecular motors driven by the hydrolysis of ATP. Several metal cations including both zinc and bismuth were capable of inhibiting RecA and these findings are presented in Chapter 2. This work has been prepared as a manuscript that we expect to submit to the *Journal of Inorganic Biochemistry*.

As RecA depends on the binding and hydrolysis of ATP for its in vivo activities, we investigated several classes of nucleotide analogs as potential inhibitors of RecA. Nucleotide analogs were first segregated according to their ability to act as substrates for hydrolysis, and all non-substrate nucleotides were classified into 3 groups based on whether they (1) had no inhibitory effect at all, (2) inhibited RecA by stabilizing the inactive conformer of the protein, or (3) inhibited RecA by binding to the activated filament and competitively inhibiting ATP hydrolysis. The results of this study provide insights into the structural intricacies of the RecA ATP-binding site in both the active and inactive conformations of the protein and resulted in the discovery of several nucleotide analogs which were able to inhibit the in vitro activities of RecA with low micromolar affinity. We summarize the conformationally selective binding and inhibition of RecA by nucleotide analogs in Chapter 3. We have published the NTP hydrolysis data in *Biochemistry* (2006 Apr 11;45(14):4502-13) and the inhibition data was submitted for publication to *ChemBioChem*.

In search of more “drug-like” small molecules, we went about screening libraries of both natural product and synthetic small molecules for their abilities to inhibit ATP hydrolysis by RecA. As discussed in Chapter 4, we initially focused our screening efforts on a small, directed library of molecules hypothesized to interfere with bacterial DNA repair and recombination machinery, or which were known inhibitors of related proteins. Two novel enzyme-linked fluorescent ATPase assays relying on a resorufin reporter were developed and used to screen this library. The work presented in this chapter has been peer-reviewed and published in *Bioorganic and Medicinal Chemistry Letters* (2007 Jun 15;17(12):3249-53).

While the biased library of carefully selected small molecules provided a convenient starting point for our studies, we eventually expanded our screening efforts to include thousands of small molecules from larger libraries of both synthetics and natural products. In a collaboration with the Biomanufacturing Research Institute and Technology Enterprise (BRITE Center) at North Carolina Central University, a total of 2180 compounds from the National Cancer Institute, 33,600 compounds from Biogen Idec and 28,800 compounds from Asinex were screened for their ability to inhibit RecA ATPase activity. Chapter 5 presents initial results from the screen of the National Cancer Institute and Biogen Idec compounds. The initial screening results have been prepared for submission to the *Journal of Biomolecular Screening* and an in-depth analysis of the biological activity of one class of hits will be prepared as a manuscript for submission to a high-impact journal (*TBA*).

A search for inhibitors of any protein begins with one or more assays which are capable of detecting the influence that a small molecule has on the activity of that protein, be it in an in vitro or in vivo setting. We chose to develop and optimize several in vitro assays capable of detecting the inhibition of either DNA binding or ATPase activity and applied

these assays to the libraries comprised of the molecular classes listed above to mine any potential inhibitors. An analysis of the results from both the DNA-binding and ATPase assays provided a means to deduce the potential mechanism of inhibition of a particular compound, be it by preventing filament formation or by interfering with the assembled filament. As the size and complexity of the libraries increased from metal cations to nucleotide analogs to synthetic small molecules, the in vitro assays employed in the screening process were either selected, adapted or specifically designed to deliver reproducible and accurate results in reaction volumes of as little as 30  $\mu$ L, to facilitate use with potentially optically active compounds and to avoid prohibitive screening expenses. The inhibition assays were employed mainly as single-point screens, but all were nonetheless trivially configured to rigorously examine the influence of the ligand on RecA by reporting kinetic data over a specific timecourse, or at various substrate and RecA concentrations, enabling the reporting of competitive and non-competitive inhibition constants including  $K_i$  and  $IC_{50}$  values. Once the hits were verified, they were subjected to in vivo testing using loss-of-phenotype and protein expression monitoring assays.

While all of the above inhibitor studies were performed on *E. coli* RecA, we have also undertaken the purification and characterization of RecA from other species of notoriously pathogenic bacteria using harmless *E. coli* lab strains as expression vessels. With these purified RecAs in hand, we have the capability to extrapolate the activity of a particular inhibitor of *E. coli* RecA against the RecA protein from strains of bacteria which are potentially hazardous to work with. In addition to permitting an investigation on the universality of RecA inhibitors, the in vitro study of RecA from these pathogenic bacterial

species will afford functional and evolutionary comparisons of RecA from several clades of the bacterial kingdom.

The long range goal of this project is to discover a new group of antibiotic chemotherapeutics which will prevent the de novo development and transmission of antibiotic resistance genes and which will either act as standalone antibiotics and/or increase the toxicity of currently available antibiotics against a broad spectrum of bacterial species. The projects outlined in this dissertation provide methods for detecting the inhibition of RecA and have resulted in the discovery of several classes of molecules which exert an inhibitory effect on RecA. Our RecA-focused approach towards understanding and inhibiting antibiotic tolerance and resistance has attracted the attention of several private enterprises and has emerged as an intriguing alternative antibacterial chemotherapeutic avenue for exploration.



## CHAPTER II

### BISMUTH–DITHIOL AND METAL–CATION MEDIATED INHIBITION OF RECA

In *Escherichia coli*, RecA has been shown to be necessary for the robust viability of an individual bacterium and to facilitate the stress-induced adaptation of entire bacterial populations through stimulation of the SOS response and by performing a strand exchange reaction which is the basis for homologous recombination. In a health sciences context, these RecA-mediated activities increase the tolerance of *E. coli* to antibiotic chemotherapy and are also implicated in the de novo development and horizontal transfer of antibiotic resistance genes. Due to the high conservation of RecA across bacterial species and its important roles in overcoming antibacterial chemotherapy, RecA has become an attractive target for pharmacological study. However, at the time this project began, there were no known natural product inhibitors of RecA; only native bacterial proteins, antibodies raised against RecA and a few select synthetic nucleotide analogs comprised a short list of modulators of RecA.

In search of new classes of inhibitors of RecA, we were inspired by the work of the Kohn laboratory, who had previously demonstrated that certain metal cations and metal–dithiol complexes were capable of inhibiting the *E. coli* transcription termination factor, rho. Kohn and coworkers found that  $\text{Be}^{2+}$ ,  $\text{Cd}^{2+}$ ,  $\text{Ni}^{2+}$ ,  $\text{Zn}^{2+}$  and  $\text{Bi}^{3+}$  metal cations were capable of inhibiting rho, and the inhibitory effect of these metal cations was increased when the metal was complexed with a small dithiol ligand.<sup>[126-128]</sup> The rho protein is a structural and

functional homolog of RecA,<sup>[129]</sup> self-associating into a hexamer of six identical subunits which acts as an RNA-dependent, ATP-hydrolysis driven molecular motor responsible for releasing nascent mRNA transcripts.<sup>[130]</sup> Analogous to rho, RecA is a DNA-dependent ATP-hydrolysis driven molecular motor. Unlike rho, RecA is active as a nucleoprotein filament of hundreds to thousands of monomers stoichiometrically coating DNA, but in vitro the RecA protein from several species of bacteria have been observed to adopt a hexameric structure common to other bacterial ATPases such as helicases and the F<sub>1</sub>-ATPase.<sup>[131-133]</sup> While it remains to be seen if this hexameric structural state of RecA possesses any biological activity, it provides an additional analogy between these two bacterial nucleic acid motor proteins.

On account of the similarities between between the two proteins, we explored the possibility that, like rho, RecA could be inhibited by transition metals and their organometallic complexes. Our initial work revealed that RecA is inhibited in vitro by the divalent cations Zn<sup>2+</sup>, Hg<sup>2+</sup> and Cu<sup>2+</sup>.<sup>[123]</sup> These transition metals appeared to inhibit RecA by irreversibly binding to the protein and causing the formation of RecA aggregates, thereby preventing its ability to assemble into active nucleoprotein filaments and perform ATP hydrolysis. This effect was specific to the identity of the metal, as Ca<sup>2+</sup>, Ba<sup>2+</sup>, Mn<sup>2+</sup>, Co<sup>2+</sup> and Ni<sup>2+</sup> had no adverse effect on RecA activity. We expanded upon this last investigation and employed a light-scattering assay to rapidly screen various species of metals for the aggregation of RecA. Through this process, we additionally identified Ag<sup>+</sup>, Cd<sup>2+</sup> and Bi<sup>3+</sup> as metals capable of binding to and irreversibly inactivating RecA. While the bacterial toxicities of several metals have long been known,<sup>[134-137]</sup> the inhibition of RecA by bismuth warranted further investigation for the reasons discussed below.

Bismuth is a highly insoluble and relatively non-toxic heavy metal, and bismuth (III) complexes, including bismuth–dithiols, are known to be antibacterial agents which potentially exert their effect through several mechanisms.<sup>[128, 138-141]</sup> Additionally bismuth is selectively toxic to prokaryotic cells, and the absence of acute toxic side effects in eukaryotic cells has allowed it to replace the use of lead in many commercial products such as solder, lubricants, shotgun ammunition and fishing tackle.<sup>[142]</sup> Some of the earliest reports of bismuth usage were for the treatment of gastrointestinal disorders and many stomach ulcers are now treated with bismuth derivatives, such as orally available antacids containing bismuth subsalicylate (i.e. *Pepto-Bismol*), which is known to be active against *H. pylori*.<sup>[143]</sup> Taken together with its usage as a therapeutic agent, the unusual mode of action of bismuth on RecA described below led us to study the action of bismuth as a RecA inhibitor in more depth.

The bismuth cation aggregated RecA under wholly different circumstances than any of the other inhibitory metals and appeared to selectively discriminate between different conformational states of RecA. We were intrigued by the activity of the bismuth cation against RecA, as bismuth compounds have long been known to be medically relevant compounds,<sup>[144]</sup> and particularly, bismuth–dithiol compounds have been shown to elicit potent antibacterial effects<sup>[128, 139, 145-147]</sup> while demonstrating very little toxicity in eukaryotic cells. The mode of action of bismuth agents are not entirely known, but prior studies indicate that the Bi<sup>3+</sup> cation may interfere with iron transport<sup>[140, 141]</sup> or bind thiol-containing proteins.<sup>[128]</sup> In this study, we propose adding RecA to the list of biological targets of bismuth and we suggest that organometallic bismuth complexes may be developed into novel adjuvants for antibacterial chemotherapy.

## Screening metal cations for irreversible inactivation of RecA

We have previously shown that  $\text{Zn}^{2+}$ ,  $\text{Cu}^{2+}$  and  $\text{Hg}^{2+}$  irreversibly inactivate *E. coli* RecA by inducing the formation of insoluble protein aggregates. This effect was specific to the identity of the metal as  $\text{Mg}^{2+}$ ,  $\text{Ca}^{2+}$ ,  $\text{Ba}^{2+}$ ,  $\text{Mn}^{2+}$ ,  $\text{Co}^{2+}$  and  $\text{Ni}^{2+}$  did not exert the same effect on the RecA protein.<sup>[123]</sup> In these studies, we employed a light-scattering assay<sup>[148]</sup> to monitor the level of RecA aggregation caused by the addition of the metallic salts as RecA was actively hydrolyzing ATP. While the metal cations were administered as their chloride salts, further analysis of the zinc cation indicated that the inhibitory activity of the metals could be improved with a thiol-containing organic ligand such as DTT. Expanding upon these previous studies, we utilized the light-scattering assay as a rapid screen to determine if other metal cations were able to aggregate the *E. coli* RecA protein. The metals were selected to span a range of electronic configurations, preferred coordination geometries, hard/soft Lewis Acid character and ionic size. Before its use, RecA was purified using size-

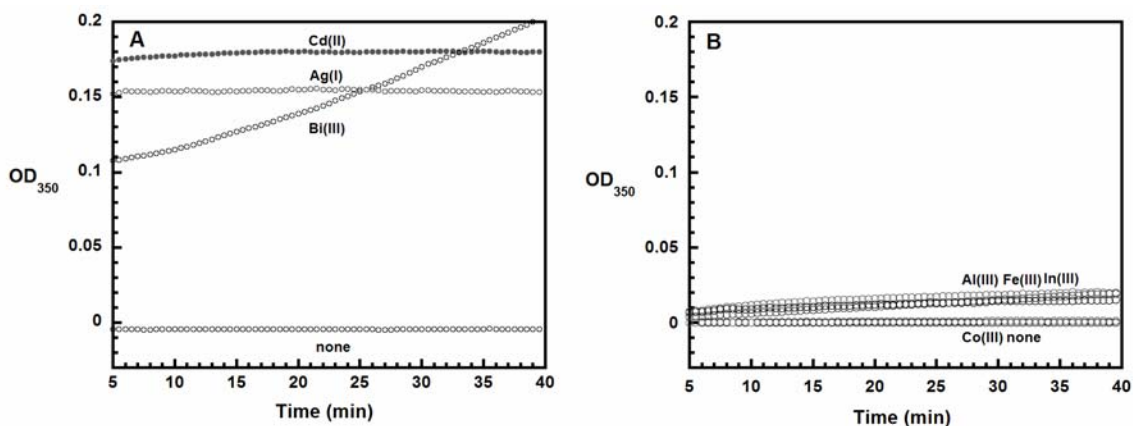


**Figure 2.1. Metal-cation induced RecA aggregation under conditions of active ATP hydrolysis. (A)** Light-scattering spectra for Cd(II), Ag(I), and Bi(III) which aggregate RecA **(B)** Light-scattering spectra for metal cations observed to have no effect on RecA solubility. Reactions were carried out in aqueous buffer tailored to the metal being assayed (see *Materials and Methods*). A stable baseline was measured for approximately 5 min, then the metal was added followed by rapid mixing of the cuvette's contents. The increase in OD<sub>350</sub> was monitored for 40 min following addition of the metal.

exclusion chromatography to remove DTT, a potential metal-chelating agent from the protein's storage buffer. Light-scattering assays performed on RecA that was actively hydrolyzing ATP using conditions as described in our previous effort<sup>[123]</sup> were performed, and we determined that AgNO<sub>3</sub>, CdCl<sub>2</sub> and Bi(NO<sub>3</sub>)<sub>3</sub> caused aggregation of RecA while Co[(NH<sub>3</sub>)<sub>6</sub>]Cl<sub>3</sub>, Al(NO<sub>3</sub>)<sub>3</sub>, FeCl<sub>2</sub>, FeCl<sub>3</sub>, CdCl<sub>2</sub>, and InCl<sub>3</sub> did not cause any aggregation (see Figure 2.1). Appropriate controls were performed to ensure that the metal cations were not precipitating by themselves and that they were causing the aggregation of RecA and not of poly(dT), ATP, Mg<sup>2+</sup> or its counterion, acetate.

The irreversible inactivation of RecA observed here and in our previous work<sup>[123]</sup> occurred under conditions where RecA was actively hydrolyzing ATP. While Ag<sup>2+</sup> and Cd<sup>2+</sup> caused a maximal level of precipitation immediately, Bi<sup>3+</sup> caused an increasing amount of precipitation over the course of 40 min. This suggested that the kinetics of irreversible inactivation of RecA by the bismuth cation was specific to a particular conformation of RecA being attained as the RecA filament was turning over ATP.

### **Investigating the dependence of ATPase cofactors for RecA aggregation**

To determine whether the inactivation of RecA by the metals assayed here and in our previous effort<sup>[123]</sup> was discriminate for the presence of RecA complexed to one or more of its substrates or cofactors, we performed the light-scattering assay using only RecA in aqueous buffer, leaving out all other components. We observed that Ag<sup>2+</sup>, Zn<sup>2+</sup>, Hg<sup>2+</sup>, Cu<sup>2+</sup> and Cd<sup>2+</sup> still induced significant aggregation of RecA alone, and only Bi<sup>3+</sup> did not precipitate RecA alone (data not shown). Therefore, we concluded that Bi<sup>3+</sup> inhibited RecA by a mechanism that differed from the other five metal species. It is interesting to note that

bismuth belongs to group VB, while the other five metals arbitrarily aggregating RecA are exclusively group IB and IIB transition metals, which can be characterized as soft Lewis Acids.<sup>[144, 149]</sup>

### **Effect of thiol ligands on RecA inhibition by the bismuth cation**

Several considerations led us to explore the effect of several thiol-containing ligands on the activity of bismuth. Bismuth–dithiols are stable complexes in aqueous environments<sup>[145]</sup> and are known to be modest antibacterials.<sup>[87]</sup> While it is hypothesized that organic thiol-containing ligands enhance the lipophilicity of bismuth to improve its antibacterial activity,<sup>[145-147, 150]</sup> thiol-containing ligands are also suspected to enhance the overall solubility and stability in aqueous environments.<sup>[145]</sup> In addition, the previous studies of our lab and that of the Kohn group demonstrate that the *in vitro* inhibition effected by the zinc cation was increased when it was complexed with DTT.<sup>[151]</sup> Kohn and coworkers have also recently demonstrated that BiBAL, bismuth (III) complexed to 2,3-dimercapto-1-propanol, a thiol-containing ligand also known as British anti-Lewisite (BAL), was a potent inhibitor of the *E. coli* transcription termination factor rho.<sup>[128]</sup> Since the ratio of Bi<sup>3+</sup> to dithiol ligand was optimized for activity against rho at 3 to 1, we used the same formulation in our studies.

We chose to examine bismuth complexed to four thiol-containing ligands including one monothiol, two 1,2-dithiols and a 1,3-dithiol (Figure 2.2, left) to determine if the inhibitory activity of bismuth against RecA is sensitive to the identity of the bismuth complex. On the day of use, fresh complexes of bismuth–thiols were made such that the ratio of the bismuth cation to thiol ligand was kept constant at 3 Bi<sup>3+</sup> to 2 thiol groups:

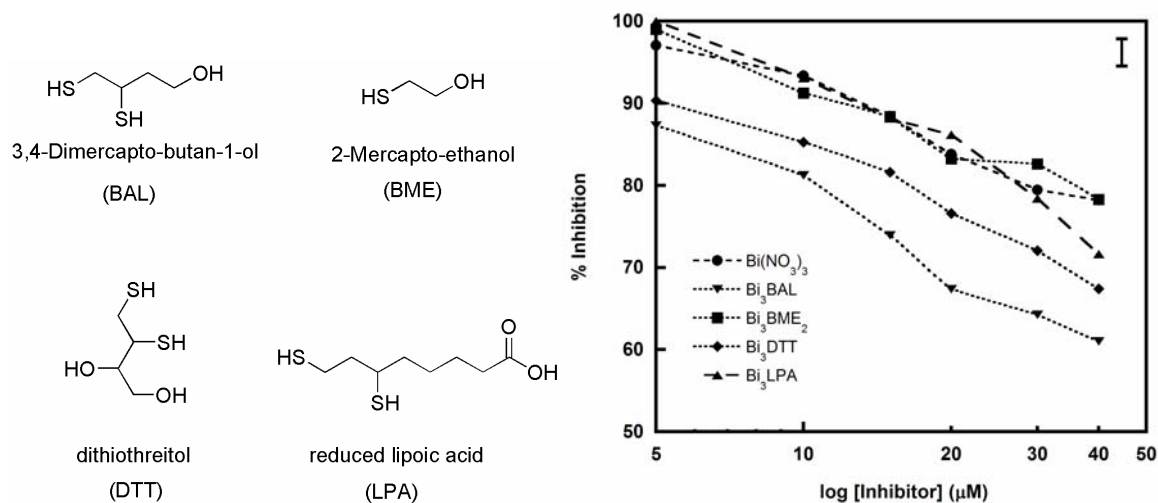


**Figure 2.2. Left Panel: Thiol ligands assayed for enhancement of ATPase inhibition by the bismuth cation.** We investigated the ability of one monothiol, two 1,2-dithiols and a 1,3-dithiol to enhance the inhibitory activity of bismuth against RecA. The ratio of bismuth to the thiol groups was kept constant at 3 Bi<sup>3+</sup> to 1 thiol for all bismuth–dithiol complexes. **Right Panel: Relative single-stranded DNA-dependent ATP hydrolysis of RecA in the presence of the ligands depicted in the left panel.** The inhibition of steady-state ATP hydrolysis by Bi(NO<sub>3</sub>)<sub>3</sub>, Bi<sub>3</sub>BME<sub>2</sub>, Bi<sub>3</sub>DTT, Bi<sub>3</sub>BAL and Bi<sub>3</sub>LPA was measured using an NADH-coupled spectrophotometric assay to detect the release of ADP. The average of three trials is plotted and the mean standard deviation is represented by the error bar in the top right corner of the plot. Control experiments (not shown) were performed to ensure that the metal complexes, 1,2-propanediol and absence of DTT did not affect the enzymatic coupling system of the assay.

Bi<sub>3</sub>BME<sub>2</sub>, Bi<sub>3</sub>BAL, Bi<sub>3</sub>DTT and Bi<sub>3</sub>LPA. When supplied with poly(dT), Mg<sup>2+</sup> and ATP, RecA forms an activated nucleoprotein filament that hydrolyzes ATP with a steady state  $k_{cat}$  of approximately 20 min<sup>-1</sup>,<sup>[124, 152, 153]</sup> thus ATPase activity serves as a reliable indicator of RecA activation. We assayed the inhibition RecA ATPase activity in the presence of 0-40 μM of the bismuth–thiol solutions indicated above, and we included the nitrate salt of bismuth for the no-ligand control (Figure 2.2, right). Again, the DTT present in the RecA storage buffer was removed using size exclusion chromatography. The assay buffer was supplemented with 10% (v/v) 1,2-propanediol to enhance the solubility and stability of the bismuth cation. Control experiments indicated that the addition of 10% (v/v) 1,2-propanediol had no effect on RecA activity. Likewise, the enzymes of the kinetic coupling system for the

spectrophotometric ATPase assay, pyruvate kinase and lactate dehydrogenase, were able to fully catalyze their respective reactions in up to 1.2 mM  $\text{Bi}^{3+}$  and were not affected by the presence of the 10% (v/v) 1,2-propanediol.

We observed a modest increase in ATPase inhibition when the bismuth cation was complexed to BAL, DTT and LPA than when it was in a complex with BME or was present as naked  $\text{Bi}^{3+}$ . From these studies it becomes apparent that  $\text{Bi}^{3+}$  more effectively inhibits RecA ATPase activity when complexed to a dithiol than when it is complexed to a monothiol or no thiol at all. It has been stated that dithiols form more stable complexes with bismuth than do monothiol<sup>[154]</sup> and there is a correlation between our observations and this claim. Of the 4 thiol-containing ligands tested, the BAL ligand potentiated the inhibitory effect of bismuth on RecA to the greatest extent. We conclude that  $\text{Bi}_3\text{BAL}$ , which has already been identified as a potent inhibitor the *E. coli* nucleic acid motor protein rho,<sup>[128]</sup> was also the most potent inhibitor of *E. coli* RecA.

### **Mechanism of RecA inhibition by $\text{Bi}_3\text{BAL}$**

Further insight into the mechanism by which  $\text{Bi}_3\text{BAL}$  inhibits RecA was achieved by analyzing poly(dT)-dependent RecA ATPase assay kinetics and by examining the conditions which were able to cause significant precipitation of the RecA protein. To evaluate whether the mechanism of inhibition of RecA by  $\text{Bi}_3\text{BAL}$  was competitive in nature, we separately titrated  $\text{Bi}_3\text{BAL}$  with the two substrates of RecA, ssDNA and ATP, in ATPase assays. As described earlier, the assay buffer was supplemented with 10% (v/v) 1,2-propanediol to enhance bismuth stability and DTT was removed from the RecA storage buffer.  $\text{Bi}_3\text{BAL}$  was titrated from 0-20  $\mu\text{M}$  and ATP and poly(dT) were individually titrated from 0-1 mM



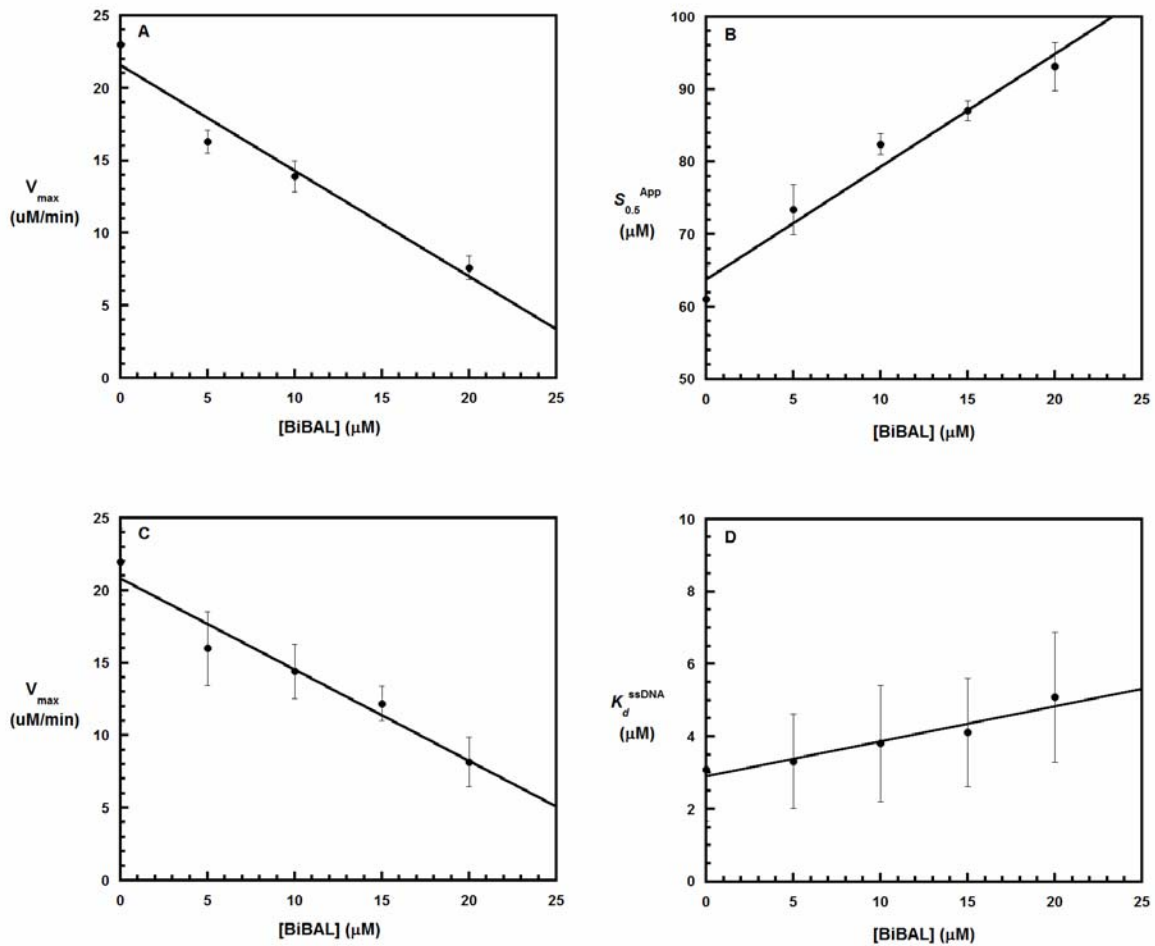


**Figure 2.3. (A & B) The affinity of RecA for ATP decreases while the maximal rate of ATP hydrolysis decreases as Bi<sub>3</sub>BAL concentration is increased.** ATP hydrolysis by RecA in the presence of various concentrations of Bi<sub>3</sub>BAL and ATP with the poly(dT) present at a fixed concentration. Steady-state ATP hydrolysis was measured using an NADH-coupled spectrophotometric assay to detect ADP production. **(C & D) The affinity of RecA for ssDNA decreases while the maximal rate of ATP hydrolysis decreases as Bi<sub>3</sub>BAL concentration is increased.** ATPase assays were performed in identical fashion as in (A) & (B), except that the ATP concentration was fixed and poly(dT) was titrated from 0-15 μM nts. Assays were performed in triplicate and averages are plotted with the error bars representing the standard deviation of three experiments.

and 0-15 μM nts, respectively. In the ATPase assays where ATP was titrated, as the Bi<sub>3</sub>BAL concentration was increased, the  $S_{0.5}^{ATP}$  was seen to increase in linear fashion while the  $V_{max}$  was seen to decrease linearly (Figures 2.3A and 2.3B). Conversely, in the ATPase assays where poly(dT) was titrated, the  $K_d^{ssDNA}$  was seen to increase linearly as Bi<sub>3</sub>BAL concentration was increased, but again, there was a linear inverse relationship between  $V_{max}$

and Bi<sub>3</sub>BAL concentration (Figures 2.3C and 2.3D). The modulation of  $V_{\max}$ ,  $S_{0.5}^{\text{ATP}}$  and  $K_d^{\text{ssDNA}}$  by Bi<sub>3</sub>BAL suggest that it is neither competitive with ATP or ssDNA binding and this is an agreement with the mechanism of action of a non-competitive irreversible enzyme inactivator.

### **Conformationally selective inhibition of RecA by Bi<sub>3</sub>BAL**

Under the conditions of the light-scattering assay in Fig. 1, when Bi<sub>3</sub>BAL > 50  $\mu\text{M}$ , visible precipitation of RecA can be seen in the assay cuvette, again demonstrating that Bi<sub>3</sub>BAL is an irreversible inactivator of RecA that causes the protein to form insoluble aggregates. RecA undergoes conformational changes upon binding ssDNA & ATP or ADP<sup>[155]</sup> and it is possible that bismuth targets one or more of these states. Having demonstrated that RecA alone in aqueous buffer is not aggregated by Bi<sub>3</sub>BAL, we endeavoured to determine which ATPase cofactors render RecA susceptible to aggregation. If a requirement for specific cofactors for aggregation was observed, we could then extrapolate the conformer of RecA to which Bi<sub>3</sub>BAL was preferentially binding. Therefore, to probe this apparent conformationally selective inhibition, we performed light-scattering assays in the presence of all permutations of ssDNA, Mg<sup>2+</sup>, and either ADP or ATP (Figure 2.4). In the assays Bi<sub>3</sub>BAL was present at 50  $\mu\text{M}$ , the threshold concentration at which visible precipitation of RecA is observed to be caused.

We observed that RecA was vulnerable to aggregation by Bi<sub>3</sub>BAL when ADP and Mg<sup>2+</sup> were present, irrespective of the presence of ssDNA. This is evident by the high level of aggregation of RecA observed immediately upon mixing with ADP, Mg<sup>2+</sup> and Bi<sub>3</sub>BAL in the presence or absence of ssDNA (Figure 2.4). Under these circumstances, the aggregation

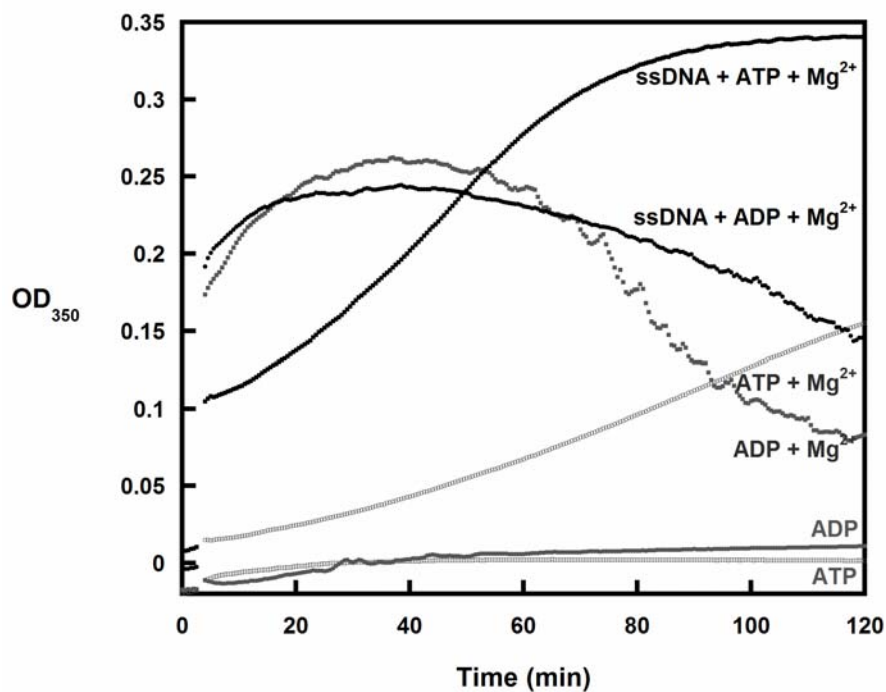


**Figure 2.4. Mechanistic exploration of inactivation of RecA by Bi<sub>3</sub>BAL using a light-scattering assay to measure protein aggregation.** RecA was incubated with the indicated components. All reactions were monitored for 5 min to ensure a stable baseline, and the aggregation assays were initiated by adding 50 μM Bi<sub>3</sub>BAL and the OD<sub>350</sub> was recorded for 120 min. The light-scattering effect for the curves corresponding to RecA-Mg<sup>2+</sup>-ADP and RecA-Mg<sup>2+</sup>-ADP-ssDNA appear to decrease at around 40 min, but this is due to the precipitated RecA falling to the bottom of the cuvette and out of the light path of the spectrophotometer.

occurs rapidly and completely and although the light-scattering effect decreases at around 40 min, this is due to the aggregated RecA–bismuth precipitating from solution and out of the path of light in the spectrophotometer. In the absence of Mg<sup>2+</sup>, RecA and ADP alone are not sufficient to cause precipitation by Bi<sub>3</sub>BAL.

In comparison to the results with ADP, a slowly increasing amount of aggregation is also observed when RecA, ATP, Mg<sup>2+</sup> and Bi<sub>3</sub>BAL are present but when ssDNA is excluded, conditions not permitting hydrolysis of the bound ATP. These results suggest that Bi<sub>3</sub>BAL more than likely binds a nucleotide-bound conformation of RecA, but has a much higher affinity for the ADP-bound RecA (Figure 2.5).

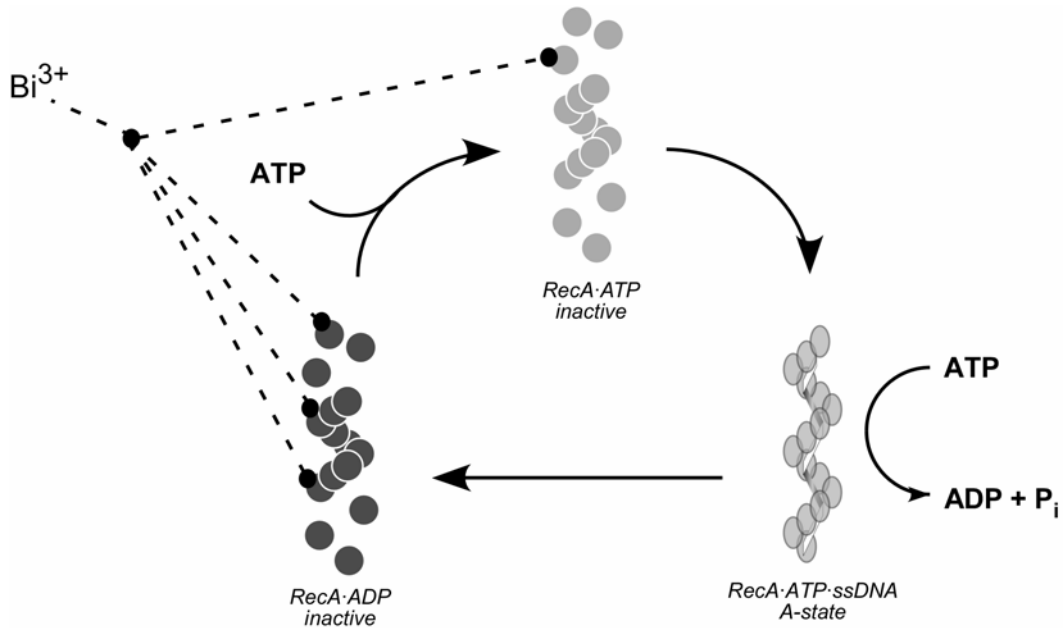


**Figure 2.5. Cartoon depicting the conformational states of RecA which are targeted by bismuth.** Bismuth has a much higher affinity for the inactive ADP-bound conformation, but can still cause aggregation of the inactive ATP-bound conformation. Bismuth is unable to target RecA that is actively hydrolyzing ATP, but readily targets the ADP-bound RecA that is the by-product of ATP hydrolysis.

When RecA is present with ATP,  $Mg^{2+}$ , ssDNA and  $Bi_3BAL$ , we observed aggregation to increase steadily as the assay progressed (Figure 2.4). These conditions promote the hydrolysis of ATP to ADP and we attribute this result to the aggregation of RecA-ADP- $Mg^{2+}$  by  $Bi_3BAL$  as this complex builds up when ADP is generated by the ATPase activity of RecA. Furthermore, based on our observation that  $Mg^{2+}$  is required to form a complex that is susceptible to aggregation, it is unlikely that  $Bi^{3+}$  is simply displacing  $Mg^{2+}$  from its native binding site on RecA.

We conclude a RecA-ADP- $Mg^{2+}$  complex must be present that for aggregation to occur, and we suspect this structure adopts a preferable conformation in which key residues are exposed and subsequently interact with the  $Bi^{3+}$  cation (Figure 2.5).

### **In vivo studies of Bi<sub>3</sub>BAL vs. RecA: using a reporter gene assay to follow SOS induction**

The in vitro activities of Bi<sub>3</sub>BAL against RecA ATPase activity led us to examine the effect of sublethal Bi<sub>3</sub>BAL doses against RecA using GY7313 *E. coli*. This species contains the *lacZ* gene encoding  $\beta$ -galactosidase regulated by the *sfiA* promoter on the chromosomal DNA, in addition to housing the *E. coli recA* gene on a plasmid. RecA activation and its subsequent stimulation of the SOS response can be monitored using a well-characterized reporter-gene assay where the *sfiA* promoter is activated in the late stages of the SOS response, leading to expression of varying levels of  $\beta$ -galactosidase. The amount of  $\beta$ -galactosidase expressed is quantified by the cleavage of *o*-nitrophenyl- $\beta$ -D-galactopyranose (ONPG), which is a colorometric substrate for  $\beta$ -galactosidase.<sup>[156-158]</sup>

The GY7313 *E. coli* were exposed to Bi<sub>3</sub>BAL and mitomycin C, a DNA-damaging agent known to induce the SOS response. We hypothesized that if Bi<sub>3</sub>BAL could inhibit RecA in vivo, then the level of apparent SOS induction by mitomycin C would be reduced in the presence of Bi<sub>3</sub>BAL. The GY7313 *E. coli* were exposed to 0-4  $\mu$ M Bi<sub>3</sub>BAL and 0.5  $\mu$ g/mL mitomycin C. Control reactions were performed using cells lacking the plasmid containing the *E. coli recA* gene and in the absence of Bi<sub>3</sub>BAL and mitomycin C such that all combinations of RecA, Bi<sub>3</sub>BAL and mitomycin C were covered and the results are displayed in Figure 2.6A.

Cells capable of expressing RecA showed the highest level of SOS induction when exposed to mitomycin C. Bi<sub>3</sub>BAL effected a modest reduction in SOS induction when given to the cells 15 min following mitomycin C treatment. The level of SOS induction decreased linearly as the concentration of Bi<sub>3</sub>BAL was increased up to 4  $\mu$ M. Control experiments with cells lacking the plasmid expressing RecA showed that in the absence of any RecA, SOS was

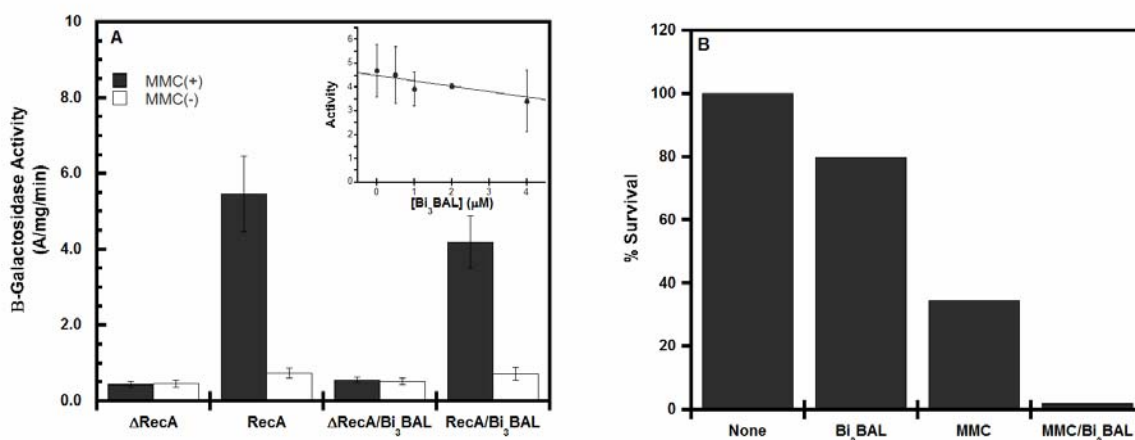


**Figure 2.6. (A) In vivo experiments exploring the effect of  $\text{Bi}_3\text{BAL}$  on SOS induction.** GY7313 *E. coli* with or without a plasmid harboring the *recA* gene were subjected to treatment with 0.5  $\mu\text{g}/\text{mL}$  mitomycin C, 2  $\mu\text{M}$   $\text{Bi}_3\text{BAL}$  or both. Induction of SOS by RecA results in expression of  $\beta$ -galactosidase is quantified by monitoring the cleavage of ONPG by the cell lysate following 2.5 h incubation with mitomycin C and  $\text{Bi}_3\text{BAL}$ . A linear relationship between increasing  $\text{Bi}_3\text{BAL}$  concentration and decreasing SOS induction is observed to occur (inset). The data plotted is the average of 3 trials and the standard error is indicated. **(B) Antibacterial synerism of  $\text{Bi}_3\text{BAL}$  and mitomycin C administration.** JM107 *E. coli* were subjected to treatment with 0.5  $\mu\text{g}/\text{mL}$  mitomycin and 2  $\mu\text{M}$   $\text{Bi}_3\text{BAL}$ , or both. Following 30 minutes of incubation with the compounds, the cells were plated onto LB-agar media and grown overnight at 37  $^\circ\text{C}$ . Colonies were counted and compared to the condition with no inhibitor to determine the % survival of the JM107 *E. coli* to determine if an antibacterial synergy could be observed between mitomycin C and  $\text{Bi}_3\text{BAL}$ .

not induced above background levels. At a concentration of 4  $\mu\text{M}$   $\text{Bi}_3\text{BAL}$  yields an approximate 25% reduction in SOS induction by mitomycin C.

While this assay provides a direct measure of the level of SOS induction caused under specified conditions, we can not confirm that this was due to the action of  $\text{Bi}_3\text{BAL}$  on RecA alone. Other members of the RecA family of ATPases and nucleic acid motor proteins may be a target of  $\text{Bi}_3\text{BAL}$ , a fact that is exemplified by its inhibition of rho activities.<sup>[128]</sup> Despite the lack of certainty about the molecular target(s), we can conclude that  $\text{Bi}_3\text{BAL}$  mitigates induction of the SOS response.

### **In vivo studies of Bi<sub>3</sub>BAL: antibacterial synergism with mitomycin C**

The SOS induction assay indicated that Bi<sub>3</sub>BAL interferes with the SOS response to DNA damage, possibly through the inactivation of RecA, which is responsible for initiating the SOS response. To determine if there is an antibacterial synergy between Bi<sub>3</sub>BAL and a DNA-damaging agent, we exposed a culture of JM107 *E. coli* cells containing the wild-type *E. coli recA* gene to 0.5 µg/mL mitomycin C and 2 µM Bi<sub>3</sub>BAL. Following 30 min of exposure to both of these agents, the viability of the cells was assayed by plating them onto LB-agar media and counting the resulting colonies after 24 h of growth. Similarly, the influence of mitomycin C and Bi<sub>3</sub>BAL on cell viability were separately measured to allow comparisons with the effect seen when both agents were present (Figure 2.6B).

Consistent with our expectation, there was an apparent antibacterial synergy between Bi<sub>3</sub>BAL and mitomycin C. 2 µM Bi<sub>3</sub>BAL alone only reduced cell viability by ~20%, and 0.5 µg/mL mitomycin C alone reduced cell viability by ~65%. When both were administered simultaneously, no colonies were visible on the LB-agar media after plating and incubation. These results indicate that Bi<sub>3</sub>BAL appears to enhance the cell death resulting from a chemical DNA-damaging agent such as mitomycin C. In conjunction with the results seen in Figure 2.6B we hypothesize that the lessened ability of GY7313 *E. coli* to survive DNA damage may be in part due to the inactivation of RecA by Bi<sub>3</sub>BAL, leading to a reduction of its effective cellular concentration, therefore reducing the level of SOS induction, a cellular response which is crucial to the repair of this damage.

## Conclusions

Our studies indicate that Bi<sub>3</sub>BAL is an inhibitor of *Escherichia coli* RecA that is neither competitive with respect to ATP or ssDNA, and that functions by irreversibly inactivating the RecA protein. Bi<sub>3</sub>BAL appears to discriminately target a RecA-nucleotide-Mg<sup>2+</sup> complex, particularly when the nucleotide is ADP. This implies that particular residues in the RecA-nucleotide-Mg<sup>2+</sup> complex targeted by bismuth are exposed in a conformation of RecA that is readily attained when the identity of the nucleotide bound is ADP. Bi<sub>3</sub>BAL also acts synergistically with the DNA damaging agent mitomycin C to prevent induction of the SOS response and inhibit bacterial growth, potentially by reducing the effective cellular concentration of RecA. These findings have identified RecA as a potential cellular target of bismuth–dithiols in addition to the *Escherichia coli* transcription termination factor rho. Bismuth–dithiols are therefore simple lead compounds for the design of new RecA inhibitors and may certainly have more than one biological target.

## Materials and Methods

### *Materials and equipment*

The *Escherichia coli* RecA protein was purified as previously described<sup>[159]</sup> to ≥ 97% homogeneity and stored in aqueous buffer [25 mM Tris·HCl (pH 7.5), 1 mM DTT and 5% glycerol] at –80 °C. The protein concentration was determined using a monomer extinction coefficient of  $2.2 \times 10^4 \text{ M}^{-1} \text{ cm}^{-1}$  at 280 nm. Bio-Spin 6 size exclusion chromatography columns were purchased from Bio-Rad (Hercules, CA). Poly(dT) (average length of 319 nucleotides) was purchased from Amersham Biosciences (Piscataway, NJ). Clear 96-well flat-bottom microplates were purchased from Evergreen Scientific (Los Angeles, CA).



JM107 *E. coli* cells were purchased from American Type Culture Collection (Manassas, VA). All other reagents were obtained from Sigma-Aldrich at the highest level of purity possible. All light-scattering assays were performed on a Perkin Elmer Lambda 20 UV/Vis spectrophotometer with a thermostatted 6-cell changer regulated by a Peltier temperature control system. RecA ATPase kinetics assays were performed on a Perkin Elmer HTS7000 Plus Bioassay Reader with a  $380 \pm 10$  nm band-pass filter (Corion).

#### *Screening metal cations for irreversible inactivation of RecA*

The precipitation of RecA was measured by recording the increase in optical density (OD) at a wavelength of 350 nm at 37 °C in a 0.4 x 1.0 cm cuvette in 600  $\mu$ L total assay volume. RecA was passed through a Bio-Spin 6 size-exclusion chromatography column prior to use to remove dithiothreitol (DTT) from the storage buffer. RecA (1  $\mu$ M) was incubated in the presence of combinations of 10 mM MgOAc<sub>2</sub>, 3 mM ATP, 3 mM ADP and 15  $\mu$ M (nts) poly(dT) so that all permutations were covered. If ATP was being added to the reaction it was added last and was not present for more than 5 min before the metal was added. Buffers for the reaction were selected such that the metal species being assayed as a precipitator of RecA was stable to precipitation itself in the reaction media. The metals were added at the following final concentrations and in the indicated buffers: AgNO<sub>3</sub> was dissolved in 25 mM HEPES (pH 7.5) with 5% (v/v) glycerol at a final concentration of 400  $\mu$ M. FeCl<sub>2</sub> was dissolved in 25 mM Bis-Tris·HOAc, 5% glycerol (pH 7.1) at a final concentration of 400  $\mu$ M. CuOAc<sub>2</sub>, CdCl<sub>2</sub>, HgCl<sub>2</sub>, ZnCl<sub>2</sub>, Co[(NH<sub>3</sub>)<sub>6</sub>Cl<sub>3</sub>], Al(NO<sub>3</sub>)<sub>3</sub>, FeCl<sub>3</sub> and InCl<sub>3</sub> were dissolved in 25 mM Tris·HOAc (pH 7.5) with 5% (v/v) glycerol at a final concentration of 400  $\mu$ M. Bi(NO<sub>3</sub>)<sub>3</sub>·5 H<sub>2</sub>O and Bi<sub>3</sub>BAL were dissolved in 25 mM

Tris·HOAc (pH 7.5) with 5% (v/v) glycerol and 10% (v/v) 1,2-propanediol at a final concentration of 150  $\mu$ M and 50  $\mu$ M respectively. A stable baseline was measured for approximately 5 minutes, then the metal was added, followed by rapid mixing of the cuvette's contents. The increase in the OD<sub>350</sub> of the solution in the cuvette was then monitored for at least 40 minutes following addition of the metal. Cuvettes were also visually inspected following the light-scattering assay to ensure the increase in OD<sub>350</sub> was due to precipitation of RecA–metal complexes and not due to absorbance properties of the metal.

#### *Preparation of bismuth–thiol solutions*

Bi<sub>3</sub>BAL was prepared fresh before use essentially as previously described.<sup>[127, 128, 139, 145]</sup> Bi(NO<sub>3</sub>)<sub>3</sub>·5 H<sub>2</sub>O (0.03 g) was dissolved in 1,2-propanediol (412  $\mu$ L) at a final concentration of 150 mM. A 50 mM solution of 2,3-dimercapto-1-propanol (BAL) was made by adding 3  $\mu$ L of BAL to 997  $\mu$ L of autoclaved deionized water. 5 mM Bi<sub>3</sub>BAL in 10% (v/v) 1,2-propanediol was made by adding 10  $\mu$ L of 150 mM Bi(NO<sub>3</sub>)<sub>3</sub> and 10  $\mu$ L of 50 mM BAL to 80  $\mu$ L of autoclaved deionized water. Upon mixing of the Bi(NO<sub>3</sub>)<sub>3</sub> and BAL, which are both colourless, a bright yellow precipitate forms and then redissolves, yielding a faint yellow solution.

Bismuth– $\beta$ -mercaptoethanol (3:2) (Bi<sub>3</sub>BME<sub>2</sub>) was prepared similarly. Bi<sub>3</sub>BME<sub>2</sub> was obtained at a concentration of 5 mM in 10% (v/v) 1,2-propanediol by mixing 10  $\mu$ L of 150 mM Bi(NO<sub>3</sub>)<sub>3</sub> with 10  $\mu$ L of 100 mM  $\beta$ -mercaptoethanol and 80  $\mu$ L of autoclaved deionized water.

Bismuth–DTT (3:1) ( $\text{Bi}_3\text{DTT}$ ) was prepared at a final concentration of 5 mM in 10% (v/v) 1,2-propanediol by mixing 10  $\mu\text{L}$  of 150 mM  $\text{Bi}(\text{NO}_3)_3$  with 10  $\mu\text{L}$  of 50 mM DTT and 80  $\mu\text{L}$  of autoclaved deionized water.

Bismuth–lipoic acid (3:1) ( $\text{Bi}_3\text{LPA}$ ) was prepared at a final concentration of 5 mM in 10% (v/v) 1,2-propanediol by mixing 10  $\mu\text{L}$  of 150 mM  $\text{Bi}(\text{NO}_3)_3$  with 10  $\mu\text{L}$  of 50 mM reduced lipoic acid and 80  $\mu\text{L}$  of autoclaved deionized water.

#### *Effect of ligands on the inhibition of RecA ATPase activity by bismuth–thiols*

The spectrophotometric ATPase kinetic measurements were carried out essentially as previously described<sup>[160, 161]</sup> at 37 °C in buffer containing 25 mM Tris·HOAc (pH 7.5), 5% (v/v) glycerol and 10% (v/v) 1,2-propanediol. DTT was removed from RecA storage buffer as described in the preceding section. Reactions (100  $\mu\text{L}$ ) were initiated in a microplate by adding ATP (3 mM) to solutions of the selected bismuth–thiol (0–40  $\mu\text{M}$ ), RecA (1  $\mu\text{M}$ ),  $\text{MgOAc}_2$  (10 mM), poly(dT) (15  $\mu\text{M}$  nts), NADH (2 mM), phosphoenolpyruvate (2.3 mM), pyruvate kinase (5 U/ml) and lactic dehydrogenase (5 U/ml). The decrease in  $A_{380}$  was measured as a function of time for 30 minutes. The  $v^\circ_{\text{obs}}$  values of steady-state ATP hydrolysis were determined using  $\Delta\varepsilon_{380} = 1210 \text{ M}^{-1}\cdot\text{cm}^{-1}$  and the % inhibition was calculated relative to the velocity in the absence of any added inhibitor.

#### *Mechanism of action of $\text{Bi}_3\text{BAL}$ vs. RecA*

The hydrolysis of ATP was measured similarly to the method described in the previous sections. DTT was removed from the RecA storage buffer as described in the preceding sections. Reactions (100  $\mu\text{L}$ ) were initiated in a microplate by adding a solution

containing RecA (1  $\mu\text{M}$ ),  $\text{MgOAc}_2$  (10  $\text{mM}$ ), NADH (2  $\text{mM}$ ), phosphoenolpyruvate (2.3  $\text{mM}$ ), pyruvate kinase (5  $\text{U/ml}$ ) and lactic dehydrogenase (5  $\text{U/ml}$ ) in 25  $\text{mM}$  Tris·HOAc (pH 7.5), 5% (v/v) glycerol and 10% (v/v) 1,2-propanediol and  $\text{Bi}_3\text{BAL}$  (0-20  $\mu\text{M}$ ). Depending on the nature of the titrant, ATP was varied from 0-960  $\mu\text{M}$  while poly(dT) was kept constant at 15  $\mu\text{M}$  nts or poly(dT) was varied from 0-15  $\mu\text{M}$  nts while the concentration of ATP was held constant at 3  $\text{mM}$ . The change in  $A_{380}$  was monitored in a microplatereader at 37  $^\circ\text{C}$  for 30 minutes. The  $v_{\text{obs}}^\circ$  values of steady-state ATP hydrolysis were determined using  $\Delta\varepsilon_{380} = 1210 \text{ M}^{-1}\cdot\text{cm}^{-1}$ . The ATP and  $\text{Bi}_3\text{BAL}$  titration was analyzed using a Michaelis-Menten equation modified for substrate cooperativity as described previously<sup>[162, 163]</sup>:

$$v_{\text{obs}}^\circ = k_{\text{cat}} \cdot R_0 \cdot \frac{[\text{ATP}]^3}{[\text{ATP}]^3 + S_{0.5}^3} \quad (1)$$

where  $R_0$  is the total concentration of RecA and  $S_{0.5}$  is the  $[\text{ATP}]$  when the velocity is half of its maximum value, much like a  $K_m^{\text{ATP}}$  value but that has been adjusted for cooperativity between individual RecA monomers. The  $V_{\text{max}}$  ( $k_{\text{cat}}$ ) and  $S_{0.5}$  were separately plotted against  $[\text{Bi}_3\text{BAL}]$  to determine the relationship between increasing  $\text{Bi}_3\text{BAL}$  concentration and these parameters describing RecA ATP hydrolysis kinetics. The poly(dT) and  $\text{Bi}_3\text{BAL}$  titration was analyzed using the following equation to determine the velocity of the reaction and the DNA binding stoichiometry value:

$$v_{\text{obs}}^\circ = \frac{V_{\text{max}}}{2} \cdot \left( R_0 + \frac{D_0}{n} + K_d - \sqrt{\left( R_0 + \frac{D_0}{n} + K_d \right)^2 - \left( 4R_0 \frac{D_0}{n} \right)} \right) \quad (2)$$

where  $V_{\text{max}}$  is the maximum velocity of the reaction,  $R_0$  is the total concentration of protein in

the reaction,  $D_0$  is the total DNA concentration in nucleotides,  $n$  is the DNA/RecA stoichiometry (nts per monomer), and  $K_d$  is the apparent dissociation constant for DNA binding (usually set to zero). The value  $n$  was too small to measure with precision in our platereader, but the  $V_{\max}$  is reliably measured in the poly(dT) titration. The  $V_{\max}$  ( $k_{\text{cat}}$ ) was plotted against  $[\text{Bi}_3\text{BAL}]$  to determine the relationship between increasing  $\text{Bi}_3\text{BAL}$  concentration and these parameters describing RecA ATP hydrolysis kinetics.

*In vivo studies of  $\text{Bi}_3\text{BAL}$  vs. RecA: using a reporter gene assay to follow SOS induction*

Assays of the ability of  $\text{Bi}_3\text{BAL}$  to inhibit SOS induction were performed essentially as previously described.<sup>[160]</sup> GY7313 cells<sup>[156]</sup> containing the *E. coli recA* gene on a plasmid derived from pTrc99A plasmid (Amersham Biosciences) were grown to saturation overnight. The saturated culture was inoculated into 5 mL of fresh LB-ampicillin media and grown to an  $\text{OD}_{600} > 0.6$ . In 12 x 75 mm tubes, the cells were diluted to  $\text{OD}_{600} = 0.3$  in 2 mL of LB in the presence or absence of 0-4  $\mu\text{M}$   $\text{Bi}_3\text{BAL}$  and 0.5  $\mu\text{g}/\text{mL}$  mitomycin C. After a 2.5 h incubation at 37 °C, 2 mL of cells was pelleted in 1.5 mL microcentrifuge tubes and resuspended in 0.5 mL of Z buffer (60 mM  $\text{Na}_2\text{HPO}_4$ , 40 mM  $\text{NaH}_2\text{PO}_4$ , 10 mM KCl, 1 mM  $\text{MgSO}_4$  and 50 mM 2-mercaptoethanol at pH 7.0). The cells were lysed by sonication (10 pulses, 75 W) and spun down at 10,000 rpm for 1 min at 4 °C to remove the membrane fraction. The clarified lysate was removed to a new 1.5 mL microcentrifuge tube and assayed for ONPG cleavage and total protein concentration.

ONPG cleavage was measured in a 96-well microplate. To each well was added 50  $\mu\text{L}$  of Z buffer, 50  $\mu\text{L}$  of clarified lysate, and 20  $\mu\text{L}$  of 4 mg/mL ONPG. Reactions were incubated at room temperature for 6 min to cleave ONPG and were quenched with 50  $\mu\text{L}$  of 1

M Na<sub>2</sub>CO<sub>3</sub>. The absorbance was recorded at 405 nm using a Perkin Elmer HTS7000+ Bioassay Reader equipped with a 405 ± 10 nm band-pass filter (Corion). Total protein concentration was determined by Bradford assay using Bio-Rad Protein Assay Reagent in a 96-well microplate format with a 595 ± 25 nm band-pass filter (Corion). The SOS induction is measured in Activity Units (A.U.) using the following equation:

$$Activity = \frac{A_{405}}{\left(\frac{x}{1000}\right) * \left(\frac{V_{ONPG}}{V_{Bradford}}\right) * T_{ONPG}} \quad (3)$$

where  $x$  is the total amount of protein (µg) present in the 1mL of clarified lysate,  $V_{ONPG}$  is the volume (µL) of clarified lysate assayed for ONPG cleavage,  $V_{Bradford}$  is the volume (µL) of clarified lysate assayed in the Bradford assay, and  $T_{ONPG}$  is the time for the ONPG cleavage reaction to develop.

*In vivo studies of Bi<sub>3</sub>BAL: antibacterial synergism with mitomycin C*

JM107 cells were grown at 37 °C overnight in LB media to saturation. Fresh 5 mL LB cultures were inoculated to an OD<sub>600</sub> = 0.05 with the overnight cultures and grown at 37 °C to an OD<sub>600</sub> = 0.6. 2 mL of cells were then added to a 12 x 75 mm tube with or without 0.5 µg/mL mitomycin C and incubated at 37 °C without shaking for 15 min. Bi<sub>3</sub>BAL was added to a final concentration of 2 µM and the cells were incubated at 37 °C without shaking for 30 min. The cells were then diluted 10<sup>5</sup> in LB and 150 µL of this dilution was spread onto an LB plate and grown overnight at 37 °C. Bacterial colonies were counted using a Syngene GeneGenius photodocumentation system with Genetools software (Frederick, MD) and compared to the condition without any inhibitor to determine % survival.

## CHAPTER III

### THE NUCLEOTIDE BINDING SPECIFICITY OF ESCHERCHIA COLI RECA:

#### A LIGAND-BASED ANALYSIS OF THE ATP-BINDING SITE

#### AND THE DESIGN OF FUNCTIONALLY SELECTIVE NUCLEOTIDE ANALOG INHIBITORS

Antibiotic resistance is an ever-increasing problem in the modern chemotherapy of bacterial infectious diseases.<sup>[113-115]</sup> Although the mechanisms that facilitate the de novo development, clonal spread and horizontal transfer of resistance factors are not fully understood, the rapid rate at which antibiotic-resistant bacteria arise is largely due to mutations introduced during stress-induced DNA repair<sup>[14, 117-119]</sup> and gene transfer between organisms.<sup>[15, 120]</sup> Recently, RecA has emerged as a crucial player in these phenomena.<sup>[15, 117-120]</sup> Moreover, RecA has long been known to influence the ability of bacteria to overcome the metabolic stress induced by a range of antibacterial agents,<sup>[3, 15, 20, 77, 80, 82, 164-176]</sup> and RecA-mediated functions are important for many aspects of bacterial pathogenicity.<sup>[13, 55, 76, 77, 80, 81, 177]</sup> Although RecA is highly conserved and likely plays similar roles in many bacteria,<sup>[22, 178]</sup> RecA-dependent processes have not been elucidated in many pathogens of interest and no small molecule natural product inhibitors of RecA have been identified

Bacteria are continuously challenged by DNA damage, and must resolve a dynamic conflict between the needs to preserve and vary their genetic information in the face of these assaults: DNA repair is essential for the maintenance of heritable genetic information while

genetic variation drives evolutionary adaptation.<sup>[119]</sup> RecA is at the center of these dichotomous pathways, detecting the influence of environmental stress on DNA replication and initiating the SOS response by stimulating LexA repressor autoproteolysis in a switch-like signaling manner.<sup>[35, 37, 38]</sup> The SOS response to DNA damage consists of a programmed gene expression profile that initially up-regulates DNA repair activities, but if DNA damage persists error-prone DNA synthesis is initiated to promote global genome-wide mutagenesis.<sup>[53, 178-181]</sup> RecA expression is also activated during the SOS response to amplify this pathway, and to perform motor-like recombinational duties which are the basis for large-scale DNA repair and horizontal gene transfer.<sup>[16, 49, 71]</sup> In essence, both the signaling and motor activities of RecA are capable of either maintaining or mutating genetic information.

In spite of the remarkably diverse set of biological activities mediated by RecA, all of the protein's known functions require the formation of an active RecA-DNA filament comprising multiple ATP-bound monomers of RecA stoichiometrically coating DNA to form a multimeric right-handed helical filament with about 6 RecA monomers and 18 DNA bases per turn.<sup>[182]</sup> A pair of active filaments (pitch  $\approx 95$  Å) with high affinity for DNA form in the presence of ATP or its unhydrolyzable isosteres (i.e. ATP $\gamma$ S). Of the active states of the RecA protein, the A-state is observed when ATP-bound RecA assembles on ssDNA, while the P-state (pairing-enhanced) is observed when RecA is complexed with multiple strands of DNA during recombination. Both forms of the active RecA filament are capable of ATP hydrolysis. An inactive collapsed filament (pitch = 75 Å) with lower affinity for ssDNA forms in the absence of ATP or in the presence of ADP.



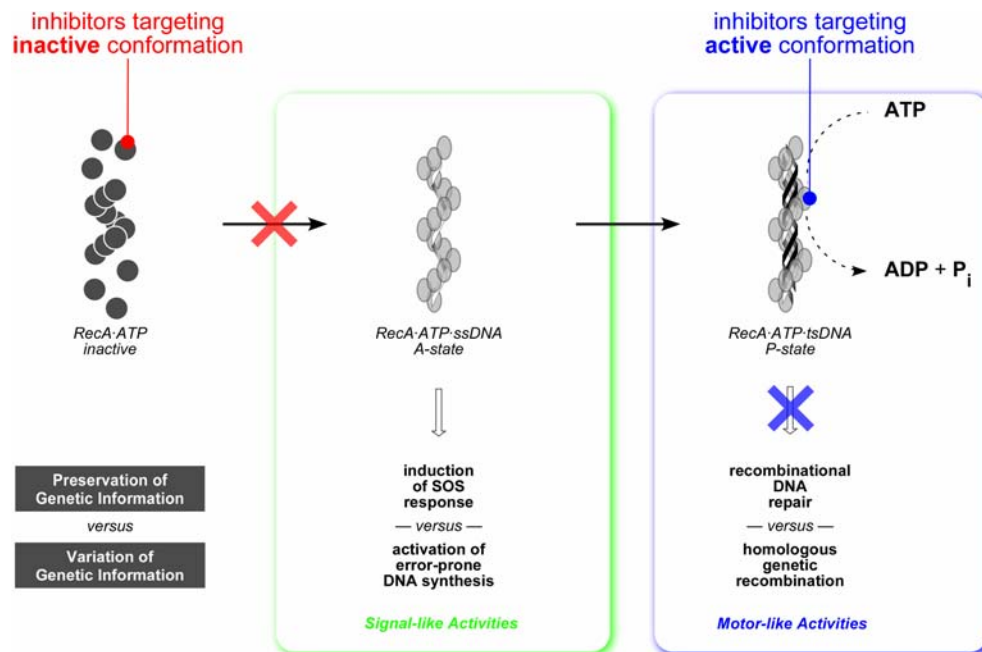


**Figure 3.1. Nucleotides can be classified based on their mode of inhibition of RecA.** The roles of RecA in both DNA repair and mutagenesis resulting in antibiotic resistance could be better understood with functionally selective inhibitors capable of separating the switch- and motor-like activities of RecA. While inhibitors of the active conformation would negate the recombinational activities of RecA dependent on ATP-hydrolysis, inhibitors targeting the inactive conformation would deny both the induction of the SOS response and the recombinational activities of RecA.

The development of ATP-competitive inhibitors represents a conceptually straightforward approach to attenuating RecA function: the conformational states of the RecA filament and their corresponding activities depend upon ATP binding and hydrolysis, therefore a structural analog of ATP can be employed to prevent access of ATP to its binding site. Towards the goal of developing potent ATP-competitive inhibitors of RecA we describe: (1) a structural overview of RecA including an in-depth analysis of the ATP-binding site, (2) a ligand-based analysis of the NTP hydrolysis substrate specificity of RecA, and (3) the analytical segregation of non-substrate nucleotides into ligands capable of inhibiting RecA by binding either the active or inactive conformations of RecA (or nucleotides which do not bind RecA at all). Our results provide insight into the design of a bioorthogonal set of functionally selective inhibitors which may be used to independently

investigate the roles of RecA-mediated SOS-signaling and recombination in the evolution and acquisition of drug resistance (see Figure 3.1).

### **Criteria for ATP-competitive inhibitor design**

The design of potent and target-selective ATP-competitive inhibitors is not a trivial exercise. Considering the myriad ATP-binding proteins known in both prokaryotic and eukaryotic proteomes, achieving selectivity is paramount: non-specific binding would result in off-target effects, convoluting the understanding of the compound's biological activity and would result in increased toxicity if said compound was intended for use as a therapeutic.

With respect to the design of ATP-competitive inhibitors of ATP-dependent enzymes such as protein kinases, the potential for selectivity can be rationalized in terms of the overall differences between the ATP-binding sites in the proteins, the conformation of the bound nucleotide and the interactions of the adenosine nucleotide and the amino acid side chains present in the ATP-binding site.<sup>[183]</sup> Therefore selectivity is dependent upon the exploitation of structural differences of the ATP-binding site, and this mantra of ATP-competitive inhibitor design is greatly enhanced by targeting a unique conformation of the ATP-dependent enzyme. While a high level of structural similarity in the ATP-binding site can be detected among the active conformers of ATP-dependent enzymes, striking structural differences emerge when their inactive conformers are compared<sup>[183]</sup> (see Figure 3.2). Therefore, ATP-competitive inhibitors designed to interact with the inactive conformer of a protein may offer more opportunities for the optimization of binding selectivity.

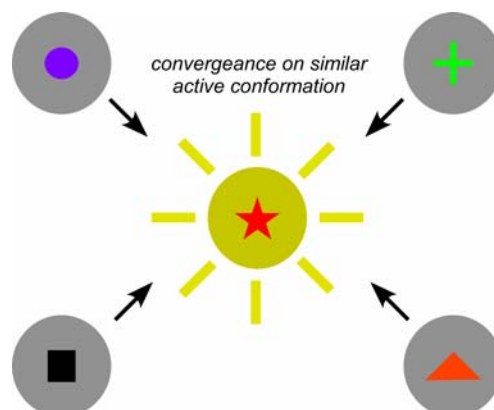


**Figure 3.2. Targeting the inactive vs. active conformations of NTP-binding proteins.** While the NTP-binding site in the active conformation more closely resemble one another, the same region can be grossly different in the proteins' inactive conformations and offer opportunity for selectivity.

Despite the limitations of homology which must be considered for designing an inhibitor binding to the active conformation targeting the ATP-binding site of the active conformation has its advantages. It can be said that the ATP-binding site of the active conformation requires conservation of 3D structure and therefore is less tolerant to mutations which may confer resistance to the inhibitor. Also, the ATP-binding site in the active conformation may still contain less conserved features such as unique residues and additional pockets which may be exploited in inhibitor design.<sup>[183]</sup> To account for both structural rationales relating to conformationally selective binding specificity, we considered features of the ATP-binding site in both the inactive and active conformers of RecA for our inhibitor design.

### **Structural analysis of the RecA ATP-binding site**

Whereas the structural features of the inactive RecA conformer have been extensively characterized, a high-resolution structure of the active conformation of RecA has not been

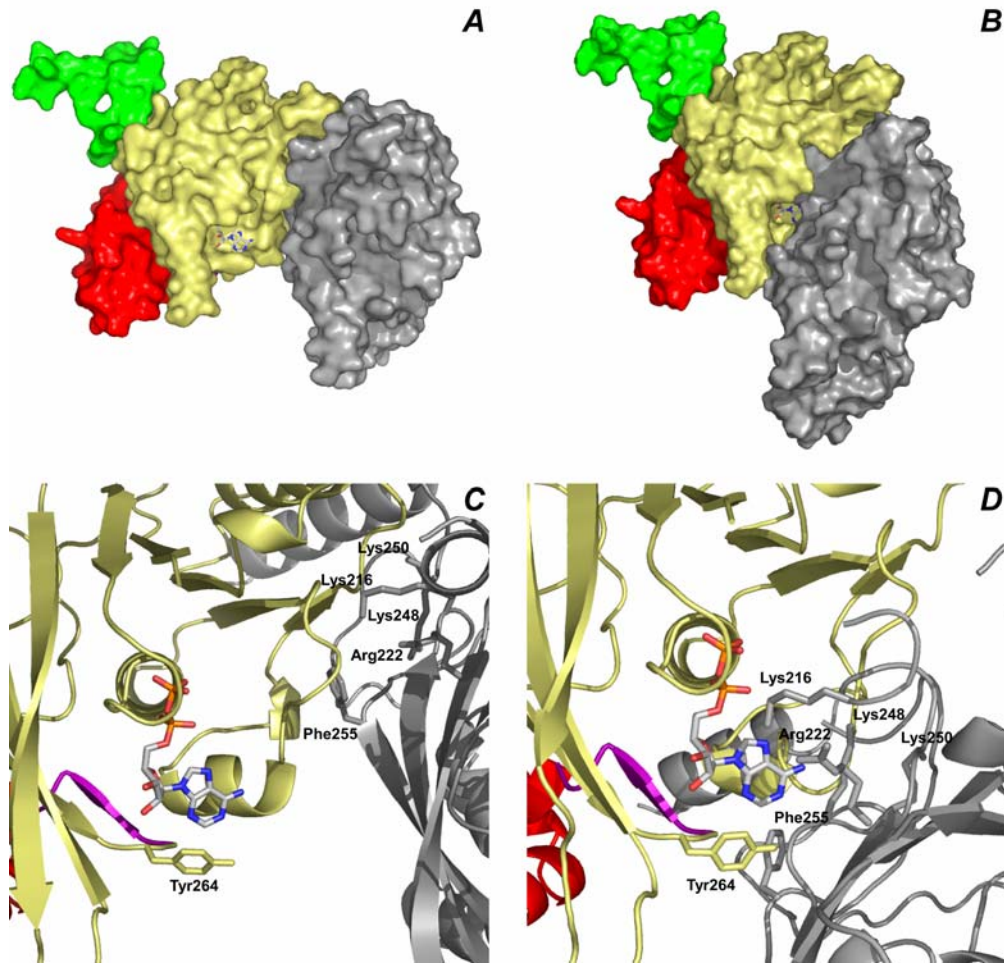


**Figure 3.3. Structural models of the RecA ATP binding site.** RecA is depicted in the inactive (panels A and C) and active (panels B and D) filament conformations with adjacent RecA monomers during filament assembly. Each panel depicts a RecA dimer wherein one subunit is colored according to its domain structure and the second monomer is gray. The domain coloring is as follows: N-terminal domain is green (residues 1-33), core/ATP-binding domain (residues 34-260) is yellow, C-terminal domain (residues 271-323) is red, and the tether between the core and C-terminal domains (residues 261-270) is magenta. **(A)** A RecA dimer from the crystal structure of the inactive filament state.<sup>[2]</sup> The proteins are rendered as their Connolly surfaces and the bound ADP molecule as a stick model. **(B)** A RecA dimer from the VanLoock et al. structural model<sup>[6]</sup> of the active filament state, rendered as in panel A. **(C)** An enhanced view of an ATP binding site from the crystal structure of the inactive filament state. The proteins are rendered as ribbon cartoons. The individual residues involved in interactions with the bound nucleotide are shown as stick models and labeled (see text for details). **(D)** An enhanced view of an ATP binding site from the VanLoock et al. structural model<sup>[6]</sup> of the active filament state, rendered as in panel C.

reported. However, the groups of Egelman and Campbell recently reported an 18-Å EM reconstruction of the extended NPF from which they developed a pseudoatomic model depicting the activated A-state of RecA.<sup>[6]</sup> A remarkable feature of the model, which has

been substantiated by analyses of the crystal structures of RecA homologs in extended filaments,<sup>[2, 155, 184]</sup> is the reorientation of RecA monomers with respect to their crystallographic locations such that the ATP-binding site is now located between adjacent monomers and comprises highly conserved residues on both monomers (Figure 3.3). Specifically, the model of the A-state RecA nucleoprotein filament describes the complete ATP-binding site as being composed of two neighboring RecA monomers, such that ATP interacts with the P-loop and several key residues of one RecA monomer (the primary site), and the adjacent RecA subunit completes the binding pocket around the adenine moiety (Figure 3.3D and Figure 3.4D).<sup>[6]</sup> Importantly, this structural model of the ATP-binding site of the A-state filament is more similar to that of other ATP-binding proteins in that the adenine moiety is fully enveloped by protein sidechains (see Figure 3.3D).

### **Comparative analysis of the RecA ATP-binding site**

As outlined above, in order to facilitate the design of nucleotide-based ATP-competitive inhibitors of RecA, a complete understanding of the protein in its inactive and active conformations is required, particularly with regards to the features of the ATP-binding site in these conformational states. To this end we comparatively analyzed the ATP-binding site of *E. coli* RecA against those of homologous ATP-binding motor proteins to identify unique structural elements which may be exploited in the design potent and selective inhibitors targeting this region of the protein.

A wealth of high-resolution structural information is available for the *E. coli* RecA protein in an inactive conformation.<sup>[5, 155, 185]</sup> We comparatively analyzed the RecA ATP-binding site with those of homologous motor proteins, such as F<sub>1</sub>-ATPase, T7 helicase, and

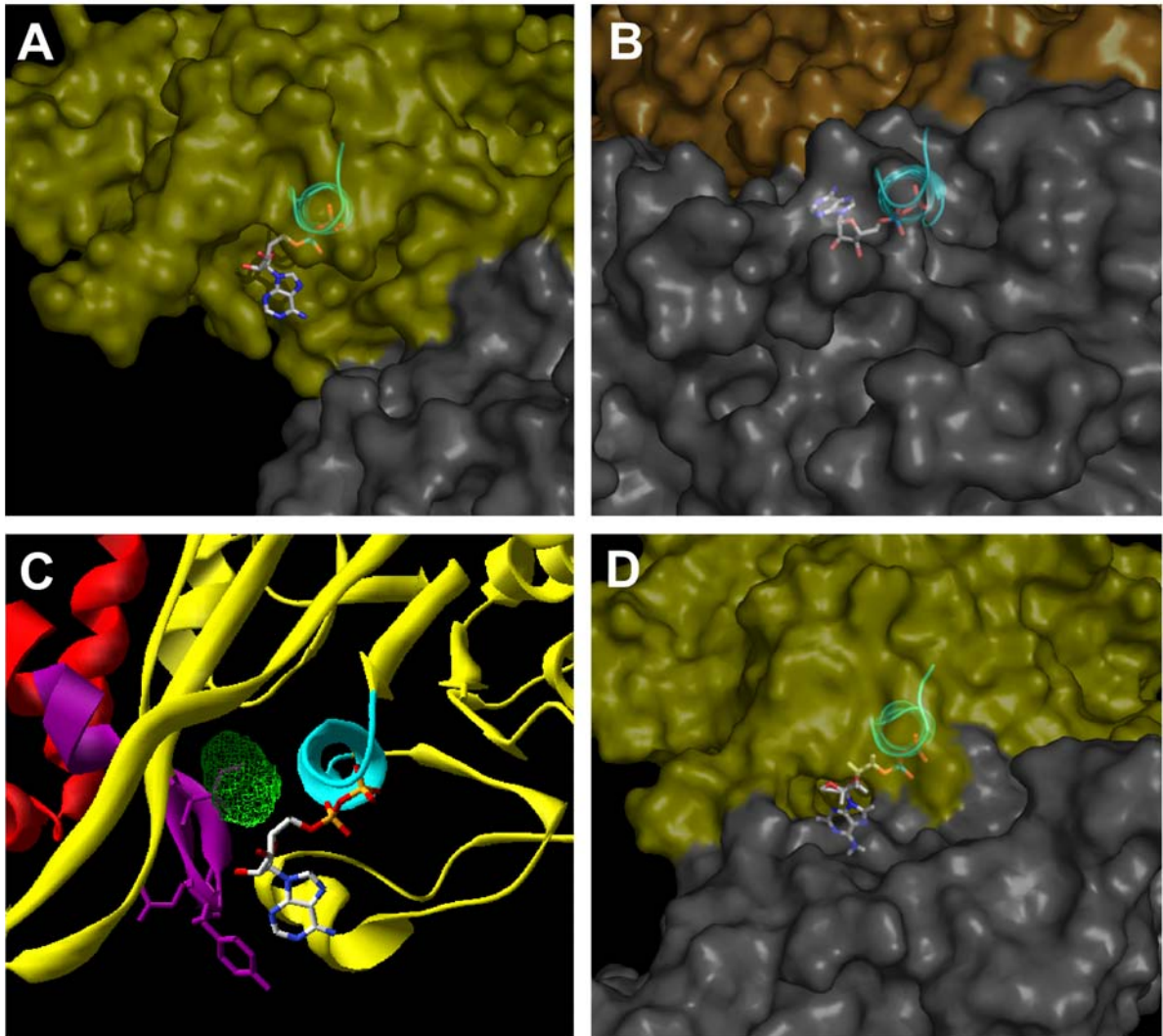


**Figure 3.4. Comparative analysis of the RecA ATP-binding site.** (A) The inactive RecA crystal structure model depicting two adjacent monomers with bound ADP exposed on the surface cavity of one monomer. (B) F<sub>1</sub>-ATPase showing two adjacent monomers. (C) A detailed view of the internal cavity near the ribose 2' and 3' hydroxyls. (D) A model of the active RecA filament showing two adjacent monomers with the bound nucleotide at the monomer-monomer interface. Note that the orientation of the bound ADP in the shallow cleft on the surface of one RecA monomer in the inactive filament (panel A) and sandwiched between two monomers in the active filament (panel D) is opposite to the relative to the orientation of the ADP buried between two monomers in the F<sub>1</sub>-ATPase (panel B). This difference in orientation of the bound nucleotide offers two cavities near N<sup>6</sup> and the 2' and 3' positions which may be exploited by introducing modifications increasing both the selectivity and affinity of a potential inhibitory ligand directed at the ATP-binding site.

the rho transcription terminator, as well as other NTPases and kinases possessing a P-loop.

The structures were aligned using the C $\alpha$  atoms of the consecutive residues in the super-secondary structural element containing the phosphate-binding loop (P-loop): specifically, the residues of the P-loop, the  $\alpha$ -helix preceding it, and the  $\beta$ -strand following the P-loop

were included. The orientation of the adenosine nucleotide relative to the P-loop that defines this super-family of enzymes could then be visualized (Figure 3.4). To facilitate comparison, the F<sub>1</sub>-ATPase, an important component of a crucial metabolic complex and a close structural homolog of RecA, is also depicted in Figure 3.4B. Importantly, the ATP-binding site of the F<sub>1</sub>-ATPase is largely representative of those of the other proteins mentioned above.

### **ADP is bound in an unusual orientation**

Steitz and coworkers reported the first observation that the relative orientation of ADP bound to protein in RecA crystals was different from those of nucleotides bound to related NTP-binding proteins.<sup>[186]</sup> We have now extended that investigation to include many structurally related enzymes. In RecA, the adenosine moiety is located in a wide, shallow, solvent-accessible cleft on the surface of the protein (Figure 3.4A) rather than having adenine buried in a hydrophobic pocket as in other ATP-binding proteins<sup>[187]</sup> (Figure 3.4B). This difference provides an important rationale for our preceding observation that the inactive conformation of RecA has a more relaxed specificity for nucleotide binding than does the activated A-state filament.

### **Internal cavity adjacent to ADP**

A second important difference between the ATP-binding site of RecA and those of related enzymes was revealed by analysis of the surfaces of the proteins and their internal cavities using Swiss-PDB Viewer. An unusual cavity was identified near the ribose 2' and 3' hydroxyl functional groups in the RecA crystal structure (Figure 3.4C). This cavity is also proximal to the protein residues Phe260, Ile262, and Tyr264. All three residues are highly

conserved<sup>[5]</sup> and mutational analysis has shown that Tyr264 is crucial for proper RecA function.<sup>[188, 189]</sup> When either Phe260 or Ile262 are replaced by alanine or glycine residues, the resulting mutant proteins have significant deficits in several in vivo RecA activities as well as in vitro DNA-dependent ATP hydrolysis (Wigle & Singleton, unpublished observations). The untolerated mutations of the amino acid residues surrounding the unique cavity suggest that it may be a functionally important feature of the RecA ATP-binding site.

### **Merging structural knowledge of RecA ATP-binding site with nucleotide analog binding data**

Based on our analysis of the RecA ATP-binding site, we were able to hypothesize that the inactive conformer RecA would have a much higher tolerance for binding nucleotides and their modified analogs than would the active conformation. To test these predictions for the purpose of further understanding how subtle differences in the active conformation and more pronounced differences in the inactive structural state affect the binding of nucleotide analogs to the ATP-binding site of RecA, we developed a stratagem for segregating nucleotides into those binding the active vs. inactive conformations. In terms of nucleotide analogs we examined for binding to RecA, there were three main classes considered. As RecA, like most ATP-binding proteins, also binds ADP strongly, we examined both NTPs and NDPs. Additionally we investigated the binding of nucleotide-like analogs bearing neither a di- or triphosphate moiety to the ATP-binding site.



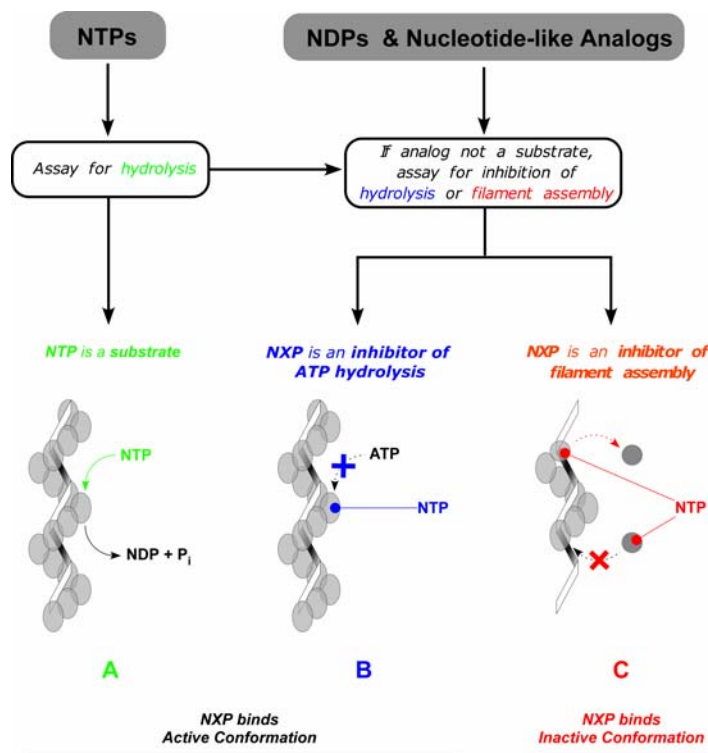


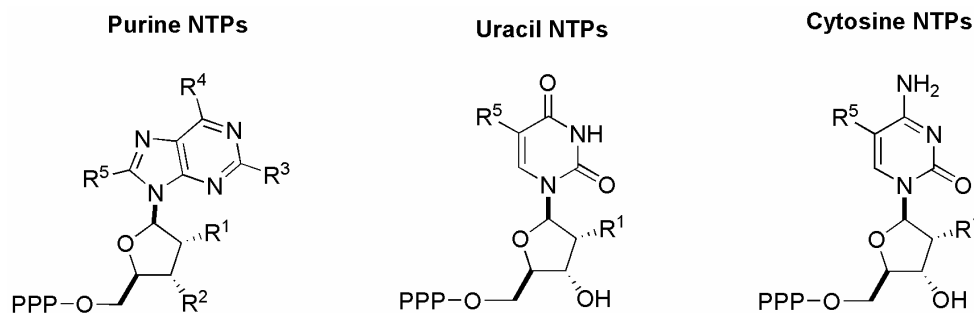
**Figure 3.5. Flowchart for analyzing the binding of nucleotide analogs to RecA.** (A) NTP are first examined for their ability to serve as substrates for hydrolysis. If an NTP was not a substrate it was grouped with NDPs and nucleotide-like analogs and assayed for inhibition of (B) ATP hydrolysis or (C) RecA-DNA filament formation.

NTPs were first screened for their potential to be hydrolyzed by RecA and the resulting hydrolysis kinetic data inferred on the ability of an NTP analog to bind and activate RecA. If an NTP was not able to activate RecA and undergo hydrolysis, it was grouped with other analogs incapable of acting as substrates, namely NDPs and nucleotide-like analogs. This group of analogs was then subjected to assays measuring the inhibition of RecA-DNA filament formation or inhibition of ATP hydrolysis and segregated into those which respectively bound to either the inactive or active conformations of RecA (see Figure 3.5). Taken together, the data collected from this screen was used to identify the structural determinants of nucleotide analogs which may serve as leads for the design of ATP-competitive inhibitors of RecA.

## Probing the substrate specificity of RecA

Our initial work explored the extent to which modification of the nucleotide base or ribose functional groups affected the ability of RecA to hydrolyze NTPs. We chose to examine 28 analogs of the eight canonical ribo- and 2'-deoxyribonucleotides that span a range of steric and electronic modifications on the purine and pyrimidine heterocycles and the 2' and 3' positions of the ribose ring (Figure 3.6).

Normally, active nucleoprotein filament formation occurs when RecA is simultaneously bound to ATP and ssDNA, and results in ATP hydrolysis. Hence, ssDNA-dependent NTP hydrolysis serves as a useful indicator that an NTP promotes active filament formation in vitro. We monitored the steady-state kinetics of the poly(dT)-dependent NTPase activity of RecA using a known enzyme-coupled continuous spectrophotometric assay for the detection of inorganic phosphate.<sup>[190]</sup> Quantitative control experiments to evaluate the potential influence of the substrates or products of the coupled reaction on the steady-state kinetic parameters for ATP turnover by RecA revealed no measurable effects on  $V_{\max}$ ,  $S_{0.5}$  for ATP, or  $K_d^{\text{app}}$  for poly(dT) binding. Further control experiments for each NTP confirmed that the hydrolysis activity was poly(dT)-dependent and that the enzyme of the coupling system, PNP, was not affected by the NTP (data not shown). For each of the 28 NTPs, the initial steady-state rates of  $P_i$  formation were plotted as a function of the total NTP concentration, and non-linear least squares curve fitting using eq. 1 yielded the rate constant for catalytic turnover,  $k_{\text{cat}}$ , and the NTP concentration required for half-maximal velocity,  $S_{0.5}$  (Table 3.1). To facilitate comparisons among the NTPs, specificity constants relative to that of ATP were also tabulated. Considering the data for the 20 NTPs that were hydrolyzed at a measurable rate, it is clear that the  $S_{0.5}$  values span a much wider range (> 40-fold) than that



Entry	Nucleoside	R <sup>1</sup>	R <sup>2</sup>	R <sup>3</sup>	R <sup>4</sup>	R <sup>5</sup>	Abbreviation
ATP Analogs							
1	araadenosine	OH <sup>a</sup>	OH	H	NH <sub>2</sub>	H	Ara-ATP
2	2'- <i>O</i> -methyladenosine	OMe	OH	H	NH <sub>2</sub>	H	2'OMe-ATP
3	3'- <i>O</i> -methyladenosine	OH	OMe	H	NH <sub>2</sub>	H	3'OMe-ATP
4	2'-aminoadenosine	NH <sub>2</sub>	OH	H	NH <sub>2</sub>	H	2'NH <sub>2</sub> -ATP
5	2'-fluoroadenosine	F	OH	H	NH <sub>2</sub>	H	2'F-ATP
6	6-chloropurineriboside	OH	OH	H	Cl	H	6-Cl-PTP
7	2,6-diaminopurineriboside	OH	OH	NH <sub>2</sub>	NH <sub>2</sub>	H	2-NH <sub>2</sub> -ATP
8	8-bromoadenosine	OH	OH	H	NH <sub>2</sub>	Br	8-Br-ATP
9	<i>N</i> <sup>6</sup> -phenyladenosine	OH	OH	H	NHPh	H	<i>N</i> <sup>6</sup> Phe-ATP
10	<i>N</i> <sup>6</sup> -benzyladenosine	OH	OH	H	NHCH <sub>2</sub> Ph	H	<i>N</i> <sup>6</sup> Bn-ATP
11	<i>N</i> <sup>6</sup> -1-naphthyladenosine	OH	OH	H	NH-1-Naphthyl	H	<i>N</i> <sup>6</sup> Np-ATP
12	<i>O</i> <sup>6</sup> -methylguanosine	OH	OH	NH <sub>2</sub>	OMe	H	<i>O</i> <sup>6</sup> Me-GTP
CTP Analogs							
13	5-methylcytidine	OH	–	–	–	Me	5-Me-CTP
UTP Analogs							
14	2'- <i>O</i> -methyluridine	OMe	–	–	–	H	2'OMe-UTP
15	5-methyluridine	OH	–	–	–	Me	5-Me-UTP
16	5-propynyl-2'-deoxyuridine	OH	–	–	–	C≡CCH <sub>3</sub>	5-propynyl-dUTP

**Figure 3.6. Non-natural nucleotide triphosphate analogs examined as substrates for hydrolysis by RecA.** The abbreviation “PPP” indicates that a triphosphate moiety (P<sub>3</sub>O<sub>7</sub><sup>4-</sup>) is appended at the 5'-*O*-position of each depicted nucleotide. <sup>a</sup> The stereochemistry of this OH is opposite that of the representative purine NTP shown.

of the  $k_{\text{cat}}$  values (2-fold). Interestingly, nine NTPs were not hydrolyzed under the experimental conditions, even at concentrations as high as 1 mM (20-fold greater than  $S_{0.5}$  for ATP). The structure-activity relationships summarizing the key structural elements that influence the hydrolysis of purine- or pyrimidine-based NTP analogs are illustrated in Figure 3.7.

<b>Table 3.1: Kinetics of NTP Hydrolysis by the RecA Protein<sup>a</sup></b>			
Nucleotide	$k_{\text{cat}}$ ( $\text{min}^{-1}$ )	$S_{0.5}$ ( $\mu\text{M}$ )	$(k_{\text{cat}}/S_{0.5})_{\text{rel}}$
ATP	20 ± 1	50 ± 2	1.0
dATP	22 ± 1	39 ± 1	1.4
Ara-ATP	22 ± 1	86 ± 8	0.65
2'OMe-ATP	n.d. <sup>b</sup>	>1000	–
3'OMe-ATP	19 ± 1	56 ± 8	0.82
2'NH <sub>2</sub> -ATP	27 ± 2	110 ± 20	0.62
2'F-ATP	15 ± 1	110 ± 30	0.33
6-Cl-PTP	17 ± 1	99 ± 8	0.42
2-NH <sub>2</sub> -ATP	27 ± 1	54 ± 5	1.2
8-Br-ATP	18 ± 1	140 ± 10	0.33
N <sup>6</sup> Ph-ATP	24 ± 3	49 ± 6	1.2
N <sup>6</sup> Bn-ATP	33 ± 1	280 ± 30	0.29
N <sup>6</sup> Np-ATP	n.d.	>1000	–
GTP	15 ± 1	1400 ± 200	0.03
dGTP	21 ± 1	620 ± 30	0.08
O <sup>6</sup> Me-GTP	n.d.	>1000	–
ITP	22 ± 1	240 ± 10	0.23
dITP	21 ± 1	600 ± 20	0.09
CTP	21 ± 1	290 ± 20	0.09
dCTP	25 ± 1	200 ± 10	0.32
5-Me-CTP	n.d.	>1000	–
UTP	25 ± 1	350 ± 40	0.09
dUTP	25 ± 1	110 ± 30	0.58
5-propynyl-dUTP	n.d.	>1000	–
5-Me-UTP	n.d.	>1000	–
TTP	n.d.	>1000	–
2'OMe-UTP	n.d.	>1000	–

<sup>a</sup> Kinetics of ATP hydrolysis were measured using the MESG/PNP system to detect release of free phosphate. Each kinetic parameter was determined in triplicate and the error shown is the standard deviation of three trials. <sup>b</sup> n.d. denotes hydrolysis was not detected at concentrations of 1000  $\mu\text{M}$ .

For the eight canonical (r,d)NTPs, the data obtained using the PNP-coupled system recapitulated previously reported conclusions.<sup>[191]</sup> Specifically, the order of decreasing  $k_{\text{cat}}/S_{0.5}$  was (r,d)ATP > UTP > (r,d)CTP > (r,d)GTP >> TTP. While ATP is the preferred substrate, it is not necessarily the purine ring that leads to the selectivity. GTP and ITP, both of which are purine nucleotides, were only able to stimulate RecA activation with  $S_{0.5}$  values of 240  $\mu\text{M}$  and 1400  $\mu\text{M}$ , respectively. ITP and GTP have a carbonyl group at position C6 in lieu of the exocyclic amine of ATP and this appears to attenuate the ability of those

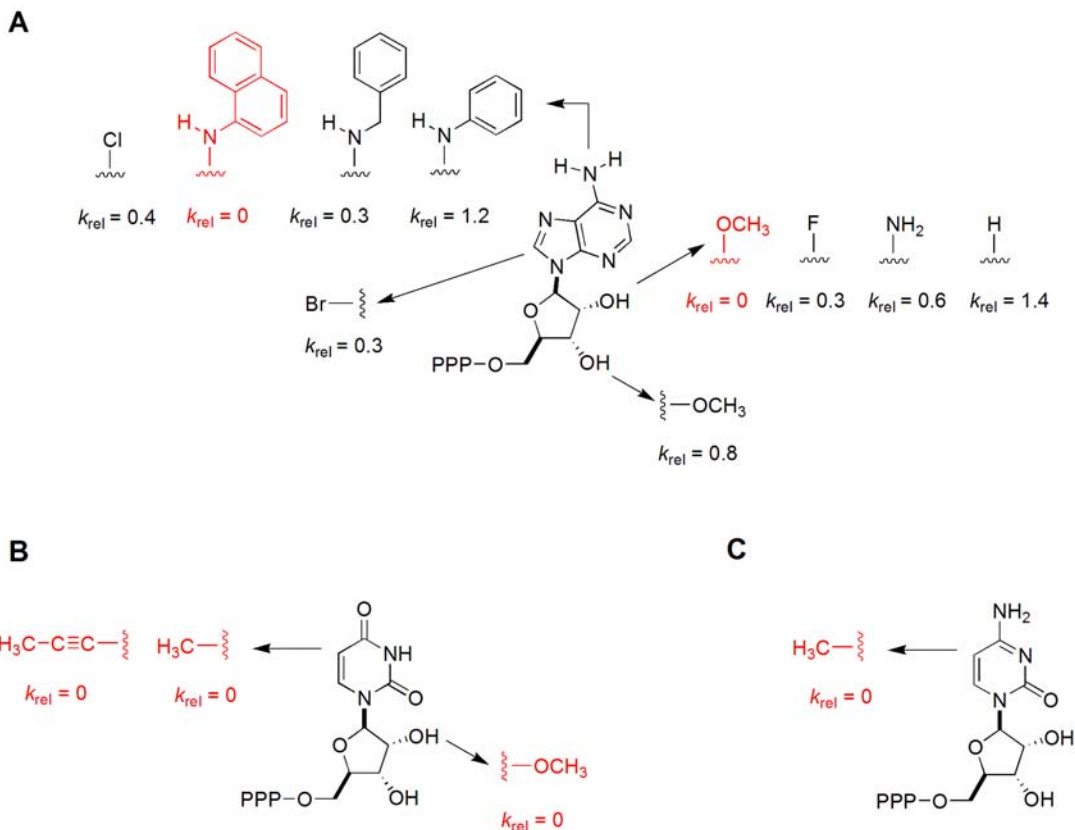


**Figure 3.7. Analysis of structure-activity relationships for RecA-catalyzed NTP hydrolysis of ATP analogs (A), UTP analogs (B), and CTP analogs (C).** The kinetic constants are compared to that of ATP using  $k_{rel} = (k_{cat}/S_{0.5})_{NTP}/(k_{cat}/S_{0.5})_{ATP}$  (see Table 1). Modifications abrogating all RecA NTPase activity are shown in red.

nucleotides to activate RecA. Previous studies by the Bryant laboratory have suggested that the specificity of RecA for ATP was due in part to a hydrogen bond between the Asp100 carboxylate and the exocyclic 6-amino group of ATP.<sup>[192]</sup> We have observed that the specificity for ATP over GTP and ITP does not appear to be entirely related to hydrogen bonding as 6-Cl-PTP, which is unable to hydrogen bond with the D100 position, is an efficient substrate of RecA.

Several aspects of the kinetic results (Figure 3.7) are not readily explained by examination of the open ATP-binding site observed in crystal structures of RecA bound to different nucleotides.<sup>[2, 186, 193]</sup> For example, ATP modifications such as 2'-F or 2'-NH<sub>2</sub>,

which change the electronic character but not the steric size of the 2' position, were well tolerated by RecA. However, the slight steric increase arising from the replacement of the 2'-OH group with 2'-OMe abolished the hydrolytic activity of RecA. Hydrogen bonding by the C2' substituent was not a requirement for RecA's NTPase activity as dATP and Ara-ATP resulted in hydrolysis kinetics essentially identical to those of ATP. Remarkably, the effect of the OH → OMe change was restricted to C2': when the 3'-OH group was replaced with a 3'-OMe group, there was no substantial change in the kinetic parameters of NTP hydrolysis. The inability of RecA to hydrolyze NTPs modified with groups larger than a hydroxyl at the C2' position also extended to pyrimidines as 2'OMe-UTP was not turned over by RecA. Moreover, MANT-ATP, which was utilized as a mixture of regioisomers with an aromatic substituent at either the ribose 2' or 3' hydroxyl was not a substrate for RecA NTPase activity.

The substitution of a methyl group for the hydrogen atom at the C5 position of pyrimidine NTPs also eliminated the ability of RecA to utilize such nucleotides as substrates. Indeed, the natural nucleotide TTP, as well as the C5-substituted nucleotides 5-Me-UTP, 5-Me-CTP, and 5-propynyl-dUTP were not RecA substrates. Presumably, the 5-methyl groups of such pyrimidine NTPs occupies an area of space corresponding to the likely positions of prospective substituents at the N7 and C8 positions of a purine NTP. The idea that a similar effect would be produced by adding a CH<sub>3</sub>-sized substituent at N7 or C8 of ATP was only partially confirmed: we observed 8-Br-ATP to be a modest substrate of RecA NTPase activity.

Contrary to the tight tolerances on the size of substituents at C2' of all NTPs and at C5 of pyrimidine NTPs, RecA was able to accommodate aromatic modifications at the N<sup>6</sup>

position of adenosine. A phenyl ring appended to the  $N^6$ -amino group had essentially no effect on hydrolysis, while a benzyl group at the  $N^6$  position, which has more rotational degrees of freedom than the phenyl substituent, increased  $k_{\text{cat}}$  significantly but also increased  $S_{0.5}$ . A naphthyl substitution at the  $N^6$  position yielded an adenosine nucleotide that was not hydrolyzed by RecA.

Although the active site for ATP hydrolysis can accommodate sterically demanding substituents as large as a benzyl group, replacement of the exocyclic  $\text{-NH}_2$  group by an  $\text{-OMe}$  group at position 6 of a purine to produce  $O^6\text{Me-GTP}$  abrogated ATP hydrolysis. Three trivial structural rationales for this observation can be ruled out by internal controls. First, the presence of an exocyclic  $\text{-NH}_2$  group at  $C2$  of  $O^6\text{Me-GTP}$  likely has little influence on its resistance to hydrolysis by RecA because the same functional group in the context of the adenine heterocycle (2- $\text{NH}_2$ -ATP) had only modest effects on the kinetic parameters. A second possible explanation for the 6- $\text{NH}_2$  to 6- $\text{OMe}$  effect is the removal of a hydrogen bond donor. However this possibility is ruled out as replacement of the  $\text{NH}_2$  group by a Cl atom (6- $\text{Cl-PTP}$ ) had only a modest effect on RecA's NTPase activity. Likewise, purine riboside-5'- $O$ -triphosphate, which has no exocyclic functional groups, has been shown to be a substrate for RecA-catalyzed hydrolysis.<sup>[194]</sup> Finally, the potential impact of a syn glycosidic torsional preference for unbound  $O^6\text{Me-GTP}$ <sup>[195]</sup> is minimized by the observation that 8- $\text{Br-ATP}$  which has a similar syn preference<sup>[196, 197]</sup> was hydrolyzed similarly to ATP.

The molecular determinants of attenuation of the DNA-dependent NTPase activity of RecA can be summarized as follows. Substitution at the  $C2'$  position of the ribose ring with groups larger than a hydroxyl moiety prevented both purine- and pyrimidine-based NTPs from acting as substrates for RecA NTPase activity. Replacement of  $N^6$ -amino group of the

adenine ring with aromatic groups larger than benzyl disrupted the ability of RecA to use the NTP as a substrate. Likewise, addition of a methyl group or propynyl group at the C5 position of pyrimidine NTPs produced the same effect.

Of the 28 NTPs tested a potential substrates for hydrolysis by RecA, 9 were unable to activate the protein. Our results demonstrate that the activation of the RecA protein by modified NTP analogs is exquisitely sensitive to modifications at certain positions and surprisingly tolerant to others. While these 9 NTPs were unhydrolyzable by RecA, we hypothesized that there was still the possibility that they could bind RecA without activating it, and potentially inhibit the protein. We envisioned two possibilities (Figure 3.5): (1) if non-substrate NTPs were able to bind and stabilize the inactive state of the protein, then they would prevent formation of RecA-DNA filament assembly or (2) if non-substrate NTPs were able to bind the active conformation without activating RecA hydrolysis, then they would allow filament formation but would competitively inhibit ATP hydrolysis. To assess the ability of these NTPs to inhibit RecA by either one of these mechanisms, we developed a systematic approach that rapidly allowed us to screen and delineate the effect of non-substrate NTPs on the conformational state of RecA. The results of this study allowed us to refine our understanding of the structure-activity relationship between nucleotide analogs and RecA as described below.

### **Probing the ability of non-substrate nucleotide analogs to bind and inhibit RecA**

In addition to probing the ability of the non-substrate NTPs to bind and inhibit RecA, we were interested in the examining the effect of nucleotides which are inherently unable to act as substrates for RecA. Nucleotides of this class included diphosphates and nucleotide-

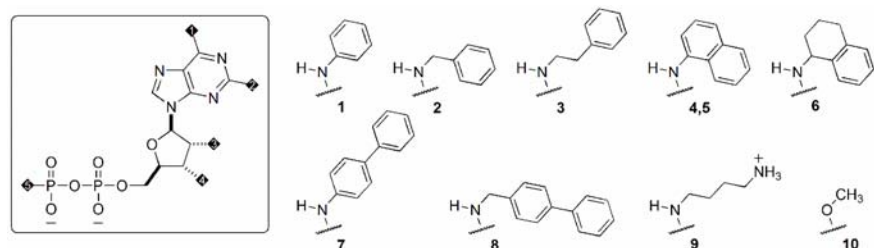


like molecules, all of which lack a hydrolyzable  $\gamma$ -phosphate group. As mentioned in the preceding section, we predicted that non-substrate nucleotides could potentially exert an inhibitory effect on RecA by binding either the inactive or active conformation of the protein and out-competing ATP. ADP and ATP $\gamma$ S can be considered as exemplary members of two orthogonal sets of functionally selective RecA inhibitors that attenuate the function of RecA by binding different states of the protein.<sup>[198]</sup> ADP stabilizes the inactive conformer and inhibits the assembly of active RecA-DNA filaments.<sup>[124, 148, 191, 199-202]</sup> Inhibitors of this type would abrogate all activities of the RecA-DNA filament, including both signaling and processive recombinational activities. In contrast, ATP $\gamma$ S induces the structural changes necessary to achieve an active conformation, but is a competitive inhibitor of ATP-hydrolysis.<sup>[203]</sup> As a result, ATP $\gamma$ S supports the biochemical activities necessary for SOS induction but prevents ATP-hydrolysis driven RecA motor activities.<sup>[203]</sup>

### **Application of selectivity filters to ADP and ATP analogs**

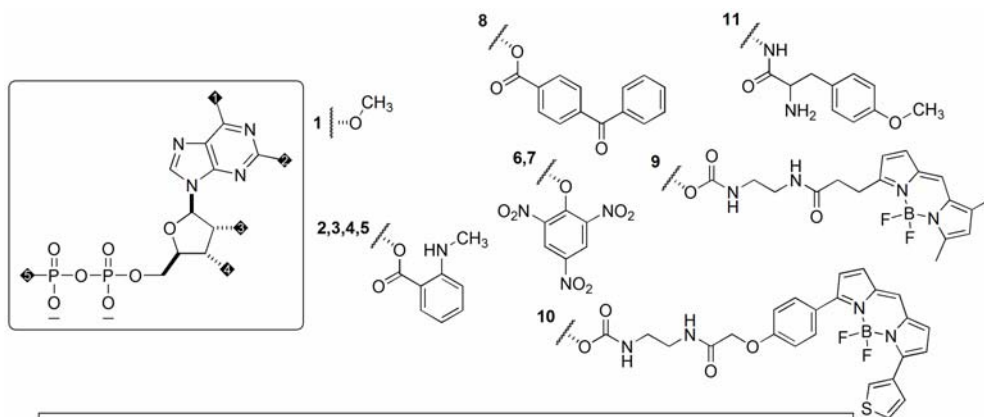
Expanding upon this last observation regarding ADP and ATP $\gamma$ S, we examined the ability of a total of 46 non-substrate nucleotides to bind either conformation of RecA and inhibit the protein. Based on our structural analysis of the ATP-binding site and coupled with the observations that certain purine nucleotides are unhydrolyzable by RecA, we reasoned that the adenosine scaffold could be modified to yield a potent RecA-specific inhibitor. This led us to consider the two groups of prospective RecA inhibitors depicted in Figure 3.8 and 3.9.

As described in the analysis of the ATP-binding site, the inactive RecA conformer binds ADP in an unusual configuration wherein the adenine  $N^6$  position appears to be



Entry	[1]	[2]	[3]	[4]	[5]	[Abbreviation]
1	NHPh	H	OH	OH	O <sup>-</sup>	N <sup>6</sup> Ph-ADP
2	NHBn	H	OH	OH	O <sup>-</sup>	N <sup>6</sup> Bn-ADP
3	NH(2-phenethyl)	H	OH	OH	O <sup>-</sup>	N <sup>6</sup> PE-ADP
4	NH(1-naphthyl)	H	OH	OH	O <sup>-</sup>	N <sup>6</sup> Np-ADP
5	NH(1-naphthyl)	H	OH	OH	OPO <sub>3</sub> <sup>2-</sup>	N <sup>6</sup> Np-ATP
6	NH(1-tetrahydronaphthyl)	H	OH	OH	O <sup>-</sup>	N <sup>6</sup> THN-ADP
7	NH(4-biphenyl)	H	OH	OH	O <sup>-</sup>	N <sup>6</sup> BP-ADP
8	NH(4-biphenylmethyl)	H	OH	OH	O <sup>-</sup>	N <sup>6</sup> BPM-ADP
9	NH(4-amino-1-butyl)	H	OH	OH	O <sup>-</sup>	N <sup>6</sup> AB-ADP
10	OMe	NH <sub>2</sub>	OH	OH	OPO <sub>3</sub> <sup>2-</sup>	O <sup>6</sup> Me-GTP

**Figure 3.8.** *N*<sup>6</sup>-modified purine analogs examined as inhibitors of RecA. Modifications at the 6 position of an adenosine scaffold were examined for their ability to exploit the fact that RecA appears to be uniquely tolerant of binding nucleotides with added bulk in this location.



Entry	[1]	[2]	[3]	[4]	[5]	[Abbreviation]
1	NH <sub>2</sub>	H	OMe	OH	OPO <sub>3</sub> <sup>2-</sup>	2'OMe-ADP
2	NH <sub>2</sub>	H	O-(N'-methylanthraniloyl)	OH	O <sup>-</sup>	MANT-ADP
3	NH <sub>2</sub>	H	O-(N'-methylanthraniloyl)	OH	OPO <sub>3</sub> <sup>2-</sup>	MANT-ATP
4	NH <sub>2</sub>	H	O-(N'-methylanthraniloyl)	OH	NHPO <sub>3</sub> <sup>2-</sup>	MANT-AMPPNP
5	OH	NH <sub>2</sub>	O-(N'-methylanthraniloyl)	OH	OPO <sub>3</sub> <sup>2-</sup>	MANT-GDP
6	NH <sub>2</sub>	H	O-(2,4,6-trinitrophenyl)	OH	O <sup>-</sup>	TNP-ADP
7	NH <sub>2</sub>	H	O-(2,4,6-trinitrophenyl)	OH	OPO <sub>3</sub> <sup>2-</sup>	TNP-ATP
8	NH <sub>2</sub>	H	O-(4-benzoylbenzoyl)	OH	OPO <sub>3</sub> <sup>2-</sup>	BzBz-ATP
9	NH <sub>2</sub>	H	O-(BODIPY TR)	OH	O <sup>-</sup>	BODIPY-ADP
10	NH <sub>2</sub>	H	O-(BODIPY FL)	OH	NHPO <sub>3</sub> <sup>2-</sup>	BODIPY-AMPPNP
11	NMe <sub>2</sub>	H	OH	NH-(O-methyltyrosyl)	OPO <sub>3</sub> <sup>2-</sup>	PrmTP

**Figure 3.9.** Ribose-modified purine analogs examined as inhibitors of RecA. Modifications at the 2' and 3' position of an adenosine scaffold were examined for their ability to exploit the internal cavity on the primary RecA monomer formed by F260, I262 and Y264, directing substituents capturing positive interactions with the hydrophobic side chains of these residues.

directed into the solvent and away from the protein (Figures 3.3 & 3.4). Thereby, we reasoned that the ATP-binding site of inactive RecA could accommodate sterically demanding substituents on the purine ring. In contrast, the ATP-binding sites of other ATPases and kinases maintain close contact with the edge and both faces of adenine, mitigating their potential interactions with many modified adenosine nucleotide analogs.<sup>[204-206]</sup> We chose to evaluate the ability of a variety of  $N^6$ -substituted ADP and ATP analogs to inhibit RecA (Figure 3.8).

The observation that mutations surrounding the unique cavity near the 2' and 3' hydroxyl groups of ADP bound in the inactive conformer (see Figure 3.4C) are untolerated suggests that it may be a functionally important feature of the RecA ATP-binding site. We therefore chose to evaluate putative inhibitors that direct space-occupying substituents into the cavity. Based on our observation that ATP derivatives bearing 2'-*O*-alkyl or -aryl substituents bind to the RecA ATP-binding site but do not serve as substrates for hydrolysis by RecA (Table 3.1), we chose to evaluate 2'-*O*- and 3'-*O*-substituted ADP and ATP analogs (Figure 3.9).

These first two approaches towards the design of a selective inhibitor of RecA rely on the principles of negative design: specificity is achieved by the introduction of substituents that prevent inhibition of non-targeted enzymes. Our preliminary observation that  $N^6$ Np-ADP selectively inhibits RecA provided important proof that addition of a naphthyl group at the  $N^6$  position of an adenosine nucleotide creates a selective RecA inhibitor.<sup>[202]</sup> Affinity for the ATP-binding site can be generated by the introduction of substituents on the adenosine nucleotide scaffold that capture new interactions with proximal amino acid side-chains.

Select members of the groups of nucleotide analogs depicted in Figures 3.8 and 3.9 may serve as leads for future rational modification procedures using positive design principles.

### Prospective inhibitors in other structural classes

In addition to analogs of the adenosine nucleotides, we elected to investigate two other groups of nucleotide-like compounds as prospective inhibitors of RecA. First, a number of TTP analogs were chosen and screened for inhibitory activities (Figure 3.10). This group was selected based on our previously reported observation that TTP binds RecA but is not hydrolyzed (Table 3.1). In the absence of any structural data for RecA-TTP interactions, the structure-activity data gathered for these compounds would help elucidate the structural basis for RecA inhibition by TTP.

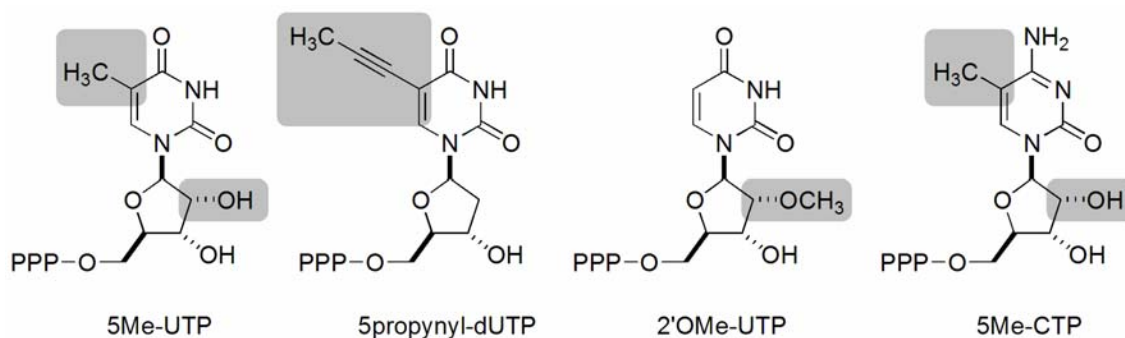
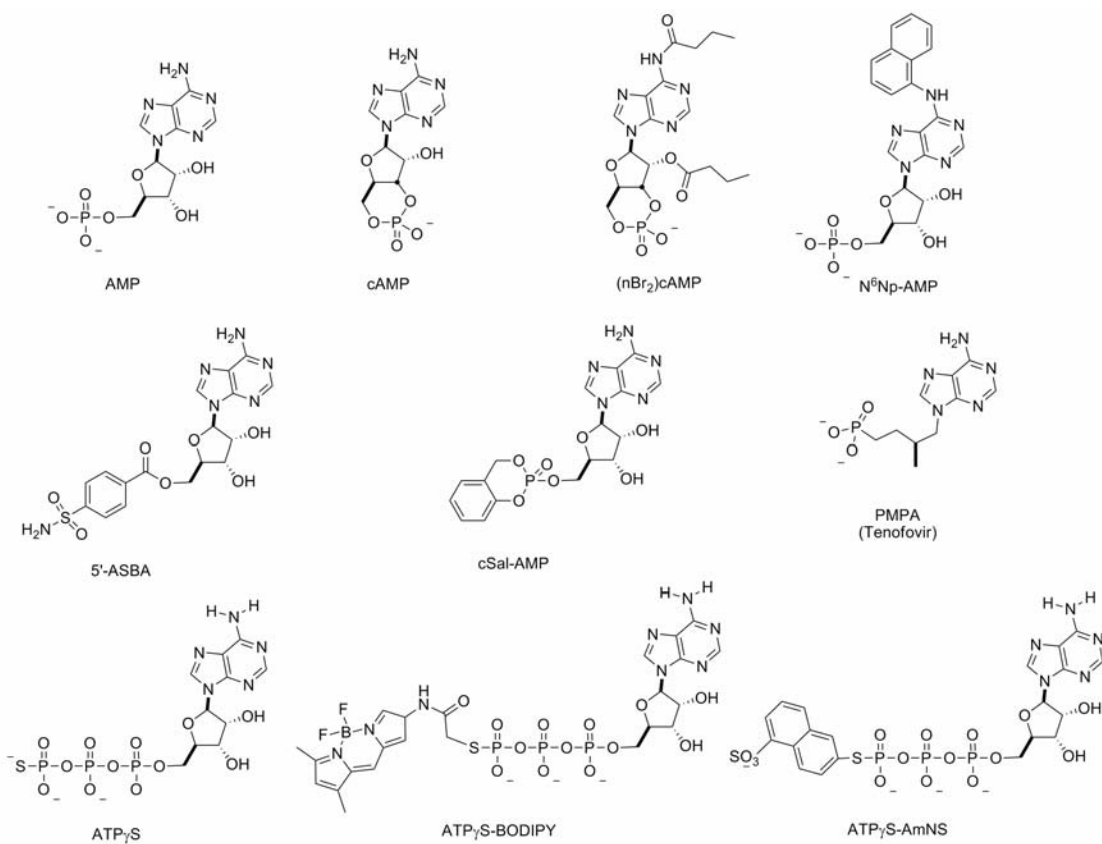


Figure 3.10. TTP analogs screened as potential inhibitors of RecA.

An important consideration in the design of prospective RecA inhibitors is to synthesize ATP competitors that could be effective in live bacteria. Unfortunately, di- and triphosphates are likely to be of little utility in this regard due to membrane-impermeability caused by the negative charges on the 5'-di- and triphosphate moieties at physiological pH. However, substantial progress has been made in the development of effective strategies for

the intracellular delivery of nucleotide prodrugs (pronucleotides), particularly for use as anticancer and antiviral therapeutics.<sup>[207-211]</sup> As an initial attempt to characterize potential inhibitors with modified phosphate groups, we chose to investigate a number of phosphate mimics and replacements as shown in Figure 3.11.



**Figure 3.11. Nucleotide analogs with di- and triphosphate replacements screened as potential inhibitors of RecA.** These molecules were examined to understand the effect of modifying the phosphate group. Some compounds were specifically chosen to examine the effect of an electrically neutral phosphate replacement.

### Molecular screening assays for RecA activities

The purpose of the second phase of our study was to identify and characterize nucleotide-based inhibitors of RecA-DNA filament assembly, ATP hydrolysis, or both. Towards this goal we have developed a complementary pair of rapid microplate assays which

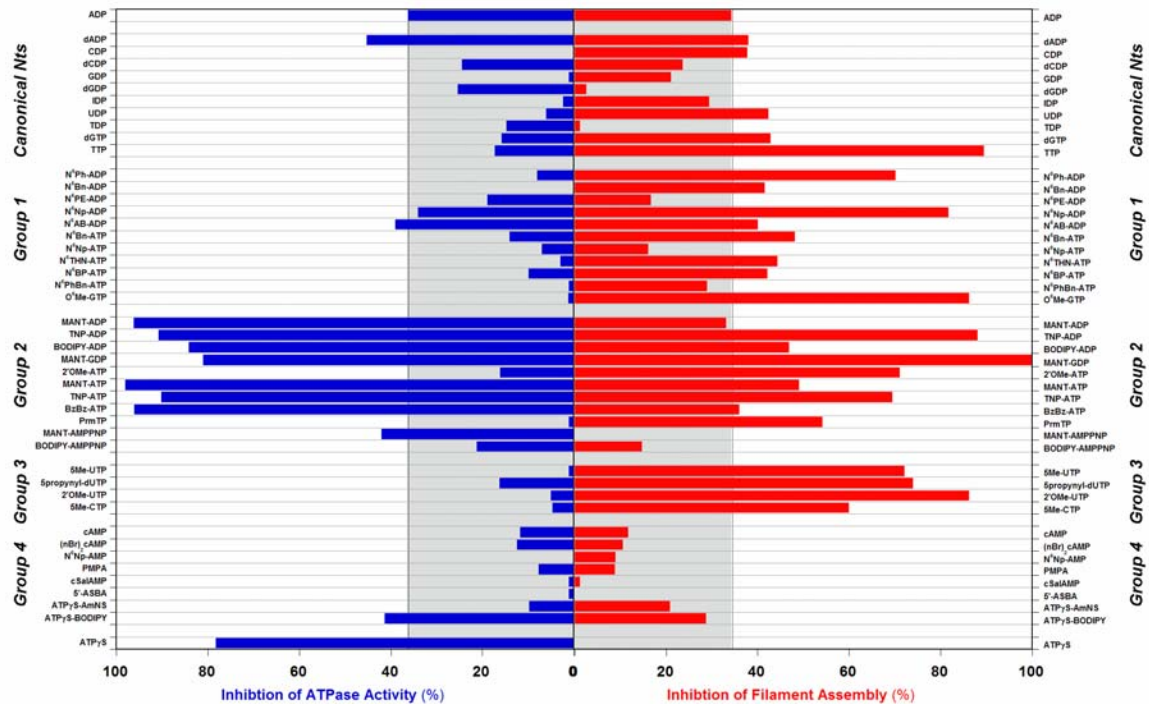


**Figure 3.12. Activities of nucleotide analogs screened against RecA in the ATPase and filament assembly assays.** The nucleotide analogs were examined at a concentration of 100  $\mu$ M to inhibit either activity. The % ATPase inhibition is represented by the blue bars (left), and the % inhibition of RecA-DNA filament assembly is represented by the red bars (right).

detect binding of nucleotides to either the inactive RecA conformer or the activate A-state conformation.<sup>[17, 124]</sup> These assays were adapted as high-throughput molecular screening assays to detect the inhibition of RecA-DNA filament assembly and the inhibition of DNA-dependent hydrolysis of ATP by RecA, respectively. A set of nucleotides deemed to be unhydrolyzable by RecA or which are inherently able to act as substrates for hydrolysis were subjected to this two-tier screen. The nucleotides were carefully selected based on a structure-activity profile predicted from a structural analysis of the ATP-binding site or from our initial efforts to describe the potential of NTPs to activate the RecA protein. Altogether, 46 compounds (Figures 3.8 – 3.11) were investigated for inhibitory activities using the two-

tiered screening assay to determine whether they significantly affected RecA DNA-dependent ATPase activity or perturbed the RecA-DNA filament assembly.

The relative inhibition of ATPase activity and RecA-DNA filament assembly effected by each compound is plotted in Figure 3.12. By comparing the length of the activity bars in Figure 3.12, it may be generally concluded that the compounds do not possess equivalent inhibitory activities in the two different screening assays. In the following sections, the structure-activity relationships elucidated by these inhibition data are described.

### **Inhibition of RecA-DNA filament ATPase activity**

The first step in both RecA-mediated SOS induction and recombinational DNA repair is the binding of RecA to ATP and ssDNA to form an active RecA-DNA filament. Active filament assembly is necessary for signaling SOS induction and normally results in the ATP hydrolysis which is required to drive recombinational activities. As a result, ATP hydrolysis serves as a useful indicator of filament activity, and the abrogation of ATPase activity would be an important aspect of RecA inhibition. We have previously optimized and quantitatively validated methods which rapidly and accurately detect the influence of a potential inhibitor on RecA by detecting one of the by-products of ATP hydrolysis, ADP and inorganic phosphate (Figure 3.13).<sup>[212-214]</sup> The fractional ATPase activity of the RecA-DNA filament measured over the course of 30 min in the presence of 100  $\mu$ M putative inhibitor (final concentration) manifests its ability to bind and inhibit the A-state filament. For each NTP assessed using this method, it was first established that the NTP did not serve as a substrate for hydrolysis by RecA at concentrations at or below 500  $\mu$ M.<sup>[212]</sup>

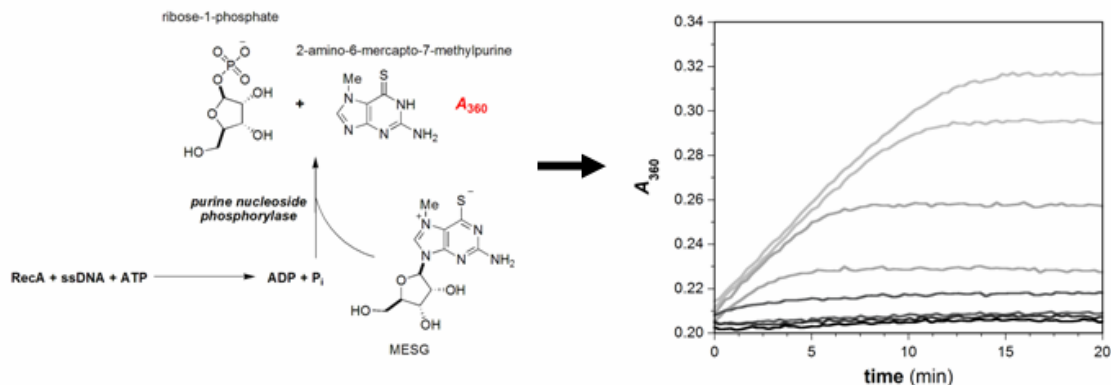


**Figure 3.13. MESG-coupled ATPase assay used to screen for nucleotide analog inhibitors of ATP hydrolysis by RecA.** The free phosphate generated when RecA hydrolyzes ATP enzymatically reacted with 2-amino-6-mercapto-7-methylpurine riboside (MESG) to produce ribose-1-phosphate and 2-amino-7-mercapto-7-methylpurine, which has an absorbance maximum of 360 nm. The absorbance at 360 nm can be measured periodically over time to construct a kinetic ATPase curve or can be measured in endpoint mode to determine the fractional inhibition of ATPase activity.

Like many ATPases, RecA is inhibited by ADP in a natural feedback mechanism. Accordingly, in the rapid screening assay ADP inhibited RecA DNA-dependent ATPase activity by 36%. The unhydrolyzable ATP isostere, ATP $\gamma$ S was even more effective than ADP, inhibiting the RecA-DNA filament ATPase by nearly 80%. The 5'-O-diphosphates corresponding to other canonical NTPs which are not well-tolerated substrates for hydrolysis by RecA were poor inhibitors of ATPase activity. Specifically, GDP, IDP, UDP, CDP and TDP did not significantly reduce the RecA ATPase activity in our screen (Figure 3.12).

Substitutions at the adenine  $N^6$  position did not result in adenosine nucleotide analogs with abilities to bind and inhibit the A-state filament. Although  $N^6$ Np-ADP and  $N^6$ AB-ADP, two ADP analogs with sterically encumbering substituents at the  $N^6$  position, inhibited ATP hydrolysis by 27% and 39%, respectively, none of the other analogs in this group (Figure 3.8) were as potent as ADP.

Nucleotides with aromatic groups substituted at either  $C2'$  or  $C3'$  were among the most effective inhibitors of RecA poly(dT)-dependent ATPase activity. Indeed, MANT-



ADP, MANT-ATP, MANT-GDP, TNP-ADP, TNP-ATP, BODIPY-ADP and BzBz-ATP all inhibited RecA poly(dT)-dependent ATPase activity more strongly than ATP $\gamma$ S. An aromatic group substitution at one ribose hydroxyl appears to greatly enhance the binding affinity of a nucleotide for the active filament ATP-binding site. This effect is further established by a comparison of the ATPase inhibition effected by GDP and its analog MANT-GDP. While GDP has no detectable impact on RecA ATPase activity, addition of a MANT group to the O2'(O3') position results in an extremely potent inhibitor of RecA ATPase activity. This may indicate that the aromatic ribose modification may not be sufficient to create a RecA-specific inhibitor and a nucleotide analog inhibitor of RecA would require additional modifications to generate specificity. Purine nucleotides having MANT group substitutions have previously been shown to inhibit adenylate cyclase enzymes with  $K_i$  values of less than 1  $\mu$ M<sup>[215, 216]</sup>, and have been used as fluorescent reporter molecules to measure the binding kinetics of ATP and GTP to various purine NTP-binding enzymes,<sup>[217, 218]</sup> including Escherichia coli replication machinery such as DnaB, DnaC and RepA.<sup>[219-225]</sup> Of the 11 members of this group (Figure 3.9), only 2'OMe-ATP, PrmTP, and BODIPY-AMPPNP are less potent than ADP. It is interesting that all three are triphosphates (or isosteres thereof). PrmTP is the only nucleotide analog with a substituent fixed at O3'. With the exception of 2'OMe-ATP, all the other analogs with substituents on the ribose ring can exist as a mixture of regioisomers due to migration of the ester or activated phenyl substituents. We speculate that RecA may accommodate 2'- but not 3'-substituted ribose. Crystal structures of other enzymes had revealed that they may select one of the two possible regioisomers.<sup>[226]</sup>

The ability to bind competitively to the ATP-binding site of RecA and inhibit its ATPase function was restricted to nucleotides bearing di- or triphosphate moieties or their isosteres. Indeed, RecA ATPase activity was not inhibited by the monophosphate species AMP, cAMP and dibutyryl-cAMP. Moreover, neither of the adenosine derivatives 5'-aminosulfonylbenzoyl-adenosine (5'-ASBA) or *cycloSal* adenosine monophosphate (*cSal*-AMP), which contain 5'-benzenesulfonamide and 5'-*cycloSal*igenyl phosphotriester groups, respectively (Figure 3.11), inhibit RecA to any appreciable extent. The lack of inhibition by 5'-ASBA, which can be considered the sulfonamide derivative of the known irreversible inhibitor 5'-fluorosulfonylbenzoyl-adenosine (5'-FSBA),<sup>[227-229]</sup> demonstrates the importance of the interaction between the phosphate ester anion and the P-loop macrodipole for binding to the ATP-binding site.

### **Inhibition of RecA-DNA filament assembly**

The second assay was designed to evaluate the inhibition of RecA-DNA filament assembly by direct monitoring of the protein released from a ssDNA substrate resulting from the addition of a putative inhibitor. Our laboratory recently reported the optimization and validation of a method to assess the effects of small molecules on the binding of RecA to ssDNA.<sup>[212, 213]</sup> Briefly, (dT)<sub>36</sub> covalently attached to biotin (biotin-(dT)<sub>36</sub>) was incubated with RecA and putative inhibitor was added to a final concentration of 100 μM. The biotin-(dT)<sub>36</sub>, with any RecA remaining bound to it, was pulled down using streptavidin-coated paramagnetic particles, while the supernatant was assessed for protein content. The amount of RecA remaining in the supernatant reflected the affinity of the ligand for the inactive

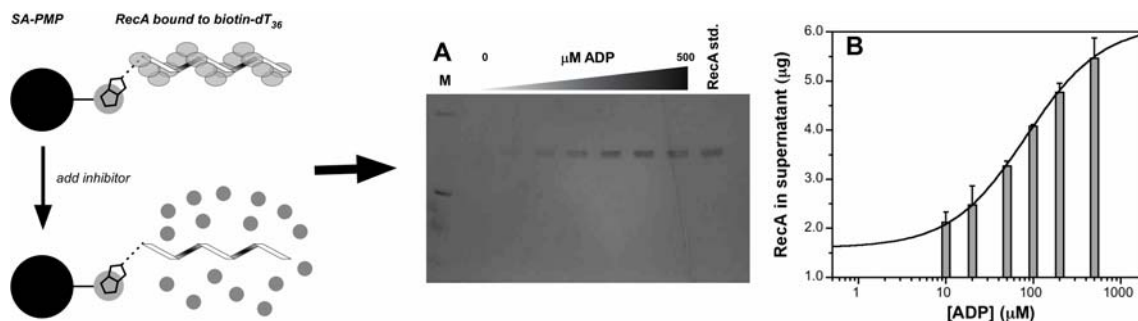


**Figure 3.14. Biotin-dT<sub>36</sub> magnetic pull-down assay used to screen for inhibitors of RecA-DNA filament assembly.** A 36mer oligonucleotide is incubated with RecA to allow filament assembly, then a putative inhibitor (in this case ADP) is added. If filament assembly on the biotin-dT<sub>36</sub> is disrupted any RecA remaining in the supernatant can be detected by and quantified by Coomassie staining after the RecA-bound biotin-dT<sub>36</sub> is pulled down using streptavidin-coated paramagnetic particles.

RecA conformer and the extent to which it inhibited RecA-DNA filament assembly (Figure 3.14).

It is established that the addition of ADP to a complex of RecA with an oligonucleotide results in disassembly of the complex.<sup>[199]</sup> In accord with this observation, ADP inhibits RecA-DNA filament assembly by 34% in the rapid molecular screening assay. Among the nucleotide analogs screened as potential inhibitors of RecA, a greater fraction were effective for inhibition of RecA-DNA filament assembly than were able to impede ATP hydrolysis.

In vitro, RecA-DNA filaments can hydrolyze NTPs other than ATP, but the substrate tolerance is exquisitely sensitive to certain modifications of the nucleoside scaffold.<sup>[124]</sup> The RecA-DNA filament assembly assay indicates that non-substrate nucleotide triphosphates bind RecA but fail to activate it for DNA binding. Indeed, dGTP and TTP are more effective at inhibiting filament assembly than ADP. Moreover, the diphosphate products of RecA NTPase substrates also bind RecA and prevent RecA-DNA filament assembly. RecA hydrolyzes UTP and CTP with essentially identical  $k_{cat}$ , and UDP and CDP cause 42% and

38% RecA-ssDNA dissociation, respectively. The diphosphates of the poorest RecA NTPase substrates, GTP and ITP, are less effective as inhibitors of RecA-DNA filament assembly (< 30%).

Analogs of ADP with modifications at the  $N^6$  position show potential as efficacious inhibitors of RecA-DNA filament assembly. In particular,  $N^6$ Ph-ADP,  $N^6$ Np-ADP, and  $O^6$ Me-GTP showed inhibition levels substantially higher than that of ADP: 70%, 82%, and 87%, respectively. ADP analogs bearing larger substituents at  $N^6$  were not as effective, especially when the C atom bonded to  $N^6$  was not aromatic. This indicates that the steric or electronic character of the  $N^6$  substituent is important not only to the binding affinity of the ADP analog for the inactive conformation ATP-binding site, but also for the efficacy of the RecA-ssDNA dissociation induced as a result of this binding. It is also noteworthy that the triphosphates were generally not as efficacious as the diphosphates. One exception to this generalization is exemplified by  $O^6$ Me-GTP. We have previously reported that the substrate tolerance by active RecA-DNA filaments is sensitive to subtle electronic and steric effects. The relative inhibitory efficacy of this modified GTP suggests that non-adenine-like electronic configurations of the purine heterocycle may be useful in future inhibitor designs.

ADP analogs with aromatic groups substituted at either  $C2'$  or  $C3'$  were also effective inhibitors of RecA-DNA filament assembly. Indeed, all but one member of Group 2 (Figure 3.9) inhibited the filament assembly activity at least as strongly as ADP. The only exception to this rule, BODIPY-AMPPNP, lacks a true triphosphate moiety.

It appears that most NTP analogs containing modifications that prevent their hydrolysis by RecA in its active state are capable of inhibiting RecA-DNA filament assembly. For example, a substitution larger than a hydroxyl at the  $C2'$  position of a

nucleotide such as a 2'-OMe group prevents its usage as an NTPase substrate and results in a good inhibitor of RecA-ssDNA binding. This is apparent for 2'OMe-ATP and 2'OMe-UTP which are not hydrolyzed and actually cause 71% and 86% inhibition of RecA-ssDNA association despite their parent molecules, ATP and UTP, being turned over readily. The structural analogs of UTP modified at position C5 with a methyl or propynyl group are also non-hydrolyzable and cause an appreciable level of RecA-ssDNA dissociation. This is exemplified by TTP, 5Me-UTP, 5propynyl-dUTP and 5Me-CTP which cause 90%, 72%, 74% and 60% RecA-ssDNA dissociation respectively. This suggests that uridine analogs may be also useful in future inhibitor designs.

### **Inhibition of RecA-mediated DNA three-strand exchange reaction**

RecA-mediated homologous genetic recombination involves multiple processes.<sup>[230]</sup> After the formation of an A-state RecA-DNA filament, the filament's DNA strand is paired with a segment of homologous dsDNA to create a RecA-tsDNA filament in the P conformational state. In the subsequent phases of recombination, several hundred bases of heteroduplex product DNA are formed as the base-pairing between strands is rapidly switched, the heteroduplex regions are extended, and the nascent ss- and dsDNA products are resolved.<sup>[231]</sup> Importantly, the latter two processes require the hydrolysis of ATP by the P-state filament. While both the A- and P-state RecA-DNA filaments actively hydrolyze ATP, the screening assays described above only evaluate ATPase activity of the A-state filament. Thus, it was necessary to assess the ability of ATPase inhibitors to modulate the activity of RecA in the P state.

The recombinational activity of RecA can be reconstituted in vitro and when supplied with linear dsDNA, circular cssDNA and ATP, RecA promotes an ATP-dependent DNA strand exchange reaction<sup>[232, 233]</sup> that provides a biochemical paradigm for RecA's role in the physiologic processes of homologous recombination and recombinational DNA repair.<sup>[34]</sup> ATP hydrolysis has been shown to be necessary to resolve the two new products of this reaction, nicked circular dsDNA and linear ssDNA.<sup>[62]</sup> To demonstrate that a small-molecule inhibitor of RecA ATP hydrolysis could prevent the recombinational activity of RecA, we performed the strand exchange reaction in the absence and presence of 100  $\mu$ M TNP-ADP. As demonstrated by Figure 3.15, TNP-ADP abrogates RecA-mediated DNA strand exchange, even over the course of 90 min in the presence of 3 mM ATP.

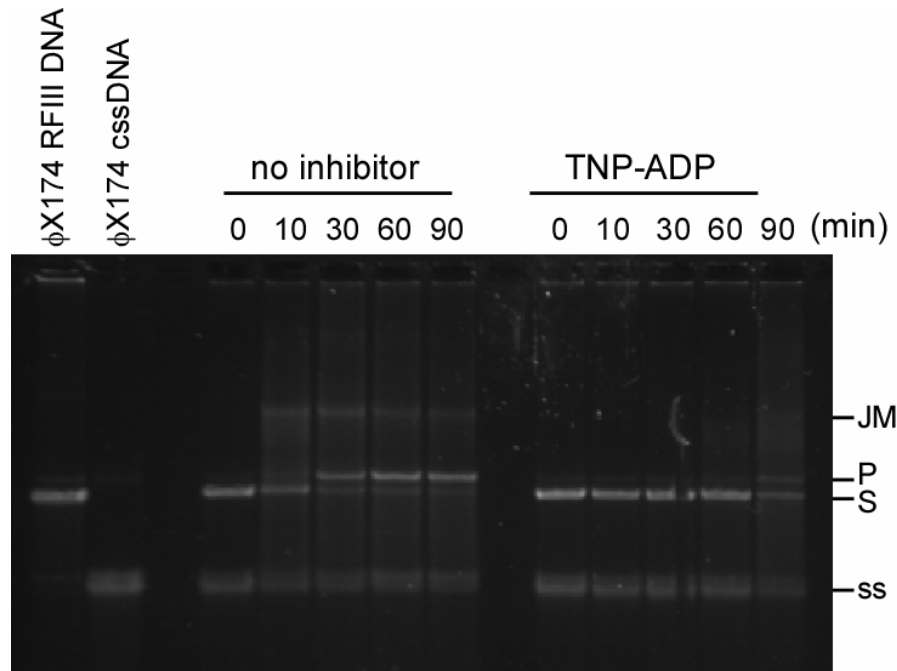


**Figure 3.15. Inhibition of RecA-mediated three-strand exchange assay by TNP-ADP.** In the absence of inhibitor, the formation of joint molecules (JM) and new nicked circular dsDNA product (P) from circular dsDNA (S) and homologous ssDNA is observed. In the presence of TNP-ADP however, JM and P are not observed until 90 minutes, and are only present at low levels.

## Functionally selective inhibition of RecA

We envisaged the two screening assays as a coupled pair that would serve to provide complementary information on two of RecA's coincident functions: (1) signaling activities inducing the cellular SOS response, and (2) ATP-hydrolysis driven motor activity resulting in recombination. This feature is critical to the strategic development of functionally selective ligands that would allow separation of the motor-like and signaling functions of RecA, and thereby permit dissection of resistance gene development and transmission pathways in bacterial pathogens. To assess the degree to which the nucleotide analog inhibitors are selective, a correlation plot was constructed (Figure 3.16) comparing the extent

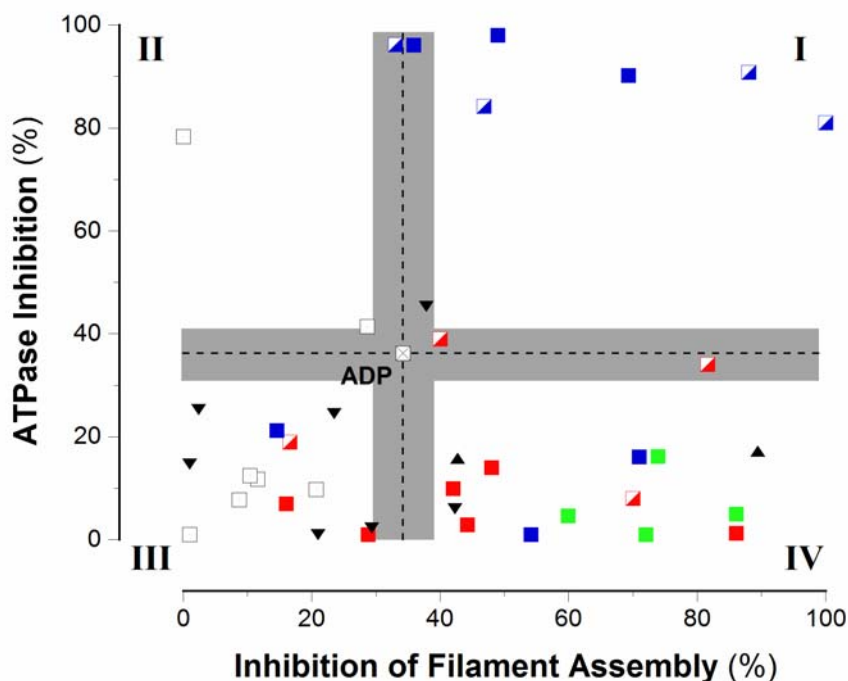


**Figure 3.16. Functionally selective inhibition of RecA.** The inhibitory activities of each nucleotide analog can be separated in a two-dimensional scatter plot. Canonical nucleotide diphosphate are shown as black downward triangles, and their triphosphate counterparts are shown as black upward triangles. Nucleotide analog diphosphates are represented as half squares, while the triphosphates are fully shaded squares and these correspond to the following colour scheme:  $N^6$ -modified nucleotide analogs are shown in red, 2' and 3' modified nucleotide analogs are shown in blue, pyrimidine nucleotide analogs are shown in green. Nucleotides possessing phosphate isosteres are shown as white squares.

to which each nucleotide analog inhibited RecA's ATPase activity with the extent to which the compound inhibited RecA-DNA filament assembly. The inhibitory properties of ADP were used as a reference for comparison of the activities of each nucleotide analog inhibitor.

Nucleotide analogs that were less inhibitory than ADP in both screening assays (Cartesian quadrant III, lower left) can be disregarded as "inactive". This quadrant is largely populated by the nucleotide-like compounds that lack a di- or triphosphate moiety (Figure 3.11). The failure to discover a RecA inhibitor among these compounds suggests that the binding of such ligands to the RecA ATP-binding site relies on interactions between the anionic di- or triphosphate moiety and the positive macrodipole of the  $\alpha$ -helix preceding the P-loop. Furthermore, the requirement for a 5'-*O*-diphosphate (or -triphosphate) suggests that the development of an inhibitor with potent *in vivo* activity will not be a trivial exercise.

Of higher interest are those nucleotide analogs that are more inhibitory than ADP in the ATPase assay (quadrant II, upper left), including ATP $\gamma$ S, MANT-ADP, MANT-ATP, BzBz-ATP, and BODIPY-ATP (see Figure 3.8). ATP-competitive ATPase inhibition constants ( $K_{ic}$ ), were measured for these nucleotides. The  $K_{ic}$  for ADP is similar to that of the  $S_{0.5}$  for ATP, being measured as 63  $\mu$ M and 50  $\mu$ M, respectively. Nucleotides that abrogated RecA's ATPase activity in the rapid screening assay were found to bind RecA with an affinity 40-100 fold higher than ADP as measured by their  $K_{ic}$  values, but generally were observed to be incapable of preventing RecA-DNA filament assembly. These compounds only weakly bind RecA in its inactive conformation, but are high-affinity binders of the active RecA-DNA filament.

Nucleotide analogs that were more inhibitory than ADP in both screening assays (quadrant I, upper right) suppressed all RecA activities, including both RecA-DNA filament



assembly and ATP hydrolysis. Inhibitors in this quadrant included TNP-ADP, TNP-ATP, and MANT-GDP (see Figure 3.9). These compounds prevent the assembly of active RecA-DNA filaments altogether, presumably by stabilizing the inactive RecA conformer. Indeed, as described above, TNP-ADP completely suppressed the three-strand exchange reaction. As it relates to inhibition of filament assembly, the superiority of the 2' modified nucleotides over their counterparts such as MANT-ADP, MANT-ATP, BODIPY-ADP and Bz-Bz-ATP lies in the nature of the substitution and the electronic character of the nucleobase. TNP-AxP analogs can exist with the trinitrophenyl moiety in aromatic form, isolated to either the 2' or 3' hydroxyl of the ribose, or as a Meisenheimer complex simultaneously bound to both hydroxyls. This is in contrast to the other above mentioned analogs which may only exist on the 2' or 3' hydroxyl, but not both simultaneously. In the case of MANT-GDP, the guanine nucleobase presents a substantially different electronic configuration than does the adenine scaffold.

Nucleotide analogs that were more inhibitory than ADP in the filament assembly assay but not the ATPase assay (quadrant IV, lower right) –  $N^6$ Np-ADP,  $N^6$ Ph-ADP,  $O^6$ Me-GTP, 2'OMe-UTP, 2'OMe-ATP, TTP, 5Me-UTP, and 5Propynyl-UTP – provide additional insight. Although such compounds apparently prevent RecA-DNA filament assembly without inhibiting the subsequent ATP hydrolysis, this cannot be the true interpretation because RecA-DNA filament assembly is obligatory for ATP hydrolysis. Consideration of the ATP concentration in the different screening assays is important for unraveling this apparent conundrum. In particular, the ATPase assay is conducted in the presence of 0.5 mM ATP, while the filament assembly assay is conducted with only sub-stoichiometric ATP $\gamma$ S (2  $\mu$ M). Indeed, quantitative inhibition assays with these nucleotides revealed  $K_{ic}$  values greater

than  $S_{0.5}$  for ATP in each case. We conclude that nucleotide analogs found in quadrant IV are capable of selectively stabilizing the inactive RecA conformer, but can be competed off by ATP at elevated concentrations. This further suggests that such compounds are likely to be weakly-binding competitive inhibitors. Although compounds in this group will not be good candidates for in vivo inhibition, their properties will be important for the elucidation of structure-activity relationships among ligands for the inactive RecA conformation.

While a di- or triphosphate moiety is required for inhibition of either ATPase activity or RecA-DNA filament assembly, the type of inhibition effected by a particular nucleoside scaffold does not depend on whether the 5' substituent is a di- or triphosphate moiety. This is exemplified by MANT-, TNP-, and  $N^6$ Np-substituted ADP/ATP pairs. The group of nucleotides which inhibited RecA-DNA filament assembly were also found to consist of a mix of di- and triphosphates. This pattern can be generalized to the following statements: (1) non-substrate NTP analogs were effective inhibitors of RecA-DNA filament assembly; and (2) NDPs derived from good RecA NTPase substrates were effective inhibitors of RecA-DNA filament assembly.

A principle conclusion of this work is that analogs of NDPs and NTPs can be readily segregated into two classes of RecA inhibitors based on their activities in a complementary pair of molecular screening assays: (1) those that preferentially bind the active RecA-DNA filament and competitively inhibit ATP hydrolysis (Figure 3.16; quadrant II); (2) those that preferentially bind the inactive RecA conformation and inhibit RecA-DNA filament assembly (Figure 3.16; quadrants I and IV). Importantly, the abilities of inhibitors in the former class to modulate the ATP turnover that is required for RecA's recombinational motor activities would allow the motor-like function of RecA to be segregated from its signal-like

functions (see Figure 3.1). In contrast, those inhibitors of the latter class possessing sufficient affinity to compete with ATP for a common binding site (Figure 3.16; quadrant I) will abrogate both signaling and processive recombinational activities of RecA. Clearly, key nucleotide functional groups, in combination with those of specific residues in the RecA protein, provide the molecular basis for the functional selectivity exhibited by the different classes of inhibitors and this has important implications as discussed below.

### **Structural bases for inhibition by ADP and ATP analogs**

In the first phase of our study on the interaction of nucleotide analogs with the RecA ATP-binding site, we demonstrated the exquisite sensitivity of the A-state conformation of RecA towards utilizing modified nucleotide triphosphates analogs as substrates for hydrolysis.<sup>[212]</sup> In the second phase of this study, we have extended these observations to non-substrate nucleotide di- and tri-phosphates and their abilities to discriminately bind and inhibit the inactive and inactive conformers of RecA. As described above, we identified two structural features of RecA's ATP-binding site in the inactive conformation that could be exploited for the design of selective ATP-competitive inhibitors. These features were the open, shallow cleft in which the adenine moiety binds and the internal cavity located near the ribose hydroxyl groups and protein residues Phe260, Ile262, and Tyr264. These features were respectively probed using *N*<sup>6</sup>-modified nucleotide analogs (Figure 3.8) and 2'(3')-modified nucleotide analogs (Figure 3.9). The relative efficacies of these nucleotide analogs for selectively binding the inactive RecA conformer and inhibiting active RecA-DNA filament assembly could be evaluated from the dispersion of data points in the horizontal dimension of the correlation plot (Figure 3.16). Both *N*<sup>6</sup>-modified (red symbols) and 2'(3')-

modified (blue symbols) ADP/ATP analogs span activities from 10% to nearly 100%. Taken together, these data provide evidence that both structural features can be exploited for the development of ATP-competitive RecA inhibitors.

We have observed that only  $N^6$ Ph-ATP and  $N^6$ Bn-ATP were efficient substrates for hydrolysis,<sup>[124]</sup> while ATP analogs bearing larger  $N^6$  substituents such as 1-naphthyl, 4-biphenyl, 1-tetrahydronaphthyl and 2-phenethyl do not serve as substrates. Most of the  $N^6$ -substituted ADP analogs were not efficacious as competitive inhibitors of ATP hydrolysis. (The exceptions are  $N^6$ Np-ADP and  $N^6$ AB-ADP.) These observations demonstrate that the ATP-binding site of the A-state RecA-DNA filament is exquisitely sensitive to the size of the substituent and only permits  $N^6$ -substituents of limited size. In contrast, the observation that  $N^6$ -substituted ADP analogs are all effective inhibitors of RecA-DNA filament assembly suggests that the ATP-binding site of the inactive RecA conformer accommodates large substituents at the 6-position of the purine heterocycle. This observation can be rationalized by examination of the crystallographic structure of the inactive filament and the pseudoatomic model of the active filament: in the inactive structure,  $N^6$  groups would be accommodated in a shallow cleft, while in the A-state filament such groups would create a steric clash with the residues from the neighboring RecA monomer that form the adenine-binding pocket. The ability to bind to and stabilize the inactive conformer of RecA prevents assembly of active RecA-DNA filaments in the conformational A state.

The efficacy of most of the  $N^6$ -substituted ADP analogs can be ascribed to the steric occlusion of RecA's ATP-binding site. An additional structural feature may be exploited by  $N^6$ AB-ADP, which is the only  $N^6$ -modified ADP bearing a formal positive charge on the substituent. We have previously hypothesized that Coulomb forces between adjacent

filament subunits, dominated by the negatively charged Asp100 residue of one RecA monomer and the positively charged Lys and Arg residues of its neighbor, regulate the transduction of ATP binding into conformational activation for DNA binding and higher-order processes.<sup>[234]</sup> We speculate that the ammonium cation of *N*<sup>6</sup>AB-ADP may disrupt electrostatic complementarity between adjacent RecA monomers, thereby preventing access to the fully active conformation of the filament.

In addition to the inhibitory activity effected by substituents on the purine heterocycle, the abilities of both pyrimidine and purine nucleotides to inhibit RecA's activities were extremely sensitive to modifications of the ribose. In particular, substituents at the ribose 2' position abrogated the abilities of NTPs to serve as RecA substrates and 2'(3')-substituted NDPs and NTPs were effective inhibitors of RecA ATPase activity. These observations may be rationalized by considering the proximity of the ADP 2'- and 3'-hydroxyl groups to the unusual cavity observed near residues Phe260, Ile262, and Tyr264 in the RecA-ADP cocrystal structure (Figure 3.4C). Of these residues, Tyr264 is the closest to the 2' and 3' positions of the ribose moiety and is part of a loop that connects RecA's ATPase domain with its C-terminal domain. It has been suggested that the C-terminal domain acts as regulatory switch that modulates RecA's DNA-binding and ATP-hydrolysis activities.<sup>[155, 186, 235-237]</sup> Moreover, analysis of low-resolution structures from EM have revealed that the state of the bound nucleotide is correlated with the relative orientation of the C-terminal domain, and Egelman and coworkers have speculated that allosteric coupling between the ATPase and C-terminal domains may be communicated in both directions.<sup>[6]</sup> We speculate that the Tyr264-containing tether may provide a means of transmitting allosteric information between the ATP binding site and the regulatory C-terminal domain. Nucleotides substituted at the 2'

position with groups at least as large as a methyl group could suppress the conformational changes in the Tyr264-containing tether that facilitate the rearrangement of the C-terminal domain.

It is interesting to note that substituents at the ribose 3' position are tolerated differently from those at the 2' position. For example, we observed that 3'-*O*-methyl-ATP is an efficient substrate for hydrolysis by RecA while its regioisomer, 2'*OMe*-ATP is not hydrolyzed at all.<sup>[212]</sup> In the present study, we noted that PrmTP, which is modified at the 3' position (Figure 3.9), is not an effective RecA inhibitor while 2'(3')-modified ADP and ATP analogs bearing ester or activated phenyl substituents that can migrate are generally effective. We hypothesize that the 2'-*O*-modified nucleotide is the high-affinity regioisomer, and experiments are underway to test this theory.

### **Implications for future rational modification procedures**

The purpose of the present study was to elucidate the structural requirements for the development of potent and selective ATP-competitive inhibitors of RecA. We identified two unusual structural features of the ATP-binding site of the inactive RecA conformer, and a number of nucleotide analogs were evaluated for their abilities to exploit these features. This approach tests a principle of negative design whereby inhibitor specificity is achieved by the introduction of substituents that prevent the formation of complexes with non-targeted enzymes. In addition, the evaluation of a range of substituents on the adenosine nucleotide scaffold was designed to identify inhibitor structure-activity relationships that would reveal new interactions with the protein's sidechains.

While modifications at both the  $N6$  and  $C2'$  positions of an adenylate nucleotide, which were directed to the shallow adenine-binding cleft and the internal cavity, respectively, produced effective inhibitors, the potency and conformational selectivity of the inhibition depended on the position of the substituent (see Figure 3.17). For example, while  $N^6$ Ph-ADP,  $N^6$ Np-ADP, and  $O^6$ Me-GTP were among the most effective inhibitors of RecA-DNA filament assembly, none of the three was more effective than ADP at inhibiting ATP hydrolysis. In contrast, TNP-ATP, TNP-ADP, and MANT-GDP were effective inhibitors of both filament assembly and ATPase activities. We tentatively conclude that this difference between the two groups arises from differences in their relative affinities for the ATP-binding site: 2'-modified nucleotides compete effectively with ATP under the experimental conditions whereas 6-modified nucleotides do not.

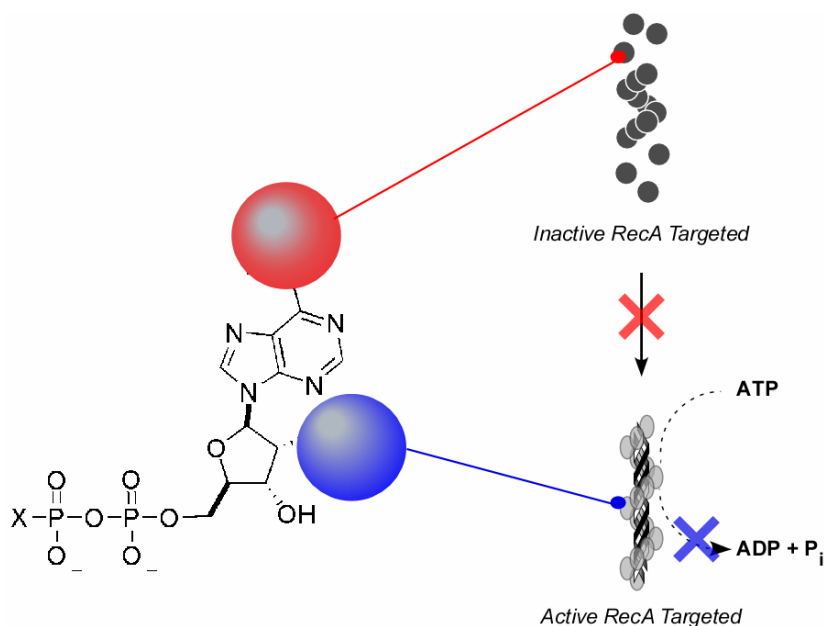


**Figure 3.17. Adenosine scaffold substitutions create conformationally selective inhibitors.** Large  $N^6$  modifications target the shallow adenine binding cleft and increase affinity for the inactive conformer. Large aromatic 2' modifications target an internal cavity in the ATP-binding site and increase affinity for the active conformer.

We speculate that  $\pi$ -stacking interactions between an aromatic group at the 2' position of a nucleotide analog and the phenol sidechain of Tyr264 may enhance the affinity of the nucleotide analog, allowing it to more effectively compete for the ATP-binding site. Nucleotides with smaller non-aromatic substituents at 2' (e.g., 2'OMe-ATP) or substituents at 3' (e.g., PrmTP) apparently interact with ATP-binding site of the inactive RecA conformer without garnering sufficient additional interactions to compete with ATP.

Substituents at the ribose 2' position lead to nucleotide analogs with enhanced abilities to inhibit RecA's activities relative to ADP. It is noteworthy that 2'(3')-modified purine nucleotides such as TNP-ATP and MANT-GTP also bind other ATP- and GTP-dependent enzymes.<sup>[219, 226, 238, 239]</sup> Thus, unless the affinity of a specific modified nucleotide is selectively enhanced for RecA, 2'(3') modifications are generally unlikely to afford selective RecA inhibitors.

Whereas nucleotide analogs bearing substituents at the 2' position can effectively compete with ATP for a common binding site on RecA, 6-modified nucleotide analogs do not. Indeed, the ATP-competitive ATPase inhibition constants ( $K_{ic}$ ) measured for such nucleotide analogs were essentially identical to the  $S_{0.5}$  value for ATP<sup>[198, 200, 240, 241]</sup> and within the range of  $K_d$  and  $K_i$  values for ADP.<sup>[198, 242, 243]</sup> The observation that the affinities of a variety of 6-substituted adenosine nucleotides, ADP, and ATP are similar recapitulates the guiding negative design principle.  $N^6$ -modified ATP analogs have been successfully used to control the functions of bioengineered (mutant) myosins, protein kinases, and kinesins.<sup>[204-206]</sup> In part, the utility of these compounds stems from the fact that they do not bind the wild-type enzymes. The superiority of  $N^6$ -substituted adenosine nucleotides for the inhibition of wild-type RecA likely results from its shallow surface crevice in which the modified



nucleotides are accommodated. This conclusion extends our preliminary observation that  $N^6$ Np-ADP (300  $\mu$ M) led to no reduction in the rates of the ATP hydrolysis reactions catalyzed by *E. coli* rho transcription terminator, chicken muscle myosin, and rabbit muscle pyruvate kinase.<sup>[202]</sup>

Taken together, the conclusions elaborated above suggest that substituents at the adenosine nucleotide ribose 2' position can lead to high-affinity ATP-competitive inhibitors of RecA while substituents at the purine 6 position can lead to high-specificity inhibitors. In the context of future rational modification procedures, it is interesting to note that MANT-GDP was characterized by more potent inhibitory activities than MANT-ATP or MANT-ADP. This suggests that the structural and energetic perturbations effected by ribose substituents may be coupled with those effected by purine substituents.

## **Conclusions**

In summary, we have thoroughly probed the ATP-binding site of RecA using nucleotide analogs and rapid microplate screening assays. As a result, we have identified two unusual structural features of the ATP-binding site of the inactive RecA conformer and discovered structure-activity patterns in the binding profiles of RecA to nucleotide analogs with inhibitory implications. Non-substrate nucleotide analogs were readily segregated into two classes based on their activities in the complementary pair of molecular screening assays: (1) those that preferentially bind the active RecA-DNA filament and competitively inhibit ATP hydrolysis; (2) those that preferentially bind the inactive RecA conformation and inhibit RecA-DNA filament assembly.

The development of inhibitors of RecA remains an important step towards fully understanding the roles of RecA within bacterial pathogens. Importantly, the abilities of inhibitors in the first class to modulate the ATP turnover that is required for RecA's recombinational motor activities would allow the motor-like function of RecA to be segregated from its signal-like functions. In contrast, those inhibitors of the second class possessing sufficient affinity to compete with ATP for a common binding site will abrogate both signaling and processive recombinational activities of RecA.

A further product of this effort was the elucidation of structural requirements for the development of potent and selective ATP-competitive inhibitors of RecA. Indeed, key nucleotide functional groups, in combination with those of specific residues in the RecA protein, were identified as providing the molecular basis for the functional selectivity exhibited by the different classes of inhibitors.

These structure-activity relationships may be exploited in future rational modification procedures for the synthesis of microbiological tools to tease apart the roles of RecA in various aspects of pathogenicity. We envision that such inhibitors may be developed into novel adjuvants for antibiotic chemotherapy that moderate the development and transmission of antibiotic resistance genes and increase the antibiotic therapeutic index.

## **Materials and Methods**

*Source of nucleotides used in this work.* The compounds used in this project were obtained from the commercial sources listed in the following table or were synthesized as described below.

**Table 3.2. Commercial Sources of Nucleotides Used**

<b>Nucleotide</b>	<b>Source</b>
ATP	<i>Sigma-Aldrich</i>
dATP	<i>Sigma-Aldrich</i>
Ara-ATP	<i>Tri-Link Biotechnologies</i>
8-Br-ATP	<i>Sigma-Aldrich</i>
2'-F-ATP	<i>Tri-Link Biotechnologies</i>
2'NH <sub>2</sub> -ATP	<i>Tri-Link Biotechnologies</i>
2'OMe-ATP	<i>Tri-Link Biotechnologies</i>
3'OMe-ATP	<i>Tri-Link Biotechnologies</i>
MANT-ATP	<i>AXXORA</i>
Bz-ATP	<i>Sigma-Aldrich</i>
TNP-ATP	<i>AXXORA</i>
N <sup>6</sup> Bn-ATP	<i>AXXORA</i>
N <sup>6</sup> Ph-ATP	<i>AXXORA</i>
PrmTP	<i>Tri-Link Biotechnologies</i>
6-Cl-PTP	<i>Tri-Link Biotechnologies</i>
ATPyS	<i>Sigma-Aldrich</i>
ATPyS-BODIPY	<i>Molecular Probes</i>
ATPyS-AmNS	<i>Molecular Probes</i>
BODIPY-AMPPNP	<i>Sigma-Aldrich</i>
MANT-AMPPNP	<i>Molecular Probes</i>
ADP	<i>Sigma-Aldrich</i>
MANT-ADP	<i>AXXORA</i>
BODIPY-ADP	<i>Molecular Probes</i>
TNP-ADP	<i>Molecular Probes</i>
N <sup>6</sup> -PE-ADP	<i>AXXORA</i>
N <sup>6</sup> -Bn-ADP	<i>AXXORA</i>
N <sup>6</sup> -Ph-ADP	<i>AXXORA</i>
α,β-CH <sub>2</sub> -ADP	<i>AXXORA</i>
AMP	<i>Sigma-Aldrich</i>
butyryl-cAMP	<i>Sigma-Aldrich</i>
dibutyryl-cAMP	<i>Sigma-Aldrich</i>
GTP	<i>Sigma-Aldrich</i>
dGTP	<i>Sigma-Aldrich</i>
O-Me-GTP	<i>Tri-Link Biotechnologies</i>
GDP	<i>Sigma-Aldrich</i>
MANT-GDP	<i>AXXORA</i>
ITP	<i>Sigma-Aldrich</i>
dITP	<i>Sigma-Aldrich</i>
IDP	<i>Sigma-Aldrich</i>
UTP	<i>Sigma-Aldrich</i>
5-Me-UTP	<i>Tri-Link Biotechnologies</i>

5-propynyl-dUTP	<i>Tri-Link Biotechnologies</i>
TTP	<i>Sigma-Aldrich</i>
TDP	<i>Sigma-Aldrich</i>
CTP	<i>Sigma-Aldrich</i>
dCTP	<i>Sigma-Aldrich</i>
5-Me-CTP	<i>Tri-Link Biotechnologies</i>
CDP	<i>Sigma-Aldrich</i>

*Synthesis of 5'-modified nucleotide analogs.*

*2',3'-O-Isopropyliden-5'-O-(4-sulfamoylbenzoyl)adenosine*: To a well-stirred, ice-cooled solution of 2',3'-*O*-isopropylidene adenosine (1.226 g, 3.99 mmol) and 4-sulfonamidobenzoic acid (0.883 g, 4.39 mmol) in anhydrous DMF (10 mL) was added DMAP (0.049 g, 0.399 mmol). Then a solution of DCC (0.905 g, 4.39 mmol) in DMF (2 mL) was added dropwise. The ice-bath was removed and the reaction mixture was warmed to room temperature and stirred for 14 h. The white precipitate was filtered and washed with DMF (5 mL). The filtrate was diluted with chloroform (50 mL) and water (100 mL). The organic layer was separated, washed with water (3 x 100 mL) and concentrated on a rotary evaporator to about 50 mL when the product precipitated as white solid. This was filtered, dried and used in the next step without further purification (1.267 g, 2.58 mmol, 65%).  $R_f$  (CH<sub>3</sub>OH/CH<sub>2</sub>Cl<sub>2</sub>: 10/90) = 0.438. <sup>1</sup>H NMR (300 MHz, DMSO-*d*<sub>6</sub>):  $\delta$  = 8.31 (s, 1H), 8.13 (s, 1H), 8.09 (dd,  $J$  = 8.8, 1.9 Hz, 2H), 7.94 (dd,  $J$  = 8.8, 1.9 Hz, 2H), 7.59 (s, 2H), 7.37 (s, 2H), 6.23 (d,  $J$  = 2.5 Hz, 1H), 5.56 (dd,  $J$  = 6.3, 2.5 Hz, 1H), 5.21 (dd,  $J$  = 6.3, 3.3 Hz, 1H), 4.62–4.45 (m, 3H), 1.57 (s, 3H), 1.36 (s, 3H). <sup>13</sup>C NMR (75 MHz, DMSO-*d*<sub>6</sub>):  $\delta$  = 164.3, 156.0, 152.6, 148.7, 148.0, 139.8, 131.9, 129.9, 125.9, 119.1, 113.5, 89.0, 83.3, 83.0, 80.7, 79.1, 64.6, 26.9, 25.2. ESI-MS:  $m/z$  491.5 [M+H]<sup>+</sup>, 513.0 [M+Na]<sup>+</sup>.

*5'-O-(4-Sulfamoylbenzoyl)adenosine*: 2',3'-*O*-Isopropylidene-5'-*O*-(4-sulfamoylbenzoyl)-adenosine (0.664 g, 1.35 mmol) was dissolved in trifluoroacetic acid (9 mL) and water (1 mL), and the resulting solution was stirred at room temperature for 1 h. The excess of trifluoroacetic acid was removed by blowing argon gas through the flask. The remaining reaction mixture was neutralized with concentrated ammonium hydroxide solution, concentrated in vacuo, dissolved in methanol and purified by flash chromatography using 10-12% CH<sub>3</sub>OH/CH<sub>2</sub>Cl<sub>2</sub> to afford the desired product as light yellow solid (0.421 g, 0.935 mmol, 69%).  $R_f$  (CH<sub>3</sub>OH/CH<sub>2</sub>Cl<sub>2</sub>: 10/90) = 0.111. <sup>1</sup>H NMR (300 MHz, CD<sub>3</sub>OD):  $\delta$  = 8.28 (s, 2H), 8.26 (s, 1H), 8.23 (s, 2H), 8.09 (s, 1H), 8.07 (d,  $J$  = 8.8 Hz, 2H), 7.95 (d,  $J$  = 8.8 Hz, 2H), 6.02 (d,  $J$  = 4.1 Hz, 1H), 4.75 (dd,  $J$  = 12.0, 3.3 Hz, 1H), 4.63–4.55 (m, 2H), 4.38–4.37 (m, 1H), 3.34 (s, 1H). <sup>13</sup>C NMR (75 MHz, CD<sub>3</sub>OD):  $\delta$  = 166.4, 165.6, 156.1, 152.0, 151.1, 149.2, 142.3, 134.2, 131.2, 127.4, 91.0, 83.5, 74.9, 71.8, 65.4. ESI-MS:  $m/z$  451.0 [M+H]<sup>+</sup>.

*N*<sup>6</sup>-*naphthyl-2',3'-O-benzylidene adenosine*: To a well-stirred suspension of *N*<sup>6</sup>-naphthyladenosine (0.491 g, 1.25 mmol) and benzaldehydedimethyl acetal (0.94 mL, 6.24 mmol) in anhydrous acetonitrile at 0 °C was added freshly distilled POCl<sub>3</sub> (0.23 mL, 2.50 mmol) dropwise. The resulting yellow coloured suspension was stirred at 0 °C for 1 h and upon warming to room temperature fully dissolved to yield a yellow solution. Stirring was continued for the next 1 h when, TLC examination showed that the starting material had completely disappeared. At this point saturated aqueous NaHCO<sub>3</sub> solution was added (100 mL). The solution was extracted with EtOAc (3 x 50 mL), and the combined organic layer was washed with brine, dried over Na<sub>2</sub>SO<sub>4</sub> and concentrated by rotoevaporation. The crude residue was then purified by flash chromatography on silica gel using EtOAc to obtain the desired product as white foam (0.376 g, 0.781 mmol, 63%),  $R_f$  (EtOH/EtOAc: 2/98) = 0.531.

$^1\text{H}$  NMR (300 MHz,  $\text{CDCl}_3$ ):  $\delta$  = 8.42 (s, 1H), 8.21 (s, 1H), 8.05–8.01 (m, 2H), 7.91–7.89 (m, 1H), 7.83 (s, 1H), 7.79 (d,  $J$  = 8.2 Hz, 1H), 7.60–7.47 (m, 8H), 6.66 (dd,  $J$  = 11.5, 1.9 Hz, 1H), 6.08 (s, 1H), 6.01 (d,  $J$  = 4.9 Hz, 1H), 5.38 (dd,  $J$  = 6.0, 4.9 Hz, 1H), 5.24 (dd,  $J$  = 6.3, 0.8 Hz, 1H), 4.73 (s, 1H), 4.05–4.00 (m, 1H), 3.89–3.84 (m, 1H).  $^{13}\text{C}$  NMR (75 MHz,  $\text{CDCl}_3$ ):  $\delta$  = 154.1, 152.8, 148.2, 140.5, 135.9, 134.4, 132.6, 130.0, 128.7, 128.6, 128.4, 126.6, 126.5, 126.4, 126.2, 125.7, 122.0, 121.9, 121.5, 107.6, 94.0, 85.6, 83.9, 82.9, 77.2, 63.4. ESI-MS:  $m/z$  482.2  $[\text{M}+\text{H}]^+$ .

*cyclo-Saligenyl-5'-O-[(N<sup>6</sup>-1-naphthyl)-2',3'-O-benzylideneadenosine]-phosphate*: To a well-stirred solution of *N<sup>6</sup>-(1-naphthyl)-2',3'-O-benzylideneadenosine* (0.311 g, 0.646 mmol) in anhydrous acetonitrile (10 mL) at 0 °C was added *cyclo-salphosphoramidite* (0.360 g, 1.42 mmol) causing the clear solution to become turbid. Then, imidazolium triflate (0.564 g, 2.58 mmol) was added with continued stirring and within 10 min the reaction mixture turned clear. Then stirring was continued for the next 1.5 h at 0 °C when a TLC examination showed complete disappearance of the starting adenosine derivative. Then, *tert*-butylhydroperoxide (0.15 mL, 1.36 mmol) was added dropwise and stirring was continued at 0 °C for 1 h at which point reaction was found to be incomplete as seen from TLC. Hence, an additional 0.1 mL (0.7 eq) of *tert*-butylhydroperoxide was added and stirring continued for 30 min when the reaction went to completion. Concentration of the solvent followed by flash chromatography (silica gel, EtOAc) afforded the desired product as white solid (0.203 g, 0.313 mmol, 49%),  $R_f$  (EtOH/EtOAc: 1/99) = 0.611.  $^1\text{H}$  NMR (two diastereomers, 300 MHz,  $\text{CDCl}_3$ ):  $\delta$  = 8.41 (s, 1H), 8.40 (s, 1H), 8.20 (d,  $J$  = 7.1 Hz, 1H), 8.09 (d,  $J$  = 6.9 Hz, 1H), 8.10–8.04 (m, 2H), 7.90 (d,  $J$  = 6.3 Hz, 1H), 7.86 (s, 1H), 7.85 (s, 1H), 7.80 (d,  $J$  = 6.6 Hz, 1H), 7.59–7.40 (m, 18H), 7.23–6.88 (m, 7H), 7.06 (dd,  $J$  = 6.3, 1.1 Hz, 1H), 6.23 (dd,  $J$  =

3.6, 1.9 Hz, 1H), 6.16 (dd,  $J = 3.3, 1.9$  Hz, 1H), 6.03 (s, 1H), 6.01 (s, 1H), 5.68 (dd,  $J = 6.6, 1.9$  Hz, 1H), 5.64 (dd,  $J = 6.6, 1.9$  Hz, 1H), 5.27–5.15 (m, 8H), 4.49–4.42 (m, 4H).  $^{31}\text{P}$  NMR (120 MHz,  $\text{CDCl}_3$ ):  $\delta = -8.42, -8.47, -8.50$  and  $-8.56$  (4s, diastereomeric mixture). ESI-MS:  $m/z$  672.2  $[\text{M}+\text{Na}]^+$ .

*cyclo-Saligenyl-5'-O-[(N<sup>6</sup>-1-naphthyl)adenosine]phosphate*: To a well-stirred solution of *cyclo-Saligenyl-5'-O-[(N<sup>6</sup>-1-naphthyl)-2',3'-O-benzylideneadenosine]phosphate* (0.053 g, 0.082 mmol) in methanol (3 mL) at room temperature was added 2 mL of trifluoroacetic acid (50% aqueous solution). The resulting solution was stirred overnight, until a TLC examination showed the reaction to be complete. The solvent was removed and the residue was purified by flash chromatography (silica gel,  $\text{CH}_3\text{OH}/\text{CH}_2\text{Cl}_2$ : 5/95) to afford the product as oil (0.028 g, 0.05 mmol, 61%),  $R_f$  ( $\text{CH}_3\text{OH}/\text{CH}_2\text{Cl}_2$ : 5/95) = 0.163.  $^1\text{H}$  NMR (300 MHz,  $\text{DMSO}-d_6$ ):  $\delta = 9.10$  (s, 1H), 8.50 (s, 1H), 8.49 (s, 1H), 8.16 (d,  $J = 7.4$  Hz, 1H), 8.01–7.99 (m, 1H), 7.92 (d,  $J = 8.0$  Hz, 1H), 7.63–7.43 (m, 4H), 7.23–7.01 (m, 4H), 5.94 (d,  $J = 5.2$  Hz, 1H), 5.51–5.50 (m, 1H), 5.35 (s, 1H), 5.24–5.22 (m, 1H), 5.22–5.19 (m, 2H), 3.80–3.62 (m, 3H).  $^{31}\text{P}$  NMR (120 MHz,  $\text{DMSO}-d_6$ ):  $\delta = -5.49$  and  $-5.52$  (2s, diastereomeric mixture). ESI-MS:  $m/z$  562.2  $[\text{M}+\text{H}]^+$ .

### Synthesis of N<sup>6</sup>-modified nucleotide analogs

*General methods for the preparation of N<sup>6</sup>-modified adenosines*: <sup>[244]</sup> 6-Chloro-2',3'-bis(*O*-Benzoyl)Adenosine was prepared according to the previously reported procedures <sup>[245, 246]</sup> Analysis of the product ( $^1\text{H}$  NMR in  $\text{CDCl}_3$ ) was identical to previously reported data.<sup>[246]</sup> The corresponding amine (4.85 mmol, 6.0 eq) was added to a stirred suspension of 6-chloro-2',3'-bis(*O*-benzoyl)adenosine (1) (0.4 g, 0.8 mmol, 1.0 eq) in ethanol (10 mL). The reaction

mixture was refluxed for 3–11 h, and then cooled to room temperature to crystallize the product. If crystallization did not occur upon cooling to room temperature, the reaction mixture was placed at 4 °C overnight to encourage crystallization. The crystallized product was filtered and washed with cold ethanol and hexanes. The analytical data (<sup>1</sup>H NMR, <sup>13</sup>C NMR and ESI-MS) for each *N*<sup>6</sup>-substituted adenosine derivative is shown below.

*N*<sup>6</sup>-[1-(1,2,3,4-Tetrahydronaphthyl)]adenosine-2',3'-O-dibenzoate: Light pink solid (0.334 g, 0.55 mmol, 68%). <sup>1</sup>H NMR (300 MHz, DMSO-*d*<sub>6</sub>): δ = 8.49 (s, 1H), 8.33 (s, 1H), 8.25 (d, *J* = 8.2 Hz, 1H), 8.01 (d, *J* = 7.1 Hz, 2H), 7.82 (d, *J* = 7.1 Hz, 2H), 7.71 (t, *J* = 7.4 Hz, 1H), 7.66–7.49 (m, 3H), 7.45–7.36 (m, 2H), 7.24–7.02 (m, 4H), 6.59 (d, *J* = 6.6 Hz, 1H), 6.34 (t, *J* = 6.0 Hz, 1H), 5.95 (dd, *J* = 5.5, 2.2 Hz, 2H), 5.66 (s, 1H), 4.58 (d, *J* = 2.2 Hz, 1H), 3.94–3.76 (m, 1H), 2.84–2.7 (m, 2H), 2.1–1.68 (m, 4H). <sup>13</sup>C NMR (75 MHz, DMSO-*d*<sub>6</sub>): δ = 164.9, 164.4, 154.4, 152.8, 139.8, 137.9, 134.0, 129.4, 129.3, 128.9, 128.7, 128.3, 127.7, 126.6, 125.7, 85.9, 84.0, 73.4, 72.5, 61.4, 48.3, 47.7, 29.6, 28.9. ESI-MS: *m/z* 606.1 [M+H<sup>+</sup>].

*N*<sup>6</sup>-(4-Phenylbenzyl)adenosine-2',3'-O-dibenzoate: White solid (0.50 g, 0.78 mmol, 96%). <sup>1</sup>H NMR (300 MHz, DMSO-*d*<sub>6</sub>) δ = 8.66 (s, 1H), 8.52 (s, 1H), 8.29 (s, 1H), 8.00 (dd, *J* = 7.1, 1.4 Hz, 2H), 7.79 (dd, *J* = 8.2, 1.4 Hz, 2H), 7.73–7.66 (m, 1H), 7.65–7.50 (m, 7H), 7.48–7.30 (m, 7H), 6.57 (d, *J* = 6.6 Hz, 1H), 6.32 (t, *J* = 6.1 Hz, 1H), 5.94 (dd, *J* = 5.3, 2.5 Hz, 1H), 5.87 (dd, *J* = 7.1, 4.7 Hz, 1H), 4.82–4.70 (m, 2H), 4.56 (q, *J* = 2.8 Hz, 1H), 3.92–3.74 (m, 2H). <sup>13</sup>C NMR (75 MHz, DMSO-*d*<sub>6</sub>) δ = 164.8, 164.4, 154.6, 152.7, 148.4, 140.0, 139.9, 139.1, 138.6, 133.9, 129.3, 129.2, 128.8, 128.7, 128.2, 127.7, 127.2, 126.6, 126.5, 119.8, 85.9, 84.0, 73.4, 72.4, 61.3, 42.6. ESI-MS: *m/z* 642.2 [M+H<sup>+</sup>].



*N*<sup>6</sup>-(4-Biphenyl)adenosine-2',3'-O-dibenzoate: White solid from CH<sub>2</sub>Cl<sub>2</sub>/hexanes (0.230 g, 0.43 mmol, 53%). <sup>1</sup>H NMR (300 MHz, CDCl<sub>3</sub>) δ = 8.56 (s, 1H), 8.24–8.00 (m, 3H), 7.96–7.79 (m, 5H), 7.68–7.26 (m, 13H), 6.79 (d, *J* = 10.2 Hz, 1H), 6.51–6.42 (m, 1H), 6.30 (d, *J* = 7.4 Hz, 1H), 6.10 (d, *J* = 5.2 Hz, 1H), 4.63 (s, 1H), 4.18–3.94 (m, 2H). <sup>13</sup>C NMR (75 MHz, CDCl<sub>3</sub>) δ = 165.6, 165.0, 152.9, 148.6, 140.8, 140.5, 137.6, 137.1, 133.9, 130.0, 129.4, 129.0, 128.8, 128.7, 127.9, 127.3, 127.1, 122.2, 121.2, 89.3, 86.8, 73.8, 73.7, 63.0. ESI-MS: *m/z* 628.2 [M+H<sup>+</sup>], 650.1 [M+Na<sup>+</sup>].

*N*<sup>6</sup>-(2-Naphthyl)adenosine-2',3'-O-dibenzoate: White solid from CH<sub>2</sub>Cl<sub>2</sub>/hexanes (0.307 g, 0.51 mmol, 56%). <sup>1</sup>H NMR (300 MHz, CDCl<sub>3</sub>) δ = 8.58 (s, 1H), 8.44 (d, *J* = 1.9 Hz, 1H), 8.41 (s, 1H), 8.10–8.03 (m, 2H), 7.92 (s, 1H), 7.88–7.72 (m, 6H), 7.66–7.26 (m, 8H), 6.45 (dd, *J* = 7.7, 5.5 Hz, 1H), 6.30 (d, *J* = 7.7 Hz, 1H), 6.10 (dd, *J* = 5.5, 1.1 Hz, 1H), 4.94 (s, 1H), 4.63 (d, *J* = 1.1 Hz, 1H), 4.14–3.95 (m, 2H). <sup>13</sup>C NMR (75 MHz, CDCl<sub>3</sub>): δ = 165.6, 165.0, 152.9, 148.5, 140.4, 135.9, 134.1, 133.9, 130.7, 129.9, 129.4, 129.0, 128.8, 128.6, 127.9, 127.8, 126.7, 125.1, 122.1, 121.0, 117.4, 89.2, 86.8, 73.8, 62.9. ESI-MS: *m/z* 602.1 [M+H<sup>+</sup>].

*N*<sup>6</sup>-(1-Naphthyl)adenosine-2',3'-O-dibenzoate: White solid from EtOH (0.236 g, 0.392 mmol, 49%). <sup>1</sup>H NMR (300 MHz, DMSO-*d*<sub>6</sub>): δ = 10.16 (s, 1H), 8.62 (s, 1H), 8.20 (s, 1H), 7.99 (t, *J* = 7.4 Hz, 3 H), 7.94–7.85 (m, 3H), 7.82 (d, *J* = 7.1 Hz, 2H), 7.75–7.37 (m, 10H), 6.61 (d, *J* = 6.6 Hz, 1H), 6.35 (t, *J* = 5.8 Hz, 1H), 5.96 (dd, *J* = 2.8, 2.8 Hz, 1H), 4.58 (d, *J* = 2.8 Hz, 1H), 3.92–3.76 (m, 2H). <sup>13</sup>C NMR (75 MHz, DMSO-*d*<sub>6</sub>): δ = 164.8, 164.4, 154.3, 152.3, 149.3, 140.5, 134.4, 133.9, 133.8, 130.0, 129.3, 129.2, 128.8, 128.7, 128.2, 128.0,

126.2, 126.0, 125.9, 125.6, 124.3, 123.4, 119.9, 85.8, 83.9, 73.4, 72.3, 61.3. ESI-MS:  $m/z$  602.2 [M+H<sup>+</sup>], 624.4 [M+Na<sup>+</sup>].

*General procedure for the preparation of the N<sup>6</sup>-substituted adenosine triphosphates<sup>[247]</sup>*: A solution of salicylphosphochloridite (55.6 mg, 0.275 mmol, 1.1 eq) in CH<sub>2</sub>Cl<sub>2</sub> (0.4 mL) was slowly added dropwise under argon to a solution of the corresponding N<sup>6</sup>-substituted adenosine derivative (0.25 mmol, 1.0 eq) in DMF (1.5 mL) and pyridine (0.1 mL). The reaction mixture was stirred for 15 min and then a freshly prepared 0.5 M solution of bis(tri-*n*-butylammonium)pyrophosphate (0.375 mmol, 1.5 eq) in DMF and tri-*n*-butylamine (0.24 mL, 1 mmol, 4.0 eq) were simultaneously injected into the reaction flask. The reaction mixture was stirred for 10 min followed by addition of a 5.0–6.0 M solution of *tert*-butyl hydroperoxide in decane (0.06 mL, 0.275 mmol, 1.1 eq). The reaction mixture was stirred at room temperature for 1 h, then de-ionized water (1 mL) was added and the organic solvents were removed by rotoevaporation. The reaction mixture was diluted with de-ionized water (10 mL) and extracted with diethyl ether (3 x 10 mL). The aqueous layer was frozen and lyophilized. A solution of aqueous ammonia (7 mL) was added to the lyophilized residue and the reaction mixture was stirred overnight at room temperature. After rotoevaporation of the solvent, the residue was purified by the ion-exchange chromatography (DEAE DE-52 cellulose, 0.005–1.0 M ammonium bicarbonate buffer, pH 8). The nucleotide-containing fractions were frozen and lyophilized. The solid was dissolved in de-ionized water and subjected to a salt exchange column (Dowex 50WX8-200, Na<sup>+</sup> form). The aqueous solution containing the sodium salt of the NTP analog was frozen and lyophilized. The analytical data (<sup>1</sup>H NMR, <sup>31</sup>P NMR and ESI-MS) for each N<sup>6</sup>-substituted adenosine triphosphate analog is shown below.

$N^6$ -[1-(1,2,3,4-Tetrahydronaphthyl)]adenosine-5'-O-triphosphate: White solid (0.035 g, 0.056 mmol, 22%).  $^1H$  NMR (300 MHz,  $D_2O$ ):  $\delta$  = 8.39 (s, 1H), 8.23 (s, 1H), 7.28–6.85 (m, 4H), 6.11 (d,  $J$  = 5.5 Hz, 0.2H), 6.06 (d,  $J$  = 5.8 Hz, 0.8H), 5.26 (s, 1H), 4.80–4.66 (m, 2H), 4.59 (t,  $J$  = 4.7 Hz, 1H), 4.48–4.40 (m, 1H), 4.38–4.28 (m, 2H), 2.88–2.60 (m, 2H), 2.04–1.75 (m, 4H).  $^{31}P$  NMR (120 MHz,  $D_2O$ ):  $\delta$  = -8.32 (d,  $J$  = 18.9 Hz), -9.29 (d,  $J$  = 19.9 Hz), -20.64 (t,  $J$  = 19.4 Hz). ESI-MS:  $m/z$  726.4  $[M+H^+]$ .

$N^6$ -(4-Phenylbenzyl)adenosine-5'-O-triphosphate: White solid (0.009 g, 0.013 mmol, 5%).  $^1H$  NMR (300 MHz,  $D_2O$ ):  $\delta$  = 8.46 (s, 1H), 8.10 (s, 1H), 7.54–7.30 (m, 10H), 6.05 (d,  $J$  = 4.9 Hz, 1H), 4.80–4.64 (m, 3H), 4.62–4.54 (m, 1H), 4.44–4.36 (m, 1H), 4.36–4.20 (m, 2H);  $^{31}P$  NMR (120 MHz,  $D_2O$ ):  $\delta$  = -7.60 (d,  $J$  = 17.8 Hz), -10.16 (d,  $J$  = 19.6 Hz), -21.43 (t,  $J$  = 19.5 Hz). ESI-MS:  $m/z$  762.0  $[M+H^+]$ .

$N^6$ -(4-Biphenyl)adenosine-5'-O-triphosphate: White solid (0.061 g, 0.083 mmol, 33%).  $^1H$  NMR (300 MHz,  $D_2O$ ):  $\delta$  = 8.38 (s, 1H), 7.99 (s, 1H), 7.26–7.02 (m, 9H), 5.92 (d,  $J$  = 3.6 Hz, 1H), 4.68–4.44 (m, 2H), 4.43–4.22 (m, 3H).  $^{31}P$  NMR (120 MHz,  $D_2O$ ):  $\delta$  = -8.14 (d,  $J$  = 17.8 Hz), -9.96 (d,  $J$  = 20.76 Hz), -21.06 (t,  $J$  = 17.8 Hz). ESI-MS:  $m/z$  749.1  $[M+H^+]$ , 770.9  $[M+Na^+]$ .

$N^6$ -(2-Naphthyl)adenosine-5'-O-triphosphate: White solid (0.014 g, 0.020 mmol, 8%).  $^1H$  NMR (300 MHz,  $D_2O$ ):  $\delta$  = 8.44 (s, 1H), 8.04 (s, 1H), 7.93 (s, 1H), 7.70–7.54 (m, 3H), 7.47 (d,  $J$  = 9.1 Hz, 1H), 7.38–7.26 (m, 2H), 6.00 (d,  $J$  = 5.2 Hz, 1H), 4.80–4.73 (m, 1H), 4.63 (t,  $J$  = 3.8 Hz, 1H), 4.46–4.39 (m, 1H), 4.37–4.22 (m, 2H).  $^{31}P$  NMR (120 MHz,  $D_2O$ ):  $\delta$  = -6.67 (d,  $J$  = 20.8 Hz), -10.05 (d,  $J$  = 17.8 Hz), -20.99 (t,  $J$  = 20.8 Hz). ESI-MS:  $m/z$  722.0  $[M+H^+]$ , 743.9  $[M+Na^+]$ .

*N*<sup>6</sup>-(1-Naphthyl)adenosine-5'-O-triphosphate: White solid (0.069 g, 0.095 mmol, 38%). <sup>1</sup>H NMR (300 MHz, D<sub>2</sub>O):  $\delta$  = 8.47 (s, 1H), 7.84 (s, 2H), 7.81–7.64 (m, 2H), 7.57 (d, *J* = 7.1 Hz, 1H), 7.50–7.34 (m, 3H), 6.06 (d, *J* = 5.2 Hz, 1H), 4.82–4.62 (m, 2H), 4.50–4.22 (m, 3H). <sup>31</sup>P NMR (120 MHz, D<sub>2</sub>O):  $\delta$  = -4.72 (d, *J* = 20.8 Hz), -9.87 (d, *J* = 20.8 Hz), -20.23 (t, *J* = 20.8 Hz). ESI-MS: *m/z* 722.0 [M+H<sup>+</sup>], 744.0 [M+Na<sup>+</sup>].

<sup>1</sup>H and <sup>13</sup>C NMR were recorded using a Varian Gemini 300 MHz spectrometer and <sup>31</sup>P NMR were recorded using a Varian 500 spectrometer. Electrospray ionization mass spectroscopy (ESI-MS) was recorded using a Thermofinnigan ion trap detection instrument.

### ***Other reagents***

The *E. coli* RecA protein was purified as described<sup>[159]</sup> to  $\geq 97\%$  homogeneity and stored in aqueous buffer (25 mM Tris·HCl, pH 7.5, 1 mM DTT, 5% glycerol) at  $-80$  °C. The protein concentration was determined using the monomer extinction coefficient  $2.2 \times 10^4 \text{ M}^{-1} \cdot \text{cm}^{-1}$  at 280 nm.<sup>[248]</sup> The EnzChek Phosphate Assay Kit, which includes purine nucleoside phosphorylase enzyme (PNP) and 7-methyl-thioguanosine substrate (MESG), was purchased from Invitrogen (Carlsbad, CA). Poly(dT) ssDNA (average length = 319 nts) was purchased from Amersham Biosciences (Piscataway, NJ). Biotin-(dT)<sub>36</sub> was purchased desalted from Sigma Genosys (The Woodlands, TX) and used without further purification. Streptavidin Paramagnetic Particles (SA-PMP) were from Promega (Hercules, CA). Clear 96-well flat-bottom microplates were purchased from Evergreen Scientific (Los Angeles, CA). Unless otherwise stated all reagents used in the synthesis of the nucleotide analogs were obtained

from Sigma-Aldrich (St. Louis, MO). All solvents employed in the reactions were obtained from Sigma-Aldrich (St. Louis, MO) and anhydrous solvents were used without distillation.

### ***Assays & other procedures***

*Nucleotide Triphosphate Hydrolysis Assays.* The hydrolysis of NTPs by RecA was measured using a published enzyme-coupled continuous spectrophotometric assay for inorganic phosphate release.<sup>[190]</sup> Reactions (100  $\mu\text{L}$  final volume) were initiated in a 96-well microplate by adding a pre-incubated solution containing 0.5  $\mu\text{M}$  RecA, 10 mM  $\text{Mg}(\text{OAc})_2$ , 1 mM DTT, 15  $\mu\text{M}$ -nts poly(dT), 0.3 mM MESG, and 1 U/mL PNP in 25 mM Tris·HOAc, pH 7.5 at 25  $^\circ\text{C}$ , 5% (v/v) glycerol, to various concentrations of nucleotide triphosphate (0 – 1000  $\mu\text{M}$ ). The  $A_{360}$  was monitored every 30 s in the microplate reader at 37  $^\circ\text{C}$  for 30 min using a Perkin-Elmer HTS 7000+ Bioassay Reader with a  $360 \pm 5$  nm bandpass filter. The initial, steady-state reaction velocity ( $v_{\text{obs}}^{\circ}$ ,  $\mu\text{M}\cdot\text{min}^{-1}$ ) for each NTP was calculated from the change in absorbance as a function of time ( $\partial A/\partial t$ ) using  $\Delta\epsilon_{360} = 6.0 \times 10^{-4}$   $\mu\text{M}^{-1}$  as measured in the microplate reader. Each set of data, corresponding to a range of NTP concentrations, was analyzed using a Michaelis-Menten equation modified for substrate cooperativity as described previously<sup>[162, 163]</sup>:

$$v_{\text{obs}}^{\circ} = k_{\text{cat}} \cdot R_0 \cdot \frac{[\text{NTP}]^3}{[\text{NTP}]^3 + S_{0.5}^3} \quad (1)$$

where  $R_0$  is the total concentration of RecA and  $S_{0.5}$  is the [NTP] when the velocity is half of its maximum value.

*Inhibition of ATPase Activity by Selected Nucleotides.* A solution containing 0.5  $\mu\text{M}$  RecA, 100  $\mu\text{M}$  nucleotide, 10 mM  $\text{Mg}(\text{OAc})_2$ , 1 mM DTT, 0.3 mM MESG and 1 U/mL PNP in 25 mM  $\text{Tris}\cdot\text{HOAc}$ , pH 7.5 at 25  $^\circ\text{C}$ , with 5% (v/v) glycerol for 5 min at 37  $^\circ\text{C}$ . The ATPase reactions were initiated by the addition of a solution containing ATP and poly(dT) (500  $\mu\text{M}$  and 1.5  $\mu\text{M}$ -nts final concentrations, respectively) to achieve a final reaction volume of 600  $\mu\text{L}$ . The change in  $A_{360}$  was recorded for 30 min at 37  $^\circ\text{C}$  in a Perkin Elmer Lambda 20 UV/Vis spectrophotometer with a thermostated 6-cell changer regulated by a Peltier temperature control system. The  $v^\circ_{\text{obs}}$  values were determined using  $\Delta\varepsilon_{360} = 1.1 \times 10^4 \text{ M}^{-1}\cdot\text{cm}^{-1}$  and the % inhibition was calculated relative to the velocity in the absence of any added inhibitor using the following equation:

$$\% \text{inhibition} = \left( 1 - \frac{V_{\text{inh}}}{V_{\text{none}}} \right) \times 100 \quad (2)$$

where  $V_{\text{inh}}$  is the velocity of the reaction in the presence of inhibitor and  $V_{\text{none}}$  is the velocity of the reaction in the absence of added inhibitor.

*Inhibition of ssDNA Binding by Selected Nucleotides.* RecA (4  $\mu\text{M}$ ) was incubated at 37  $^\circ\text{C}$  for 20 min with 100  $\mu\text{M}$  nucleotide, 18  $\mu\text{M}$ -nts biotin-(dT)<sub>36</sub>, 2  $\mu\text{M}$   $\text{ATP}\gamma\text{S}$ , 60 mM NaCl, and 1 mM DTT in 1X Assay Buffer (25 mM  $\text{Tris}\cdot\text{HOAc}$ , pH 7.5 at 25  $^\circ\text{C}$ , 5% (v/v) glycerol, 10 mM  $\text{Mg}(\text{OAc})_2$ ) in a total volume of 50  $\mu\text{L}$ . In optimization trials, the inclusion of NaCl and sub-stoichiometric amounts of  $\text{ATP}\gamma\text{S}$  were found to maximize the signal-to-background ratio for the assay, where the signal is defined as the amount of RecA released in the

presence of 100  $\mu\text{M}$  ADP and the background is defined as the amount of RecA released in the absence of any additional nucleotide (data not shown). SA-PMP beads were washed three times with 1X Assay Buffer by resuspension in buffer followed by pelleting with a magnet and removal of the supernatant. The entire 50  $\mu\text{L}$  reaction volume was added to the washed SA-PMP beads and was mixed thoroughly to ensure coating of the beads with the reaction mixture. The reactions with beads were incubated for 20 min at 37  $^{\circ}\text{C}$  in an Eppendorf Thermomixer R microplate incubator. After the incubation period, the SA-PMP beads were pulled down with a microplate magnet and 10  $\mu\text{L}$  of supernatant was removed to a second microplate. To this supernatant was added 200  $\mu\text{L}$  of Protein Assay Reagent (Biorad), and the absorbance of the resulting solution was measured in the microplate reader using a  $595 \pm 25$  nm bandpass filter. The  $A_{595}$  value was converted to [RecA] by comparison with a RecA standard curve to quantify the RecA remaining in the supernatant. The apparent dissociation constants ( $K_d^{\text{app}}$ ) were determined by nonlinear least squares analysis of the resulting titration isotherms using the following equation:

$$A_{595} = A_{\min} + (A_{\max} - A_{\min}) \cdot \frac{[\text{NTP}]}{[\text{NTP}] + K_d^{\text{app}}} \quad (3)$$

where  $A_{\min}$  and  $A_{\max}$  are the minimum and maximum absorbance values, respectively.

*RecA-mediated strand exchange inhibition assay:* Circular  $\phi\chi 174$  cssDNA and dsDNA were from New England Biolabs. The  $\phi\chi 174$  dsDNA was linearized to RFI form using XhoI endonuclease (New England Biolabs). Single-stranded DNA binding protein (SSB) was purchased from Promega. RecA protein was purified as previously described.<sup>[159]</sup> Strand

exchange promoted by RecA was monitored essentially as described.<sup>[232, 233]</sup> RecA (10  $\mu$ M) was incubated at 37 °C for 10 min with  $\phi\chi$ 174 cssDNA (20  $\mu$ M-nts) in 1X Reaction Buffer (25 mM Tris·HOAc, 5% glycerol, pH = 7.5) with Mg(OAc)<sub>2</sub> (10 mM), phosphocreatine (12 mM), creatine phosphokinase (10 U/mL) and in the presence or absence of TNP-ADP (100  $\mu$ M). After the initial incubation,  $\phi\chi$ 174 linear dsDNA form III (20  $\mu$ M-nts) was added and the mixture was incubated for another 10 min at 37 °C. During this second incubation, 10  $\mu$ L was removed as the 0 min aliquot and added to RecA stop dye (60 mM EDTA, 5% (w/v) SDS, 25% (w/v) glycerol, 0.2% bromophenol blue) (3.3  $\mu$ L) to inactivate the RecA and stop the strand exchange reaction. A cocktail of ATP (3 mM) and SSB (2  $\mu$ M) was added to the reaction which was allowed to proceed at 37 °C. Aliquots (10  $\mu$ L) were taken at 10, 30, 60 and 90 min after the addition of ATP. The aliquots were run on a 0.8% agarose gel for 12 h. at 30 V, and the gel was stained for 1.5 h with 1X Sybr Gold (Molecular Probes) for visualization.

#### *Molecular model building for active filament conformation.*

The all-atom model of the active RecA filament was constructed by superimposing the  $C_{\alpha}$  backbone of the Xing and Bell crystal structure (PDB code 1XMV;<sup>[2]</sup>) onto the  $C_{\alpha}$  backbone of two adjacent RecA-filament subunits of the Egelman laboratory electron microscopy model of the active filament (PDB code 1N03;<sup>[6]</sup>). A simple minimization of the superimposed, all-atom structure was then performed using Insight II (Accelrys) to relieve steric clashes between residues due to adjustments in their position made during alignment.



## CHAPTER IV

### DIRECTED MOLECULAR SCREENING FOR RECA ATPASE INHIBITORS

Drug resistance is an ever-increasing problem in the chemotherapy of bacterial infectious diseases. The de novo development and clonal spread of drug-resistant bacteria, and the horizontal transfer of resistance factors among bacteria have resulted in a dramatic increase in the incidence of drug-resistant infections. One strategy to improve the efficacy of existing antibacterial drugs involves countering bacterial mechanisms of drug resistance. In this context, RecA has emerged as a potential target because its activities allow bacteria to overcome the metabolic stress induced by a range of antibacterial agents, and promote the de novo development and transmission of antibiotic resistance genes.<sup>[15, 16, 117-119]</sup> Although potent and selective inhibitors of RecA could be used to modulate its activities in the development of antibiotic resistance, no small-molecule natural product inhibitor of RecA's activities has been reported. Herein, we report the development of two novel enzyme-coupled fluorescent ATPase assays detecting the generation of either free phosphate or ADP. The assays were optimized as microvolume molecular screening assays and implemented in the directed screening of prospective inhibitors of RecA's ATPase activity.

#### **Selection of a focused mini-library of potential inhibitors**

We have previously demonstrated that select NDP and NTP analogs inhibit RecA ATP hydrolysis (see Chapter 3).<sup>[17, 124, 213]</sup> Because nucleotide analogs are largely unsuited



for use in cell-based assays, we screened a small, focused set of commercially available compounds to discover non-nucleotide inhibitors of RecA. The compounds we elected to study were carefully selected to slant the odds of finding an inhibitor in our favor and they are ordered into five groups (Figure 4.1). The first group comprises vanillin,<sup>[249-251]</sup> cinnamaldehyde,<sup>[252]</sup> curcumin,<sup>[253]</sup> and the soy-derived compounds genistin and genistein,<sup>[254]</sup> all of which have been predicted to inhibit RecA based on their activities in microbiological assays. The second group includes adenosine nucleotide-like compounds<sup>[227, 255]</sup> that may extend upon our previous success with nucleotide analogs. The third group is composed of inhibitors of the gyrase-Hsp90-like (GHL) family of ATPases.<sup>[256, 257]</sup> The fourth group includes adenine-like inhibitors of protein kinases.<sup>[258]</sup> The fifth group comprises compounds related to the non-nucleotide inhibitors of purine nucleotide receptors, suramin and PPADS.<sup>[259, 260]</sup>

### **Development of novel HTS-compatible fluorescent ATPase assays**

High-throughput screening is a useful method for the identification of novel inhibitory scaffolds. Recently, we reported a coupled enzyme assay that was optimized for determination of *E. coli* RecA's ssDNA-dependent ATPase activity,<sup>[124, 213]</sup> which is a useful indicator of active RecA-DNA filament assembly (refer to Figure 3.13 for MESG/PNP assay scheme). It was undesirable to use this assay to screen a larger, more diverse library because many of the compounds may be UV active at 360 nm and this interfering absorbance would lead to false negatives in a high-throughput screening project.

To address this concern, we developed two robust and reproducible microplate assays for RecA's ATPase activity that are suitable for screening collections of small molecules as

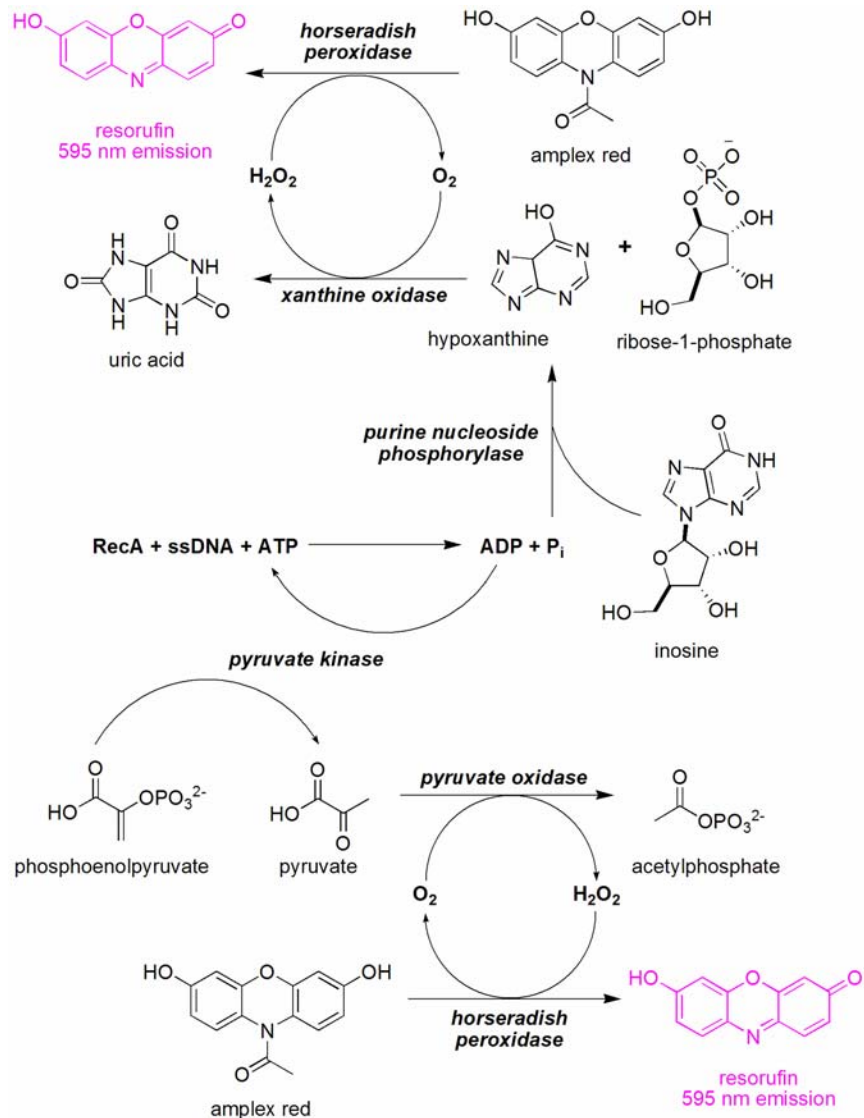


**Figure 4.2. Two fluorescent ATPase assays developed to monitor ATP hydrolysis by RecA in the presence of small molecules which may be UV-active.** In the top scheme, inorganic phosphate resulting from ATP (or NTP) hydrolysis reacts with inosine and purine nucleoside phosphorylase, yielding hypoxanthine and ribose-1-phosphate. The hypoxanthine undergoes O<sub>2</sub>-dependent oxidation in the presence of xanthine oxidase, producing uric acid and H<sub>2</sub>O<sub>2</sub>, the latter of which is used to horseradish peroxidase to oxidize amplex red to resorufin. In the bottom scheme, the ADP produced from ATP hydrolysis and phosphoenolpyruvate serve as substrates for the enzyme pyruvate kinase to regenerate ATP and produce pyruvate, the latter of which undergoes O<sub>2</sub>-dependent oxidation by pyruvate oxidase, yielding acetylphosphate and H<sub>2</sub>O<sub>2</sub>. Identical to the top scheme, horseradish peroxidase uses H<sub>2</sub>O<sub>2</sub> to oxidize amplex red to resorufin. The resorufin fluorophore has an excitation maximum at 485 nm and an emission maximum of 595 nm, which makes it ideal for use with UV-active compounds.

prospective RecA inhibitors without the potential for signal interference generated by UV-active compounds (Figure 4.2). Each variation of the assay utilizes one product of ATP

hydrolysis, either ADP or  $P_i$ , as a substrate for commercially available enzymes and, for every molecule of ATP hydrolyzed by RecA, one molecule of amplex red is ultimately oxidized to resorufin, which has a unique fluorescence emission at 595 nm.<sup>[261]</sup> In one variant of the assay,  $P_i$  and inosine serve as substrates for PNP in the production of hypoxanthine and ribose-1-phosphate. In turn, the  $O_2$ -dependent oxidation of hypoxanthine by xanthine oxidase produces uric acid and  $H_2O_2$ , the latter of which is used by horseradish peroxidase to oxidize amplex red to resorufin. In the other assay variant, ADP and phosphoenolpyruvate serve as substrates for the commercially available enzyme pyruvate kinase to produce ATP and pyruvate, the latter of which is a substrate for  $O_2$ -dependent oxidation by pyruvate oxidase in the production of acetylphosphate and  $H_2O_2$ .<sup>[262]</sup> Identical to the first assay, horseradish peroxidase uses  $H_2O_2$  to catalyze the oxidation of amplex red to resorufin.



**Figure 4.3.** The resorufin ADP/ $P_i$  reporter molecule provides a convenient colorimetric indicator that the reaction is complete. On the left, a complete positive control reaction is dark pink at the end of the experiment, while on the right, a negative control reaction is essentially colourless.

It is to the advantage of the screener to use a spectrophotometric reporter such as resorufin that has an emission maximum of 595 nm. Observing the extreme red-shifted

emission of the resorufin reporter rather than a reporter molecule's absorbance in the 260-500 nm range avoids the pitfall of an interfering signal from the compound being screened as an inhibitor. This was the case with the 2-amino-6-mercapto-7-methylpurine reporter in the MESG/PNP assay, whose absorption maximum at 360 nm overlaps with several compounds we attempted to screen. Another established ATPase assay that has been well-characterized for use with RecA where NADH is stoichiometrically oxidized to NAD<sup>+</sup> for every ATP molecule hydrolyzed<sup>[161]</sup> relies on the disappearance of an absorbance signal at 380 nm, and UV-active compounds in this range would create false positives. A further useful feature of the resorufin reporter molecule lies in the fact that amplex red is nearly colourless and when it undergoes oxidation, and the resulting resorufin is bright pink, providing a convenient colorimetric indicator that is visible to the human eye (see Figure 4.3).

To determine if these novel fluorescent ATPase assays were suitable for high-throughput screening, we assessed their robustness and reproducibility using statistical analysis.<sup>[263]</sup> In our hands, the ADP-linked ATPase assay was more useful as a screening assay because the P<sub>i</sub>-linked assay was sensitive to variations in the residual phosphate contaminating enzyme and DNA preparations. For the ADP-linked ATPase assay optimized for 96-well microplates, positive and negative control experiments were performed on three different days with 48 wells per condition to simulate the day-to-day and well-to-well variability between assays (Figure 4.4). Statistical evaluation of the results yielded a reproducible *Z'* factor of 0.83, demonstrating the excellent utility of the assay for reproducibly differentiating normal activity from inhibition. Furthermore, the inclusion of the two most potent NTP-analog inhibitors discovered in our previous work described in

Chapter 3, verified that known RecA ATPase inhibitors would prevent resorufin production using this assay system (Figure 4.4).

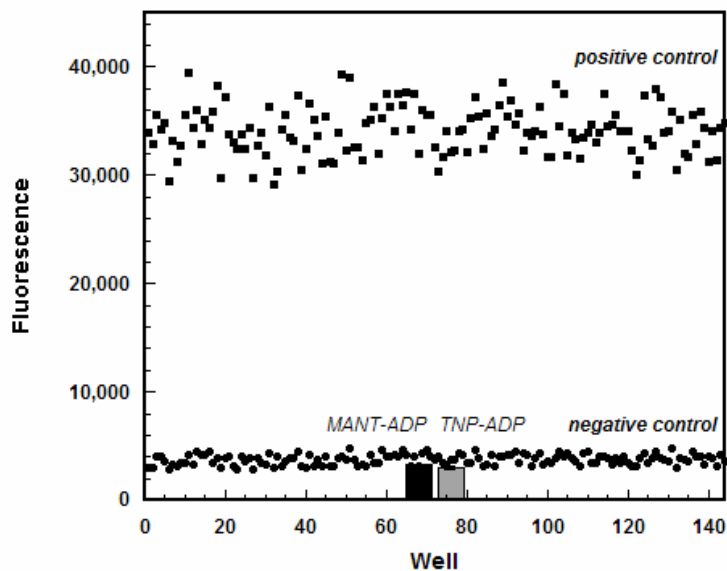


**Figure 4.4. Interday and intercolumn precision for the ADP-linked fluorescent ATPase assay.** The raw fluorescence measurements are represented as a scatter plot for the positive and negative control reactions. The previously characterized nucleotide analog inhibitors MANT-ADP and TNP-ADP were assayed at a concentration of 100  $\mu\text{M}$  to ensure that the assay would identify a known inhibitor of ATP hydrolysis. The  $Z'$  factor for the fluorescent ATPase HTS assay is 0.87.

### Screening the focused library

With a suitable ATPase assay in hand, we assessed the abilities of the 18 compounds in our directed mini-library (Figure 4.1) to inhibit RecA's ATPase activity at 100  $\mu\text{M}$ . The fractional inhibition observed in the presence of each compound was obtained by comparing the total fluorescence in wells containing the reaction in the presence and absence of inhibitor (Figure 4.5). Only curcumin from Group 1 and the polysulfated naphthyl compounds, suramin, Congo Red and bis-ANS, from Group 5, appeared to inhibit RecA's ATPase activity under these conditions.

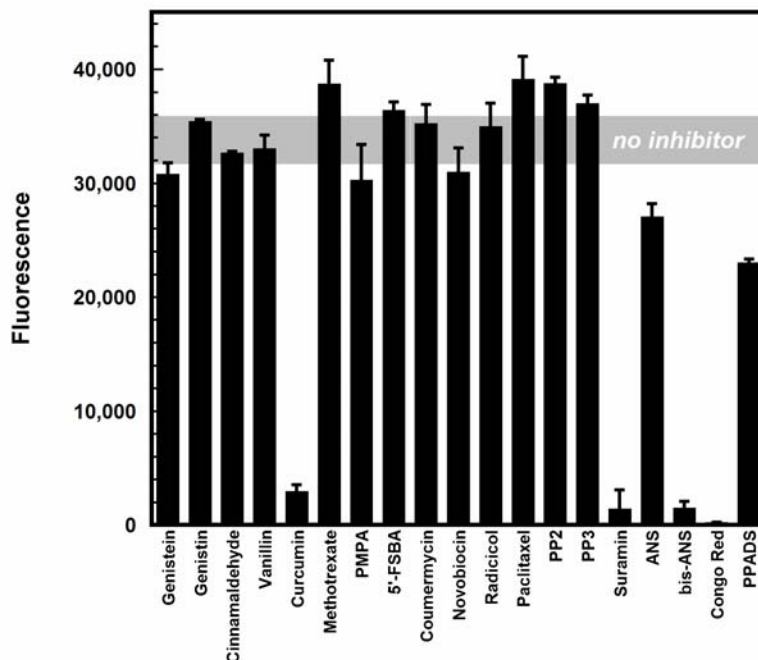


**Figure 4.5. Results of the directed screen of 18 selected compounds against RecA ATP hydrolysis activity.** Reactions (100  $\mu$ L) proceeded for 25 min at 37  $^{\circ}$ C, and contained RecA (0.5  $\mu$ M), polyd(T) ssDNA (5  $\mu$ M nts), ATP (0.5 mM) and an enzyme-linked reporter system as indicated in the materials and method section. The resorufin emission signal was detected in a microplate reader using an excitation filter of 485 nm and a emission filter of 595 nm.

Upon the identification of molecules that attenuated resorufin production, it was necessary to determine whether these compounds were selectively inhibiting RecA or other components of the coupled assay system. Therefore, four compounds were evaluated in subsequent control reactions in the presence of 500  $\mu$ M ADP, but in the absence of RecA. Because all four of these compounds also inhibited pyruvate kinase in the control assay, we evaluated their abilities to inhibit RecA's ATPase activity using the  $P_i$ -linked fluorescence ATPase assay described above. Suramin, Congo Red, and bis-ANS, but not curcumin, inhibited ATP hydrolysis by RecA.

It is important to note that none of the compounds expected to inhibit RecA based on prior biological activity studies (Group 1) inhibited RecA's ATPase activity in vitro. Possible explanations for the apparent inconsistency include the following: (1) these



compounds may inhibit RecA-associated proteins rather than RecA itself; or (2) these compounds may interfere with RNA or protein synthesis. Of additional importance is the observation that no known inhibitor from Group 2, 3 or 4 substantially inhibited RecA's ATPase activity. The failure to discover a RecA inhibitor among these compounds suggests that the development of a potent RecA inhibitor will not be a trivial exercise. However, the same lack of cross-inhibition of RecA by known inhibitors of other ATP-dependent enzymes also suggests the likelihood of ultimately discovering a specific inhibitor of RecA's activities.

### **Insights into the mechanism of inhibition by polysulfated naphthyl compounds**

Although we did not observe inhibition of RecA by any of the molecules in Groups 1, 2, 3, or 4, we did find that the polysulfated naphthyl compounds, Congo Red, suramin, and bis-ANS, strongly inhibited the ATPase activity of RecA. The nature of the inhibition by these compounds is reputed to be promiscuous. Indeed, it has been established that, in aqueous solution, Congo Red self-assembles into supramolecular aggregates<sup>[264, 265]</sup> that can result in apparent inhibition by the reversible sequestration of enzyme.<sup>[266, 267]</sup> In contrast, suramin, which is also active against many different enzymes<sup>[268]</sup> and is structurally similar to Congo Red, does not form aggregates and does not inhibit model enzymes that are sensitive to supramolecular ligands.<sup>[266, 267]</sup> The possibility that suramin may be a structure- or mechanism-specific inhibitor of RecA is supported by the observation that PPADS does not inhibit RecA's ATPase activity, despite the fact that both compounds are potent antagonists of the P2X<sub>1</sub> nucleotide receptors.<sup>[260]</sup> Finally, it is noteworthy that select transition metal cations trap inactive RecA as insoluble aggregates,<sup>[123]</sup> but no visible precipitates were

formed in the presence of suramin, Congo Red, or bis-ANS.

To probe this class of polysulfated naphthyl compounds further, we characterized the nature of the inhibition of RecA by suramin. While suramin inhibited RecA's ATPase activity with an  $IC_{50}$  of approximately 2  $\mu$ M, the inhibition was not competitive with respect to ATP or ssDNA binding (data not shown). We speculate that suramin modulates RecA's activity by binding to an allosteric region of the protein and trapping the protein in its inactive conformation.

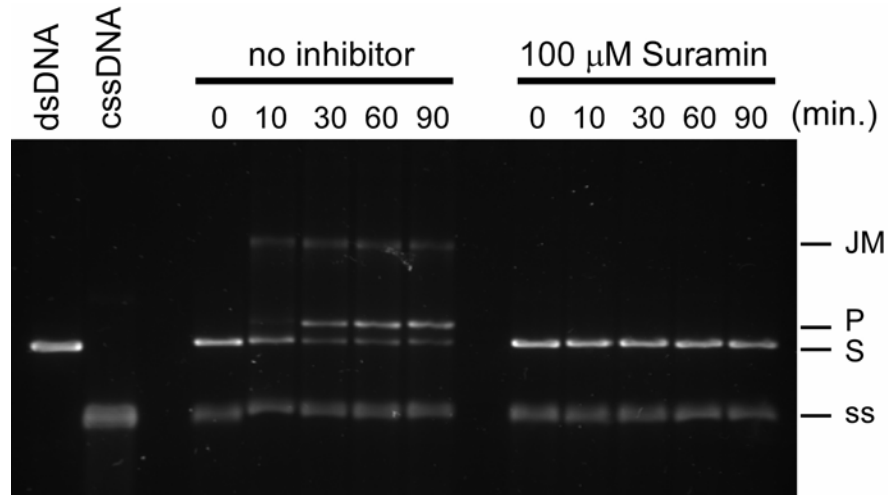


**Figure 4.6. Suramin inhibits the RecA-mediated DNA three strand exchange reaction.** In the absence of inhibitor, the formation of joint molecules (JM) and new nicked circular dsDNA product (P) from circular dsDNA (S) and homologous ssDNA is observed. In the presence of suramin however, JM and P are not observed until 90 minutes, and are only present at low levels.

Importantly, we demonstrated that suramin interferes with the RecA-mediated DNA strand exchange reaction, an established RecA activity that serves as an *in vitro* model for its physiologic recombinational functions.<sup>[34]</sup> It is known that RecA must hydrolyze ATP in order to carry out the strand exchange reaction between  $\phi\chi 174$  cssDNA and homologous, linear dsDNA (S) to yield a nicked circular dsDNA product (P), which migrates more slowly under electrophoretic conditions than the substrate DNA molecules. The presence of

suramin (100  $\mu\text{M}$ ) in this reaction completely abrogated the formation of nicked circular dsDNA product, even over the course of 90 min (see Figure 4.6).

## Conclusions

In conclusion, we have reported two new fluorescence-based assays for screening potential inhibitors of RecA's ATPase activity. We previously developed HTS-compatible screening assays for RecA's ATPase and filament assembly activities,<sup>[17, 124, 213]</sup> and the new molecular screening assays complement and extend the previous assays by providing an observable parameter that is not influenced adversely by UV-active compounds. Moreover, the assays reported herein were optimized for use with RecA based on its production of either free phosphate or ADP. We further reported that suramin, Congo Red, and bis-ANS strongly inhibit RecA's ATPase assay and compose a new structural class of RecA inhibitors. We expect that polysulfated naphthyl compounds such as these are likely to be of little therapeutic utility due to membrane-impermeability caused by their negative charges. Nonetheless these compounds may be used in future rational modification procedures for the synthesis microbiological tools to tease apart the roles of RecA in various aspects of pathogenicity. We envision that such inhibitors may ultimately be developed into novel adjuvants for antibiotic chemotherapy that moderate the development and transmission of antibiotic resistance genes and increase the antibiotic therapeutic index.

## Materials and Methods

**Source of reagents used:** The *E. coli* RecA protein was purified as described<sup>[159]</sup> to  $\geq 97\%$  homogeneity and stored in aqueous buffer (25 mM Tris·HCl, pH 7.5, 1 mM DTT, 5%

glycerol) at  $-80\text{ }^{\circ}\text{C}$ . The protein concentration was determined using the monomer extinction coefficient  $2.2 \times 10^4\text{ M}^{-1}\cdot\text{cm}^{-1}$  at  $280\text{ nm}$ .<sup>[248]</sup> Poly(dT) ssDNA (average length = 319 nts) was purchased from Amersham Biosciences (Piscataway, NJ). Black 96-well flat-bottom microplates were purchased from Corning (Corning, NY). ATP, Amplex red, inosine, phosphoenolpyruvate, horseradish peroxidase, pyruvate kinase (type VII from rabbit muscle), bacterial pyruvate oxidase and xanthine oxidase were purchased from Sigma-Aldrich (St. Louis, MO). Purine nucleoside phosphorylase was obtained from Invitrogen (Carlsbad, CA).  $\Phi\chi 174$  DNA and XhoI endonuclease were obtained from New England Biolabs (Ipswich, MA). Creatine phosphokinase and phosphocreatine were obtained from Sigma-Aldrich (St. Louis, MO).

**Table 4.1. Commercial sources of the focused library**

<b>Compound</b>	<b>Source</b>
Genistein	<i>Sigma-Aldrich</i>
Genistin	<i>Sigma-Aldrich</i>
Cinnamaldehyde	<i>Sigma-Aldrich</i>
Vanillin	<i>Sigma-Aldrich</i>
Curcumin	<i>K.H. Lee (UNC)</i>
Methotrexate	<i>Sigma-Aldrich</i>
PMPA	<i>Drug Bank</i>
5'-FSBA	<i>Synthesized (Chapter 3)</i>
Coumermycin	<i>Sigma-Aldrich</i>
Novobiocin	<i>Sigma-Aldrich</i>
Radicicol	<i>Sigma-Aldrich</i>
PP2	<i>AG Scientific</i>
PP3	<i>AG Scientific</i>
Suramin	<i>Sigma-Aldrich</i>
ANS	<i>Sigma-Aldrich</i>
Bis-ANS	<i>Sigma-Aldrich</i>
Congo Red	<i>Sigma-Aldrich</i>
PPADS	<i>Sigma-Aldrich</i>

### *Fluorescent ATPase Assays*

The conditions for the endpoint based fluorescent ATPase assays are described below. Positive control reactions were performed in the absence of any inhibitor and negative control reactions lacked polyd(T) ssDNA to simulate the complete inhibition of ATP hydrolysis. Note that these assays were optimized for use as endpoint inhibitor screens with RecA in 100  $\mu$ L volume in 96-well blackplates, but they have also been optimized for use in kinetic mode in 25  $\mu$ L volumes in 384-well blackplates (data not shown).

*ADP-linked ATPase assay for RecA activity.* Reactions (100  $\mu$ L) were carried out in 96-well blackplates and contained RecA (0.5  $\mu$ M), polyd(T) ssDNA (5  $\mu$ M-nts), MgOAc<sub>2</sub> (10 mM), ATP (500  $\mu$ M), phosphoenolpyruvate (250  $\mu$ M), amplex red (200  $\mu$ M), pyruvate kinase (1 U/mL), pyruvate oxidase (1 U/mL), horseradish peroxidase (1 U/mL), 5% glycerol and 25 mM Tris·HOAc, pH = 7.5. After a 25 min incubation of all the reagents at 37 °C the reaction was excited at 485 nm and emission was observed at 595 nm in a BMG Polarstar microplatereader.

*Phosphate-linked NTPase assay for RecA activity.* Reactions (100  $\mu$ L) were carried out in 96-well blackplates and contained RecA (0.5  $\mu$ M), polyd(T) ssDNA (5  $\mu$ M-nts), MgOAc<sub>2</sub> (10 mM), ATP (500  $\mu$ M), inosine (1 mM), amplex red (200  $\mu$ M), purine nucleoside phosphorylase (1 U/mL), xanthine oxidase (1 U/mL), horseradish peroxidase (1 U/mL), 5% glycerol and 25 mM Tris·HOAc, pH = 7.5. After a 25 min incubation of all the reagents at 37 °C the reaction was excited at 485 nm and emission was observed at 595 nm in a BMG Polarstar microplatereader.

For both variations of the fluorescent ATPase assay the % inhibition effected by each compound was calculated using the following formula:

$$\%inhibition = \left( 1 - \left( \frac{Em^{595}_{inh} - \mu_{min}}{Em_{max} - \mu_{min}} \right) \right) \times 100 \quad (1)$$

where  $Em^{595}$  is the emission measured at 595 nm in the presence of inhibitor,  $\mu_{min}$  is the plate average minimum  $Em^{595}$  signal control value, and  $\mu_{max}$  is the plate averaged maximum  $Em^{595}$  signal control.

To assess the quality of the assay for HTS applications, the  $Z'$  factor was determined using the following formula<sup>[263]</sup>:

$$Z' = 1 - \left( \frac{3\sigma_{max} + 3\sigma_{min}}{|\mu_{max} - \mu_{min}|} \right) \quad (2)$$

where  $\sigma_{max}$  and  $\sigma_{min}$  is the standard deviation for the respective positive and negative controls and  $\mu_{max}$  and  $\mu_{min}$  are the average values of the respective positive and negative controls.

### ***RecA-mediated strand exchange inhibition assay***

The  $\phi\chi 174$  dsDNA was linearized to RFI form using XhoI endonuclease. Single-stranded DNA binding protein (SSB) was purchased from Promega. RecA protein was purified as previously described.<sup>[159]</sup> Strand exchange promoted by RecA was monitored essentially as described.<sup>[232, 233]</sup> RecA (10  $\mu$ M) was incubated at 37 °C for 10 min with  $\phi\chi 174$  cssDNA (20  $\mu$ M-nts) in 1X Reaction Buffer (25 mM Tris·HOAc, 5% glycerol, pH = 7.5) with Mg(OAc)<sub>2</sub> (10 mM), phosphocreatine (12 mM), creatine phosphokinase (10 U/mL)

and in the presence or absence of suramin (100  $\mu$ M). After the initial incubation,  $\phi\chi$ 174 linear dsDNA form III (20  $\mu$ M-nts) was added and the mixture was incubated for another 10 min at 37  $^{\circ}$ C. During this second incubation, 10  $\mu$ L was removed as the 0 min aliquot and added to RecA stop dye (60 mM EDTA, 5% (w/v) SDS, 25% (w/v) glycerol, 0.2% bromophenol blue) (3.3  $\mu$ L) to inactivate the RecA and stop the strand exchange reaction. A cocktail of ATP (3 mM) and SSB (2  $\mu$ M) was added to the reaction which was allowed to proceed at 37  $^{\circ}$ C. Aliquots (10  $\mu$ L) were taken at 10, 30, 60 and 90 min after the addition of ATP. The aliquots were run on a 0.8% agarose gel for 12 h. at 30 V, and the gel was stained for 1.5 h with 1X Sybr Gold (Molecular Probes) for visualization.

**CHAPTER V:**  
**HIGH-THROUGHPUT SCREENING FOR INHIBITORS OF RECA**

Antibiotic resistant bacteria are rendering the current supply of available antibacterial drugs ineffective at an alarming rate and there is a dearth of novel drug targets for the treatment of bacterial infectious diseases. Recent evidence suggests that RecA-controlled processes are responsible for an increased tolerance to antibiotic chemotherapy and in pathways which ultimately lead to full-fledged antibiotic resistance. A small molecule capable of inhibiting RecA would impact these pathways which include DNA repair, SOS mutagenesis and recombination-based horizontal gene transfer. It has been shown that bacteria having loss-of-function mutations in the *recA* gene are exquisitely sensitive to antibiotic treatment and develop resistance much more slowly or not at all.<sup>[3]</sup> A chemotherapeutic agent imparting this phenotype could act synergistically with currently prescribed antibiotics, greatly enhancing their potency and preventing the accumulation of populations which are resistant to them. Therefore, cell-permeable small molecules which specifically target RecA are required to demonstrate that RecA holds potential as a new druggable target in the treatment of bacterial infections; however, no such natural products or synthetic small molecules are known to exist.

High-throughput screening (HTS) is recognized as a powerful tool in drug discovery, and represents a blunt-force approach in the identification of target-specific lead compounds.



While HTS was previously only accessible to drug companies with sufficient resources to support screening endeavours, the continued establishment of private and academic HTS-screening centres and companies tailoring their services to these enterprises has made it increasingly feasible for academic laboratories to gain access to this drug discovery tool. In the Research Triangle area, one such screening centre has been created at the Biomanufacturing and Research Institute and Technology Enterprise (BRITE) located at North Carolina Central University (NCCU). We have been fortunate to collaborate with the Director Li-An Yeh and Professor Jonathon Sexton of the BRITE Center in our efforts to identify chemical probes which target RecA. Towards the goal of validating RecA as an important and novel target for the chemotherapeutic treatment of bacterial infectious diseases, we have screened 35,780 small molecules against RecA at the BRITE Center.

As ssDNA-dependent ATP hydrolysis is a useful indicator that the RecA protein is active, we elected to screen the compounds using a phosphomolybdate blue ATPase assay to identify compounds which prevented the generation of inorganic phosphate from ATP. In total, 80 small molecules were identified as primary hits and could be clustered in five groups based on molecular structure. The most potent class of hits was further examined in microbiological assays, and compound A1 was found to effect a reduction in RecA-dependent SOS expression in K-12 *Escherichia coli* and enhanced cell-killing efficacy of ciprofloxacin up to 10,000-fold in SC30RP *Escherichia coli*. Compound A1 represents the first small molecule demonstrating an ability to inhibit the bacterial SOS and is evidence that small molecule inhibitors of RecA hold enormous potential as synergistic antibacterial agents.

## Assay optimization and validation

Once a target has been established, the next step in HTS is the development and optimization of a robust assay suited to screening thousands of compounds in a short period of time. The assay must minimize the cost and occurrence of false positives and negatives, while maximizing the speed efficiency with which inhibitors are identified. Since RecA is activated in the presence of ssDNA and ATP, forming a nucleoprotein filament that hydrolyzes ATP, ssDNA-dependent ATP hydrolysis serves as a useful indicator of RecA activation and we chose to monitor the reduction of ATPase activity as a diagnostic for small-molecule mediated inhibition of RecA. The *in vitro* screening was performed using a phosphomolybdate blue (PMB) phosphate detection assay to identify compounds that abrogated ATP hydrolysis by RecA.<sup>[269, 270]</sup> The PMB ATPase assay relies on the interaction of a molybdate-ascorbic acid complex with inorganic phosphate to produce an aggregate phosphomolybdate complex having a strong absorbance in the 600-700 nm range (Figure 5.1). This assay has the advantage of being more cost effective than the fluorescent ATPase assay presented in Chapter 4.

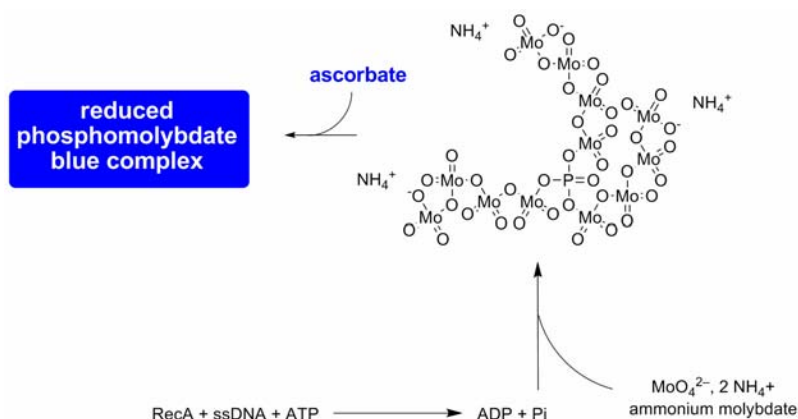


**Figure 5.1. PMB ATPase assay used to identify inhibitors of RecA.** In the assay,  $\text{P}_i$  generated from ATP hydrolysis by RecA forms a complex with molybdate and is reduced by ascorbic acid. The resulting phosphomolybdate complex absorbs strongly in the 600-700 nm region.

To identify compounds binding RecA with reasonable affinity we had to first consider an appropriate concentration of compound to screen in our adapted assay. To optimize the assay for detection of ATP hydrolysis by RecA, we determined that 0.5  $\mu\text{M}$  RecA and 0.75 mM ATP reacted in the presence of saturating poly(dT) (5  $\mu\text{M}$  nucleotides) for 35 min at 37  $^{\circ}\text{C}$  would keep the results in the linear range of detection of the system. Due to the fact that RecA is only active as a filament and is present at a relatively high concentration in the assay (0.5  $\mu\text{M}$ ), we elected to screen all compounds at a concentration of 17  $\mu\text{M}$  so that for every RecA monomer there were approximately 34 molecules of potential inhibitor. DNA was present at a concentration of 5  $\mu\text{M}$  nucleotides (nts), and RecA binds DNA with an approximate stoichiometry of 3 nucleotides to 1 monomer of RecA, therefore RecA was saturated nearly 3.3-fold by poly(dT) ssDNA. In our microplate reader, the  $A_{650}$

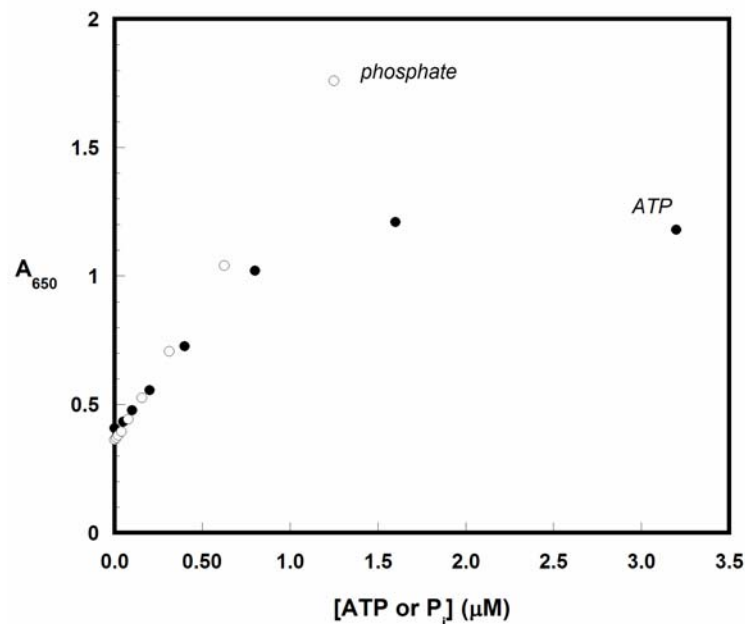


**Figure 5.2. Optimization of the phosphomolybdate blue ATPase adapted for use with RecA.** Inorganic phosphate ( $\text{P}_i$ ) was titrated with phosphomolybdate blue dye, while various concentrations of ATP were reacted in the presence of RecA (0.5  $\mu\text{M}$ ) and polyd(T) ssDNA (5  $\mu\text{M}$  nts) for 1 h at 37  $^{\circ}\text{C}$  to generate  $\text{P}_i$ . While the  $A_{650}$  signal remains linear until at least 1.25 mM for the  $\text{P}_i$  titration (open circles), the signal for  $\text{P}_i$  generated from ATP only remains linear until 0.75 mM ATP (filled circles) due to the build-up of ADP, a natural feedback inhibitor of RecA.

signal of the PMB phosphate detection assay remains linear to at least 1.25 mM  $P_i$ , but we needed to tailor the ATP concentration using this phosphate detection system as an ATPase assay with RecA. We established that beyond 0.75 mM ATP, the absorbance signal at 650 nm corresponding to generation of free phosphate increases non-linearly with increasing  $P_i$  concentration, due to the build-up of ADP, a natural feedback inhibitor of RecA (see Figure 5.2). Therefore an ATP concentration of 0.75 mM was selected so that we could have the maximum amount of ATP in the assay that would allow our results to remain in the linear range of detection of the system.

The quality of the PMB HTS ATPase assay for RecA activity was assessed by determining its  $Z'$  factor<sup>[263]</sup>, which defines the difference between the positive and negative controls of the dynamic signal being measured and the data variation of that signal. Robust and reproducible assays have a  $Z'$  factor ranging from 0.5 to 1. Consistent with a high-quality assay, the  $Z'$  factor was 0.73 (see Figure 5.3).

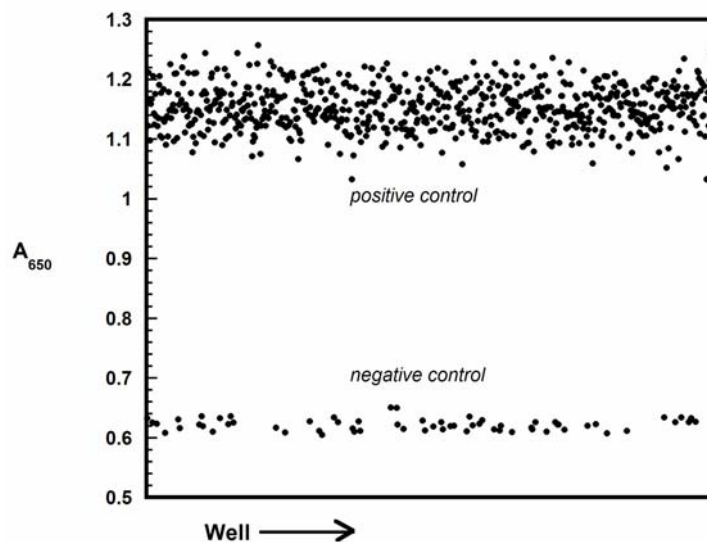


**Figure 5.3.  $Z'$  factor determination for the phosphomolybdate blue ATPase assay adapted for use with RecA.** A scatter plot of the  $A_{650}$  data used to calculate the  $Z'$  factor is shown for the positive and negative control reactions at the end of 35 min. The negative control reaction does not contain polyd(T) ssDNA, an essential component for RecA-mediated ATP hydrolysis.

## PMB ATPase assay trial run on the National Cancer Insititute Libraries

Once the PMB assay was validated for use with RecA by virtue of robust and reproducible controls, the assay was further validated by screening 2180 compounds combined from the National Cancer Institute (NCI) Challenge, Diversity and Natural Product library sets. The three NCI libraries were screened using the previously validated fluorescent ATPase assay in Chapter 4, and the results obtained were compared to those obtained with the PMB ATPase assay. The PMB ATPase assay had a 0.32% hit rate, yielding seven primary hits above 50% inhibition, four of which were confirmed as true hits in an  $IC_{50}$  study (Figure 5.4A). Of the four confirmed hits, three were found in common between both screening attempts of the NCI libraries employing the fluorescent ATPase assay and the PMB ATPase assay and they appear to share a remarkably similar scaffold (Figure 5.4B).

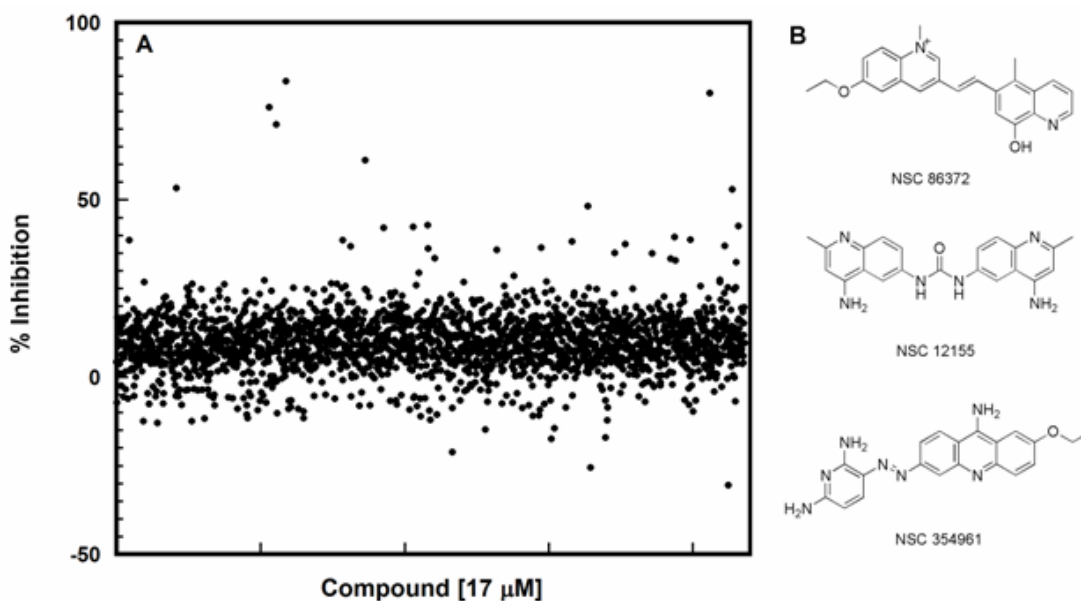


**Figure 5.4. Scatter plot of the ATPase inhibition effected by 2180 NCI compounds.** Reactions proceeded for 35 min at 37 °C and contained RecA (0.5 μM), polyd(T) ssDNA (5 μM nts), ATP (0.75 mM) and compounds were assayed at a final concentration of 17 μM. The screening results are represented as a scatter plot of inhibition (%) effected by each compound. There were 7 primary hits above a threshold of 50% inhibition.

The IC<sub>50</sub> values for these compounds spanned a range of 4-8  $\mu$ M, but unfortunately they possessed no biological activity against bacterial cultures. Nevertheless, the ability of the PMB assay and fluorescent ATPase assay<sup>[214]</sup> to mine the same hits from the NCI library reveals that the PMB ATPase assay is also a reliable method which may be employed to search for inhibitors of RecA in multi-thousand compound libraries.

### Screening a 33,600 compound library against RecA

The ability to efficiently identify the above mentioned NCI compounds as inhibitors of RecA (IRAs) using the PMB ATPase assay prompted us to screen a 350,000-compound library donated to the BRITE Center by Biogen Idec. Using compound and reagent concentrations identical to those described above, we performed a screen of 33,600 representative compounds selected to represent the overall diversity of the parent library.

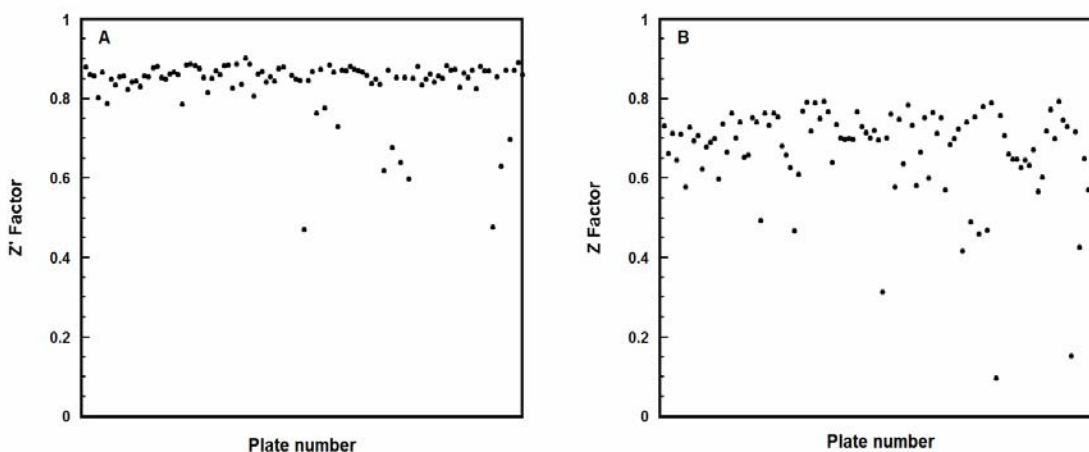


**Figure 5.5.** Statistical analyses of each 384-well plate to determine the quality of the HTS assay performed on the donated Biogen Idec compounds. **(A)** Z' factor analysis was performed on each plate and the average Z' factor value was 0.83. **(B)** A Z factor analysis was performed on each plate and the average Z factor value was 0.67. Three plates had a Z factor below 0.4 and were rejected during data analysis.

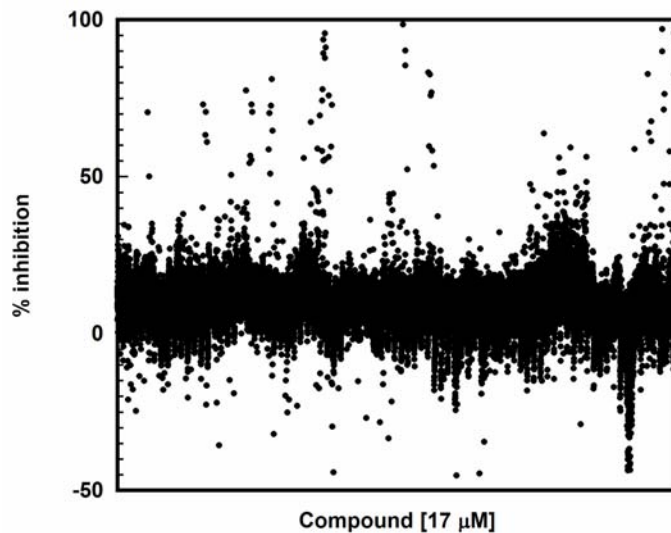


**Figure 5.6.** A total of 33,600 compounds were screened using the phosphomolybdate blue ATPase assay. Reactions proceeded for 35 min at 37 °C and contained RecA (0.5 μM), polyd(T) ssDNA (5 μM nts), ATP (0.75 mM) and compounds were assayed at a final concentration of 17 μM. The screening results are represented as a scatter plot of inhibition (%) effected by each compound. There were 73 primary hits above a threshold of 50% inhibition

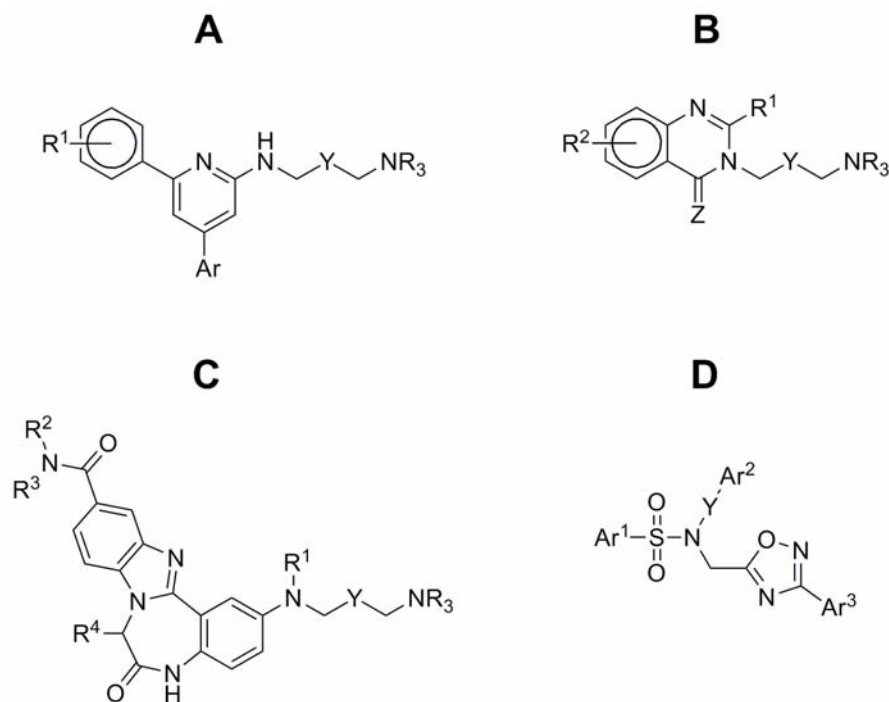


**Figure 5.7.** Four classes of hits mined in the Biogen library. Of the 73 total hits, 69 could be placed into one of the four groups, labeled A-D. There were the following number of hits belonging to the following classes: A – 34, D – 20, C – 10 and D – 5.

The HTS assay had an average  $Z'$  factor of 0.83 and a  $Z$  factor of 0.67, demonstrating robust and reproducible behaviour from plate to plate (see Figure 5.5). Three plates had a  $Z$  factor below 0.4 and were rejected during data analysis. Again, using a threshold of 50% inhibition, there were 73 hits for a hit rate of 0.22% (Figure 5.6). Interestingly, 69 of the 73 hits could be categorized into four classes based on their scaffold similarity and shared pharmacophores and we will refer to these classes as groups A-D, with 34, 20, 10 and 5 compounds in groups A-D, respectively (Figure 5.7). It would appear that the screen effectively mined the library, systematically identifying molecules belonging to one of these 4 groups.

Select representative members from 3 of the 4 scaffold classes were independently synthesized and were successfully confirmed as validated hits in  $IC_{50}$  analyses (see Figure 5.8 - Figure 5.10). Extrapolating these observations to the rest of the compounds belonging to the four scaffold classes, it appears that the false-positive rate was remarkably low.

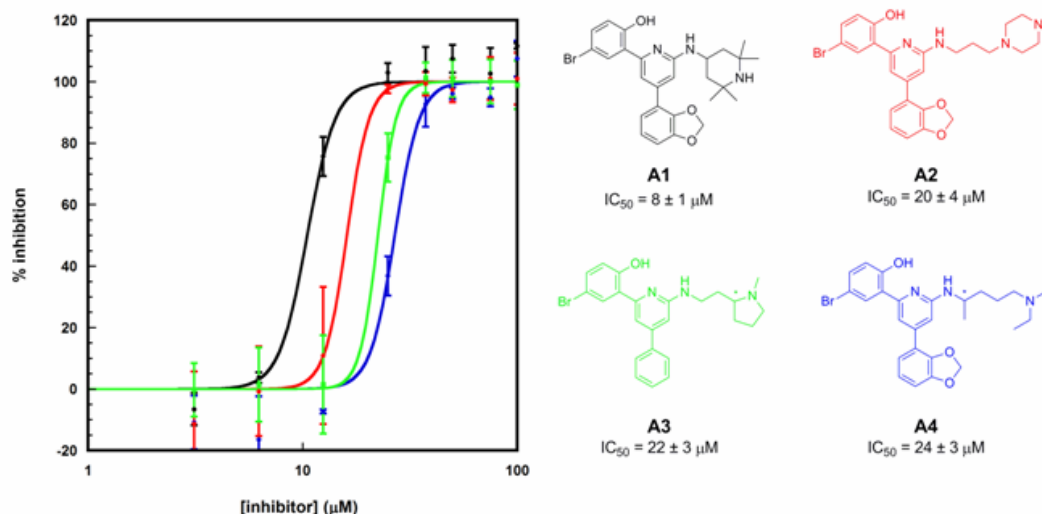


**Figure 5.8.  $IC_{50}$  study for selected scaffold class A compounds.** Four representative Group A compounds from a pool of 34 hits were synthesized and were subjected to  $IC_{50}$  analysis using the PMB ATPase assay. Group A compounds had the most potent  $IC_{50}$  values, with all  $IC_{50}$ 's < 25  $\mu\text{M}$ . Compound A1 was found to have an effect on the viability of *E. coli* cell cultures and was further examined in microbiological assays for in vivo inhibition of RecA. The error bars represent the standard deviation of three experiments.



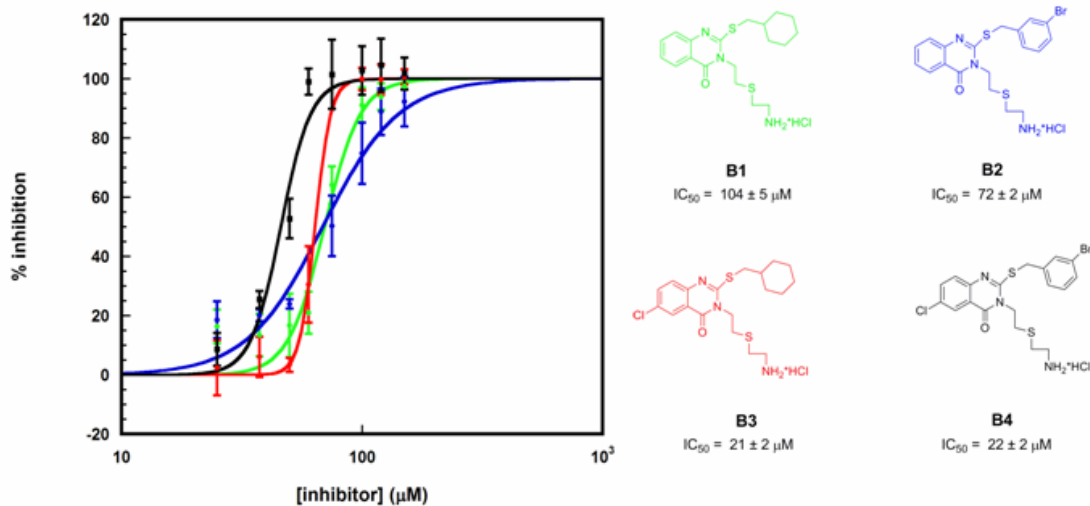


**Figure 5.9.  $IC_{50}$  study for selected scaffold class B compounds.** Four representative compounds from group B from a pool of 20 hits were synthesized and subjected to  $IC_{50}$  analysis using the PMB ATPase assay. Group B compounds possessed no biological activity against *E. coli* cell cultures and was this class of compounds was not studied further. The error bars represent the standard deviation of three experiments.

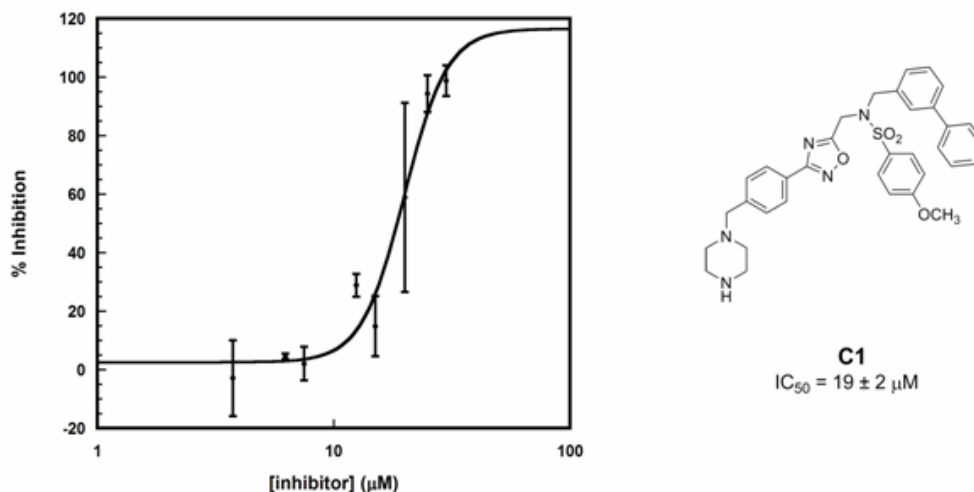


**Figure 5.10.  $IC_{50}$  study for selected scaffold class C compounds.** One representative compound from a pool of 10 hits was synthesized and subjected to  $IC_{50}$  analysis. Group C compounds possessed no biological activity against *E. coli* cell cultures and was this class of compounds was not studied further. The error bars represent the standard deviation of three experiments.

Compounds in group A had the most potent  $IC_{50}$  values (all below 25  $\mu\text{M}$ ) and this class was studied in further detail to determine their mode of action against RecA and were found to be active against live cell cultures as described below.

### Investigating the mechanism of action of Group A compounds

From our efforts to confirm the four classes of compounds as authentic inhibitors by quantifying their  $IC_{50}$  values, we determined that compound class A, consisting of heterocycles with molecular weights less than 550 g/mol, had the largest inhibitory effect against RecA in vitro. The most potent inhibitor from scaffold group A, compound A1 having an  $IC_{50}$  of  $8 \pm 1 \mu\text{M}$ , was found to effect a reduction in bacterial viability in combination with ciprofloxacin using a single-point microbiological screening assay (data not shown) and was examined more closely to elucidate the method by which it was inhibiting the ATPase activity of RecA. To explore the possible mode of action of group A compounds against RecA, we separately titrated ATP and poly(dT) with A1 in ATP hydrolysis assays (Figure 5.11). When ATP and A1 were titrated, we observed the  $S_{0.5}^{\text{ATP}}$  to

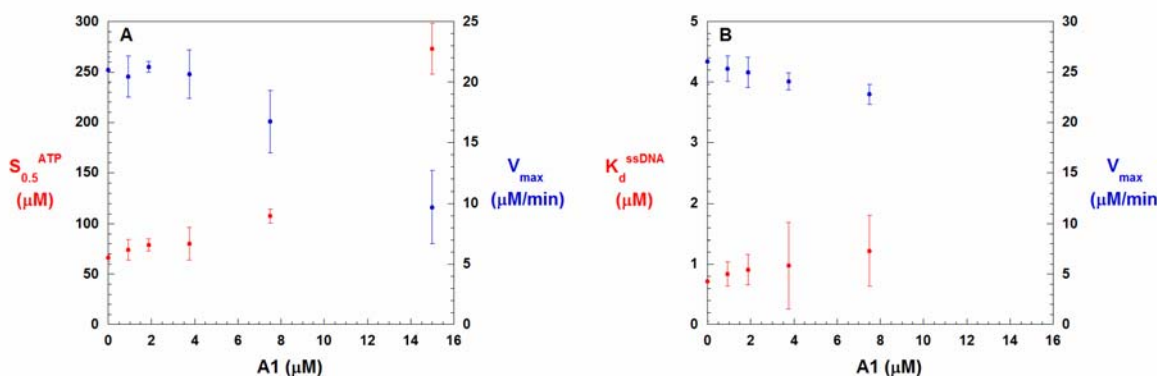


**Figure 5.11. Determining if A1 is competitive with respect to ATP or ssDNA.** (A) A1 and ATP were titrated, while the poly(dT) concentration was held constant. The  $S_{0.5}^{\text{ATP}}$  (left y-axis) and the  $V_{\text{max}}$  was (right y-axis) were plotted as a function of A1 concentration. (B) A1 and poly(dT) were titrated while ATP was held constant. The  $K_d^{\text{ssDNA}}$  (left y-axis) and  $V_{\text{max}}$  (right y-axis) were plotted as a function of A1 concentration. The standard error of three experiments is indicated by the error bars.

increase as the concentration of A1 was increased, and likewise when poly(dT) was titrated with A1, the  $K_d^{ssDNA}$  increased monotonically. In both cases  $V_{max}$  decreased monotonically as the A1 concentration was increased. From these experiments we conclude that A1 is neither competitive with respect to ATP or ssDNA. In addition a RecA-DNA binding assay described previously<sup>[124, 271]</sup> was performed and indicated that A1 did not prevent the interaction of RecA and ssDNA, but rather enhanced it. From these experiments we concluded that A1 is neither competitive with ATP or ssDNA. Rather, A1 appears to bind the A-state filament at an allosteric site, preventing cooperative activation of RecA to the transition state required for ATP hydrolysis.

We further examined the ability of A1 to inhibit the DNA strand exchange reaction catalyzed by RecA using an in vitro assay which provides a paradigm for the in vivo recombinational activity of RecA.<sup>[34]</sup> In the assay, RecA is supplied with ATP, linear dsDNA, circular ssDNA and resolves the two DNA substrates into nicked circular dsDNA

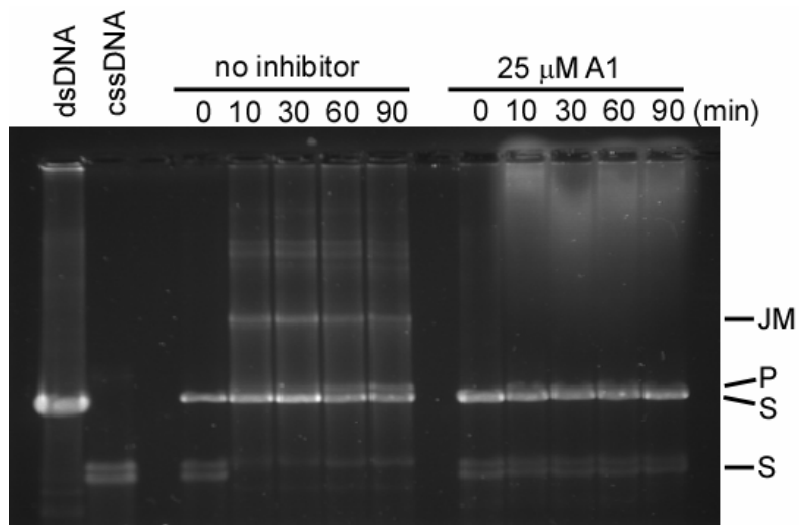


**Figure 5.12. RecA mediated three-strand exchange is inhibited by A1.** In the absence of inhibitor, the formation of joint molecules (JM) and new nicked circular dsDNA product (P) from circular dsDNA and homologous cssDNA substrates (S) is observed. In the presence of A1 (25  $\mu$ M) however, JM and P are not observed even after course of 90 minutes and higher molecular weight structures which migrate very slowly under electrophoretic conditions are observed near the wells.

and linear ssDNA using ATP-hydrolysis induced conformational rearrangements to facilitate the formation of three-stranded joint molecules (JM) and perpetuate branch migration, yielding a new nicked circular dsDNA product that migrates more slowly in agarose electrophoresis than does intact cssDNA. The presence of 25  $\mu$ M A1 completely inhibited this reaction, and judging by the higher molecular weight structures visible on the agarose gel on which the reaction was analyzed, it appears that a RecA-DNA aggregate is formed in the presence of A1 (see DNA staining near wells in Figure 5.12). Taken together with the DNA binding assay, and the ATP- and poly(dT)-dependent titrations, these results suggest that A1 strongly induces the formation of a RecA-DNA aggregate incapable of performing ATP hydrolysis and the associated DNA strand exchange reaction that is the basis for the physiologic recombinational activities of RecA.

### **Group A compounds effect a reduction in RecA-dependent SOS expression**

After demonstrating that group A compounds were the most effective in vitro inhibitors of RecA discovered from the PMB ATPase screen, compound A1 was subjected to an analysis of its ability to effect a RecA-dependent reduction in SOS induction in *E. coli* cell cultures. The Sandler group recently reported the ability to measure SOS expression in K-12 *E. coli* having a *sulA-gfp* fusion reporter gene inserted into the chromosomal DNA (strain SS996).<sup>[4]</sup> The *sulA* promoter is LexA-regulated, and the gene product of *sulA* is thought to bind FtsZ to inhibit cell division until DNA damage can be repaired.<sup>[272]</sup> LexA is known to bind the *sulA* promoter much more tightly than other SOS promoters. *SulA* is expressed 100-fold during the SOS response.<sup>[4]</sup> We used these SS996 *E. coli* to determine the differential SOS expression effected by A1 following treatment with ciprofloxacin, a GyrA specific

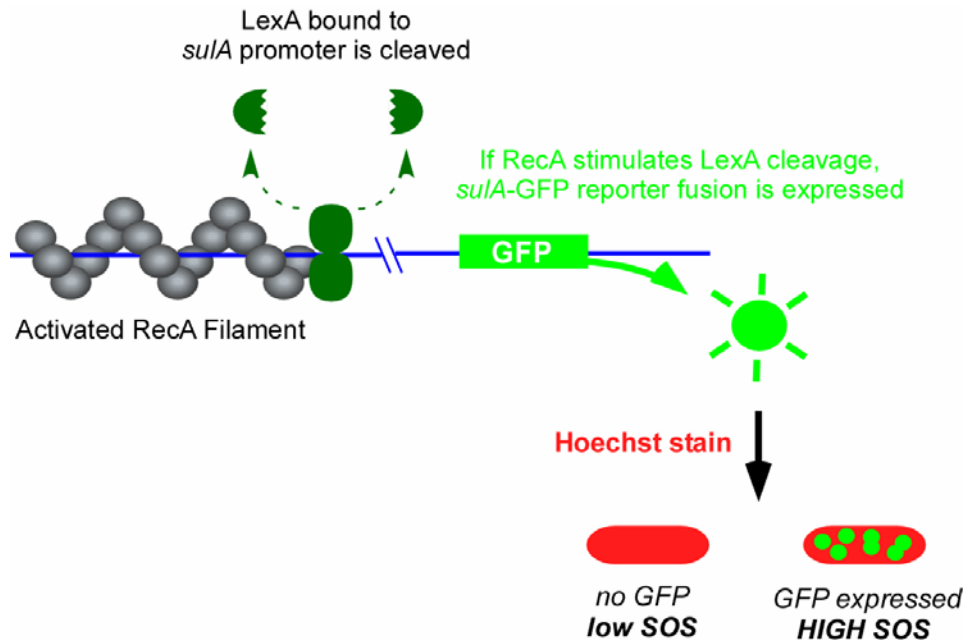


**Figure 5.13. The ciprofloxacin-induced SOS response measured by a GFP reporter gene expression assay.** We obtained K-12 *E. coli* engineered by the Sandler group<sup>[4]</sup> which have the GFP reporter gene inserted into the chromosomal DNA under the control of the *sulA* promoter. In the late stages of the SOS response, the *sulA* promoter is normally activated when RecA cleaves LexA, and in this engineered strain, this results in the large scale expression of GFP which can be measured using epifluorescence confocal microscopy.

DNA-damaging antibiotic known to stimulate SOS (see Figure 5.13 for assay scheme).<sup>[20]</sup>

The RecA-dependent expression of GFP could be individually measured among single cells in a population of bacteria exposed to ciprofloxacin and comparatively analyzed to GFP expression among cells given a combination of ciprofloxacin and A1.

Mid-log phase ( $OD_{600} = 0.3$ ) cultures of SS996 *E. coli* were given either no compound, A1 only, ciprofloxacin only or a combination of varying doses of A1 (0-100  $\mu\text{M}$ ) and a fixed amount of ciprofloxacin (25 ng/mL), then allowed to incubate for 90 min at 37  $^{\circ}\text{C}$ . The bacteria were fixed with formaldehyde and stained with Hoechst dye, then examined by high-content epifluorescence microscopy using a 40X objective and filters selected for Hoechst and GFP (see Figure 5.14, Left panel). The fluorescence intensities in the Hoechst and GFP channels was analyzed and a ratio of GFP/Hoechst intensities was calculated to

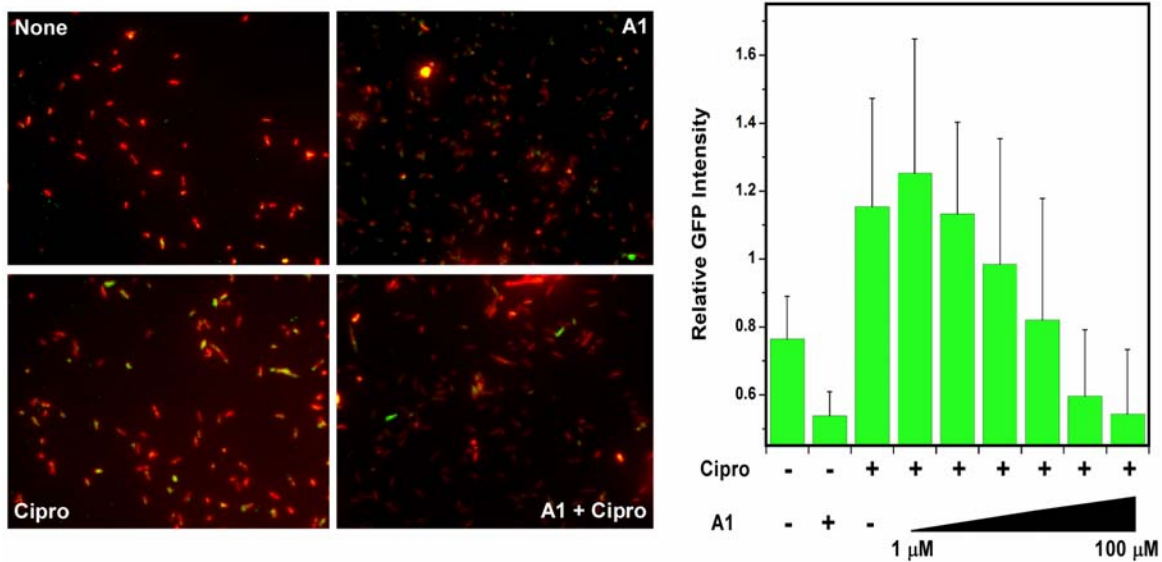


**Figure 5.13. Inhibition of SOS induction by A1. (Left) Superimposition of the GFP and Hoechst channel images.** All bacteria are stained with Hoechst dye, and an image is taken of the Hoechst (red) and GFP (green) channels. The relative GFP/Hoechst ratio is calculated to determine the level of RecA-controlled SOS induction per cell (see Figure 5.14). A1 completely inhibits the cipro-inducible GFP expression at 100  $\mu\text{M}$ . Controls reactions contained either no compounds at all, 100  $\mu\text{M}$  A1 only or 25 ng/mL cipro only. **(Right) The SOS response measured by *sulA*-GFP expression shows is attenuated with increasing doses of A1.** All cultures are given 25 ng/mL cipro and varying doses of A1. The relative GFP/Hoechst ratio is calculated to determine the level of RecA-controlled SOS induction per cell (see Figure 5.13). A1 completely inhibits the cipro-inducible RecA-controlled GFP expression at 100  $\mu\text{M}$  and this effect decreases as A1 is reduced to 1  $\mu\text{M}$ . Controls reactions contained either no compounds at all, 100  $\mu\text{M}$  A1 only or 25 ng/mL cipro only. The error bars represent the standard deviation in > 250 individual bacteria defined as individual regions of interest.

determine the relative GFP expression per cell. There was a noticeable decrease in SOS expression in the presence of A1, and this phenomenon was dose-responsive (see Figure 5.14 Right panel).

From our results it was clearly apparent that A1 effected a dose-dependent decrease in the expression of GFP resulting from ciprofloxacin exposure (see Figure 5.14). *E. coli* exposed to ciprofloxacin showed a higher level of SOS expression than untreated bacteria (1.15 to 0.76 as measured by relative GFP intensity). In the presence of the highest concentration of A1, bacteria both treated and untreated with ciprofloxacin were characterized by a very similar SOS expression profile ( $\sim 0.54$  as measured by relative GFP

intensity) and this ratio was observed to increase as the A1 concentration was reduced. Taken together, this indicates that A1 was capable of abrogating the induction of the SOS under conditions simulating natural environmental stress and also under conditions of enhanced stress stimulated by the antibiotic ciprofloxacin. The effect seen in the presence of A1 can not be attributed to cytotoxicity or inhibition of protein translation as 100  $\mu$ M A1 on alone was found to have a negligible impact on the growth rate or viability of *E. coli* cultures as described in the proceeding section. Overall, these results represent the first evidence that a selective small molecule inhibitor targeting RecA will mitigate a powerful inhibitory effect on the SOS response in vivo.

### **Group A compounds display antibacterial synergism with ciprofloxacin**

After demonstrating that group A compounds were the most effective in vitro inhibitors of RecA discovered from the PMB ATPase screen, compound A1 was subjected to a bacterial viability study<sup>[273]</sup> to determine if it possessed biological activity against RecA activities in live *E. coli* cell cultures. The Collins group demonstrated that RecA<sup>-</sup> SOS-deficient *E. coli* were ultra-sensitive to ciprofloxacin than wild-type *E. coli*. Extending this observation, we hypothesized that a small-molecule inhibitor of RecA that diminishes the SOS response would result in a ciprofloxacin-sensitive phenotype. To evaluate this hypothesis, cultures of SC30RP *E. coli* were given either no compound, 100  $\mu$ M A1 only, 25 ng/mL ciprofloxacin only or a combination of varying amounts of A1 (1-100  $\mu$ M) and 25 ng/mL ciprofloxacin and their growth was monitored by observing the optical density (OD) of the culture over a period of 8 h. In addition, the number of viable bacteria in the bacterial

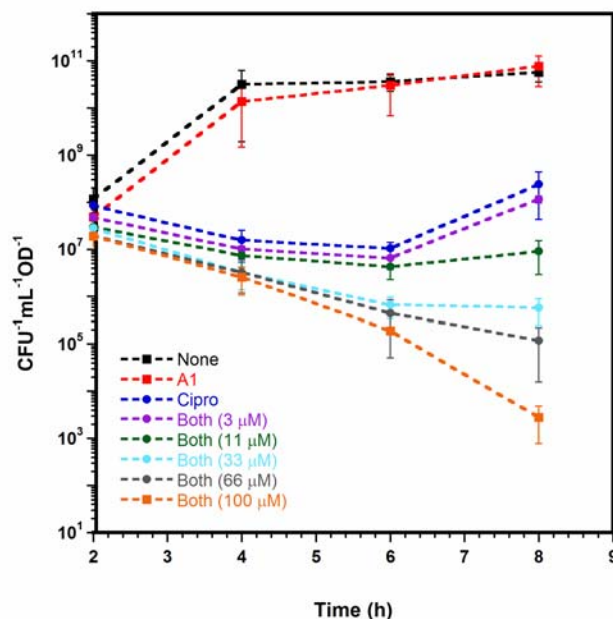


**Figure 5.15. Compound A1 synergistically enhances the toxicity of ciprofloxacin in *E. coli*.** All cultures were given 25 ng/mL cipro and varying doses of A1 (with the A1 dose listed in the brackets) and then incubated for 8 h. At 2 h intervals, the optical densities (OD) of the cultures were checked and an aliquot was plated on LB-agar media to count to the number of viable colony forming bacteria per OD/mL (CFU/OD/mL). Control reactions lacked both cipro and A1 (none), had only 100  $\mu$ M A1 or had only 25 ng/mL cipro.

cultures was quantified at the same time intervals by plating a sample of the culture on LB-agar media (see Figure 5.15). The OD of the control cultures with no antibiotic or containing only A1 increased exponentially and showed a constant number of colony forming units per milliliter per OD unit ( $\text{CFU}\cdot\text{mL}^{-1}\cdot\text{OD}^{-1}$ ). We conclude that A1 has no impact on bacterial growth and viability, as evident by the negligible decrease in OD and CFU parameters. The cultures containing ciprofloxacin or the combination of ciprofloxacin and A1 showed severely impeded growth rates; however the culture containing the combination of both compounds (having at least 33  $\mu$ M A1) showed an approximate 100-10,000 fold decrease in number of  $\text{CFU}\cdot\text{mL}^{-1}\cdot\text{OD}^{-1}$ . While the optical density of these two cultures was similar, we speculate that the decrease of viable bacteria in the culture treated with both ciprofloxacin and higher concentrations of A1 suggests the presence of a higher number of lysed cells



having released their cellular contents into the growth media. The reduction in viability of ciprofloxacin-treated bacteria by A1 was dose responsive and compound A1 can be said to synergistically enhance the antibacterial effect of ciprofloxacin as predicted.

## **Conclusions**

In summary, current antibiotic chemotherapeutics inherently stimulate the development of resistance, most likely in part to the activation RecA-dependent processes. Therefore, current antibiotics could have their effective shelf lives extended and have their potency increased by a small molecule inhibitor of RecA. We have screened 35,780 small molecules for inhibition of RecA using a phosphomolybdate blue ATPase assay to detect the generation of free phosphate. The hits obtained could be classified into one of five groups based on scaffold similarity and shared pharmacophores. Compound A1, having the most potent effect on RecA in vitro, was tested in live *E. coli* cultures and abrogated the SOS response, both under naturally occurring conditions and resulting from exposure to ciprofloxacin, an antibiotic agent known to upregulate SOS expression. Moreover, compound A1 potentiated the effect of a low dose of ciprofloxacin, and this cocktail of compounds killed bacteria with an efficiency of up to 10,000 times that of ciprofloxacin by itself. Compounds represented in class A display a unique biological activity previously unseen in known antibacterial chemotherapeutics and may serve as lead candidates for the development of adjuvants for the treatment of bacterial infectious diseases. More importantly, using a cell-permeable small molecule exerting control over RecA, we have provided proof-of-principle that RecA may be a novel target for antibacterial chemotherapy not belonging to the traditional classes of traditional antibiotics.

## Materials and Methods

### *RecA and ATPase reagents*

RecA was purified as previously described.<sup>[159]</sup> Poly(dT) single-stranded DNA (average length = 319 bases) was purchased from Amersham Biosciences (Piscataway, New Jersey). Crystalline L-Ascorbic acid and sulfuric acid were purchased from Fisher Scientific.  $\phi\chi 174$  circular single-stranded DNA (cssDNA) and double stranded DNA (dsDNA) were purchased from New England Biolabs (Ipswich, MA). Unless otherwise stated all other reagents were purchased from Sigma-Aldrich (St. Louis, MO) at the highest level of purity possible. K-12 *E. coli* containing the *sula-gfp* reporter gene (SS996 strain)<sup>[4]</sup> were a generous gift from Dr. Steven Sandler at the University of Massachusetts at Amherst.

The phosphomolybdate blue dye was made as a 10X stock by mixing 87 mL concentrated sulfuric acid to 50 mL autoclaved MilliQ de-ionized water, adding 30 g ammonium molybdate and adjusting the final volume to 250 mL with autoclaved MilliQ de-ionized water. On the day of use, fresh 1X phosphomolybdate blue dye was made by diluting the 10X stock in autoclaved MilliQ de-ionized water and ascorbic acid and SDS were added to final concentrations of 10% w/v and 1% w/v respectively.

### *Compound libraries*

The Challenge, Diversity and Natural Product library sets were obtained from the National Cancer Institute (NCI), Drug Synthesis and Chemistry Branch (Bethesda, MD) as 10 mM stocks in DMSO. A 1 mM stock was made in DMSO using a TOMTEC 96-channel pipet tower (TOMTEC, Hamden, CT).

The BRITE compound collection consists of a library of ~350,000 compounds generated by combinatorial chemistry synthetic routes, which was donated from Biogen-Idec in 2006. Upon acquisition, compounds were placed into 100% DMSO at an initial concentration of 10 mM. All of the compound plates were stored in polypropylene deep-well blocks at 4 °C without humidity controls. Using a Biomek NX unit (Beckman-Coulter, Fullerton, CA), 0.5 µL of a 1 mM stock of library compounds in DMSO was pre spotted onto Costar clear flat-bottom 384-well assay plates (Corning, Lowell, MA). In the left and right two columns of the assay plates 0.5 µL DMSO was spotted for the respective negative and positive control reactions.

#### *Phosphomolybdate blue ATPase assay*

The ATPase reactions were carried out in the 384-well plates that the compounds were spotted in, and the final volume in each well was 30.5 µL, giving final concentrations of 17 µM for the library compounds and 1.6 % for DMSO. A 2.25 mM stock of ATP was prepared in H<sub>2</sub>O and 10 µL of this was added to all wells of the assay plates using a Thermo Multidrop 384-well dispenser (Thermo Fisher, Waltham, MA), yielding a final ATP concentration of 0.75 mM. To columns 3-24 of the assay plates, using a Thermo Multidrop 384-well dispenser, was added 20 µL of a cocktail of containing RecA, poly(dT) ssDNA, MgOAc<sub>2</sub> and Tris·Glycerol buffer (pH = 7.5) such that the final concentrations were 0.5 µM RecA, 5 uM nts poly(dT), 10 mM MgOAc<sub>2</sub>, 25 mM Tris·HOAc and 5 % v/v glycerol. For the negative control, 20 µL of an identical solution containing no poly(dT) was added to columns 1 and 2 using a Thermo Multidrop 384-well dispenser. The assay plates were processed in batches of 20, and upon addition of all reagents the plates were transferred to a

37 °C air incubator and the ATPase reaction was allowed to proceed for 35 min. Subsequently, the plates were removed from incubator and 30 μL of the 1X phosphomolybdate blue dye was added to all wells using a Thermo Multidrop 384-well dispenser. After 5 min of incubation at room temperature, the plates were scanned for absorbance at 650 nm using a Spectramax Plus<sup>384</sup> (Molecular Devices, Sunnyvale, CA). Screening data informatics were processed using ActivityBase, XLfit (ID Business Solutions, Bridgewater, NJ) and Microsoft Excel 2003 (Microsoft, Redmond, WA). The percent-inhibition of RecA ATPase activity was analyzed on a plate-to-plate basis by comparing the  $A_{650}$  value per compound well with the plate-averaged control wells using the following relationship (1):

$$\%inhibition = \left( 1 - \left( \frac{A_{650} - \mu_{\min}}{\mu_{\max} - \mu_{\min}} \right) \right) \times 100 \quad (1)$$

where  $A_{650}$  is the absorbance value at 650 nm in the presence of inhibitor,  $\mu_{\min}$  is the plate average minimum  $A_{650}$  signal control value, and  $\mu_{\max}$  is the plate averaged maximum  $A_{650}$  signal control.

To assess the quality of the assay for HTS applications, the  $Z'$  factor and Z-factor was determined using the following formulas (2) and (3) [263]:

$$Z' = 1 - \left( \frac{3\sigma_{\max} + 3\sigma_{\min}}{|\mu_{\max} - \mu_{\min}|} \right) \quad (2)$$

where  $\sigma_{\max}$  and  $\sigma_{\min}$  is the standard deviation for the respective positive and negative controls and  $\mu_{\max}$  and  $\mu_{\min}$  are the average values of the respective positive and negative controls; and

$$Z - factor = 1 - \left( \frac{3\sigma_{CMPD} + 3\sigma_{PC}}{|\mu_{CMPD} - \mu_{PC}|} \right) \quad (3)$$

$\sigma_{CMPD}$  is the standard deviation in the compound data,  $\sigma_{PC}$  is the standard deviation in the 100% inhibition control,  $\mu_{CMPD}$  and  $\mu_{PC}$  are the average values for the compound data and the 100% inhibition control.

#### *Small molecule inhibition of RecA-mediated three-strand exchange reaction*

The  $\phi\chi 174$  dsDNA was linearized to the RFI form using XhoI endonuclease (New England Biolabs). Single-stranded DNA binding protein (SSB) was purchased from Promega. Strand exchange promoted by RecA was monitored essentially as described.<sup>[232, 233]</sup> RecA (10  $\mu$ M) was incubated at 37 °C for 10 min with  $\phi\chi 174$  cssDNA (20  $\mu$ M-nts) in 1X Reaction Buffer (25 mM Tris·HOAc, 5% glycerol, pH = 7.5) with Mg(OAc)<sub>2</sub> (10 mM), phosphocreatine (12 mM), creatine phosphokinase (10 U/mL) and in the presence or absence of A1 (25  $\mu$ M). After the initial incubation,  $\phi\chi 174$  linear dsDNA form III (20  $\mu$ M-nts) was added and the mixture was incubated for another 10 min at 37 °C. During this second incubation, 10  $\mu$ L was removed as the 0 min aliquot and added to RecA stop dye (60 mM EDTA, 5% (w/v) SDS, 25% (w/v) glycerol, 0.2% bromophenol blue) (3.3  $\mu$ L) to inactivate the RecA and stop the strand exchange reaction. A cocktail of ATP (3 mM) and SSB (2  $\mu$ M) was added to the reaction which was allowed to proceed at 37 °C. Aliquots (10  $\mu$ L) were

taken at 10, 30, 60 and 90 min after the addition of ATP. The aliquots were run on a 0.8% agarose gel for 12 h at 30 V, and the gel was stained for 1.5 h with 1X Sybr Gold (Invitrogen, Carlsbad, CA) for visualization.

#### *Small molecule inhibition of RecA-dependent SOS activation*

We assessed the ability of compound A1 to impact the RecA-dependent induction of the SOS response using K-12 *E. coli* having the *sulA* SOS promoter fused to the green fluorescent protein (*gfp*) reporter gene inserted at *attλ* on the chromosome (strain SS996)<sup>[4]</sup>. Fresh 2 mL LB cultures were inoculated with saturated overnight cultures of SS996 K-12 *E. coli* to OD<sub>600</sub> = 0.3 in the presence and absence of 25 ng/uL Ciprofloxacin and 0-100 μM A1. The highest final concentration of DMSO attained from the addition of these compounds was 0.15% and considered negligible. The cultures were grown in a shaking incubator at 37 °C for 90 min. At the end of this incubation, the cells were stained for 5 min at 25 °C directly in the LB medium with the addition of 3.7% formaldehyde and 10 μg/mL Hoechst stain or 10 μg/mL 4',6-diamidino-2-phenylindole (DAPI). Following staining, 1.6 mL of cells was centrifuged at 13000 rpm (RCF?) for 1 min and the supernatant was removed. The cells were washed three times with 10 mM MgSO<sub>4</sub> (1 mL) and finally resuspended in 10 mM MgSO<sub>4</sub> (500 μL). The cells were diluted (1:10) in clear, flat-bottom 384-well imaging microplates (Greiner, Monroe, NC) in a volume of 50 μL, sealed and centrifuged for 15 min at 3000 rpm and imaged in a BD pathway 855 high-content epifluorescence confocal microscope, equipped with an Olympus 40X/0.90NA objective and a Hamamatsu Orca CCD camera. Multiplexed two-color images were acquired using the following filters; GFP: 488nm/10nm bandwidth excitation filter, FURA/FITC epifluorescence dichroic and 515 LP

emission filter. DAPI: 380nm/10nm bandwidth excitation filter, 400dclp dichroic and 435nm long-pass emission filter. Bacterial cell binary masks were generated using the Attovision software (BD Biosciences, San Jose, CA) to delineate the cell boundaries using the DAPI channel. A normalized GFP intensity was calculated by integrating the GFP signal divided by the integrated DAPI intensity within the cell boundary. The average normalized GFP response per bacterium for a particular well was calculated and compared to other wells.

#### *Growth inhibition and quantitation of viable E. coli*

We assessed the ability of A1 to impact the viability and growth rates of SC30RP *E. coli*<sup>[274]</sup> using a modified procedure described by Elwell et al.<sup>[273]</sup> Fresh 25 mL LB cultures were inoculated with SC30RP *E. coli* to OD<sub>600</sub> = 0.05 in the presence and absence of 25 ng/uL Ciprofloxacin and 0-100 μM A1. The cultures were grown in a shaking incubator at 37 °C and samples were removed at various time intervals over 12 h to monitor the OD<sub>600</sub> and diluted for plating (30 μL) onto LB-agar. The amount of viable cells were quantified by counting the colonies formed after 24 h incubation at 37 °C so that the CFU<sup>-1</sup>·mL<sup>-1</sup>·OD could be determined.

## **CHAPTER VI:**

### **CONCLUSIONS**

The introduction and widespread use of antibiotics beginning in the World War II era led the health community to believe that humanity was rid of its greatest and most persistent threat, disease-causing bacteria. But today, just over 50 years later, the ever-increasing number of bacterial strains that display resistance to antibiotics indicates that this struggle is far from over. While antibiotics are traditionally classified into 6 categories based on their mode of action, only 2 of these classes of antibiotics have been introduced in the past 40 years, and the most currently prescribed work-horse antibiotics are now available as generics and misused to the point where resistance has slowly eroded their utility.<sup>[275]</sup> Exacerbating this problem is the tepid enthusiasm with which Big Pharma has approached the development of new antibacterials. From their point of view, why spend billions of dollars and 10-20 years developing a new FDA-approved antibiotic if it will become obsolete in a matter of years due to resistance?<sup>[9]</sup> In this regard, new drug targets and novel strategies are required in the chemotherapeutic intervention of bacterial infectious diseases. Towards this end, we have proposed inhibiting the bacterial RecA protein to ultimately target the underlying mechanisms behind antibiotic tolerance and resistance.

RecA's involvement in DNA repair, stress-induced mutagenesis and horizontal gene transfer contributes to the ability of bacteria to evade antibacterial chemotherapy, and in the absence of any known natural product inhibitors, we sought to develop small molecule



inhibitors of RecA to dissect and further understand the importance of these pathways. This dissertation has examined two approaches towards the discovery of such molecules: (1) directed screening of small compound libraries predicted to have a high probability of interacting with RecA, and (2) random screening of large compound libraries to discover lead compounds and scaffolds which interact with RecA. The search for an inhibitor of any protein begins with an assay capable of detecting the influence that a small molecule has on the activation state of protein. Over the course of this dissertation, several assays have been employed to identify RecA inhibitors. As RecA is a DNA-dependent ATPase, we have used assays monitoring RecA-DNA binding or ATP hydrolysis to determine the effect of small molecules on RecA. As the size and complexity of the libraries increased, we had to tailor our assays to meet the requirements they imposed, and known assays were adapted appropriately or novel original assays were developed specifically to meet our needs.

The first compound class looked at as inhibitors was metal cations, specifically bismuth–dithiols. Inspired by the inhibition of the *E. coli* rho transcription terminator by zinc and bismuth cations,<sup>[126-128]</sup> we examined the effects of several metal cations on RecA. Several metal cation species were found to irreversibly inactivate RecA by aggregating the protein, including bismuth. We found that bismuth preferentially targeted an ADP-bound conformation of RecA and that its inhibitory activity was enhanced when it was complexed to dithiol-containing ligands. In vivo testing indicated that bismuth–dithiols were moderately effective at reducing the SOS response and that they displayed antibacterial synergism with the DNA-damaging agent mitomycin C. It is known that bismuth compounds have multiple biological targets and that they have long been known to possess antibacterial activity, and we add RecA to the list of cellular targets of bismuth.

Next, we examined nucleotide analogs as inhibitors of RecA. This compound class was selected as RecA requires the binding and hydrolysis of ATP to perform its biological activities. Nucleotide analogs were first segregated based on their ability to act as substrates for hydrolysis by RecA, and the non-substrates were further segregated on their abilities to bind and inhibit the inactive or the active conformation of the protein. The former class of inhibitors was identified using a RecA-DNA binding assay, while the latter class of inhibitors was identified using an ATPase inhibition assay. We demonstrate that *N*<sup>6</sup>-modified adenosine analogs are well-tolerated by the RecA ATP-binding site (but not by the ATP-binding sites of many other ATP-binding proteins) and that aromatic 2'-*O* modifications greatly increases the affinity of nucleotide analogs for the RecA ATP-binding site. Our findings lend support to a structural model of the active RecA filament where a cooperative ATP-binding site comprising two adjacent RecA monomers is the active site for hydrolysis. Additionally we identify several features of the ATP-binding site in both the active and inactive conformation ATP-binding site which can be exploited in the design of potent and selective ATP-competitive inhibitors. More importantly we demonstrate the ability to discern the preferred conformation to which a ligand binds to inhibit RecA and we speculate that conformationally selective inhibitors can be used to dissect the roles of RecA-mediated SOS induction and RecA-mediated recombination in antibiotic tolerance and resistance.

In search of more “drug-like” small molecule inhibitors of RecA, we went about screening a small, focused library of 18 compounds predicted to interact with RecA based their ability to inhibit related proteins or which have been reported to inhibit RecA based on their ability to interfere with bacterial DNA repair and recombination machinery in microbiological assays. We discovered that suramin and structurally related polysulfated

naphthyl compounds indeed inhibit RecA, although these compounds are likely to be of little therapeutic utility as they are charged and do not traverse biological membranes. Nevertheless, they may serve as lead compounds in future rational design procedures for the development of biologically active tools to examine the roles of RecA in the antibiotic response and in pathogenicity. Additionally, two novel fluorescent ATPase assays relying on a resorufin reporter were developed specifically for this project, and may be of value to other researchers attempting to measure the rates of ATP hydrolysis or  $P_i$  generation by other proteins.

In my last project, I was fortunate to have the opportunity to perform high-throughput screening of several large libraries of small molecules against RecA. In total, I screened over 64,000 molecules from several sources against RecA using a phosphomolybdate blue ATPase assay. The compounds comprised 2180 synthetics and natural products from the National Cancer Institute repositories, 33,600 small molecules from a Biogen Idec library and 28,000 small molecules from Asinex. While the NCI and Biogen Idec screening results are presented in this dissertation, the results from the Asinex library are of commercial interest and are not discussed here. Compound group A from the Biogen Idec library was the most potent group of small molecules against the *in vitro* activities of RecA, and more importantly this inhibition carried over to *in vivo* studies. The most potent compound, A1 ( $IC_{50} = 8 \pm 1 \mu M$ ), was studied in great detail and found to reduce the induction of the SOS response as measured using a strain of K-12 *E. coli* having a *sulA*-GFP reporter fusion. Bacterial cultures exposed to ciprofloxacin and A1 were observed in high-content epifluorescence microscopy and as the dose of A1 was increased, the GFP expression corresponding to SOS induction was seen to diminish. After determining that A1 limited the

RecA-mediated SOS induction in live bacteria exposed to ciprofloxacin, we sought to test the hypothesis that such a small molecule may act synergistically with a bactericidal antibiotic such as ciprofloxacin to kill bacteria. Experiments monitoring bacterial growth and viability confirm this hypothesis: A1 increased the toxicity of ciprofloxacin up to 10,000-fold. Compound A1 sabotaged the ability of bacteria to withstand exposure to ciprofloxacin, presumably by blocking the SOS response and the DNA repair pathways which repair ciprofloxacin induced double-stranded DNA breaks. Therefore, compound A1 displays a previously unseen and unique biological activity and may serve as a lead compound for the design of adjuvants for the treatment of bacterial infectious diseases.

Taken together, the work presented in this dissertation provides a foundation for future studies on the inhibition of the RecA protein. More importantly, we provide proof-of-principle that RecA is a potentially modern and exciting new “druggable” target in the treatment of bacterial infectious diseases. We hope that this work will continue to evolve and that one day health care professionals will uniformly prescribe antibiotic cocktails which include a RecA inhibitor to prevent the occurrence of drug tolerance and resistance that currently causes regimens of antibiotic chemotherapy to fail.

## REFEREED PUBLICATIONS

All of the work presented in this dissertation has been or will be peer-reviewed for publication. The following is a list of publications listed chronologically by publication date, or by the date they were or are expected to be submitted for publication:

**Wigle, T. J.**, Lee, A. M., and Singleton, S. F. (2006) Conformationally selective binding of nucleotide analogues to *Escherichia coli* RecA: a ligand-based analysis of the RecA ATP binding site, *Biochemistry* 45, 4502-13.

Lee, A. M., **Wigle, T. J.**, and Singleton, S. F. (2007) A complementary pair of rapid molecular screening assays for RecA activities, *Anal. Biochem.* 367(2), 247-58.

**Wigle, T. J.**, and Singleton, S. F. (2007) Directed molecular screening for RecA ATPase inhibitors, *Bioorg. Med. Chem. Lett.* 17(12), 3249-53

**Wigle, T.J.**, Gromova, A. V., Hadimani, M.B. and Singleton, S.F. (2007) Towards Functionally Selective Inhibitors of RecA From Bacterial Pathogens, *ChemBioChem*, submitted for publication.

**Wigle, T.J.**, Lee, A.M., Zeng, B.B. and Singleton, S.F. (2007) Metal-Cation and Bismuth-Dithiol Mediated Inhibition of *E. coli* RecA, *J. Inorg. Biochem*, submitted for publication.

**Wigle, T.J.**, Sexton, T.J., Gromova, A.V., Hadimani, M.B., Hughes, M.A., Smith, G.R., Yeh, L.A. and Singleton, S.F. (2007) High-throughput Screening for Novel Inhibitors of *Escherichia coli* RecA ATPase Activity, *J. Biomol. Screen*, submitted for publication.

**Wigle, T.J.**, Sexton, T.J., Gromova, A.V., Flanagan, K. and Singleton, S.F. (2007) Potentiating the Toxicity of Ciprofloxacin with an Inhibitor of RecA, *Science*, in preparation for submission.

## CONFERENCE PRESENTATIONS

Some of the work outlined in this dissertation was or will be presented at the following conferences:

### Posters

Lee, A.M., **Wigle, T.J.** and Singleton, S.F. *A Molecular Target for the Suppression of the Evolution of Antibiotic Resistance: Inhibition of the E. coli RecA Protein by Select Small Molecules.* Experimental Biology Meeting, San Diego, CA, USA, April 2005

**Wigle, T.J.** and Singleton, S.F. *Targeting RecA to Prevent the Evolution of Antibiotic Resistance: HTS-Screening Strategies and ATP-Competitive Inhibitors.* Gordon Conference on Bioorganic Chemistry, Oxford, England, August 2006

**Wigle, T.J.** and Singleton, S.F. *Targeting RecA to Prevent the Evolution of Antibiotic Resistance: HTS-Screening Strategies and ATP-Competitive Inhibitors.* American Chemical Society Fall Meeting, San Francisco, CA, USA, September 2006

Gromova, A.V., **Wigle, T.J.** and Singleton, S.F. *Sabotaging Antibiotic Tolerance and Resistance with Inhibitors of RecA.* American Chemical Society Spring Meeting, New Orleans, LA, USA, April 2007

## REFERENCES

1. Clatworthy, A. E., Pierson, E., and Hung, D. T. (2007) Targeting virulence: a new paradigm for antimicrobial therapy, *Nat Chem Biol* 3, 541-548.
2. Xing, X., and Bell, C. E. (2004) Crystal structures of Escherichia coli RecA in complex with MgADP and MnAMP-PNP, *Biochemistry* 43, 16142-52.
3. Kohanski, M. A., Dwyer, D. J., Hayete, B., Lawrence, C. A., and Collins, J. J. (2007) A common mechanism of cellular death induced by bactericidal antibiotics, *Cell* 130, 797-810.
4. McCool, J. D., Long, E., Petrosino, J. F., Sandler, H. A., Rosenberg, S. M., and Sandler, S. J. (2004) Measurement of SOS expression in individual Escherichia coli K-12 cells using fluorescence microscopy, *Mol. Microbiol.* 53, 1343-57.
5. Roca, A. I., and Cox, M. M. (1997) RecA protein: structure, function, and role in recombinational DNA repair, *Prog Nucleic Acid Res Mol Biol* 56, 129-223.
6. VanLoock, M. S., Yu, X., Yang, S., Lai, A. L., Low, C., Campbell, M. J., and Egelman, E. H. (2003) ATP-mediated conformational changes in the RecA filament, *Structure (Camb)* 11, 187-96.
7. Sears, C. L. (2005) A dynamic partnership: celebrating our gut flora, *Anaerobe* 11, 247-51.
8. Fleming, A. (2001) On the antibacterial action of cultures of a penicillium, with special reference to their use in the isolation of B. influenzae. 1929, *Bull. World Health Organ.* 79, 780-90.
9. Projan, S. J. (2003) Why is big Pharma getting out of antibacterial drug discovery?, *Curr. Opin. Microbiol.* 6, 427-30.
10. Klevens, R. M., Morrison, M. A., Nadle, J., Petit, S., Gershman, K., Ray, S., Harrison, L. H., Lynfield, R., Dumyati, G., Townes, J. M., Craig, A. S., Zell, E. R., Fosheim, G. E., McDougal, L. K., Carey, R. B., and Fridkin, S. K. (2007) Invasive methicillin-resistant Staphylococcus aureus infections in the United States, *JAMA* 298, 1763-71.

11. Cirz, R. T., Gingles, N., and Romesberg, F. E. (2006) Side effects may include evolution, *Nat. Med.* *12*, 890-1.
12. Coleman, K., Athalye, M., Clancey, A., Davison, M., Payne, D. J., Perry, C. R., and Chopra, I. (1994) Bacterial resistance mechanisms as therapeutic targets, *J. Antimicrob. Chemother.* *33*, 1091-116.
13. Prudhomme, M., Attaiech, L., Sanchez, G., Martin, B., and Claverys, J. P. (2006) Antibiotic stress induces genetic transformability in the human pathogen *Streptococcus pneumoniae*, *Science* *313*, 89-92.
14. Cirz, R. T., Chin, J. K., Andes, D. R., de Crecy-Lagard, V., Craig, W. A., and Romesberg, F. E. (2005) Inhibition of mutation and combating the evolution of antibiotic resistance, *PLoS Biol* *3*, e176.
15. Beaber, J. W., Hochhut, B., and Waldor, M. K. (2004) SOS response promotes horizontal dissemination of antibiotic resistance genes, *Nature* *427*, 72-4.
16. Hastings, P. J., Rosenberg, S. M., and Slack, A. (2004) Antibiotic-induced lateral transfer of antibiotic resistance, *Trends Microbiol.* *12*, 401-4.
17. Lee, A. M., Ross, C. T., Zeng, B. B., and Singleton, S. F. (2005) A molecular target for suppression of the evolution of antibiotic resistance: inhibition of the *Escherichia coli* RecA protein by N(6)-(1-naphthyl)-ADP, *J. Med. Chem.* *48*, 5408-11.
18. Slack, A., Thornton, P. C., Magner, D. B., Rosenberg, S. M., and Hastings, P. J. (2006) On the mechanism of gene amplification induced under stress in *Escherichia coli*, *PLoS Genet* *2*, e48.
19. Cirz, R. T., O'Neill, B. M., Hammond, J. A., Head, S. R., and Romesberg, F. E. (2006) Defining the *Pseudomonas aeruginosa* SOS response and its role in the global response to the antibiotic ciprofloxacin, *J. Bacteriol.* *188*, 7101-10.
20. Cirz, R. T., Jones, M. B., Gingles, N. A., Minogue, T. D., Jarrahi, B., Peterson, S. N., and Romesberg, F. E. (2007) Complete and SOS-mediated response of *Staphylococcus aureus* to the antibiotic ciprofloxacin, *J. Bacteriol.* *189*, 531-9.
21. Wigle, T. J., and Singleton, S. F. (2007) Directed molecular screening for RecA ATPase inhibitors, *Bioorg. Med. Chem. Lett.*



22. Kowalczykowski, S. C., and Eggleston, A. K. (1994) Homologous pairing and DNA strand-exchange proteins, *Annu. Rev. Biochem.* 63, 991-1043.
23. Clark, A. J., and Margulies, A. D. (1965) Isolation and Characterization of Recombination-Deficient Mutants of Escherichia Coli K12, *Proc. Natl. Acad. Sci. U. S. A.* 53, 451-9.
24. VanBogelen, R. A., Kelley, P. M., and Neidhardt, F. C. (1987) Differential induction of heat shock, SOS, and oxidation stress regulons and accumulation of nucleotides in Escherichia coli, *J. Bacteriol.* 169, 26-32.
25. Courcelle, J., and Hanawalt, P. C. (2003) RecA-dependent recovery of arrested DNA replication forks, *Annu. Rev. Genet.* 37, 611-46.
26. Bjedov, I., Tenaillon, O., Gerard, B., Souza, V., Denamur, E., Radman, M., Taddei, F., and Matic, I. (2003) Stress-induced mutagenesis in bacteria, *Science* 300, 1404-9.
27. Aertsen, A., Van Houdt, R., Vanoirbeek, K., and Michiels, C. W. (2004) An SOS response induced by high pressure in Escherichia coli, *J. Bacteriol.* 186, 6133-41.
28. Janion, C., Sikora, A., Nowosielska, A., and Grzesiuk, E. (2002) Induction of the SOS response in starved Escherichia coli, *Environ. Mol. Mutagen.* 40, 129-33.
29. Little, J. W., Mount, D. W., and Yanisch-Perron, C. R. (1981) Purified *lexA* protein is a repressor of the *recA* and *lexA* genes, *Proc. Natl. Acad. Sci. U. S. A.* 78, 4199-203.
30. Schlacher, K., Pham, P., Cox, M. M., and Goodman, M. F. (2006) Roles of DNA polymerase V and RecA protein in SOS damage-induced mutation, *Chem. Rev.* 106, 406-19.
31. Schlacher, K., Leslie, K., Wyman, C., Woodgate, R., Cox, M. M., and Goodman, M. F. (2005) DNA polymerase V and RecA protein, a minimal mutasome, *Mol. Cell* 17, 561-72.
32. Cox, M. M. (1994) Why does RecA protein hydrolyse ATP?, *Trends Biochem. Sci.* 19, 217-22.

33. Cox, M. M. (2007) Motoring along with the bacterial RecA protein, *Nat Rev Mol Cell Biol* 8, 127-38.
34. Lusetti, S. L., and Cox, M. M. (2002) The bacterial RecA protein and the recombinational DNA repair of stalled replication forks, *Annu Rev Biochem* 71, 71-100.
35. Michel, B. (2005) After 30 years of study, the bacterial SOS response still surprises us, *PLoS Biol* 3, e255.
36. Little, J. W. (1984) Autodigestion of *lexA* and phage lambda repressors, *Proc. Natl. Acad. Sci. U. S. A.* 81, 1375-9.
37. Little, J. W. (1982) Control of the SOS regulatory system by the level of RecA protease, *Biochimie* 64, 585-9.
38. Little, J. W., and Mount, D. W. (1982) The SOS regulatory system of *Escherichia coli*, *Cell* 29, 11-22.
39. Kelley, W. L. (2006) Lex marks the spot: the virulent side of SOS and a closer look at the LexA regulon, *Mol. Microbiol.* 62, 1228-38.
40. Sassanfar, M., and Roberts, J. W. (1990) Nature of the SOS-inducing signal in *Escherichia coli*. The involvement of DNA replication, *J. Mol. Biol.* 212, 79-96.
41. Courcelle, J., and Hanawalt, P. C. (2001) Participation of recombination proteins in rescue of arrested replication forks in UV-irradiated *Escherichia coli* need not involve recombination, *Proc. Natl. Acad. Sci. U. S. A.* 98, 8196-202.
42. Courcelle, J., Khodursky, A., Peter, B., Brown, P. O., and Hanawalt, P. C. (2001) Comparative gene expression profiles following UV exposure in wild-type and SOS-deficient *Escherichia coli*, *Genetics* 158, 41-64.
43. Khil, P. P., and Camerini-Otero, R. D. (2002) Over 1000 genes are involved in the DNA damage response of *Escherichia coli*, *Mol. Microbiol.* 44, 89-105.
44. Janion, C. (2001) Some aspects of the SOS response system--a critical survey, *Acta Biochim. Pol.* 48, 599-610.

45. Giacomoni, P. U. (1982) Induction by mitomycin C of recA protein synthesis in bacteria and spheroplasts, *J. Biol. Chem.* 257, 14932-6.
46. Goodman, M. F. (2000) Coping with replication 'train wrecks' in Escherichia coli using Pol V, Pol II and RecA proteins, *Trends Biochem. Sci.* 25, 189-95.
47. McKenzie, G. J., Harris, R. S., Lee, P. L., and Rosenberg, S. M. (2000) The SOS response regulates adaptive mutation, *Proc. Natl. Acad. Sci. U. S. A.* 97, 6646-51.
48. Rosenberg, S. M., and Hastings, P. J. (2004) Adaptive point mutation and adaptive amplification pathways in the Escherichia coli Lac system: stress responses producing genetic change, *J. Bacteriol.* 186, 4838-43.
49. Hastings, P. J., and Rosenberg, S. M. (2002) In pursuit of a molecular mechanism for adaptive gene amplification, *DNA Repair (Amst) 1*, 111-23.
50. Trusca, D., Scott, S., Thompson, C., and Bramhill, D. (1998) Bacterial SOS checkpoint protein SulA inhibits polymerization of purified FtsZ cell division protein, *J. Bacteriol.* 180, 3946-53.
51. Bramhill, D. (1997) Bacterial cell division, *Annu. Rev. Cell Dev. Biol.* 13, 395-424.
52. Black, C. G., Fyfe, J. A., and Davies, J. K. (1998) Absence of an SOS-like system in Neisseria gonorrhoeae, *Gene* 208, 61-6.
53. Friedberg, E. C., Walker, G. C., and Siede, W. (1995) in *DNA Repair and Mutagenesis* pp 407-464, ASM Press, Washington, D.C.
54. Schlacher, K., and Goodman, M. F. (2007) Lessons from 50 years of SOS DNA-damage-induced mutagenesis, *Nat Rev Mol Cell Biol* 8, 587-94.
55. Kline, K. A., Sechman, E. V., Skaar, E. P., and Seifert, H. S. (2003) Recombination, repair and replication in the pathogenic Neisseriae: the 3 R's of molecular genetics of two human-specific bacterial pathogens, *Mol Microbiol* 50, 3-13.
56. Rauch, P. J., Palmen, R., Burds, A. A., Gregg-Jolly, L. A., van der Zee, J. R., and Hellingwerf, K. J. (1996) The expression of the Acinetobacter calcoaceticus recA gene increases in response to DNA damage independently of RecA and of

- development of competence for natural transformation, *Microbiology* 142 ( Pt 4), 1025-32.
57. Ramesar, R. S., Abratt, V., Woods, D. R., and Rawlings, D. E. (1989) Nucleotide sequence and expression of a cloned *Thiobacillus ferrooxidans* recA gene in *Escherichia coli*, *Gene* 78, 1-8.
  58. Goodman, H. J., Parker, J. R., Southern, J. A., and Woods, D. R. (1987) Cloning and expression in *Escherichia coli* of a recA-like gene from *Bacteroides fragilis*, *Gene* 58, 265-71.
  59. Edelman, W., and Kucherlapati, R. (1996) Role of recombination enzymes in mammalian cell survival, *Proc. Natl. Acad. Sci. U. S. A.* 93, 6225-7.
  60. Seitz, E. M., Haseltine, C. A., and Kowalczykowski, S. C. (2001) DNA recombination and repair in the archaea, *Adv. Appl. Microbiol.* 50, 101-69.
  61. Egelman, E. (2000) A ubiquitous structural core, *Trends Biochem. Sci.* 25, 183-4.
  62. Cox, M. M. (2003) The bacterial RecA protein as a motor protein, *Annu. Rev. Microbiol.* 57, 551-77.
  63. Cox, M. M., Goodman, M. F., Kreuzer, K. N., Sherratt, D. J., Sandler, S. J., and Marians, K. J. (2000) The importance of repairing stalled replication forks, *Nature* 404, 37-41.
  64. West, S. C., Cassuto, E., and Howard-Flanders, P. (1981) recA protein promotes homologous-pairing and strand-exchange reactions between duplex DNA molecules, *Proc. Natl. Acad. Sci. U. S. A.* 78, 2100-4.
  65. Sladek, F. M., Munn, M. M., Rupp, W. D., and Howard-Flanders, P. (1989) In vitro repair of psoralen-DNA cross-links by RecA, UvrABC, and the 5'-exonuclease of DNA polymerase I, *J. Biol. Chem.* 264, 6755-65.
  66. Smith, K. C., Wang, T. V., and Sharma, R. C. (1987) recA-dependent DNA repair in UV-irradiated *Escherichia coli*, *J. Photochem. Photobiol. B.* 1, 1-11.

67. Dixon, D. A., and Kowalczykowski, S. C. (1991) Homologous pairing in vitro stimulated by the recombination hotspot, Chi, *Cell* 66, 361-71.
68. Kowalczykowski, S. C., Dixon, D. A., Eggleston, A. K., Lauder, S. D., and Rehrauer, W. M. (1994) Biochemistry of homologous recombination in Escherichia coli, *Microbiol. Rev.* 58, 401-65.
69. Donaldson, J. R., Courcelle, C. T., and Courcelle, J. (2006) RuvABC is required to resolve holliday junctions that accumulate following replication on damaged templates in Escherichia coli, *J. Biol. Chem.* 281, 28811-21.
70. Kowalczykowski, S. C. (1994) In vitro reconstitution of homologous recombination reactions, *Experientia* 50, 204-15.
71. Volodin, A. A., Voloshin, O. N., and Camerini-Otero, R. D. (2005) Homologous recombination and RecA protein: towards a new generation of tools for genome manipulations, *Trends Biotechnol.* 23, 97-102.
72. Davison, J. (1999) Genetic exchange between bacteria in the environment, *Plasmid* 42, 73-91.
73. Riera, J., Fernandez de Henestrosa, A. R., Garriga, X., Tapias, A., and Barbe, J. (1994) Interspecies regulation of the recA gene of gram-negative bacteria lacking an E. coli-like SOS operator, *Mol. Gen. Genet.* 245, 523-7.
74. Boyle-Vavra, S., and Seifert, H. S. (1996) Uptake-sequence-independent DNA transformation exists in Neisseria gonorrhoeae, *Microbiology* 142 ( Pt 10), 2839-45.
75. Catlin, B. W., and Cunningham, L. S. (1961) Transforming activities and base contents of deoxyribonucleate preparations from various Neisseriae, *J. Gen. Microbiol.* 26, 303-12.
76. Gomez-Gomez, J. M., Manfredi, C., Alonso, J. C., and Blazquez, J. (2007) A novel role for RecA under non-stress: promotion of swarming motility in Escherichia coli K-12, *BMC Biol* 5, 14.
77. Kimmitt, P. T., Harwood, C. R., and Barer, M. R. (2000) Toxin gene expression by shiga toxin-producing Escherichia coli: the role of antibiotics and the bacterial SOS response, *Emerg. Infect. Dis.* 6, 458-65.

78. Casjens, S. (2003) Prophages and bacterial genomics: what have we learned so far?, *Mol. Microbiol.* 49, 277-300.
79. Kramer, N., Hahn, J., and Dubnau, D. (2007) Multiple interactions among the competence proteins of *Bacillus subtilis*, *Mol. Microbiol.* 65, 454-64.
80. Goerke, C., Koller, J., and Wolz, C. (2006) Ciprofloxacin and trimethoprim cause phage induction and virulence modulation in *Staphylococcus aureus*, *Antimicrob Agents Chemother* 50, 171-7.
81. Boles, B. R., Thoendel, M., and Singh, P. K. (2004) Self-generated diversity produces "insurance effects" in biofilm communities, *Proc. Natl. Acad. Sci. U. S. A.* 101, 16630-5.
82. Lewin, C. S., and Amyes, S. G. (1991) The role of the SOS response in bacteria exposed to zidovudine or trimethoprim, *J. Med. Microbiol.* 34, 329-32.
83. Power, E. G., and Phillips, I. (1992) Induction of the SOS gene (umuC) by 4-quinolone antibacterial drugs, *J. Med. Microbiol.* 36, 78-82.
84. Riesenfeld, C., Everett, M., Piddock, L. J., and Hall, B. G. (1997) Adaptive mutations produce resistance to ciprofloxacin, *Antimicrob. Agents Chemother.* 41, 2059-60.
85. Rosenberg, S. M. (2001) Evolving responsively: adaptive mutation, *Nat Rev Genet* 2, 504-15.
86. Miller, C., Thomsen, L. E., Gaggero, C., Mosseri, R., Ingmer, H., and Cohen, S. N. (2004) SOS response induction by beta-lactams and bacterial defense against antibiotic lethality, *Science* 305, 1629-31.
87. Maiques, E., Ubeda, C., Campoy, S., Salvador, N., Lasa, I., Novick, R. P., Barbe, J., and Penades, J. R. (2006) beta-lactam antibiotics induce the SOS response and horizontal transfer of virulence factors in *Staphylococcus aureus*, *J. Bacteriol.* 188, 2726-9.
88. Bisognano, C., Kelley, W. L., Estoppey, T., Francois, P., Schrenzel, J., Li, D., Lew, D. P., Hooper, D. C., Cheung, A. L., and Vaudaux, P. (2004) A recA-LexA-dependent pathway mediates ciprofloxacin-induced fibronectin binding in *Staphylococcus aureus*, *J. Biol. Chem.* 279, 9064-71.

89. Chao, L. (1986) Sensitivity of DNA-repair-deficient strains of *Escherichia coli* to rifampicin killing, *Mutat. Res.* 173, 25-9.
90. Fram, R. J., Mack, S. L., George, M., and Marinus, M. G. (1989) DNA repair mechanisms affecting cytotoxicity by streptozotocin in *E. coli*, *Mutat. Res.* 218, 125-33.
91. Herrero, M., and Moreno, F. (1986) Microcin B17 blocks DNA replication and induces the SOS system in *Escherichia coli*, *J. Gen. Microbiol.* 132, 393-402.
92. Howard, B. M., Pinney, R. J., and Smith, J. T. (1993) Function of the SOS process in repair of DNA damage induced by modern 4-quinolones, *J. Pharm. Pharmacol.* 45, 658-62.
93. Lal, D., Som, S., and Friedman, S. (1988) Survival and mutagenic effects of 5-azacytidine in *Escherichia coli*, *Mutat. Res.* 193, 229-36.
94. Mamber, S. W., Brookshire, K. W., and Forenza, S. (1990) Induction of the SOS response in *Escherichia coli* by azidothymidine and dideoxynucleosides, *Antimicrob. Agents Chemother.* 34, 1237-43.
95. Martinez, J. L., and Perez-Diaz, J. C. (1986) Isolation, characterization, and mode of action on *Escherichia coli* strains of microcin D93, *Antimicrob. Agents Chemother.* 29, 456-60.
96. McDaniel, L. S., Rogers, L. H., and Hill, W. E. (1978) Survival of recombination-deficient mutants of *Escherichia coli* during incubation with nalidixic acid, *J. Bacteriol.* 134, 1195-8.
97. Oda, Y. (1987) Induction of SOS responses in *Escherichia coli* by 5-fluorouracil, *Mutat. Res.* 183, 103-8.
98. Piddock, L. J., and Walters, R. N. (1992) Bactericidal activities of five quinolones for *Escherichia coli* strains with mutations in genes encoding the SOS response or cell division, *Antimicrob. Agents Chemother.* 36, 819-25.
99. Tamamura, T., Tsuchiya, M., Isshiki, K., Sawa, T., Takeuchi, T., Hori, M., and Sakata, N. (1988) Terpentecin, an inhibitor of DNA synthesis, *J. Antibiot. (Tokyo)*. 41, 648-54.

100. Yamamoto, K., Hiramoto, T., Shinagawa, H., and Fujiwara, Y. (1984) Genetic activity of bleomycin in *Escherichia coli*, *Chem. Biol. Interact.* 48, 145-52.
101. Pankey, G. A., and Sabath, L. D. (2004) Clinical relevance of bacteriostatic versus bactericidal mechanisms of action in the treatment of Gram-positive bacterial infections, *Clin. Infect. Dis.* 38, 864-70.
102. Smith, P. A., and Romesberg, F. E. (2007) Combating bacteria and drug resistance by inhibiting mechanisms of persistence and adaptation, *Nat Chem Biol* 3, 549-56.
103. Hotchkiss, R. D. (1951) Transfer of penicillin resistance in pneumococci by the desoxyribonucleate derived from resistant cultures, *Cold Spring Harb. Symp. Quant. Biol.* 16, 457-61.
104. Davies, J. (1996) Origins and evolution of antibiotic resistance, *Microbiologia* 12, 9-16.
105. Burrus, V., Pavlovic, G., Decaris, B., and Guedon, G. (2002) Conjugative transposons: the tip of the iceberg, *Mol. Microbiol.* 46, 601-10.
106. Hahn, J., Maier, B., Haijema, B. J., Sheetz, M., and Dubnau, D. (2005) Transformation proteins and DNA uptake localize to the cell poles in *Bacillus subtilis*, *Cell* 122, 59-71.
107. Capaldo, F. N., and Barbour, S. D. (1975) DNA content, synthesis and integrity in dividing and non-dividing cells of rec- strains of *Escherichia coli* K12, *J. Mol. Biol.* 91, 53-66.
108. Capaldo, F. N., and Barbour, S. D. (1975) The role of the rec genes in the viability of *Escherichia coli* K12, *Basic Life Sci.* 5A, 405-18.
109. Capaldo, F. N., Ramsey, G., and Barbour, S. D. (1974) Analysis of the growth of recombination-deficient strains of *Escherichia coli* K-12, *J. Bacteriol.* 118, 242-9.
110. Capaldo, F. N., and Barbour, S. D. (1973) Isolation of the nonviable cells produced during normal growth of recombination-deficient strains of *Escherichia coli* K-12, *J. Bacteriol.* 115, 928-36.



111. Mushegian, A. R., and Koonin, E. V. (1996) A minimal gene set for cellular life derived by comparison of complete bacterial genomes, *Proc. Natl. Acad. Sci. U. S. A.* 93, 10268-73.
112. Koonin, E. V. (2003) Comparative genomics, minimal gene-sets and the last universal common ancestor, *Nat Rev Microbiol* 1, 127-36.
113. Diekema, D. J., BootsMiller, B. J., Vaughn, T. E., Woolson, R. F., Yankey, J. W., Ernst, E. J., Flach, S. D., Ward, M. M., Franciscus, C. L., Pfaller, M. A., and Doebbeling, B. N. (2004) Antimicrobial resistance trends and outbreak frequency in United States hospitals, *Clin Infect Dis* 38, 78-85.
114. Smolinski, M. S., Hamburg, M. A., and Lederberg, J. (2003), National Academies Press, Washington, D.C.
115. Talbot, G. H., Bradley, J., Edwards, J. E., Jr., Gilbert, D., Scheld, M., and Bartlett, J. G. (2006) Bad bugs need drugs: an update on the development pipeline from the Antimicrobial Availability Task Force of the Infectious Diseases Society of America, *Clin Infect Dis* 42, 657-68.
116. Power, E. (2006) Impact of antibiotic restrictions: the pharmaceutical perspective, *Clin Microbiol Infect* 12 Suppl 5, 25-34.
117. Foster, P. L. (2005) Stress responses and genetic variation in bacteria, *Mutation Research* 569, 3-11.
118. Hersh, M. N., Ponder, R. G., Hastings, P. J., and Rosenberg, S. M. (2004) Adaptive mutation and amplification in *Escherichia coli*: two pathways of genome adaptation under stress, *Res. Microbiol.* 155, 352-9.
119. Matic, I., Taddei, F., and Radman, M. (2004) Survival versus maintenance of genetic stability: a conflict of priorities during stress, *Research in Microbiology* 155, 337-41.
120. Hastings, P. J., Rosenberg, S. M., and Slack, A. (2004) Antibiotic-induced lateral transfer of antibiotic resistance, *Trends Microbiol.* 12, 401-4.
121. Yang, S., VanLoock, M. S., Yu, X., and Egelman, E. H. (2001) Comparison of bacteriophage T4 UvsX and human Rad51 filaments suggests that RecA-like polymers may have evolved independently, *J Mol Biol* 312, 999-1009.

122. Yang, S., Yu, X., Seitz, E. M., Kowalczykowski, S. C., and Egelman, E. H. (2001) Archaeal RadA protein binds DNA as both helical filaments and octameric rings, *J Mol Biol* 314, 1077-85.
123. Lee, A. M., and Singleton, S. F. (2004) Inhibition of the Escherichia coli RecA protein: zinc(II), copper(II) and mercury(II) trap RecA as inactive aggregates, *J Inorg Biochem* 98, 1981-6.
124. Wigle, T. J., Lee, A. M., and Singleton, S. F. (2006) Conformationally selective binding of nucleotide analogues to Escherichia coli RecA: a ligand-based analysis of the RecA ATP binding site, *Biochemistry* 45, 4502-13.
125. Cline, D. J., Holt, S. L., and Singleton, S. F. (2007) Inhibition of Escherichia coli RecA by rationally redesigned N-terminal helix, *Org Biomol Chem* 5, 1525-8.
126. Weber, T. P., Widger, W. R., and Kohn, H. (2003) Metal dependency for transcription factor rho activation, *Biochemistry* 42, 1652-9.
127. Weber, T. P., Widger, W. R., and Kohn, H. (2003) Metal-1,4-dithio-2,3-dihydroxybutane chelates: novel inhibitors of the Rho transcription termination factor, *Biochemistry* 42, 9121-6.
128. Brogan, A. P., Verghese, J., Widger, W. R., and Kohn, H. (2005) Bismuth-dithiol inhibition of the Escherichia coli rho transcription termination factor, *J. Inorg. Biochem.* 99, 841-51.
129. Yu, X., Horiguchi, T., Shigesada, K., and Egelman, E. H. (2000) Three-dimensional reconstruction of transcription termination factor rho: orientation of the N-terminal domain and visualization of an RNA-binding site, *J Mol Biol* 299, 1279-87.
130. Ciampi, M. S. (2006) Rho-dependent terminators and transcription termination, *Microbiology* 152, 2515-28.
131. Brenner, S. L., Zlotnick, A., and Stafford, W. F., 3rd. (1990) RecA protein self-assembly. II. Analytical equilibrium ultracentrifugation studies of the entropy-driven self-association of RecA, *J Mol Biol* 216, 949-64.

132. Benight, A. S., Wilson, D. H., Budzynski, D. M., and Goldstein, R. F. (1991) Dynamic light scattering investigations of RecA self-assembly and interactions with single strand DNA, *Biochimie* 73, 143-55.
133. Yu, X., and Egelman, E. H. (1997) The RecA hexamer is a structural homologue of ring helicases, *Nat Struct Biol* 4, 101-4.
134. Singh, K., Singh, D. P., Barwa, M. S., Tyagi, P., and Mirza, Y. (2006) Antibacterial Co(II), Ni(II), Cu(II) and Zn(II) complexes of Schiff bases derived from fluorobenzaldehyde and triazoles, *J Enzyme Inhib Med Chem* 21, 557-62.
135. Chohan, Z. H., Arif, M., Akhtar, M. A., and Supuran, C. T. (2006) Metal-Based Antibacterial and Antifungal Agents: Synthesis, Characterization, and In Vitro Biological Evaluation of Co(II), Cu(II), Ni(II), and Zn(II) Complexes With Amino Acid-Derived Compounds, *Bioinorg Chem Appl*, 83131.
136. Chohan, Z. H., Arif, M., Shafiq, Z., Yaqub, M., and Supuran, C. T. (2006) In vitro antibacterial, antifungal & cytotoxic activity of some isonicotinoylhydrazide Schiff's bases and their cobalt (II), copper (II), nickel (II) and zinc (II) complexes, *J Enzyme Inhib Med Chem* 21, 95-103.
137. Kizilcikli, I., Kurt, Y. D., Akkurt, B., Genel, A. Y., Birteksoz, S., Otuk, G., and Ulkuseven, B. (2007) Antimicrobial activity of a series of thiosemicarbazones and their Zn(II) and Pd(II) complexes, *Folia Microbiol (Praha)* 52, 15-25.
138. Domenico, P., Tomas, J. M., Merino, S., Rubires, X., and Cunha, B. A. (1999) Surface antigen exposure by bismuth dimercaprol suppression of *Klebsiella pneumoniae* capsular polysaccharide, *Infect Immun* 67, 664-9.
139. Domenico, P., Baldassarri, L., Schoch, P. E., Kaehler, K., Sasatsu, M., and Cunha, B. A. (2001) Activities of bismuth thiols against staphylococci and staphylococcal biofilms, *Antimicrob Agents Chemother* 45, 1417-21.
140. Domenico, P., Reich, J., Madonia, W., and Cunha, B. A. (1996) Resistance to bismuth among gram-negative bacteria is dependent upon iron and its uptake, *J Antimicrob Chemother* 38, 1031-40.
141. Bland, M. V., Ismail, S., Heinemann, J. A., and Keenan, J. I. (2004) The action of bismuth against *Helicobacter pylori* mimics but is not caused by intracellular iron deprivation, *Antimicrob Agents Chemother* 48, 1983-8.

142. U.S. Geological Survey Website (2007).  
<http://minerals.usgs.gov/minerals/pubs/commodity/bismuth/>
143. Ables, A. Z., Simon, I., and Melton, E. R. (2007) Update on Helicobacter pylori treatment, *Am. Fam. Physician* 75, 351-8.
144. Briand, G. G., and Burford, N. (1999) Bismuth compounds and preparations with biological or medicinal relevance, *Chem Rev* 99, 2601-58.
145. Domenico, P., Salo, R. J., Novick, S. G., Schoch, P. E., Van Horn, K., and Cunha, B. A. (1997) Enhancement of bismuth antibacterial activity with lipophilic thiol chelators, *Antimicrob Agents Chemother* 41, 1697-703.
146. Kotani, T., Nagai, D., Asahi, K., Suzuki, H., Yamao, F., Kataoka, N., and Yagura, T. (2005) Antibacterial properties of some cyclic organobismuth(III) compounds, *Antimicrob Agents Chemother* 49, 2729-34.
147. Murata, T. (2006) Effects of bismuth contamination on the growth and activity of soil microorganisms using thiols as model compounds, *J Environ Sci Health A Tox Hazard Subst Environ Eng* 41, 161-72.
148. Lee, J. W., and Cox, M. M. (1990) Inhibition of recA protein promoted ATP hydrolysis. 2. Longitudinal assembly and disassembly of recA protein filaments mediated by ATP and ADP, *Biochemistry* 29, 7677-83.
149. Kasuga, N. C., Onodera, K., Nakano, S., Hayashi, K., and Nomiya, K. (2006) Syntheses, crystal structures and antimicrobial activities of 6-coordinate antimony(III) complexes with tridentate 2-acetylpyridine thiosemicarbazone, bis(thiosemicarbazone) and semicarbazone ligands, *J Inorg Biochem.*
150. Mahony, D. E., Lim-Morrison, S., Bryden, L., Faulkner, G., Hoffman, P. S., Agocs, L., Briand, G. G., Burford, N., and Maguire, H. (1999) Antimicrobial activities of synthetic bismuth compounds against Clostridium difficile, *Antimicrob Agents Chemother* 43, 582-8.
151. Lee, A. M., and Singleton, S. F. (2004) Inhibition of the Escherichia coli RecA protein: zinc(II), copper(II) and mercury(II) trap RecA as inactive aggregates, *Journal of Inorganic Biochemistry* 98, 1981-6.

152. Brenner, S. L., Mitchell, R. S., Morriscal, S. W., Neuendorf, S. K., Schutte, B. C., and Cox, M. M. (1987) recA protein-promoted ATP hydrolysis occurs throughout recA nucleoprotein filaments, *J Biol Chem* 262, 4011-6.
153. Arenson, T. A., Tsodikov, O. V., and Cox, M. M. (1999) Quantitative analysis of the kinetics of end-dependent disassembly of RecA filaments from ssDNA, *J Mol Biol* 288, 391-401.
154. Beil, W., Bierbaum, S., and Sewing, K. F. (1993) Studies on the mechanism of action of colloidal bismuth subcitrate. I. Interaction with sulfhydryls, *Pharmacology* 47, 135-40.
155. Bell, C. E. (2005) Structure and mechanism of Escherichia coli RecA ATPase, *Mol Microbiol* 58, 358-66.
156. Bailone, A., Backman, A., Sommer, S., Celerier, J., Bagdasarian, M. M., Bagdasarian, M., and Devoret, R. (1988) PsiB polypeptide prevents activation of RecA protein in Escherichia coli, *Mol Gen Genet* 214, 389-95.
157. Berger, M. D., Lee, A. M., Simonette, R. A., Jackson, B. E., Roca, A. I., and Singleton, S. F. (2001) Design and evaluation of a tryptophanless RecA protein with wild type activity, *Biochemical and Biophysical Research Communications* 286, 1195-203.
158. Griffith, K. L., and Wolf, R. E., Jr. (2002) Measuring beta-galactosidase activity in bacteria: cell growth, permeabilization, and enzyme assays in 96-well arrays, *Biochem Biophys Res Commun* 290, 397-402.
159. Singleton, S. F., Simonette, R. A., Sharma, N. C., and Roca, A. I. (2002) Intein-mediated affinity-fusion purification of the Escherichia coli RecA protein, *Protein Expr Purif* 26, 476-88.
160. Berger, M. D., Lee, A. M., Simonette, R. A., Jackson, B. E., Roca, A. I., and Singleton, S. F. (2001) Design and evaluation of a tryptophanless RecA protein with wild type activity, *Biochem Biophys Res Commun* 286, 1195-203.
161. Morriscal, S. W., Lee, J., and Cox, M. M. (1986) Continuous association of Escherichia coli single-stranded DNA binding protein with stable complexes of recA protein and single-stranded DNA, *Biochemistry* 25, 1482-94.

162. Neet, K. E. (1980) Cooperativity in enzyme function: equilibrium and kinetic aspects, *Methods Enzymol* 64, 139-92.
163. Menge, K. L., and Bryant, F. R. (1988) ATP-stimulated hydrolysis of GTP by RecA protein: kinetic consequences of cooperative RecA protein-ATP interactions, *Biochemistry* 27, 2635-40.
164. Bisognano, C., Kelley, W. L., Estoppey, T., Francois, P., Schrenzel, J., Li, D., Lew, D. P., Hooper, D. C., Cheung, A. L., and Vaudaux, P. (2004) A recA-LexA-dependent pathway mediates ciprofloxacin-induced fibronectin binding in *Staphylococcus aureus*, *J. Biol. Chem.* 279, 9064-71.
165. Chao, L. (1986) Sensitivity of DNA-repair-deficient strains of *Escherichia coli* to rifampicin killing, *Mutat. Res.* 173, 25-9.
166. Fram, R. J., Mack, S. L., George, M., and Marinus, M. G. (1989) DNA repair mechanisms affecting cytotoxicity by streptozotocin in *E. coli*, *Mutat. Res.* 218, 125-33.
167. Herrero, M., and Moreno, F. (1986) Microcin B17 blocks DNA replication and induces the SOS system in *Escherichia coli*, *J. Gen. Microbiol.* 132, 393-402.
168. Howard, B. M., Pinney, R. J., and Smith, J. T. (1993) Function of the SOS process in repair of DNA damage induced by modern 4-quinolones, *J. Pharm. Pharmacol.* 45, 658-62.
169. Lal, D., Som, S., and Friedman, S. (1988) Survival and mutagenic effects of 5-azacytidine in *Escherichia coli*, *Mutat. Res.* 193, 229-36.
170. Mamber, S. W., Brookshire, K. W., and Forenza, S. (1990) Induction of the SOS response in *Escherichia coli* by azidothymidine and dideoxynucleosides, *Antimicrob. Agents Chemother.* 34, 1237-43.
171. Martinez, J. L., and Perez-Diaz, J. C. (1986) Isolation, characterization, and mode of action on *Escherichia coli* strains of microcin D93, *Antimicrob. Agents Chemother.* 29, 456-60.

172. McDaniel, L. S., Rogers, L. H., and Hill, W. E. (1978) Survival of recombination-deficient mutants of *Escherichia coli* during incubation with nalidixic acid, *J. Bacteriol.* *134*, 1195-8.
173. Oda, Y. (1987) Induction of SOS responses in *Escherichia coli* by 5-fluorouracil, *Mutat. Res.* *183*, 103-8.
174. Piddock, L. J., and Walters, R. N. (1992) Bactericidal activities of five quinolones for *Escherichia coli* strains with mutations in genes encoding the SOS response or cell division, *Antimicrob. Agents Chemother.* *36*, 819-25.
175. Tamamura, T., Tsuchiya, M., Isshiki, K., Sawa, T., Takeuchi, T., Hori, M., and Sakata, N. (1988) Terpentecin, an inhibitor of DNA synthesis, *J. Antibiot.* *41*, 648-54.
176. Yamamoto, K., Hiramoto, T., Shinagawa, H., and Fujiwara, Y. (1984) Genetic activity of bleomycin in *Escherichia coli*, *Chem.-Biol. Interact.* *48*, 145-52.
177. Casjens, S. (2003) Prophages and bacterial genomics: what have we learned so far?, *Molecular Microbiology* *49*, 277-300.
178. Roca, A. I., and Cox, M. M. (1997) RecA protein: structure, function, and role in recombinational DNA repair, *Progress in Nucleic Acid Research and Molecular Biology* *56*, 129-223.
179. Sassanfar, M., and Roberts, J. W. (1990) Nature of the SOS-inducing signal in *Escherichia coli*. The involvement of DNA replication, *Journal of Molecular Biology* *212*, 79-96.
180. Goodman, M. F. (2000) Coping with replication 'train wrecks' in *Escherichia coli* using Pol V, Pol II and RecA proteins, *Trends in Biochemical Sciences* *25*, 189-95.
181. Courcelle, J., Ganesan, A. K., and Hanawalt, P. C. (2001) Therefore, what are recombination proteins there for?, *BioEssays* *23*, 463-70.
182. Haruta, N., Yu, X., Yang, S., Egelman, E. H., and Cox, M. M. (2003) A DNA pairing-enhanced conformation of bacterial RecA proteins, *J. Biol. Chem.* *278*, 52710-23.

183. Noble, M. E., Endicott, J. A., and Johnson, L. N. (2004) Protein kinase inhibitors: insights into drug design from structure, *Science* 303, 1800-5.
184. Wu, Y., He, Y., Moya, I. A., Qian, X., and Luo, Y. (2004) Crystal structure of archaeal recombinase RADA: a snapshot of its extended conformation, *Mol Cell* 15, 423-35.
185. McGrew, D. A., and Knight, K. L. (2003) Molecular design and functional organization of the RecA protein, *Crit Rev Biochem Mol Biol* 38, 385-432.
186. Story, R. M., and Steitz, T. A. (1992) Structure of the recA protein-ADP complex, *Nature* 355, 374-6.
187. Chene, P. (2002) ATPases as drug targets: learning from their structure, *Nat Rev Drug Discov* 1, 665-73.
188. Freitag, N. E., and McEntee, K. (1991) Site-directed mutagenesis of the RecA protein of *Escherichia coli*. Tyrosine 264 is required for efficient ATP hydrolysis and strand exchange but not for LexA repressor inactivation, *J Biol Chem* 266, 7058-66.
189. Eriksson, S., Norden, B., Morimatsu, K., Horii, T., and Takahashi, M. (1993) Role of tyrosine residue 264 of RecA for the binding of cofactor and DNA, *J Biol Chem* 268, 1811-6.
190. Webb, M. R., and Hunter, J. L. (1992) Interaction of GTPase-activating protein with p21ras, measured using a continuous assay for inorganic phosphate release, *Biochem J* 287 ( Pt 2), 555-9.
191. Ellouze, C., Selmane, T., Kim, H. K., Tuite, E., Norden, B., Mortensen, K., and Takahashi, M. (1999) Difference between active and inactive nucleotide cofactors in the effect on the DNA binding and the helical structure of RecA filament dissociation of RecA--DNA complex by inactive nucleotides, *Eur. J. Biochem.* 262, 88-94.
192. Katz, F. S., and Bryant, F. R. (2003) Three-strand exchange by the *Escherichia coli* RecA protein using ITP as a nucleotide cofactor: mechanistic parallels with the ATP-dependent reaction of the RecA protein from *Streptococcus pneumoniae*, *J Biol Chem* 278, 35889-96.



193. Xing, X., and Bell, C. E. (2004) Crystal structures of Escherichia coli RecA in a compressed helical filament, *J Mol Biol* 342, 1471-85.
194. Menge, K. L., and Bryant, F. R. (1992) Effect of nucleotide cofactor structure on recA protein-promoted DNA pairing. 1. Three-strand exchange reaction, *Biochemistry* 31, 5151-7.
195. Yamagata, Y., Kohda, K., and Tomita, K. (1988) Structural studies of O6-methyldeoxyguanosine and related compounds: a promutagenic DNA lesion by methylating carcinogens, *Nucleic Acids Res* 16, 9307-21.
196. Tavale, S. S., and Sobell, H. M. (1970) Crystal and molecular structure of 8-bromoguanosine and 8-bromoadenosine, two purine nucleosides in the syn conformation, *J Mol Biol* 48, 109-23.
197. Ikehara, M., Uesugi, S., and Yoshida, K. (1972) Conformation of purine nucleoside pyrophosphates as studied by circular dichroism, *Biochemistry* 11, 836-42.
198. Lee, J. W., and Cox, M. M. (1990) Inhibition of recA protein promoted ATP hydrolysis. 1. ATP gamma S and ADP are antagonistic inhibitors, *Biochemistry* 29, 7666-76.
199. Roca, A. I., and Singleton, S. F. (2003) Direct evaluation of a mechanism for activation of the RecA nucleoprotein filament, *J. Am. Chem. Soc.* 125, 15366-75.
200. Moreau, P. L., and Carlier, M. F. (1989) RecA protein-promoted cleavage of LexA repressor in the presence of ADP and structural analogues of inorganic phosphate, the fluoride complexes of aluminum and beryllium, *J. Biol. Chem.* 264, 2302-6.
201. Menetski, J. P., and Kowalczykowski, S. C. (1985) Interaction of recA protein with single-stranded DNA. Quantitative aspects of binding affinity modulation by nucleotide cofactors, *J. Mol. Biol.* 181, 281-95.
202. Lee, A. M., Ross, C. T., Zeng, B. B., and Singleton, S. F. (2005) A molecular target for suppression of the evolution of antibiotic resistance: inhibition of the Escherichia coli RecA protein by N(6)-(1-naphthyl)-ADP, *Journal of Medicinal Chemistry* 48, 5408-11.

203. Yasuda, T., Morimatsu, K., Kato, R., Usukura, J., Takahashi, M., and Ohmori, H. (2001) Physical interactions between DinI and RecA nucleoprotein filament for the regulation of SOS mutagenesis, *Embo J* 20, 1192-202.
204. Shah, K., Liu, Y., Deirmengian, C., and Shokat, K. M. (1997) Engineering unnatural nucleotide specificity for Rous sarcoma virus tyrosine kinase to uniquely label its direct substrates, *Proc Natl Acad Sci U S A* 94, 3565-70.
205. Gillespie, P. G., Gillespie, S. K., Mercer, J. A., Shah, K., and Shokat, K. M. (1999) Engineering of the myosin- $\beta$  nucleotide-binding pocket to create selective sensitivity to N(6)-modified ADP analogs, *J Biol Chem* 274, 31373-81.
206. Kapoor, T. M., and Mitchison, T. J. (1999) Allele-specific activators and inhibitors for kinesin, *Proc Natl Acad Sci U S A* 96, 9106-11.
207. Drontle, D. P., and Wagner, C. R. (2004) Designing a pronucleotide stratagem: lessons from amino acid phosphoramidates of anticancer and antiviral pyrimidines, *Mini Rev. Med. Chem.* 4, 404-419.
208. Krise, J. P., and Stella, V. J. (1996) Prodrugs of phosphates, phosphonates, and phosphinates, *Adv. Drug Del. Rev.* 19, 287-310.
209. Meier, C., Ruppel, M. F., Vukadinovic, D., and Balzarini, J. (2004) "Lock-in"-cycloSal-pronucleotides - a new generation of chemical Trojan Horses?, *Mini Rev. Med. Chem.* 4, 383-394.
210. Peyrottes, S., Egron, D., Lefebvre, I., Gosselin, G., and Imbach, J. L. (2004) SATE pronucleotide approaches: an overview, *Mini Rev. Med. Chem.* 4, 395-408.
211. Schultz, C. (2003) Prodrugs of biologically active phosphate esters, *Bioorg Med Chem* 11, 885-98.
212. Wigle, T. J., Lee, A. M., and Singleton, S. F. (2006) Conformationally selective binding of nucleotide analogues to Escherichia coli RecA: A ligand-based analysis of the RecA ATP binding site, *Biochemistry* 45, 4502-4513.
213. Lee, A. M., Wigle, T. J., and Singleton, S. F. (2007) A complementary pair of rapid molecular screening assays for RecA activities, *Anal. Biochem.*, (in press).

214. Wigle, T. J., and Singleton, S. F. (2007) Directed molecular screening for RecA ATPase inhibitors, *Bioorg Med Chem Lett* 17, 3249-53.
215. Gille, A., Lushington, G. H., Mou, T. C., Doughty, M. B., Johnson, R. A., and Seifert, R. (2004) Differential inhibition of adenylyl cyclase isoforms and soluble guanylyl cyclase by purine and pyrimidine nucleotides, *J. Biol. Chem.* 279, 19955-69.
216. Mou, T. C., Gille, A., Fancy, D. A., Seifert, R., and Sprang, S. R. (2005) Structural basis for the inhibition of mammalian membrane adenylyl cyclase by 2'(3')-O-(N-Methylanthraniloyl)-guanosine 5'-triphosphate, *J. Biol. Chem.* 280, 7253-61.
217. Nomanbhoy, T. K., and Cerione, R. (1996) Characterization of the interaction between RhoGDI and Cdc42Hs using fluorescence spectroscopy, *J. Biol. Chem.* 271, 10004-9.
218. Rohn, T. T., Nelson, L. K., Davis, A. R., and Quinn, M. T. (1999) Inhibition of GTP binding to Rac2 by peroxynitrite: potential role for tyrosine modification, *Free Radic. Biol. Med.* 26, 1321-31.
219. Galletto, R., Maillard, R., Jezewska, M. J., and Bujalowski, W. (2004) Global conformation of the Escherichia coli replication factor DnaC protein in absence and presence of nucleotide cofactors, *Biochemistry (Mosc)*. 43, 10988-1001.
220. Galletto, R., Jezewska, M. J., and Bujalowski, W. (2005) Kinetics of allosteric conformational transition of a macromolecule prior to ligand binding: analysis of stopped-flow kinetic experiments, *Cell Biochem. Biophys.* 42, 121-44.
221. Jezewska, M. J., Lucius, A. L., and Bujalowski, W. (2005) Binding of six nucleotide cofactors to the hexameric helicase RepA protein of plasmid RSF1010. 1. Direct evidence of cooperative interactions between the nucleotide-binding sites of a hexameric helicase, *Biochemistry (Mosc)*. 44, 3865-76.
222. Galletto, R., and Bujalowski, W. (2002) Kinetics of the E. coli replication factor DnaC protein-nucleotide interactions. II. Fluorescence anisotropy and transient, dynamic quenching stopped-flow studies of the reaction intermediates, *Biochemistry (Mosc)*. 41, 8921-34.
223. Galletto, R., and Bujalowski, W. (2002) The E. coli replication factor DnaC protein exists in two conformations with different nucleotide binding capabilities. I.

- Determination of the binding mechanism using ATP and ADP fluorescent analogues, *Biochemistry (Mosc)*. 41, 8907-20.
224. Galletto, R., Rajendran, S., and Bujalowski, W. (2000) Interactions of nucleotide cofactors with the Escherichia coli replication factor DnaC protein, *Biochemistry (Mosc)*. 39, 12959-69.
225. Bujalowski, W., and Jezewska, M. J. (2000) Kinetic mechanism of nucleotide cofactor binding to Escherichia coli replicative helicase DnaB protein. stopped-flow kinetic studies using fluorescent, ribose-, and base-modified nucleotide analogues, *Biochemistry (Mosc)*. 39, 2106-22.
226. Cheng, J. Q., Jiang, W., and Hackney, D. D. (1998) Interaction of mant-adenosine nucleotides and magnesium with kinesin, *Biochemistry* 37, 5288-95.
227. Knight, K. L., and McEntee, K. (1985) Affinity labeling of a tyrosine residue in the ATP binding site of the recA protein from Escherichia coli with 5'-p-fluorosulfonylbenzoyl adenosine, *J Biol Chem* 260, 10177-84.
228. Ohkubo, S., Matsuoka, I., Kimura, J., and Nakanishi, H. (1998) Inhibition of ATP-induced cAMP formation by 5'-p-fluorosulfonylbenzoyl adenosine in NG108-15 cells, *Naunyn Schmiedebergs Arch Pharmacol* 358, 153-9.
229. Torres, C. R., Vasconcelos, E. G., Ferreira, S. T., and Verjovski-Almeida, S. (1998) Divalent cation dependence and inhibition of Schistosoma mansoni ATP diphosphohydrolase by fluorosulfonylbenzoyl adenosine, *Eur J Biochem* 251, 516-21.
230. Xiao, J., Lee, A. M., and Singleton, S. F. (2006) Direct evaluation of a kinetic model for RecA-mediated DNA-strand exchange: the importance of nucleic acid dynamics and entropy during homologous genetic recombination, *ChemBiochem* 7, 1265-78.
231. Xiao, J., Lee, A. M., and Singleton, S. F. (2006) Construction and evaluation of a kinetic scheme for RecA-mediated DNA strand exchange, *Biopolymers* 81, 473-96.
232. Cox, M. M., and Lehman, I. R. (1981) recA protein of Escherichia coli promotes branch migration, a kinetically distinct phase of DNA strand exchange, *Proc Natl Acad Sci U S A* 78, 3433-7.

233. Roman, L. J., and Kowalczykowski, S. C. (1986) Relationship of the physical and enzymatic properties of *Escherichia coli* recA protein to its strand exchange activity, *Biochemistry* 25, 7375-85.
234. Lee, A. M., and Singleton, S. F. (2006) Intersubunit electrostatic complementarity in the RecA nucleoprotein filament regulates nucleotide substrate specificity and conformational activation, *Biochemistry* 45, 4514-29.
235. Eggler, A. L., Lusetti, S. L., and Cox, M. M. (2003) The C terminus of the *Escherichia coli* RecA protein modulates the DNA binding competition with single-stranded DNA-binding protein, *J Biol Chem* 278, 16389-96.
236. Kurumizaka, H., Aihara, H., Ikawa, S., Kashima, T., Bazemore, L. R., Kawasaki, K., Sarai, A., Radding, C. M., and Shibata, T. (1996) A possible role of the C-terminal domain of the RecA protein. A gateway model for double-stranded DNA binding, *J Biol Chem* 271, 33515-24.
237. Lusetti, S. L., Shaw, J. J., and Cox, M. M. (2003) Magnesium ion-dependent activation of the RecA protein involves the C terminus, *J Biol Chem* 278, 16381-8.
238. Maruta, S., Saitoh, J., and Asakura, T. (2000) Analysis of conformational changes at the unique loop adjacent to the ATP binding site of smooth muscle myosin using a fluorescent probe, *J Biochem (Tokyo)* 127, 199-204.
239. Plesniak, L., Horiuchi, Y., Sem, D., Meinenger, D., Stiles, L., Shaffer, J., Jennings, P. A., and Adams, J. A. (2002) Probing the nucleotide binding domain of the osmoregulator EnvZ using fluorescent nucleotide derivatives, *Biochemistry* 41, 13876-82.
240. Kowalczykowski, S. C. (1986) Interaction of recA protein with a photoaffinity analogue of ATP, 8-azido-ATP: determination of nucleotide cofactor binding parameters and of the relationship between ATP binding and ATP hydrolysis, *Biochemistry* 25, 5872-81.
241. Stole, E., and Bryant, F. R. (1996) Reengineering the nucleotide cofactor specificity of the RecA protein by mutation of aspartic acid 100, *J Biol Chem* 271, 18326-8.
242. Cotterill, S. M., Satterthwait, A. C., and Fersht, A. R. (1982) recA protein from *Escherichia coli*. a very rapid and simple purification procedure: binding of adenosine

- 5'-triphosphate and adenosine 5'-diphosphate by the homogeneous protein, *Biochemistry* 21, 4332-7.
243. Cox, M. M., Soltis, D. A., Lehman, I. R., DeBrosse, C., and Benkovic, S. J. (1983) ADP-mediated dissociation of stable complexes of recA protein and single-stranded DNA, *J Biol Chem* 258, 2586-92.
  244. Kikugawa, K., Iizuka, K., and Ichino, M. (1973) Platelet aggregation inhibitors. 4. N 6 -substituted adenosines, *J Med Chem* 16, 358-64.
  245. Maruyama, T., Kozai, S., Takamatsu, S., and Izawa, K. (2000) Introduction of a benzoyl group onto 6-chloropurine riboside in aqueous solution and its application to the synthesis of nucleoside derivatives, *Nucleic Acids Symp Ser*, 103-4.
  246. Petersen, S. G., and Rajsiki, S. R. (2005) o-nitrobenzenesulfonamides in nucleoside synthesis: efficient 5'-aziridination of adenosine, *J Org Chem* 70, 5833-9.
  247. Li, P., Xu, Z., Liu, H., Wennefors, C. K., Dobrikov, M. I., Ludwig, J., and Shaw, B. R. (2005) Synthesis of alpha-P-modified nucleoside diphosphates with ethylenediamine, *J Am Chem Soc* 127, 16782-3.
  248. Craig, N. L., and Roberts, J. W. (1981) Function of nucleoside triphosphate and polynucleotide in Escherichia coli recA protein-directed cleavage of phage lambda repressor, *J Biol Chem* 256, 8039-44.
  249. Ohta, T., Watanabe, M., Watanabe, K., Shirasu, Y., and Kada, T. (1986) Inhibitory effects of flavourings on mutagenesis induced by chemicals in bacteria, *Food Chem. Toxicol.* 24, 51-4.
  250. Sasaki, Y. F., Imanishi, H., Ohta, T., and Shirasu, Y. (1987) Effects of vanillin on sister-chromatid exchanges and chromosome aberrations induced by mitomycin C in cultured Chinese hamster ovary cells, *Mutat. Res.* 191, 193-200.
  251. Watanabe, K., Ohta, T., and Shirasu, Y. (1989) Enhancement and inhibition of mutation by o-vanillin in Escherichia coli, *Mutat. Res.* 218, 105-9.
  252. Shaughnessy, D. T., Schaaper, R. M., Umbach, D. M., and DeMarini, D. M. (2006) Inhibition of spontaneous mutagenesis by vanillin and cinnamaldehyde in Escherichia coli: Dependence on recombinational repair, *Mutat. Res.* 602, 54-64.

253. Oda, Y. (1995) Inhibitory effect of curcumin on SOS functions induced by UV irradiation, *Mutat. Res.* 348, 67-73.
254. Yang, Y., and Fix, D. (2006) Genetic analysis of the anti-mutagenic effect of genistein in *Escherichia coli*, *Mutat. Res.* 600, 193-206.
255. Scholz, G., Barritt, G. J., and Kwok, F. (1992) Affinity labelling of the active site of brain phosphatidylinositol 4-kinase with 5'-fluorosulphonylbenzoyl-adenosine, *Eur. J. Biochem.* 210, 461-6.
256. Burlison, J. A., Neckers, L., Smith, A. B., Maxwell, A., and Blagg, B. S. (2006) Novobiocin: redesigning a DNA gyrase inhibitor for selective inhibition of hsp90, *J. Am. Chem. Soc.* 128, 15529-36.
257. Corbett, K. D., and Berger, J. M. (2006) Structural basis for topoisomerase VI inhibition by the anti-Hsp90 drug radicicol, *Nucleic Acids Res* 34, 4269-77.
258. Wang, Y., Wagner, M. B., Kumar, R., Cheng, J., and Joyner, R. W. (2003) Inhibition of fast sodium current in rabbit ventricular myocytes by protein tyrosine kinase inhibitors, *Pflugers Arch.* 446, 485-91.
259. Lambrecht, G., Braun, K., Damer, M., Ganso, M., Hildebrandt, C., Ullmann, H., Kassack, M. U., and Nickel, P. (2002) Structure-activity relationships of suramin and pyridoxal-5'-phosphate derivatives as P2 receptor antagonists, *Curr. Pharm. Des.* 8, 2371-99.
260. Jacobson, K. A., Costanzi, S., Ohno, M., Joshi, B. V., Besada, P., Xu, B., and Tchilibon, S. (2004) Molecular recognition at purine and pyrimidine nucleotide (P2) receptors, *Curr Top Med Chem* 4, 805-19.
261. Zhou, M., Diwu, Z., Panchuk-Voloshina, N., and Haugland, R. P. (1997) A stable nonfluorescent derivative of resorufin for the fluorometric determination of trace hydrogen peroxide: applications in detecting the activity of phagocyte NADPH oxidase and other oxidases, *Anal. Biochem.* 253, 162-8.
262. Zhang, B., Senator, D., Wilson, C. J., and Ng, S. C. (2005) Development of a high-throughput robotic fluorescence-based assay for HsEg5 inhibitor screening, *Anal. Biochem.* 345, 326-35.

263. Zhang, J. H., Chung, T. D., and Oldenburg, K. R. (1999) A Simple Statistical Parameter for Use in Evaluation and Validation of High Throughput Screening Assays, *J Biomol Screen* 4, 67-73.
264. Stopa, B., Konieczny, L., Piekarska, B., Roterman, I., Rybarska, J., and Skowronek, M. (1997) Effect of self association of bis-ANS and bis-azo dyes on protein binding, *Biochimie* 79, 23-6.
265. Konieczny, L., Piekarska, B., Rybarska, J., Skowronek, M., Stopa, B., Tabor, B., Dabros, W., Pawlicki, R., and Roterman, I. (1997) The use of congo red as a lyotropic liquid crystal to carry stains in a model immunotargeting system--microscopic studies, *Folia Histochem. Cytobiol.* 35, 203-10.
266. McGovern, S. L., Helfand, B. T., Feng, B., and Shoichet, B. K. (2003) A specific mechanism of nonspecific inhibition, *J. Med. Chem.* 46, 4265-72.
267. McGovern, S. L., Caselli, E., Grigorieff, N., and Shoichet, B. K. (2002) A common mechanism underlying promiscuous inhibitors from virtual and high-throughput screening, *J. Med. Chem.* 45, 1712-22.
268. Stein, C. A. (1993) Suramin: a novel antineoplastic agent with multiple potential mechanisms of action, *Cancer Res.* 53, 2239-48.
269. Lin, T. I., and Morales, M. F. (1977) Application of a one-step procedure for measuring inorganic phosphate in the presence of proteins: the actomyosin ATPase system, *Anal Biochem* 77, 10-7.
270. Hergenrother, P. J., Haas, M. K., and Martin, S. F. (1997) Chromogenic assay for phospholipase D from *Streptomyces chromofuscus*: application to the evaluation of substrate analogs, *Lipids* 32, 783-8.
271. Lee, A. M., Wigle, T. J., and Singleton, S. F. (2007) A complementary pair of rapid molecular screening assays for RecA activities, *Anal Biochem* 367, 247-58.
272. Mukherjee, A., and Lutkenhaus, J. (1998) Purification, assembly, and localization of FtsZ, *Methods Enzymol.* 298, 296-305.
273. Elwell, L. P., Ferone, R., Freeman, G. A., Fyfe, J. A., Hill, J. A., Ray, P. H., Richards, C. A., Singer, S. C., Knick, V. B., Rideout, J. L., and et al. (1987) Antibacterial



activity and mechanism of action of 3'-azido-3'-deoxythymidine (BW A509U),  
*Antimicrob Agents Chemother* 31, 274-80.

274. Witkin, E. M., McCall, J. O., Volkert, M. R., and Wermundsen, I. E. (1982)  
Constitutive expression of SOS functions and modulation of mutagenesis resulting  
from resolution of genetic instability at or near the recA locus of *Escherichia coli*,  
*Mol Gen Genet* 185, 43-50.
275. Finch, R. (2007) Innovation - drugs and diagnostics, *J. Antimicrob. Chemother.* 60  
*Suppl 1*, i79-82.